Identification of Novel Biomarkers for Diabetic Retinopathy in Human Tears

Terry Nguyen-Khuong

School of Optometry and Vision Science

University of New South Wales

2011

A thesis submitted in partial fulfilment of the requirement for the degree of Doctor of Philosophy (Ph.D.)

PLEASE TYPE

THE UNIVERSITY OF NEW SOUTH WALES
Thesis/Dissertation Sheet

Surname or Family name: NGUYEN-KHUONG

First name: TERRY Other name/s:

Abbreviation for degree as given in the University calendar: PhD

School: SCHOOL OF OPTOMETRY AND VISION SCIENCE Faculty: SCIENCE

Title: IDENTIFICATION OF NOVEL BIOMARKERS FOR DIABETIC RETINOPATHY IN HUMAN TEARS

Abstract 350 words maximum: (PLEASE TYPE)

Diabetic retinopathy (DR) is a sight threatening disorder which develops in nearly all patients with diabetes mellitus (DM). DR centres on the abnormal growth and rupturing of the retinal blood vessels. Current modes of diagnostics rely on the clinical presentation of DR, at which stage, maturation of the disease and possible damage to the retinal tissue is significant. Due to the high incidence and severity of damage resulting from this disorder a diagnostic which allows early and accurate detection is essential.

It was the aim of this project to identify biomarkers in human tears which would provide the basis for development of a non-invasive diagnostic test for DM and DR. This biomarker discovery involved extensive method development for optimal identification of quantitative changes to the tear peptidome and proteome. Proteomic technologies including MALDI-MS, iTRAQ, 2-D LC MS/MS, 2-D electrophoresis, MF10 fractionation and non-labelling mass spectrometry-based strategies were assessed in terms of their utility to investigate the tear proteome and peptidome. This thesis describes the first study to use MF10 technology and peak integration analysis to investigate the peptidome fraction of tears between different subject groups. The application of spin filters to partition higher molecular weight tear proteins from analysis, vastly improved the visualization of lower molecular weight proteins and peptides of human tears using MALDI. It is also the first study to mine the peptidomic population in tears for disease associated biomarkers. From this, one hundred and nine peptides in the 1-25 kDa MF10 fractions of the tear samples were found to alter between DM and DR subjects in comparison to healthy controls. Thirteen of these peptides were sequenced, identified and subsequently validated using an MRM assay developed specifically to quantitate and verify candidate tear peptide biomarkers.

The work presented in this thesis is the first study to identify and profile tear peptide biomarkers which have correlated with the onset of DM and DR. It is envisioned that these biomarkers will form the intrinsic components of a non-invasive diagnostic for DM and DR. Furthermore, this work has established principles for future peptidomic or low abundance protein studies with complex bio-fluids. The work has demonstrated that fractionation is an important part of both biomarker discovery and validation, especially in the context of identifying biomarkers in a complex biofluid such as tears. Coupled with validation through targeted quantitative mass spectrometry, the workflow described is a powerful tool of clinical utility in biomarker discovery and validation.

Declaration relating to disposition of project thesis/dissertation

I hereby grant to the University of New South Wales or its agents the right to archive and to make available my thesis or dissertation in whole or in part in the University libraries in all forms of media, now or here after known, subject to the provisions of the Copyright Act 1968. I retain all property rights, such as patent rights. I also retain the right to use in future works (such as articles or books) all or part of this thesis or dissertation.

I also authorise University Microfilms to use the 350 word abstract of my thesis in Dissertation Abstracts International (this is applicable to doctoral theses only).

…… …… ……..……...

Signature Witness …….. Date

The University recognises that there may be exceptional circumstances requiring restrictions on copying or conditions on use. Requests for restriction for a period of up to 2 years must be made in writing. Requests for a longer period of restriction may be considered in exceptional circumstances and require the approval of the Dean of Graduate Research.

FOR OFFICE USE ONLY Date of completion of requirements for Award:

THIS SHEET IS TO BE GLUED TO THE INSIDE FRONT COVER OF THE THESIS

Originality statement

I hereby declare that this submission is my own work and to the best of my knowledge, contains no materials previously published or written by another person or substantial proportions of material which have been accepted for the award of any other degree or diploma at UNSW or any other educational institution, except where due acknowledgement is made in the thesis. Any contribution made to the research by others whom I have worked at UNSW or elsewhere is explicitly acknowledged in the thesis. I also declare that the intellectual content of this thesis is the product of my own work, except to the extent that assistance from others in the project's design and conception or in style, presentation and linguistic expression is acknowledged.

Signed

Date

Acknowledgements

First and foremost I wish to thank all of my supervisors. This thesis the product of your fantastic scientific collaboration, critical and creative thinking. Thanks goes to my supervisor Professor Mark Willcox for the tireless efforts keeping me on track. Many thanks go to Dr Bradley Walsh for the vision and valuable advice and contribution financially and scientifically. Many thanks also goes to Dr Zhenjun Zhao for helping me collect samples despite how difficult it has been. Special mention goes to Dr Anna Fitzgerald for helping me through the hard yards of the past three years. Your advice is greatly appreciated as well as your support and contribution.

To the many wonderful people at Minomic who have made my journey quite smooth and enjoyable. Your help, support, guidance and friendship are an experience I will value most. To Belinda Schiller, Shona Seeto, Shamila Khan, Jing Jing You, Stefanie Wetzel, Carlos Casanova, Tammy Malouf, Melissa Thomas and Agnes Debril, I thank you for the hilarious and warm discussions about everything. Thank you to Belinda Schiller for those endless days proof-reading and discussing points of this thesis.

I thank the people who have helped me at the BMSF. Great mention goes to Dr Valerie Wasinger for her enormous support and guidance. I have learnt a great deal from you, all of which is warmly appreciated.

To my friends who have been a constant support outside my Ph.D. To my mates; David Luu, Nicolas Triantafillou, Mark Piekarz and Mathew “Macca” McMahon; thanks guys for the hours spent hanging with me to ease those stress levels.

Thankyou to my family for the warmth, love and support over the many years since I started this project. Special mention goes to my mother who taught me well and raised me so well, passing on skills and school of thought which I have applied to the way I live. Your constant support and dedication throughout the toughest times of our lives will be greatly remembered and definitely appreciated.

Finally and most importantly, I wish to dedicate this work to my closest friend, partner and fiancée Marie. So many nights and days have been sacrificed on your part to help make my journey smooth and easier. Your support every day and constant care and love is so warmly appreciated. I definitely look forward to the rest of my life with you. May our future endeavours be fruitful.

Terry Nguyen-Khuong

Abstract

Diabetic retinopathy (DR) is a sight threatening disorder which develops in nearly all patients with diabetes mellitus (DM). DR centres on the abnormal growth and rupturing of the retinal blood vessels. Current modes of diagnostics rely on the clinical presentation of DR, at which stage, maturation of the disease and possible damage to the retinal tissue is significant. Due to the high incidence and severity of damage resulting from this disorder a diagnostic which allows early and accurate detection is essential.

It was the aim of this project to identify biomarkers in human tears which would provide the basis for development of a non-invasive diagnostic test for DM and DR. This biomarker discovery involved extensive method development for optimal identification of quantitative changes to the tear peptidome and proteome. Proteomic technologies including MALDI-MS, iTRAQ, 2-D LC MS/MS, 2-D electrophoresis, MF10 fractionation and non-labelling mass spectrometry-based strategies were assessed in terms of their utility to investigate the tear proteome and peptidome. This thesis describes the first study to use MF10 technology and peak integration analysis to investigate the peptidome fraction of tears between different subject groups. The application of spin filters to partition higher molecular weight tear proteins from analysis, vastly improved the visualization of lower molecular weight proteins and peptides of human tears using MALDI. It is also the first study to mine the peptidomic population in tears for disease associated biomarkers. From this, one hundred and nine peptides in the 1-25 kDa MF10 fractions of the tear samples were found to alter between DM and DR subjects in comparison to healthy controls. Thirteen of these peptides were sequenced, identified and subsequently validated using an MRM assay developed specifically to quantitate and verify candidate tear peptide biomarkers.

The work presented in this thesis is the first study to identify and profile tear peptide biomarkers which have correlated with the onset of DM and DR. It is envisioned that these biomarkers will form the intrinsic components of a non-invasive diagnostic for DM and DR. Furthermore, this work has established principles for future peptidomic or low abundance protein studies with complex bio-fluids. The work has demonstrated that fractionation is an important part of both biomarker discovery and validation, especially in the context of identifying biomarkers in a complex biofluid such as tears. Coupled with validation through targeted quantitative mass spectrometry, the workflow described is a powerful tool of clinical utility in biomarker discovery and validation.

Table of Contents

List of Figures

List of Tables

Abbreviations

SCGB 2A1	Secretoglobin 2A1
$[M+H]^+$	Singly charged protonated molecular ion
1-DE	One Dimensional Electrophoresis
2-D	Two-Dimension
2-D LC-MS/MS	Two-Dimensional Liquid Chromatography and Tandem Mass Spectrometry
2-DE	Two-Dimensional Electrophoresis
ACN	Acetonitrile
AMBIC	Ammonium Bicarbonate
ANOVA	Analysis of Variance
AUC	Area Under the Curve
CD	Cluster of differentiation
CE	Collision Energy
CHCA	α-cyano-4-hydroxycinnamic acid
CID	Collision-induced Dissociation
CO_2	Carbon Dioxide
Con	Control
cps	Counts per Second
Da	Dalton
DAVID	Database for Annotation, Visualisation and Integrated Discovery
DDA	Data Dependant Acquisition
dH_2O	Distilled Water
DM	Diabetes Mellitus
DNA	Deoxy-ribonucleic acid
DP	Declustering Potential
DR	Diabetic Retinopathy
DTT	Dithiothreitol
EACA	ε-aminocaproic acid
ELISA	Enzyme Linked Immunosorbent Assay
FA	Formic Acid
FACs	Fluorescence-activated cell sorting
FT-ICR	Fourier Transform Ion Cyclotron Resonance
GO	Gene ontology
HFBA	*n*-heptafluorobutyric acid
HPDR	High-Proliferative Diabetic Retinopathy
HPLC	High Performance Liquid Chromatography
iCAT	Isotope-Coded Affinity Tags
ICPL	Isotope Coded Protein Labeling
IDA	Information Dependant Acquisition
IEF	isoelectric focussing
IgA	Immunoglobulin A
IL	inter-leukin
IPG	Isoelectric pH Gradient
iTRAQ	Isobaric Tagging for Relative and Absolute Quantitation

KCl	Potassium
kDa	Kilo Daltons
KH_2PO_4	Potassium Phosphate
kVHrs	kilo-volt hours
LC-MS/MS	Liquid Chromatography-tandem Mass Spectrometry
LDH	Lactate Dehydrogenase
LTQ-FT	Linear Ion Trap Fourier Transform
m/z	Mass to Charge ratio
MALDI-MS	Matrix Assisted Laser Desorption/Ionization – Mass Spectrometry
MALDI-TOF	Matrix Assisted Laser Desorption Ionization – Time of Flight
MDH	Malate Dehydrogenase
MF10	Microflow
min	Minutes
mM	Milli Molar
MO	Macular Odema
MRM	Multiple Reaction Monitoring
mRNA	Messenger ribonucleic acid
MS	Mass Spectrometry
MS/MS	Tandem Mass Spectrometry
MW	Molecular Weight
NaN_3	Sodium azide
NPDR	Non-Proliferative Diabetic Retinopathy
Nsec	Nanoseconds
PDR	Proliferative Diabetic Retinopathy
pI	Isoelectric Point
PMM	Peptide Mass Maps
PRP	Proline rich protein
QQQ	Triple quadrupole
S.D	Standard Deviation
SCX	Strong Cation Exchange
SDS-PAGE	Sodium Dodecyl Sulfate Polyacrylamide Gel Electrophoresis
Sec	Seconds
SELDI	Surface-Enhanced Laser Desorption/Ionisation
sIgA	Secreted Immunoglobulin A
SRM	Selected Reaction Monitoring
TBP	Tri-butyl Phosphate
TFA	Trifluoroacetic Acid
TIC	Total Ion Count
TMT	Tandem Mass Tag
TOF	Time of Flight
Tris-HCl	Tris-Hydrochloric acid
uL	Micro litres
UVB	Ultra violet b radiation
V	Voltage
VIP	Vasoactive Intestinal Peptide

List of Publications

Zhao, Z., Liu, J., Wasinger, V., Malouf, T., **Nguyen-Khuong, T**., Walsh, BJ., Willcox, MDP. Tear Lipocalin is the Predominant Phosphoprotein in Human Tear Fluid. *Experimental Eye Research* Exp Eye Res. 2010 Feb; 90(2):344-9.

Nguyen-Khuong, T., Fitzgerald, A., Zhao, Z., Willcox, M., Walsh, BJ. Improvements for the visualisation of low-molecular weight protein and peptides of human tears using MALDI. *Proteomics* 2008; 8(17):3424-3432

Abstracts

Nguyen-Khuong, T., Wasinger, V., Fitzgerald, AM., Zhao, Z., Willcox, MDP., Walsh, BJ. Identification of Novel Biomarkers for Diabetic Retinopathy in Human Tears. *Human Proteome Organisation (HUPO) World Congress,* Toronto, Canada, 25-30th 2009

Nguyen-Khuong, T., Zhao, Z., Willcox, MDP., Walsh, BJ. Identification of Novel Biomarkers for Diabetic Retinopathy in type 2 diabetes. *Proteomics Symposium* Lorne, VIC, Australia, 7-10th February, 2008

Nguyen-Khuong, T., Willcox, MDP., Walsh, BJ. Low Molecular Weight Analysis of Human Tears; Novel Methods to Characterise Low Range Proteins. *Proteomics Symposium* Lorne, VIC, Australia, 2-4th February, 2007

Patents

Co-Author of provisional patent; Biomarkers for diabetes and diabetic retinopathy in human tears. – 2007

1

GENERAL INTRODUCTION

1.1 Epidemiology of Diabetic Retinopathy

Diabetic retinopathy (DR) is a common complication of diabetes. Following the increase in the incidence of diabetes, DR remains a leading cause of visual loss amongst diabetic patients in developing countries. Within Australia, 15 % of diabetic patients have some form of DR [1-3]. Amongst patients with type 2 diabetes, 22 % had developed DR, whilst 6 % of newly diagnosed patients had developed DR. Recently, studies have shown that retinopathy has a propensity to develop 7 years prior to the detection of diabetes [4-5]. There is no correlation between the prevalence of retinopathy with race, geographical location, gender, age, primary language or income [6].

1.2 Retinal Biology

The retina is comprised of four major cell-types: neurons, microglia, macroglia and microvascular cells. Together they compose a photo-sensitive tissue lining the inner surface of the eye whose primary function is to convert light stimuli into electrical impulses that are transmitted to the optic nerve and subsequently delivered to the brain for interpretation. Neurons (photoreceptors, ganglion, horizontal and amacrine cells) present in all layers of the retina seen in Figure 1.1 are primarily involved in the conversion of light stimulation into electrical impulses. Light enters through from the front of the eye and stimulates the photoreceptors on the outer segments end of the retina near the choroid and pigment epithelium. Electrical signals will travel through to horizontal cells located in the outer nuclear layer (ONL), bipolar cells and amacrine cells located in the inner nuclear layer (INL) and inner plexiform layer (IPL), the ganglion cells (in the ganglion cell layer (GCL)) before travelling through the blood retinal barrier (BRB) for interpretation by the brain. Macroglia (Muller cells and astrocytes) interface the microvascular cells (pericytes and endothelial cells) and the neurons to provide nutritional and regulatory support. Pericytes are smooth muscle cells regularly spaced along the retinal capillaries. As an undifferentiated cell, pericytes possess the capacity to support the vessels and differentiate into various cell types [7]. Together, the cells are arranged tightly to form the BRB. Like most neurons, retinal neurons rely on a stringently controlled homeostasis for normal function [8]. Breakdown of this barrier can introduce neurons to foreign bodies such as autoantibodies or a deluge of ions which disrupt the ion gradients that facilitate electrical signaling of the images received from the ocular region. The integrity of the BRB can be compromised by the onset and development of ocular pathologies such as diabetes mellitus, arterial hypertension or diabetic retinopathy [9-10].

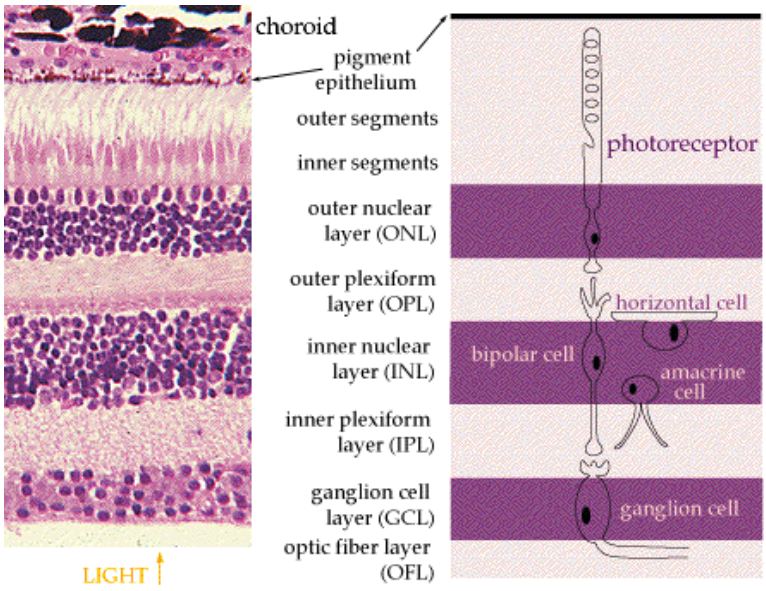

Figure 1.1 Histological and schematic of the structure of the Retina. Cells of the retina are organised into 8 layers. The rod and cone photoreceptor cell bodies, bipolar, horizontal and amacrine cell bodies are present in the inner nuclear layer, ganglion cells reside in the ganglion cell and nerve fibre layers. Images courtesy of http://www.phys.ufl.edu

The retina is integral to vision and involved in the initial processes of converting light signals from external stimuli into chemical and electrical impulses that are sent straight to the brain. Pervading the retina are blood vessels which supply the cells of the retina with nutrients and support. Damage to any of the intricate structures of the retina can compromise vision. Damage can come from a variety of sources such as photomechanical, photothermal and photochemical damage [11]. Damage is also associated with various diseases. Diabetes in particular, is a common cause of damage to the retina. Long duration of diabetes, elevated glycosylated haemoglobin levels, high blood pressure and chronic hyperglycaemia can lead to blood vessel instability. During DR disease progression, blood vessels of the retinal region swell and leak fluid. Eventually this leads to abnormal blood vessel growth, and ultimately cloudy vision or blindness.

1.3 Pathophysiology of Diabetic Retinopathy

There are several clinical signs that accompany the progression of DR. Clinically, progression of diabetic retinopathy can be defined into non-proliferative diabetic retinopathy (NPDR), severe non-proliferative diabetic retinopathy, proliferative diabetic retinopathy (PDR), high-proliferative diabetic retinopathy (HPDR) and eventually, macula

odema (MO) [12]. Currently, each stage can be diagnosed and monitored through inspection with a dilated fundus exam by a healthcare professional.

In the first stage of diabetic retinopathy, NPDR, various molecular events can occur. Tight junctions between adjacent microvascular endothelial cells will leak macromolecules such as lipoproteins, proteins and water [13-14]. The basement membrane of retinal capillaries will thicken thereby decreasing the binding of growth factors important to the structural maintenance and integrity of the membrane. Furthermore, there is a loss of micro-vascular cells around the retinal region of the eye such as pericytes and capillary epithelial cells [12]. At this stage, isolated microaneurysms can be observed in a fundus examination. With the progression of NDPR, the microaneurysms can deteriorate causing venous bleeding in the retinal regions (Figure 1.2). Recent studies established that the inner retinal region (ganglion cell, inner plexiform and inner nuclear layer) of diabetic retinopathy patients is significantly thinner than that of healthy controls [15].

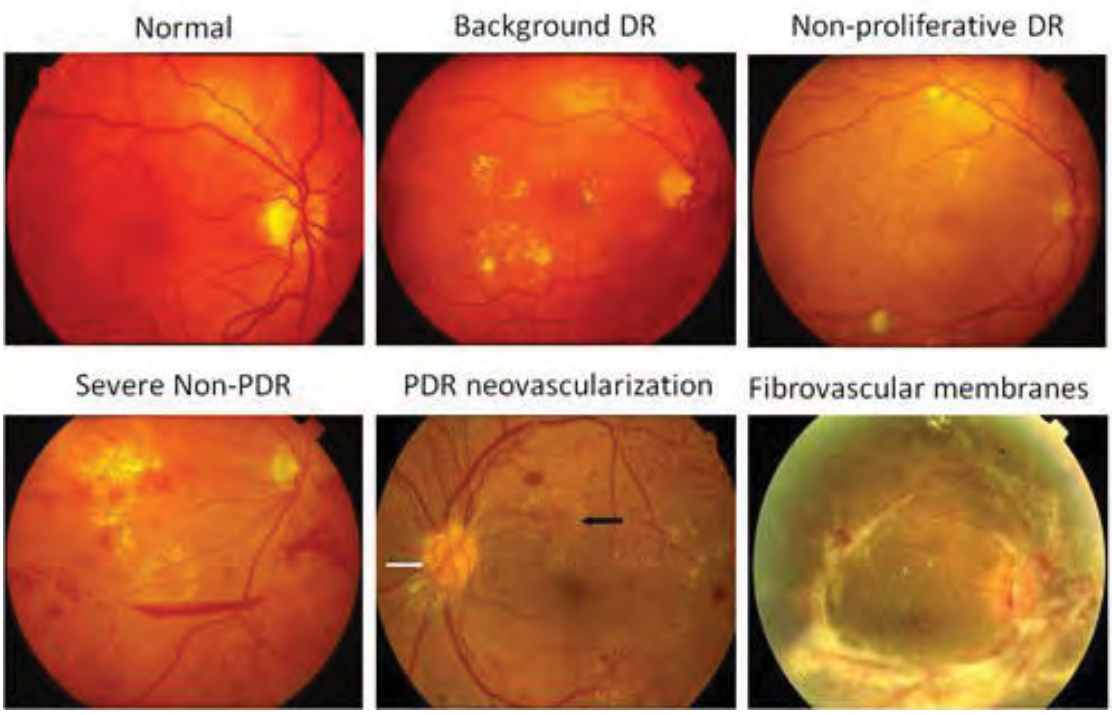

Figure 1.2 Fundus photographs of retinal region charting the progression of diabetic retinopathy. At earliest stage, microaneurysms occur. These develop to larger swellings in moderate non-proliferative retinopathy, where some of the blood vessels that nourish the retina are blocked. With severe non-proliferative retinopathy, a larger portion of blood vessels in the retina are blocked, depriving the retina of sufficient blood supply. During proliferative retinopathy the growth of new blood vessels is promoted. Unfortunately, such blood vessels are abnormal and fragile with propensity to leak blood which will lead to severe vision loss and blindness. http://www.ocularangiogenesis.nl/Images/4stagesDR.jpg

Non-proliferative diabetic retinopathy is an intermediate stage of retinopathy. This stage of the disease is primarily characterised by capillary occlusion which causes ischemia (decreased blood flow, oxygen and glucose) and development of abnormally dilated capillaries. New peripheral vessels or pre-retinal haemorrhages will dominate half of the intraretinal region (figure 1.2). Such vessels form a disorganized network that extends into the vitreous cavity of the eye and has a propensity to haemorrhage [12, 16]. Hypoxia resulting from retinal capillary occlusion will stimulate expression of effectors leading to breakdown of the blood-retinal barrier [16]. At an advanced stage of the disease visual impairment is inevitable. In most cases, vision will blur.

Proliferative diabetic retinopathy is clinically established late in the disease. Neovascularisation events accompanying fibrosis will extend into the structures of the anterior chamber of the eye. These structures will obstruct effusion of molecules from the aqueous humour, elevating intraocular pressure and exacerbating neovascular glaucoma. Vessels will become fibrotic and involute, causing retinal detachment from accompanying fibrous tissue. Visual obstruction and impairment is severe at this stage [17-18].

The final stages of diabetic retinopathy are marked by clinically apparent macular oedema and thus irreparable visual obstruction. Pathologically, plasma leaks from small vessels of the macula. Re-absorption of the fluid elements causes deposition of lipid and lipoprotein components and eventual formation of hard exudates in the macula [17-18].

1.4 Current Therapies

Experimental therapies used to treat various stages of diabetic retinopathy are many and varied. The course of action is dependent on family and medical history. Currently, glucose monitoring and control is sufficient to abate the problems at the early stages of retinopathy. Efficient glucose control can be used to limit hyperglycaemia and modifications to key retinal molecules, which in turn halts degradation to retinal vasculature. Unfortunately, glucose control may prove to be a challenge for various patients, especially when hyperglycaemia is intrinsic to the biology of additional physiologies such as pregnancy, hypertension or puberty [19-21].

Apart from strict glucose monitoring, a lot of therapies of recent interest are designed around the retinopathy biochemistries mentioned. Whilst most of these therapies do generate promising initial results, they are currently preliminary and discussion on their efficacy in treating retinopathy is limited.

For severe retinopathy, laser photocoagulation is usually utilised. Laser treatment results in the regression of new vessels and elimination of hypoxic regions. Various clinical trials support the efficacy of retinal laser photocoagulation for the treatment of DR. In a large controlled clinical trial, the Diabetic Retinopathy Study, 1758 patients exhibiting PDR were randomly selected to receive laser photocoagulation [22]. After 2 years, severe vision loss was observed in 6 % of treated and 16 % of untreated patients. Furthermore, the reduction in severe vision loss was significantly greater than 50% in those that received treatment. Similarly in a separate study, the Early Treatment Diabetic Retinopathy Study, patients with less severe DR were randomly selected for laser photocoagulation treatment [22]. In the 3711 patients selected, early pan-retinal laser photocoagulation reduced the risk by approximately 50% compared to deferral [23]. The results suggest that the benefits are more discernible amongst patients exhibiting high degree of retinopathy.

Patients with advanced retinopathy will benefit from vitrectomy. Vitrectomy is an invasive surgical technique that involves clearing small portions of the vitreous from the front of the eye. Specifically, vitrectomy is used to clear the free bleeding blood vessels or scar tissue as a result of possible retinal detachment or fibrotic vessels that result from advanced stages of diabetic retinopathy [22].

Effectiveness of the aforementioned therapies is dependent on the state of the diabetic retinopathy at the time of diagnosis. Several epidemiological studies demonstrate that glycaemic control remains the most efficacious mode of therapy for DR. The diabetes control and complications trial reported a 76% reduction in diabetic retinopathy and 54% reduction in the progression of retinopathy in patients that underwent glycaemic control [24]. The United Kingdom Prospective Diabetes Study randomized 3867 patients and found that glycaemic control reduced microvascular endpoints by 26% and the need for photocoagulation by 29% [25-26]. As previously mentioned, the Early Treatment Diabetic Retinopathy Study showed that pan retinal- and focal laser photocoagulation reduced severe vision loss by 50% [22]. Via a more invasive technique, 25% of vitrectomy patients

gained better than 20/40 vision as compared to the control group, and this was generally maintained for approximately 4 years [27]. From these statistics, it becomes evident that as the disease progresses, the effectiveness of the therapies aimed to treat various stages of the DR progression is reduced.

One of the main challenges in retinopathy disease management is to generate an efficient diagnostic to detect and monitor the onset and progression of the disease. It has been established that retinopathy has a propensity to develop 7 years prior to the detection of diabetes [4] [5]. Thus, there is a potential that at the time of diagnosis of diabetes, retinopathy may be at a developed stage. Early diagnosis is essential so treatment regimes can be administered before ocular damage is too severe or possibly irreversible.

1.5 Diagnosis

Currently, the diagnosis of DR can be made using a variety of techniques. The challenge, however, is to improve the diagnostic capabilities and possibly identify disease progression prior to any detrimental development of retinopathy. Currently, diagnostic techniques include ophthalmoscopy and surveying fundus photographs; and recent advances to technology have introduced new diagnostic techniques including tomography and oxygenation monitoring.

1.5.1 Direct and Indirect Ophthalmoscopy

Ophthalmoscopy is the examination of the back of the retina using an ophthalmoscope which is an apparatus that uses a series of mirrors and focusing lens to achieve this. Currently, ophthalmoscopy is the most commonly used technique to monitor DR. The sensitivity of most traditional ophthalmoscopy apparati is low compared with the newer seven standard fields (SSFs) photography which has now become the gold-standard for detecting diabetic retinopathy [28]. Recently, new proprietary systems have been introduced to improve diagnosis using various multiple field photography. These systems do achieve high specificity and sensitivity for detecting DR. For example, the Inoveon DR system achieves 98.2% and 89.7% sensitivity and specificity, respectively, in identifying macula oedema requiring referral Clinical evaluation of patients with diabetic retinopathy. [29]. Such high sensitivity comes with high screening costs due to the need for highly skilled technicians, the requirement for expensive and thus inaccessible instrumentation

and also may involve uncomfortable pupil dilation, which can further complicate screening. The specificity is still at a level which means that 1 out of every 10 patients will be incorrectly diagnosed with diabetic retinopathy [4].

1.5.2 Optical Coherence Tomography

During optical coherence tomography, a pair of near-infrared beams from diodes are directed through the pupil of the eye, vitreous, retina and choroid. Any structures will disrupt the integrity of the two beams generating an interference pattern which is detected by a measuring apparatus which determines the optical reflectance and anatomical thickness of the retinal surfaces [4, 30]. Unfortunately, opacities not related to vasculature such as cataracts, corneal opacities, floaters or vitreous haemorrhage can interfere and result in misdiagnosis of diabetic retinopathy. Using optical coherence tomography is therefore an unspecific diagnostic method for diabetic retinopathy.

1.5.3 Retinal Blood Flow, Vascular Leakage and Oxygenation

Diagnostic techniques involving the measurement of blood flow to the retina and oxygenation levels are invasive. These methods are based on the principles of angiography, using a medical imaging technique using a dye tracing method. It involves injection of sodium fluorescein into the vasculature. The migration of the dye through the circulation can be measured and an angiogram is obtained by photographing the fluorescence after a light at wavelength 490 nm is used to illuminate the back of the retina [12].

In one particular method, a Doppler flowmeter is used to aim a laser beam at the blood column in retinal vessels. Doppler shifts in the column of moving erythrocytes are used to quantify the extent of ocular blood flow around the retina. Unfortunately, only one vessel at a time can be measured, usually the largest vessel adjacent to the optic nerve [31].

A scanning laser ophthalmoscope produces a video fluorescein angiogram showing the movement and intensity of fluorescence along the course of the vessel over time. This allows the flow rate of the plasma column in any blood vessel in the photographic field to be calculated [12].

Retinal oxygenation can be measured by intra-retinal oxygen electrodes, an invasive technique. In functional magnetic resonance imaging, changes in oxygenation levels are calculated by comparing retinal oxygenation when a subject is breathing 100% oxygen with breathing 95%/5% CO_2. This method is accurate and is not subject to errors that can be introduced in other methods caused by events and interferences such as free eye movement, blinking and obstructions [32]. Unfortunately, the strategy can be quite invasive, often at the detriment of the patient's comfort.

1.5.4 Caveats to Retinopathy Diagnostic Tests / Improvement to Retinopathy Diagnostic

The availability of a diagnostic technology that can detect the disease early in its development is of great benefit to retinopathy disease management. Ultimately, the role of a diagnostic would be to identify the disease in its infancy at which time, strategies can be implemented to improve the quality of life of the patient. Current modes of diagnostics do not offer much benefit to disease management, because ultimately, these methods of monitoring DR are dependent upon the clinical presentation of DR, at which stage maturation of the disease and possible damage to the retinal tissue is significant.

There are several requirements for a diagnostic biomarker. Biomarkers are endogenous molecules whose presence or metabolism is objectively and directly correlated to a physiological process or disease status [33-34]. It is essential that a biomarker can be detected across different laboratories and technology platforms [33], particularly to clinicians and general practitioners who are at the forefront of healthcare. Therefore, an extensive cost to maintain a diagnostic platform would render the diagnostic ineffective and inaccessible to most patients. Primarily, an ideal diagnostic would detect diabetic retinopathy at an early stage, when disease management and preventative measures such as glycaemic control, would be less intensive and invasive. Finally, the biomarker should be derived from a non-invasive source, not necessarily indigenous to the affected organ. Ideally, tests would be fast and efficient results easily obtained from patients with minimal discomfort.

Currently, there is limited evidence of any genetic influence on diabetic retinopathy, or the presence of a gene which predisposes patients to DR [12]. The best platform to determine biomarkers for a disease is proteomics. Proteins are far more diverse than the genetic

material that encodes them (DNA and/or RNA). This is mainly due to the 100 or so currently characterized post-translational modifications, which can alter the structural information and therefore functional attributes of a protein species [35]. Additionally, fluctuations to biological events such as protein turnover, protease and protease inhibitor activity and post-translational modifications in response to internal and external stimuli do affect the concentration of a protein and peptide species *in vivo.* Unfortunately, information about such post-translational biological events will not be divulged at the genetic aspect of the cell. Thus, protein biomarkers possess the greatest potential for diabetic retinopathy disease management.

Over the last decade, protein biomarkers for ocular diseases have been derived from human tears [36-39]. As a non invasive source, tear fluid is easily accessible. Additionally, tear fluid can come in contact with the epithelium of the eye and thereby come in direct contact with blood circulation and its associated proteins [40]. Thus, variations amongst lower-dynamic range proteins and peptides in the tear film can reflect pathological conditions of, but not limited, to the eye. Clinical evidence detailing tear film instability corresponding with ocular disease is well documented [37, 41-43]. However, as yet, the aetiology and physiological changes that occur within the tear film with the onset of a disease are not as yet well defined.

1.6 The Tear Film

The tear film contributes to the maintenance and integrity of the ocular surface and presents itself as the first barrier of defense in the ocular system. The tear film consists of a complex mixture of ions, small molecules, glycoproteins and proteins whose collective functions are: to maintain a smooth surface for light refraction; lubricate the eyelids, the conjunctiva and the cornea; supply the cornea with nutrients and transport metabolic by-products from the corneal surface; provide white blood cells with access to the cornea and conjunctiva; remove foreign materials from the cornea and the conjunctiva, and defend the ocular surfaces from pathogens via specific and non-specific antibacterial substances [44].

The ocular surface contains a multilayered arrangement of cells distinguished by size and surface characteristics. These cells are organized into distinct domains, based on their junctional arrangements and are innervated by a dense and comprehensive vasculature

network. Nutrients and oxygen are partially supplied by the tear film, secreted by the lacrimal glands, located supertemporally to each eye (Figure 1.3). Through the process of blinking, lacrimal fluid flows through excretory ducts into the ocular space. Tear fluid maintains a moist and smooth optical surface, while dissolved oxygen from ambient air and nutrients present in the tear film diffuse into the nutrient-starved, avascular corneal epithelium.

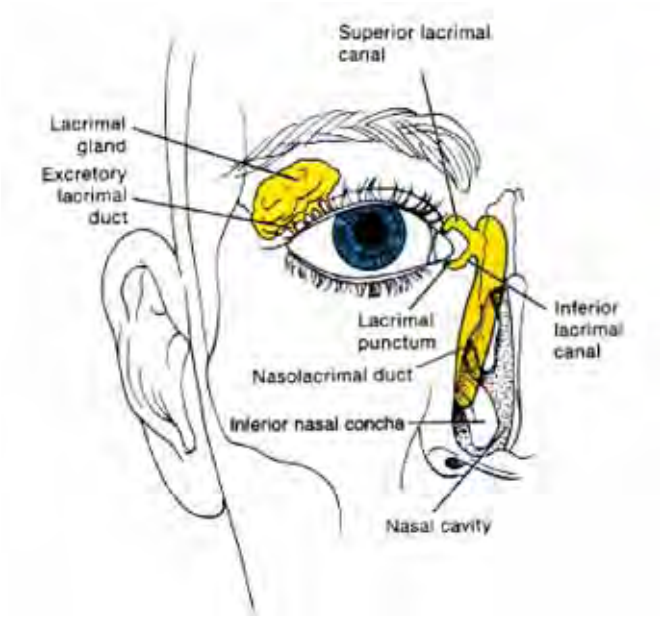

Figure 1.3 Secretion of tears via the Lacrimal gland.

http://www.xenophilia.com/

Water content of tears is altered as it passes through the lacrimal glands. IgA, cellular debris and potassium ions are channeled into the tear film as it filters through various orbs and vasculature networks of the accessory glands, ocular surface epithelia and meibomian glands of the ocular network [45].

Tear fluid pervades surfaces of the corneal epithelium palpebral and bulbar conjunctiva. Residual debris from ocular cells susceptible to desquamation and apoptosis, will channel into the tear film. Tear-asssociated mast cells, non-epithelial cells, secretory cells, meibomian products and accessory proteins leak from the tear film into the local blood circulation [46]. Through blinking, cellular debris and foreign matter are flushed to the caruncle of the eye ultimately destined for elimination [45].

1.6.1 Structure of the Tear Film

As mentioned, the tear film is composed of a complex mixture of ions, small molecules, proteins, lipids and mucins that are arranged in a trilaminar structure. Specifically, this structure is comprised of a superficial lipid layer, intermediate aqueous phase, and an underlying mucosal layer [47] (Figure 1.4).

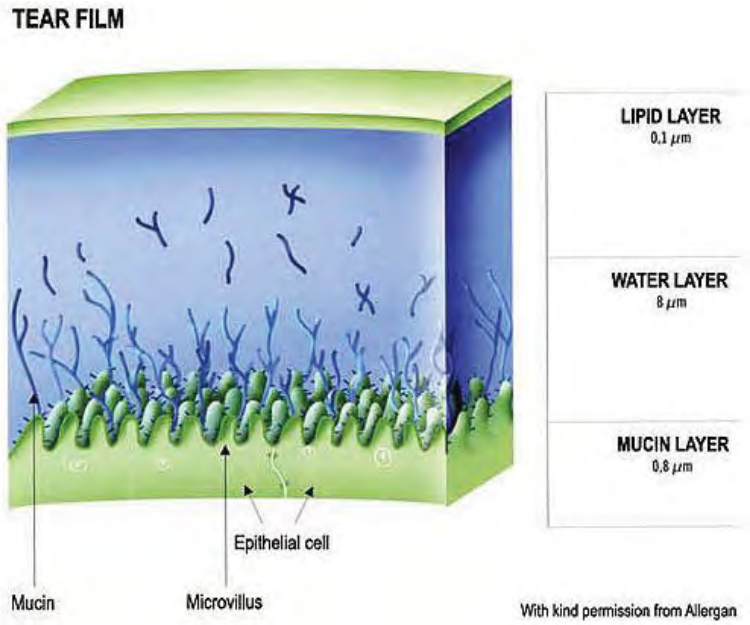

Figure 1.4 Layers of the tear film. http://www.lea-test.fi/

1.6.2 Lipid Layer

The lipid layer is produced by the tubuloacinar meimobian glands embedded in the upper and lower tarsal plates [48]. Secretion is controlled by rich innervation of para- and sympathetic nerve fibres. Through holocrine secretion, meibomian cells and their contents are released into the tear film [49]. The lipid layer acts primarily to retard the evaporation of the aqueous phases and to prevent contamination of the tear film from other lipids which have a propensity to destabilize the tear film [42]. Additionally, the tear lipid layer maintains a strong surface tension, thus structure and integrity of the tear film [50].

The lipid layer is composed of polar and non-polar lipids; a majority of which are wax and sterol esters. The lower dynamic range lipids are free sterols, free fatty acids, hydrocarbons and phospholipids. Such composition confers several properties to the tear

film [51]. For example, lipids will spread well over aqueous phases of tears, and its melting temperature holds around 19-32^{o}C [51]. The lipid layer cannot spread well over saline [52].

1.6.3 Aqueous Phase

Most of the constituents of the aqueous phase are secreted by the lacrimal gland. The lacrimal gland consists of two primary complementary lobes; the orbital and palpebral lobes. The larger orbital lobe empties through two to eight ducts into the conjuntival sac mainly at the upper temporal fornix. Ducts from the orbital lobe will empty into the smaller palpebral lobe. The interstitial tissue of the lacrimal gland is wide-meshed and rich in free cells such as eosinophils, lymphocytes, macrophages and plasma cells. A majority of the affectors of the body's adaptive immune system in tears are derived from such plasma cells, whilst the rest are derived from serum through leakage of the conjunctival vessels which innervate the lacrimal gland and the ocular surface [53].

Activation of tear secretion is controlled by parasympathetic nerves intimately positioned around acinar cells, duct cells and blood vessels. Receptors on acinar cells, once stimulated, induce vasodilation of blood vessels, in turn, increasing secretion [54]. Electrolyte, water and protein secretion is controlled via release of acetylcholine and vasoactive intestinal peptide (VIP). Sympathetic activation of the tear formation occurs through the release of noradrenaline, substance P, an enkephalin family of peptides, calcitonin gene-related peptide and neuropeptide Y [55].

1.6.3.1 **Function**

Constituents of the aqueous phase determine tear pH and osmolarlity and thus the integrity of the proteins and cellular bodies within the tear film. Electrolytes such as potassium, magnesium, calcium, chloride, bicarbonate and phosphate can be found in the tear film [56].

1.6.4 Proteins

A substantial population of tear proteins can be found within the aqueous phase. The relative proportions of proteins present in tear samples will ultimately depend on the method of tear collection [57]. For example, invasive methods exploiting filter paper or

cellulose sponges stimulate the conjunctiva, inducing serum leakage. Thus a higher proportion of serum proteins would be found in analysis.

Akin to serum, the tear film exhibits a wide dynamic range of proteins. Tear specific lipocalin, lysozyme and lactoferrin together constitute 85% of the total protein content in the tear film. Tear lipocalin is an acidic protein and although its function in tears is not fully understood, it does exhibit homology to other members of the lipocalin protein family [58-59]. Generally, lipocalins are capable of binding and transporting an extensive array of endogenous lipid molecules. Thus, it is possible tear lipocalins may be partly responsible for the transport of fatty acid ligands to the outer surface of the tear film, and thus aid in tear film integrity and stability [60].

Lysozyme accounts for 20-40% of the total tear protein content and represents the most alkaline protein in tears [61]. The long chained glycolytic enzyme is produced by lysosomes within cellular ultrastructure. Lysozyme has the ability to dissolve bacterial cell walls through the enzymatic digestion of tissue muco-polysaccharides [54]. The antibacterial properties of lysozyme are only existent in tears, nasal secretions and white blood cells, where the concentration is high. The lysozyme concentration within the tear film will decrease with progression of age and dry eye [62].

Lactoferrin is an iron binding protein produced and secreted by the lacrimal gland. Lactoferrin also possesses antibacterial properties. Its presence in the tear film is elemental to passive transport, together with serum proteins [63].

There are a significant number of lower abundant proteins in the tear film. Recent data suggests the presence of 491 proteins in tear fluid, of which there is a large number of proteases and protease inhibitors [46]. To date there is limited characterization of the endogenous peptides present in tears.

Levels of low abundance proteins and peptides can be indicative of underlying pathologies. For example, the equilibrium between the number of proteases and protease inhibitors in the tears is an indication of the integrity of the tear film and/ or state of disease of the ocular region [46]. On the other hand, the equilibrium of lactate dehydrogenase (LDH)/malate dehydrogenase (MDH) may alter during periods of corneal-

oxygen stress, with increases in LDH observed during sleep, but reduced levels of LDH observed during waking hours [61]. Furthermore, immunoglobulins are present in the tear film in concentrations approximating 20% of the level normally found in serum. Their presence in the tear film reflects changes in ocular conditions and is derived from serum leakage/diffusion from nearby blood vessels. Vital to the eye's innate immunity, immunoglobulins IgE, IgM and IgG are recruited during periods of ocular inflammation and conjunctival stimulation [54]. On the other hand, IgA, the predominant immunoglobulin secreted by the plasma cells within the lacrimal gland, is usually found as an immunological coating of the eye where it can act as the first line of immunological defence. Furthermore, there is a plentiful supply of phagocytic cells within the tear film, recruited usually to protect against organisms and foreign bodies attracted to opportunistic infection of conjunctival blood supply [64].

Protein expression and secretion into the tear film is dependent on the state of the ocular environment. Concentrations of tear proteins such as Immunoglobulin (Ig) M, secretory IgA, polymeric IgA1 and polymeric IgA2 have been reported to decrease upon stimulation implying a constitutive role, whilst concentrations of lacrimal proteins lactoferrin, TSP and lysozyme increasing imply a regulatory role of such proteins [65-66]. Studies have also demonstrated that tear film composition changes during sleep. Closed-eye tears were characterised by higher concentrations of complement proteins such as C1q, C3, factor B, C4, C5 and C9 [67-68]. Such proteins are thought to derive from conjunctival blood vessels during sleep. Changes can also be observed in the tear film after contact lens wear, particularly an increased deposition of tear proteins on contact lens after wear. Such changes tend to suggest a change in the tear film stability innate immunity response so as to counter the oxygen stress-related or pathogenicity of the ocular surface.

1.6.5 Mucous Phase

There are several sources from which constituents of the mucosal layer are secreted. Mucosal constituents are primarily secreted via the goblet cells of the conjunctiva and the crypts of henle in the fornices, whist secondary sources include non-goblet epithelial cells [64]. The pre-ocular tear film is dependent on a constant supply of mucous. The mucosal layer aids in maintenance of an ocular environment suitable for keeping the corneal and conjunctival surfaces in the proper state of hydration [69].

The mucosal layer lubricates the ocular surface. It allows the eyelid margins and palpebral conjunctiva to slide smoothly over each other through blinking and ocular rotational movements [70]. It contains high molecular weight proteins with a high carbohydrate/protein ratio. Glyco-proteins mediate the protection of epithelial surfaces, through coating and removal of foreign bodies and thus protect the cornea and conjunctiva from abrasion. In non-moist regions, mucous can overcome temporary hydrophobicity [64].

1.6.6 Tear Biomarkers

Disease associated biomarkers have been identified in both the lipid and aqueous characteristics of tears. Biomarker discovery in tears can prove challenging due to the small volumes of tears that are collected in a clinical setting [71]. The challenges are amplified amongst lipid biomarkers due to their distinctive long hydrocarbon chains and its resistance to ionization and lack of sensitive analytical methods. Recent studies have characterized the tear proteome, using a combination of sensitive mass spectrometry approaches and proteomic technology [46]. Recently, de Souza, through a combination of mass spectrometry configurations was able to identify 491 tear proteins [46]. Improvements to mass spectrometry sensitivity have not only increased the list of tear proteins, but also increased the potential list of candidate biomarkers for systemic and tear film disease.

Mounting clinical studies suggest that changes in tear film composition paralleled the onset of eye diseases such as dry eye, Sjögren's syndrome, conjunctivitis, blepharitis and other general inflammatory conditions [36-39]. Several biomarkers for non-ocular diseases have been documented, cementing theories that tear biomarkers are not necessarily only indicative of ocular instability. For example, Evans et al., reported a high association of lacryglobin in five different types of cancer – colon, prostate, breast, lung and ovarian [72]. The upregulation of collagen type IX has been associated with the onset of pseudoexfoliation syndrome [73]. Jacob and Ham [2008] reviews the most recent disease associated biomarkers present in tears as tabulated in Table 1.1[74].

Table 1.1 Tear associated protein candidate biomarkers identified in rabbit and human populations. This table was modified from Jacob *et al.,* 2008 [36, 38, 72-73, 75-84]

protein biomarker	Tear Source	Analytical method	marker specificity	regulation	Author
Lysozyme	Rabbit	HPLC-ESI/MS	Corneal Wounding	up	Zhou *et al.,* 2003
lipophilin/B-2 microglobulin/cystatin/heterodimer of lipophilins A&C/Lipophilins CL/Lipocalin/apolipoproteinD monomer/unidentified	Rabbit	1-D SDS-PAGE/MALDI-TOF/ESI-QhQ/MS	Surgically induced Dry Eye	up/down/up/down/up/up/down/up	Ham *et al.,* 2007
Neutrophile defensins NP-1 AND NP-2	Rabbit	SELDI-TOF-MS	Corneal Wounding	up	Zhou et al.,2007
Lacryglobin	Human	1-D/2-D SDS PAGE	cancer	up	Evans *et al.,* 2001
collagen type IX epitope	Human	Western Blot	Pseudoexfoliation Syndrome	up	Assouti *et al.,* 2006
Apo-A1	Human	1-D SDS-PAGE/Western Blot	Diabetic Retinopathy	up	Kawai *et al.,* 2002
Global protein profile	Human	2-D SDS-PAGE	Diabetes Mellitus Type II	up	Herber *et al.,* 2001
serum albulmin precursor/alpha-1 antitrypsin/lacritin precursor/lysozyme/Ig-k chain VIII/prolactin inducible protein/cystatin SA III/pyruvate kinase/unnamed protein	Human	2-D SDS-PAGE/ESI-QTOF	Blepharitis	down	Koo *et al.,* 2005
Lactoferrin/EGF/AQP5	Human	ELISA	Dry eye	down/down/u	Ohashi *et al.,* 2003
proline rich protein 3/proline rich protein 4/Nasopharyngeal carcinoma-associated proline-rich protein/a-1 antitrypsin/calgranulin/unnamed protein/unnamed protein	Human	SELDI-TOF-MS	Dry eye	down/down/down/up/up/down/down	Grus *et al.,* 2005
Ten proteins	Human	SELDI-TOF-MS	Sjorgren syndrome	3 up/7 down	Tomosugi *et al.,* 2005
Cystatins	Human	ELISA	Corneal transplantation	down	ter Rahe BSM *et al.,* 1998
Interleukin 6 and 8	Human	ELISA	Penetrating keratoplasty	up	Fodor *et al.,* 2006
A-defensins (HNP-1, HNP-2 and HNP-3)	Human	SELDI-TOF-MS	Pyterigium surgery	up	Zhou L *et al.,* 2004

Several studies reported changes to bioactive molecules in biofluids other than tears of patients with diabetic retinopathy, such as: prorenin, laminin, prostaglandin E1 and E2 and IL-6 in serum [85-88]; IL-8, IL-10, monocyte chemoattractant protein-1, angiopoietin 2 and vascular endothelial growth factor in vitreous[88-89]; and vascular endothelial growth factor and IL-6 in aqueous humor [90]. The most interesting development so far has been the reports of changes in the tear film of diabetic retinopathy patients, such as tear film break-up time and the Schirmer test [91] where the changes extend to the tear proteome. Herber *et al*., 2001 reported a significantly higher number of tear proteins in patients with diabetes [38]. This was later confirmed by Grus *et al*., (2002), who also reported that while higher molecular weight range proteins were not observed to alter with the onset of diabetes, the most important differences in protein patterns were observed in the 30 – 50 kDa range. However, these protein candidates were not identified [37]. Clinical evidence suggests that relatively minor changes to tear constituents can be introduced from different pathologies which, in turn, will affect ocular health. Kawai identified an increased concentration of apolipoprotein A-1 in tears of patients with diabetic retinopathy using 1D-SDS PAGE coupled with western blotting techniques [78].

Characterisation of the lower abundance proteins and peptides within the tear film significantly remains absent from tear biomarker studies to date. Proteomic and peptidomic characterization is hampered by the presence of higher abundance proteins, which “suffocate” the lower abundance proteins and peptides preventing efficient analysis. To study these peptides, a strategy needs to be put into place to either remove these problematic proteins or enrich peptides from collected tears. This becomes more challenging considering the small volumes of tears able to be collected.

1.7 Proteomics

Proteomics is a field of study that focuses on protein expression, function and interactions in cells, tissues and organisms. The aim of proteomics is to produce an inventory of proteins present in a cell/tissue/organism from which to draw comparisons. Doing so will provide a source of information about the cellular and biological activity encoded in the genome. However, the inherent challenges of proteomic analysis stem from the constant changes in protein stability and abundance within a biological system. For example, cell cycle events affect protein turnover, processing and modifications. The state of these processes will fluctuate with the influence of stimuli from physiological and external

sources on the cellular environment. Post-translational modifications will ultimately affect protein location and stability, making proteome research a complex challenge, which cannot be identified through analysis of the genome alone. Additionally, protein expression and abundance within a cell or organism can vary across at least 10 magnitudes. Thus, a protein of high abundance will be over-represented in any analysis due to the high frequency with which they are detected by instruments.

There are established methodologies which address the challenges behind studying the proteome. The most widely used of such technologies is 2-dimensional electrophoresis (2D-E) coupled with mass spectrometry (MS) identification. However, various modes of chromatography, improvements to current 2D-E methodologies, pre-fractionation techniques, shotgun proteomics and new levels of automation have been introduced in an attempt to garner increasing amounts of proteomic information.

1.7.1 Current Proteomic Paradigm

The current paradigm of most proteomic study centres upon 2-dimensional electrophoresis separation (2D-E) coupled with MS identification. A generic proteomic workflow would comprise six steps: (i) sample collection, handling and preparation; (ii) separation of proteins according to their pI using isoelectric focussing (IEF); (iii) separation of proteins based on their molecular mass (SDS PAGE); (iv) 2-DE protein pattern visualization; (v) 2-DE pattern computer-assisted analysis, and (vi) selection and digestion of protein spots for further MS analysis (Figure 1.5). Variations to any of these steps are essential to adapt a standard proteomic methodology to a specific sample or biomarker study [92-94].

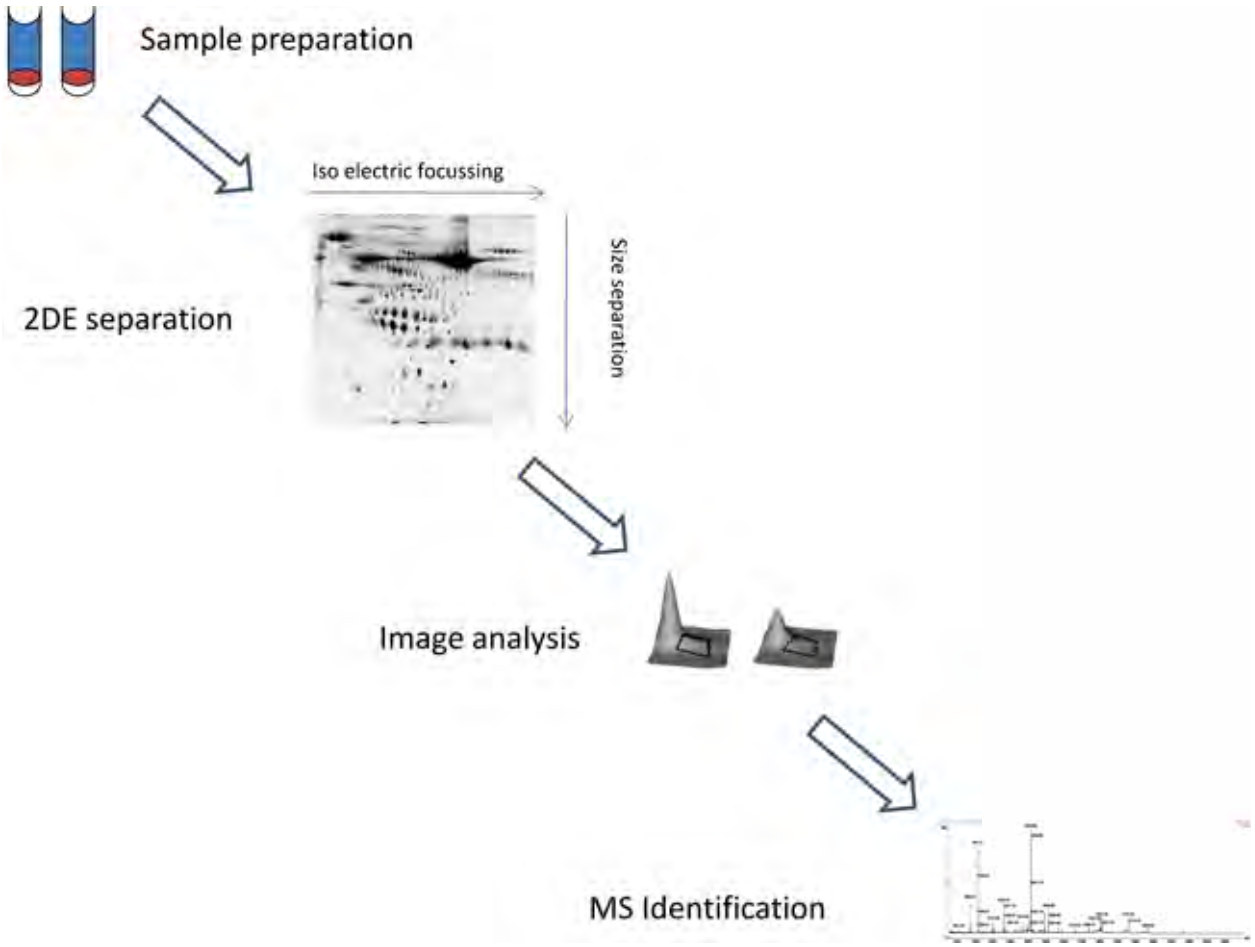

Figure 1.5 Standard proteomic workflow.

One major advantage of the described methodology is the ability to adapt the protocol to suit the type of biological sample at any stage. However, there are important caveats of such established protocols. Firstly, it is essential that samples should be prepared and collected in a way that allows evaluation of biological and technical/experimental variation. Alterations to a protocol can affect protein size, propensity for cleavage, p*I*, charge, substrate affinity and solubilization and therefore affect protein detection, identification and quantification. As such, the issue behind sample availability is emphasized and caution should be practiced against pooling limited samples because no two samples will be identical.

Researchers are becoming increasingly aware of the importance of reducing sample complexity using pre-fractionation techniques [95]. Multiple pre-fractionation techniques can be employed depending on the desired outcome. Proteins within a sample can be

separated into fractions for individual analysis based on characteristics such as size, charge, substrate affinity, solubilization and biochemical reactivity. Additionally, specific proteins can be targeted for depletion or enrichment; highly abundant proteins are often depleted from biofluid samples prior to their analysis to increase the resolution of the low abundance and potentially more informative proteins. Knowledge of the sample of interest is important when determining which type of pre-fractionation technique to employ.

Co-migration of proteins and protein complexes means that generic electrophoretic separation protocols are in some cases inadequate to accurately assess the changes in proteomic profiles between diseases. This is despite the introduction of narrow range IPG strips, and gradient gels. However, higher abundance proteins will be preferentially resolved on most gels. Additionally, hydrophobic proteins and membrane-spanning proteins are notoriously difficult sample to solubilize in an aqueous phase, even in the presence of detergents. As such, their under-representation remains a limitation of 2D-PAGE.

There are two forms of dyes which are used to visualise the protein profile on a 2D-gel so as to detect qualitative and quantitative changes in a biological sample. Each currently available stain has inherent limitations. Colorimetric stains such as colloidal coomassie blue, silver, and zinc or imidazole-zinc staining have a limited range of detection and in most cases are incompatible with mass spectrometry [94]. On the other hand, fluorescent stains such as krypton, deep purple, rubeo, flamingo and sypro ruby have a wider dynamic range of detection. Unfortunately, this stain technology does rely on expensive fluorescent imagers and detectors, which may render the technology out of reach to some investigators. A combination of colorimetric stains and fluorescent stains are often required to visualize and excise proteins of interest from a gel for further analysis.

Image analysis has always been the bottleneck to most proteomic workflows. The ultimate aim of image analysis is to compare and contrast the spatial pattern and relative abundance of the protein spots that have been focused on a 2D-E gel. The onus is on the image analysis software package to rigorously and efficiently detect the spots on a 2D-E gel, match, normalize and quantitate the intensities of the spots. Unfortunately, such a critical stage of a biomarker discovery workflow still requires correction and additional

editing through user intervention [94]. As such, current technology for proteomic related biomarker discovery can prove to be time-consuming and relatively subjective.

In summary, high-variability, user-dependency, low-sensitivity, low resolution of proteins followed by complex and lengthy image analysis processes have been shortcomings of an otherwise mature and commonly used protein separation technique [35], [96]. The multiple steps of a proteomic workflow will inevitably be subjected to errors in sample and equipment management. There is a general trend to move from gel-based proteomics approaches into mass-spectrometry focused strategies, whereby analysis would be centered on various configurations of mass spectrometry such as matrix-assisted laser desorption ionization time-of-flight mass spectrometry (MALDI-TOF MS) [76], surface enhanced laser desorption ionization time-of-flight mass spectrometry (SELDI-TOF MS) [36] and liquid chromatography tandem mass spectrometry (LC-MS/MS) [57]. Furthermore, there is an emergence of shotgun proteomics; a workflow whereby whole samples are analyzed using MS, without user intervention, in an attempt to gain high volumes of objective empirical data without the introduction of operator subjectivity.

1.8 Shotgun Proteomics

Shotgun proteomics or multi-dimensional protein identification technology (MudPIT) is a gel-free proteomic technology that rapidly and comprehensively generates proteomic profiles whilst removing the subjectivity commonly introduced through gel-dependant proteomic strategies. MudPIT involves a biphasic separation of an enzymatically digested sample. The sample is firstly bound and eluted into fractions using a strong cation exchange (SCX) column in the first dimension, before each fraction is further separated on a reverse phase liquid chromatography (RPLC) column in the second dimension that is coupled online to a mass spectrometer [96-98]. Peptides are thus separated based on two orthogonal properties; charge and hydrophobicity. This proteomic platform is readily automated, thus promoting high throughput and generation of vast volumes of data in comparatively short analysis times to that of 2D-E.

However, it must be noted that there are still certain limitations associated with the technology which investigators should be mindful of when conducting a 2D-LC/MudPIT experiment. MudPIT analysis is centered on mass spectrometry and as such, can be affected by the inherent limitations of the technology. Additional limitations include ion

suppression of low molecular weight peptides by larger species and the generation of vast volumes of data which may vary in significance and quality [99]. It is up to the user to efficiently analyse the data, with the assistance of high powered algorithms to differentiate and identify the important ions of interest. Recent developments to the sensitivity and high dynamic range capabilities of mass spectrometers are an interesting development to this area.

As with 2D-E, shotgun proteomics can suffer from issues such as co-elution of peptides in a complex solution and high variability between separations using a liquid chromatography column [100]. In a very complex peptide mixture, there is a higher preference for abundant ions to enter MS/MS fragmentation and identification. In general, low molecular weight species can be missed because: 1) ions elute at a later point in the data dependant acquisition; 2) ions can elute in a varying sequential order and 3) chromatographic elution times are too short. Thus, which ions are subjected to MS/MS appears to be a semi-random process which is dependent on sample complexity, sample resolution, ionization efficiency, ion suppression, scanning speed of the mass spectrometer and dynamic exclusion efficiency [101].

1.9 Quantitation

Mass spectrometry is not primarily quantitative, however, much improvement has been made to enable quantitative comparisons between the proteomes of multiple biological samples.

Initially, quantitation involved relative measurements using isotopic labeling of a pair of biological samples, such as comparison of O^{14}/O^{16} peaks within a pooled sample. This would require a biological sample to be labeled *in vivo.* Thus it was restricted to cultured cells grown under regimes intended to supplement their nutrients with isotopes. The areas under a peak in a mass spectrum would be calculated post-mass spectrometry analysis [93, 97, 102].

Isotope-coded affinity tags (iCAT) is a form of quantitative proteomics which involves labeling peptide species *in vitro*. ICAT labels are composed of a reactive group, with an affinity for cysteine, attached to an isotopic linker with either eight hydrogen atoms (light tag) or eight deuterium atoms (heavy tag) and a biotin tag. Samples to be compared are

labeled *in vitro* with heavy or light tags, pooled and the relative abundances assayed using MS, with subsequent identifications through MS/MS [92, 103]. Unfortunately, the limited affinity of the iCAT tag for only cysteine residues inhibits a comprehensive analysis of a sample's proteome.

The iTRAQ^{TM} (isobaric tag for relative and absolute quantitation) labeling system (Applied Biosystems) is a variation of iCAT in which different sized reporter ion tags with an affinity for amine residues are used to label proteins [104-105]. This improves the labeling efficiency. As eight different tags are available for use with this technique up to eight different biological samples can be analysed at any one time. The samples are pooled and analysed using a standard MudPIT workflow. Changes in abundance of any peptide are reflected in the relative abundance of the isobaric tags displayed with the MS/MS spectra [106]. However, the expensive nature of the dyes renders the technology inaccessible to many proteomic researchers.

More recently, relative quantitations have been performed in the absence of labeling. Analysis is usually performed post-MS analysis using either spectral counting strategies or algorithms which compare ion intensities between samples known as peak integration. The advantage which these technologies have over labeling quantitation is the wide dynamic range which is possible to analyse through this strategy. Additionally, it avoids the inefficiency of chemical labeling that can misrepresent the actual quantities of proteins and peptides within a biological sample. For these reasons, label-free technology is becoming increasingly popular and has been used to characterise differential expression in synapses [107], biomarkers for Down's syndrome in maternal serum [108] and preterm birth in human cervical-vaginal fluid [109].

Non-labeling quantitation is a semi-quantitative platform which correlates mass spectral information to abundances of a peptide or protein. Spectral counting, involves searching the collection of MS/MS spectra against a database such as MASCOT or SEQUEST. Spectral counting then operates on the assumption that the quantity of a protein is correlated to the number of spectra identified for that particular protein [110]. With peak integration, peptide signals are detected at MS level and differentiated from chemical noise through their characteristic isotopic pattern. The patterns are compared across retention time and monoisotopic mass (m/z). The total ion current of the peptide signal is integrated and used

as a quantitative measurement of the peptide [111]. Subsequent identification is then obtained using MS/MS data associated with the file generated from the same run [110].

Peak integration does afford the researcher significant advantages. As changes are dependant at the MS level, any unidentified peptides of interest which do not survive the duty cycle of the mass spectrometer, can be identified through the use of an inclusion list and re-injecting the sample back into the instrument. On the other hand, spectral counting with low abundance proteins and peptides produces few spectra leading to small numbers that are often unreliable. All spectra in the analysis are the product of those precursor ions which have survived the duty cycle of the mass spectrometer, which itself can be an unreliable source of selection [110].

As with most of these approaches, replicate analysis and sensitivity to instrument setup is a very important issue. Multiple replicate analyses are emphasised for statistical relevance and to avoid random sampling errors. This is essential with complex samples, whereby a multitude of peptides can overwhelm instrument capacity, impairing efficient sequencing of all peptides. Furthermore, peak-integration analysis algorithms such as Decyder MS (GE Healthcare) or Progenesis LC-MS (Nonlinear) rely heavily upon MS chromatograms from experiments. Thus, changes in any of the alignments and assembly of chromatography-MS setup will ultimately alter any empirical data derived from such workflows [93].

1.10 Peptidomics

Like proteomics, peptidomics is a field of study centred on the expression and function of peptides in cells, tissues and organisms [112-113]. The existence of peptides in a sample extends from bioactive molecules to products of protein degradation, protease activity or other biological metabolic processes [112]. Many peptides are bioactive molecules that mediate cellular communications such as hormones and neurotransmitters [114]. Peptide maturation, activation, and degradation emphasize the intrinsic link between the peptidome and proteome; the equilibrium between both is regulated and counter-regulated by proteases and protease inhibitors. Therefore, diverse roles in key regulatory processes accentuate a need to improve peptide discovery.

Peptidomics is a relatively new concept. The advantage of peptidomic study is that most of the principles affiliated with proteomic technology do apply to peptidomic workflows.

However, this is all that the two technologies have in common. Whereas it is not necessary to identify all the peptides in the sample in order for a protein to be identified in proteomics, this is not true of peptidomics. The success of a peptidomic study relies heavily upon the ability to isolate and enrich the peptides in a sample [112, 115]. Before engaging in a peptidomic experiment, one must consider several principles.

In comparison to proteins, endogenous peptides represent a lower abundant class. Importantly, peptides suffer from artifacts caused by endogenous proteolytic degradation [112]. To preserve the integrity of endogenous peptides, it is preferable to conduct sample preparations at low temperatures and in the presence of protease inhibitors designed to suppress proteolytic activity [112]. However protease activity and its artifacts can be a contributing factor to various diseases and their progression, thus, it may not be necessary to use protease inhibitors in biomarker studies.

Fractionation is an important consideration in peptidomic studies. In fractionation, endogenous peptides are separated from higher abundance species, thus preventing co-elution with larger proteins whose signals can mask that of the peptide. It would be advantageous if the fractionation technology used were also involved in enriching the peptide fraction to be analysed. Such examples of fractionation techniques may include various modes of chromatography such as strong cation exchange, reverse phase liquid chromatography, affinity chromatography or size exclusion [112, 116]. The availability of smaller and cheaper pre-packed chromatography columns with the aforementioned chemistries has streamlined peptidomic strategies. New fractionation instruments such as the microflow (MF10) have also contributed a great deal to fractionation technology and will be discussed later in this chapter.

Mass spectrometry was intrinsically designed for the identification of peptides. Efficient sample preparation, fractionation and enrichment of peptides render mass spectrometry identification highly accurate and definitive. There is an important caveat inherent with database searching using mass spectrometry data as there are computational problems in predicting unpredictable cleavage sites. Spectra are usually searched using algorithms such as SEQUEST and MASCOT. Such programs are biased to tryptic residues. As such, the researcher must take into account that enriched peptides might not carry either lysine or

arginine residues that are necessary for tryptic digestion. As such, most peptides do not necessarily bear basic –COOH termini, making identification difficult.

1.11 Microflow MF10

The MicroFlow MF10 is an apparatus which employs the principle behind membrane electrophoresis established by Horvath *et al*., 1994 [117]. Separation occurs in a buffered system whereby a protein's amphoteric nature determines its propensity to migrate from anode to cathode under an electric field. Proteins can be separated during the run either by size using multiple sized membranes or through its charge and mobility using unrestricted sized membranes. With the MF10 system, low volumes of samples can be separated [118]. Up to 6 fractions can be generated using multiple sized polyacrylamide membranes ranging from 1 kDa to 500 kDa. Furthermore, separation cartridges are designed to permit fractionation of two separate samples simultaneously, Figure 1.6. Recent preliminary results have seen the MF10 applied to a series of samples such as plasma and urine [118].

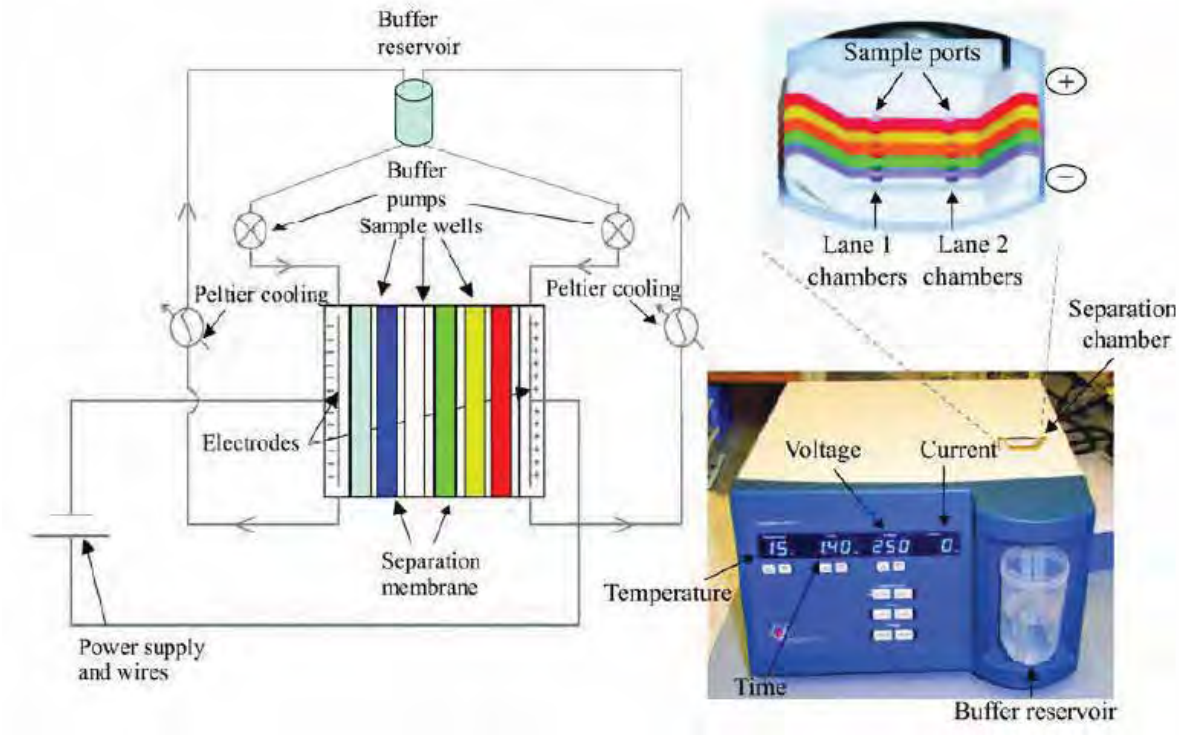

Figure 1.6 Schematic diagram of the MF10 instrument. The instrument has an internal cooling system that reduces heat of the running buffers. Buffers around the separation

membranes are sourced from the buffer reservoir, whilst buffers between the membranes are manually injected into the sample ports. Buffers facilitate the current and migration of the charged species through the chambers. Membranes can constitute up to 6 chamber designs. This diagram was modified from Wasinger *et al.*, 2008 [118].

1.12 Validation using MRM

There is an increasing need to validate biomarkers identified through the discovery phases. The current accepted paradigm of validation centres around antibody based arrays such as ELISAs, FACs, Western Blotting or tissue microarrays. Unfortunately, such strategies are expensive in terms of time, reagents and effort to produce high-quality antibody assays to test a collection of biomarkers. Limitations are further exacerbated by the difficulties of generating antibodies, particularly for novel biomarkers [119].

Multiple Reaction Monitoring (MRM) or Selected Reaction Monitoring (SRM) is a MS-based technique that presents a compelling solution to verify and validate disease-associated biomarkers. MRM exploits the capabilities of a triple quadrupole (QQQ) to measure the absolute or relative quantity of the targeted peptide. MRM requires knowledge of the analytes molecular weight and fragmentation behaviour under CID. In MRM, the first quadrupole of the instrument selects the precursor ion of interest to be fragmented in the second quadrupole by collisional excitation with a neutral gas in a pressurized collision cell. The product ions are detected and monitored for quantitation in the third quadrupole. The product ions or transitions characteristic of the precursor ion are monitored over time yielding chromatographic traces with retention time. Chromatographic traces of each transition are compared between samples [120].

1.13 Aims

An efficient diagnostic is required to detect and/or predict the onset and development of DR prior to any significant damage to the retina. As a characteristic of the disease, biomarkers are an integral constituent of diagnostics. Indigenous to the ocular region, tears are a potential source of non-invasive molecular markers for the ocular disease. Indeed, many disease associated biomarkers in tears have been described. Proteomics and peptidomic technology offer an optimistic chance to investigate the potential biomarkers in tears for diabetic retinopathy.

It was the aim of this candidature to investigate through proteomic and peptidomic workflows the presence and profile of protein and peptide molecular markers associated with DR. Several aims were addressed:

1. To develop a tear fractionation protocol from which biomarkers can be successfully derived. This was accomplished via a series of experiments:
    a. Analysing tear samples with 2-D electrophoresis.
    b. Analysing tear samples with 2-D LC MS/MS.
    c. Developing pattern-based MS monitoring using MALDI-MS.
    d. Fractionation of tear samples using spin filters.
    e. Fractionation of tear samples using Microflow MF10 fractionator.
    f. Quantitation of low abundant tear proteins and peptides via labelling strategies such as iTRAQ.
    g. Quantitation of low abundant tear proteins and peptides via non-labelling strategies using peak integration (Decyder MS and Progenesis LC-MS) and spectral counting (Scaffold).
    h. Addressing the benefits and limitations of each technology and its application to identify disease associated candidate biomarkers in human tears.

2. Application of tear fractionation protocol to characterise tear biomarkers associated with Diabetes Mellitus and Diabetic Retinopathy. This was accomplished through several phases
    a. Collection of tears from healthy controls, patients with diabetes without diabetic retinopathy and patients with diabetic retinopathy.
    b. Fractionation of tears using MF10 fractionation.
    c. Fragmentation and analysis of tear peptides using LTQ-FT MS.
    d. Non-labelling quantitative analysis and peptide profiling using peak integration.

3. Validation of candidate biomarkers using Multiple Reaction Monitoring. This was accomplished through several tasks:
    a. Development of sample processing technique to fractionate tears suitable for MRM.
    b. Development of MRM assay to quantitatively monitor the profiles of molecular markers.
    c. Validation of candidate biomarkers using MRM assay and statistical analysis.

It is hypothesised throughout this study that changes to the peptidomic population of tears would correlate well with the onset of DM and DR in its early stages.

2

GENERAL MATERIALS AND METHODS

This chapter describes the general methods and methods commonly used during this study. The procedures exclusive to a particular chapter are described accordingly in the relevant chapter.

2.1 Materials

All chemicals were from Sigma-Aldrich (St. Louis, Missouri, USA) unless stated otherwise.

Tributylphosphine (TBP), Precision plus Protein standards, were obtained from Bio-Rad (Hercules, CA, USA). MF10 polyacrylamide membranes and cartridge holders were obtained from Nusep (Lane Cove, Sydney, Australia). *n*-heptafluorobutyric acid (HFBA) was purchased from Pierce (Rockford, Illinois, USA). Sequencing grade modified trypsin was purchased from Promega (Madison, WI, USA). iTRAQ® reagents were purchased from Applied Biosystems (Foster City, CA, USA), Ultrapure water to prepare buffers and solutions was produced using an arium ultrapure water system (18Ω) from Sartorius (Aubagne, France).

2.2 Ethics Approval and Details

Ethics was approved by the South Eastern Sydney Area Health Service for collection of tears from the Diabetes Clinic at Prince of Wales Hospital. Additionally, ethics was approved for the collection of tears with the Xian Hospital, Xian; Wenzhou Hospital, Wenzhou, Peoples Republic of China. Informed consent was obtained from each of the participants and the study was performed in accordance with the guidelines of the Declaration of Helsinki.

Patient data including stage of diabetes, diabetic retinopathy and supplementary data such as body mass index and medication was collected.

2.3 Tear Collection and Storage

Sample collection was performed with the subject seated looking straight ahead (primary gaze position). The subject's head was tilted towards the shoulder ipsilateral to the eye used for sample collection was advised to facilitate tear flow (Figure 2.1). Tears were routinely collected from one of the two eyes, and the choice was usually made by the

subject; if a greater volume of tears was needed than able to be collected from one eye then they were also collected from the other eye.

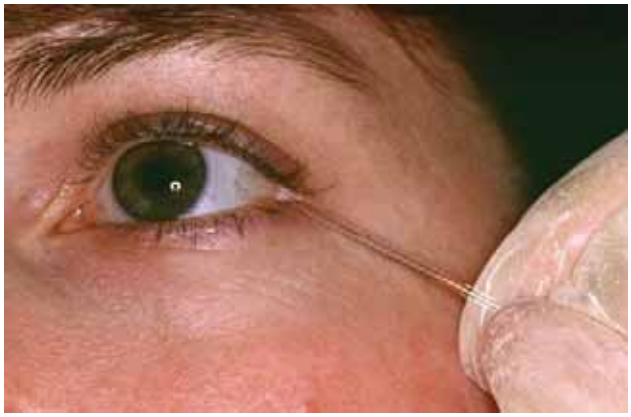

Figure 2.1 Tear sample collection. The subject was seated looking straight. A 10 µL microcapillary tube was placed on the outer canthus of the eye and tears were collected via capillary action.

A 10 µL micropipette (Blaubrand Intramark, Wertheim, Germany) was applied to the lower lid margin, close to the lateral canthus, using the index finger and thumb of the right hand for the right eye (vice versa for the left). The index finger, as well as 2-3 fingers of the other hand was used for immobilization of the subjects head and gentle retraction of the lids whenever needed. The intention was to fill the micropipette up to the black line (10 uL) of the micropipette, though this was not achieved at all times (mainly in patients with dry eyes).

A small manual pump was used to expel the tears from the micropipette into a 0.5 ml Eppendorf tube. Care was taken in all cases not to allow the used micropipette to come into contact with anything before and after transferring the sample into the Eppendorf tubes. The tube lids were closed, labelled and put on ice in an ice bucket. In most of the cases parafilm was used to seal the tube after labelling. Tubes were then stored at -80°C until required for use.

2.4 Acetone Precipitation

Cold acetone (-20^{o}C) was quickly added to the sample to be precipitated in a ratio of acetone: sample of 9:1. The sample was incubated at -20^{o}C for 1 ½ hours and was then centrifuged in a 5840R centrifuge (Eppendorf AG, Hamburg, Germany) at 11 000 x *g* for 15

minutes at 4°C. After centrifugation, the supernatant was discarded and the pellet was air-dried for 15 minutes before being frozen at -20 °C unless stated otherwise.

2.5 Protein quantitation using Fluoroprofile™

A Fluoroprofile™ protein quantitation kit (Sigma Aldrich, St Louis, MO, USA) was used to determine the protein concentration of tear samples prior to MF10 fractionation. The assay was performed according to the manufacturer's instructions with epicoconnone and bovine serum albumin used as standards. Briefly, a serial dilution of the standards and samples was prepared in 0.1% SDS. The Fluoroprofile™ Fluorescent reagent, Quantitation buffer and ultrapure water were mixed in a 1:1:8 ratio. This preparation was added to the protein standards and tear protein samples in equal volumes and allowed to incubate at 4°C in the dark. The fluorescent intensities of the analytes were measured using a BioRad Pharos FX™ Plus Molecular Imager (Bio-Rad, Hercules, CA, USA) using the Quantity One program (Bio-Rad). The analytes were measured at excitation 510 nm and emission of 620 nm.

2.6 Electrophoresis

2.6.1 Isoelectric Focussing

Isoelectric focussing (IEF) for 2D-E was performed using 11 cm linear immobilized pH gradient (IPG) strips over the pH 4-7 (Bio-Rad) or pH 6-11 (GE Healthcare, Uppsala, Sweden) range. All samples were focused using active rehydration. MiPrep M 400 lypholised rehydration buffer (Minomic Int'l' Ltd, Frenchs Forest, Australia) was reconstituted with 200 µL of ultrapure H_2O. The IPG strips were rehydrated with 250 µL of this solution for a minimum of 6 hours.

An aliquot of tears was combined with 40 µL of reconstituted MiPrep M (which contains DTT for protein reduction) and incubated at room temperature for 30 minutes. Two and a half microlitres of 25% acrylamide was then added to alkylate the proteins and the preparation was sonicated for 15 minutes before focussing.

IEF was performed using an IPGphor™ Isoelectric Focussing System (GE Healthcare). Briefly, rehydrated IPG strips were placed inside the strip holder. Electrode wicks were placed at each end of the strip and the electrode were positioned on top of the wicks.

Cups were then placed securely at each end of the IPG strip and half of the sample was loaded into each cup before mineral oil (Shell Oil Company, Houston TX, USA) was poured along the strip holders and within the cups to prevent the strips and sample drying out during focussing. IEF was then run according to table 2.1. After completion, strips were removed, drained of oil and frozen for 1 hour at -20^{o}C.

Table 2.1 IPGPhor^{TM} IEF running conditions at 20^{o}C

Current (uA/Strip)	Step	Voltage (V)	Time (Hour/s)	Minimum Total kVHrs
100	1- Step and Hold	100	2	50.3
	2- Step and Hold	300	3	
	3- Step and Hold	600	2	
	4- Step and Hold	1000	2	
	5- Step and Hold	2500	1	
	6- Step and Hold	3500	1	
	7- Step and Hold	8000	5	
	Hold step	100	10	

2.6.2 SDS -polyacrylamide Gel Electrophoresis (SDS-PAGE): 1-D and 2-D Applications

1-D gels: 2X sample buffer (Table 2.2) was added to each sample in a 1:1 volume ratio and boiled for 5-10 minutes. Samples were centrifuged at 24,000 x *g* for 5 min and 20 µL was loaded into each well of a Tris-glycine Criterion gel (Bio-Rad) for electrophoresis.

Table 2.2 2X concentrated sample buffer (Brackets designate final concentration)

Sample Buffer	Final Concentration	Volume (mL)
Tris-pH 6.8 stock	0.25 M	1.0
Glycerol	10% (v/v)	0.8
20% SDS	2% (v/v)	0.8
2-β-mercaptoethanol	10% (v/v)	0.4
Bromophenol Blue (to colour)		0.2
Ultra pure H_2O	-	To 4mL

2-D gels: IPG strips that had been frozen for 1 hour were reduced and alkylated by incubating first in reduction buffer (Table 2.3) for 15 minutes and then in alkylation buffer (Table 1.3) for a further 15 minutes. The reduced and alkylated strips were placed on a Tris-glycine Criterion gel (Bio-Rad) and precision protein marker (Bio-Rad) (7 uL) was added to the designated lane. To hold the strips in place molten agarose (0.5% agarose made up in Tris-glycine running buffer, see Table 2.4) was poured over the strips and left to set.

Table 2.3 Reduction and alkylation solutions

	Reducing solution		Alkylation solution	
Reagents	Final Concentration	Amount	Final Concentration	Amount
Urea	6M	36g	6M	36g
SDS	2%	2g	2%	2g
5X Tris/HCl gel buffer	1X	20mL	1X	20mL
50% glycerol	20%	40mL	20%	40mL
DTT	65mM	1g	-	-
25% Acrylamide solution	-	-	2.50%	10mL
Ultrapure H_2O	To 100ml		To 100ml	

Gels were placed in a Dodeca cell (Bio-Rad) containing 1X running buffer (Table 2.4). Electrophoresis was carried out for approximately 70 minutes at 200 V. Electrophoresis

was completed when the tracking dye (bromophenol blue) reached the bottom of the gel. Gels were removed and proteins were fixed with fixative (10% methanol, 7% acetic acid, ultrapure H_2O) before being stained for protein visualization.

Table 2.4 Tris/Glycine/SDS (1X) running buffer, pH 8.3

buffer reagents	final concentration	Amount (g)
Glycine	192 mM	14.4 g
SDS	0.1%(v/v)	1 g
Tris base	24.8 mM	3 g
Ultrapure H_2O	-	To 1L

2.6.3 Protein Visualization

After fixing, gels were stained using Sypro Ruby (Bio-Rad) overnight before over-staining with Coomassie Brilliant Blue. Briefly, gels were incubated with 50 mL of Sypro Ruby (filtered through Whatman number 1 filter paper to remove any dye particles) overnight. Sypro stained gels were destained for of minimum of 2 hours using fixative. Images of the Sypro stained gels were taken using BioRad Pharos FX™ Plus Molecular Imager (Bio-Rad). The analytes were measured at excitation 532 nm and emission of 620 nm.

Following imaging, gels were then stained in approximately 100 mL Coomassie Brilliant Blue G-250 (Table 2.5) and subsequently destained with 7% (v/v) acetic acid. All gels were stored and sealed in plastic bags kept at room temperature until further use.

Table 2.5 Colloidal Coomassie Brilliant Blue G-250 for Visualisation

reagents	amount	final concentration
Ammonium sulfate	340 g	17%
Phosphoric acid	60 mL	3%
Coomassie G-250	2 g	0.10%
Methanol	680 mL	34%
Ultrapure H_2O	make up to 2 L	

2.6.4 In-gel Digestion and Sample Preparation for LC-MS

Protein gel bands of interest were excised from Coomassie Brilliant Blue stained gels and washed three times in ultrapure water for 5 minutes with removal of water between each wash. Gel pieces were then further washed for 10 minutes in 100% acetonitrile (ACN) with enough volume to cover the gel piece in order to remove any remaining Coomassie Brilliant Blue. ACN was removed and the sample was dried completely in a vacuum centrifuge (CentriVap, Labconco, Kansas City, USA). Gel pieces were re-swelled at 4^{o}C for 45 minutes with 5-8 µL of 50 mM ammonium bicarbonate (AMBIC) buffer containing trypsin (5 ng/ul). This incubation was continued overnight at 37^{o}C.

Proteins were extracted with a 20 minute wash with 20 mM AMBIC followed by 3 x 20 minute washes with 5% (v/v) formic acid (FA) in 50% ACN. Supernatant containing extracted peptides was removed and pooled after each wash. Pooled supernatants were dried completely in a vacuum centrifuge. Samples were cleaned using StageTip cleanup (Section 2.8) prior to analysis with LC-MS/MS.

2.7 MF10 Assembly and Fractionation

MF10 fractionations were performed using a 4- chamber assembly. Chambers were assembled using 2.7 x 2.2 cm polyacrylamide membranes with varying pore size limits. These membranes were washed twice with ultrapure H_2O and then twice with 1X Tris-ε-aminocaproic acid (EACA)/Urea buffer (90mM Tris (hydroxymethyl) aminomethane, 10 mM EACA, 4M Urea). The lines of the MF10 were washed with ultrapure water followed with a 10 minute wash with 1X Tris/EACA/Urea buffer. All samples were also prepared in

this buffer such that the final volume and concentration would be 140 µL and 1X Tris/EACA/Urea buffer, respectively. Furthermore, 1X Tris/EACA/Urea buffer was used as a circulating buffer.

Cartridges were assembled according to schematic diagram in Figure 2.2. Briefly, cartridges were placed in increasing sizes from the anode to the cathode. The 5kDa membranes were placed at both cathode and anode so as to filter out any low molecular weight charged contaminant molecules in the sample during fractionation.

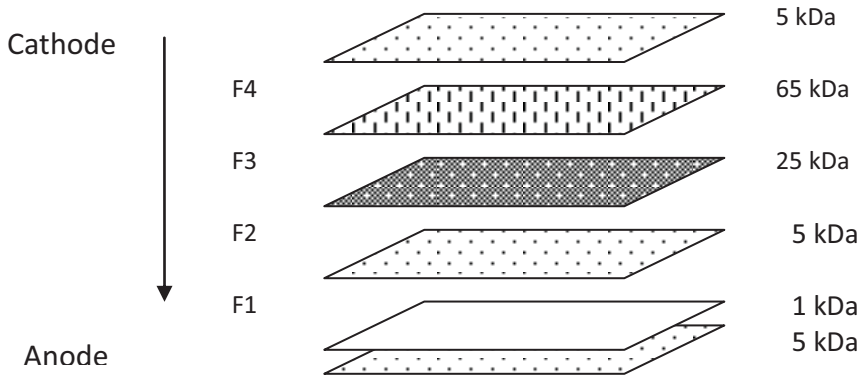

Figure 2.2 MF10 Chamber assembly for size fractionation. A four chamber system was defined by 5 cartridges. 5 kDa membranes were placed at the end of each assembly so as to filter the charged contaminants.

Each 140 µL sample was loaded at the cathode end of the apparatus between the 5 kDa and the 65 kDa membranes. Additionally, Tris/EACA/Urea buffer was added to the remaining chambers. Fractionation was performed at 50 V for 30 minutes and then at 200 V for 2 ½ hours. On completion, samples were collected from the chambers using gel loading tips. Fractions F3 and F4 (Figure 2.2) were removed and acetone precipitated whilst F1 and F2 were concentrated and desalted with C18 chromatography prior to analysis with LC-MS (see section 2.8).

2.8 Sample Preparation for LC-MS

Samples of interest were acidified to ~ pH 3 using appropriate volume of formic acid. C18 StageTips^{TM} (Proxeon) was initialized with 20 µL 80% ACN/5% FA in dH_2O (v/v) and equilibrated with 20 µL 5% FA in dH_2O. Samples were passed through the StageTips in 20 µL aliquots before the tip was washed twice with 20 µL of 5% FA in dH_2O (v/v). Peptides were eluted with 40 µL of 80% ACN/5% FA in dH_2O (v/v) into a clean 1.5 mL polypropylene

tube. The samples were then dried completely in a vacuum centrifuge and frozen at -20°C until further use.

2.9 In Solution Tryptic Digestion for LC-MS/MS

Lypholised protein samples were reconstituted with 25 µL of 50 mM AMBIC (pH 8). Trypsin was added to a final enzyme:protein ratio of 1:100 (w/w). The preparation was incubated at 37°C overnight. Reaction was stopped by acidifying the preparation to ~pH 3 using neat FA. Samples were then completely dried in a vacuum centrifuge and frozen at -20°C until further use

2.10 Label-Based Relative Quantitation

2.10.1 iTRAQ Labelling

One hundred micrograms of total protein as determined by total protein assay (Fluoroprofile™ see section 2.5) was precipitated using acetone precipitation (as per section 2.2). A 20 µL aliquot of dissolving buffer (Table 2.6) was added to each sample. The samples were vortexed continuously for approximately 5 min before being sonicated for 2-3 min.

Table 2.6 Dissolving buffer for iTRAQ labelling

Sample buffer	volume
Ultrapure H_2O	300 ul
Sodium biocarbonate (500 mM)	30 ul
2% SDS	15 ul

The samples were reduced using 2 µL 200mM tris-(2-carboxyethyl) phosphine (TBP) and the samples were incubated at 60°C for 60 minutes. Samples were then alkylated with 1 µL of iodoacetimide (200 mM). The samples were vortexed and centrifuged down briefly and incubated at room temperature for 10 minutes. Ten microlitres of reconstituted trypsin (0.4 ng/µL in ultrapure H_2O, Promega) was added to each sample and incubated overnight at 37°C.

Samples were centrifuged briefly and the pH was tested with a pH strip (Merck, Darmstadt, Germany). The pH was adjusted by adding 2.5-4 µL of sodium bicarbonate (500 mM) until the pH was basic (~pH 8). iTRAQ reagents were removed and allowed to reach room temperature. To each vial, containing a reporter mass (114, 115, 116, 117), 70 µL of ethanol was added and centrifuged briefly. The entire contents of one reconstituted reporter mass iTRAQ reagent vial was added to each sample. The samples were vortexed, centrifuged briefly and incubated at room temperature for 1 hour. Samples were then combined, vortexed and centrifuged briefly.

Samples were cleaned using cation exchange and C18 cleanup. Solutions were delivered through the C18 and cation exchange cartridges using a 5 mL S.G.E syringe. A uniform flow was applied by attaching the syringe to a syringe pump. A cation exchange cartridge (200 µL cartridge containing POROS^{TM} resin 50 HS 50 um particle size (4.0 mm X 15 mm) was washed with clean buffer (Table 2.7), followed by 2 mL of cation exchange load buffer. The flow through of all buffers was discarded. The sample was diluted 10 fold with the load buffer and the pH was adjusted between pH 2.5 – 3.3 using neat acetic acid. The samples were slowly loaded onto the cartridge (9.5 mL/hr). One milliliter of the load buffer was passed through the cartridge. Five hundred microlitres of the elute buffer was passed through the cartridge and the flow was captured into a clean 1.5 mL polypropylene tube.

Table 2.7 Buffers used in strong cation exchange

Cation exchange buffer	Composition
Load	10 mM KH_2PO_4 in 25% ACN pH 3.0
Elute	10 mM KH_2PO_4 in 25% ACN and 350 mM KCl, pH 3.0
Clean	10 mM KH_2PO_4 in 25% ACN and 1 M KCl at pH 3.0
Storage	10 mM KH_2PO_4 in 25% ACN and 0.1% NaN_3 pH 3.0

The buffers used to clean the sample using C18 cartridge are described in table 2.8. The eluate was dried down using a speedvac and resuspended in load buffer. A C18 cartridge (1 X 8 mm; Michrom Bioresources, Inc., CA, USA) was washed with 1 mL of neat ACN at a slow rate (9.5 mL/hr) before the column was washed with 1 mL of wash buffer in ultrapure H_2O. The C18 cartridge was then washed with 1 mL of the load buffer before the sample was slowly loaded (9.5 mL/hr) onto the C18 cartridge. Bound sample was desalted using

0.2% HFBA/ultrapure H_2O and eluted with 500 µL of elute buffer, and an additional 200 µL of neat ACN. The eluted samples were then stored at -20°C until required for 2D LC-MS/MS (see section 2.12.3).

Table 2.8 Buffers used in C18 cleanup

C18 Buffer	Composition
Load	0.2% HFBA/ultrapure H_2O
Wash	50% ACN/0.1% FA in ultrapure H_2O
Elute	0.1% FA/50% ACN, ultrapure H_2O

2.11 Label-Free Quantiation

Data derived from LC-MS/MS analysis was performed using the quantitative methods of Peak Integration and Spectral counting. Peak integration analysis was performed using both Decyder MS and Progenesis LC-MS programs, whilst spectral counting was analysed using Scaffold.

2.11.1 Peak Integration using Decyder MS

Peak Integration was performed using Decyder MS (GE Healthcare Uppsala, Sweden) on data files imported from LC-MS/MS analysis run on the LTQ-FT. Retention times were cropped from 13.79 – 47 minutes and the m/z range considered was 350 – 1700. Peptides were automatically aligned, detected, and their charge states assigned with the PepDetect module choosing a typical peak width of 1.2 min and a mass resolution of 0.4 amu. Charge states were set from 2 to 6. The dcms (Decyder mass spec data) files were converted into a pdws file (workspace file) which classified the peptides in a final workspace (2D LC intensity map) defined by the previously mentioned properties (charge state, resolution and peak width). Relative quantification was performed by matching peptides according to their 2D LC intensity map with the PepMatch module. Each sample was assigned to an experimental group and uniform background modeling and correction parameters were set to uniform. Data was normalized using the measured intensity distribution since there were no internal standards. Matching of the LC-MS traces was performed with a respective time and mass tolerance of 2 min and 0.5 Da.

The extent of change between each of the peptides was determined using their one-way ANOVA statistics. Additionally, the calculation of a t-test score would be used to determine the extent of change between each group. Only peptides with an ANOVA p statistic of $p<0.001$ were considered for quantitation. Peptides were chosen on the basis that they exhibited a minimum of a two-fold change and possessed a 2+ or 3+ charge. Peptide identification was performed by exporting the selected peptides into mgf.files (Mascot generic format) and searched using the NCBI database as of January 2009. The resulting *.dat files (Mascot search results) were reimported back into Decyder MS for annotation.

2.11.2 Peak Integration using Progenesis LC-MS

Progenesis LC-MS (Nonlinear Dynamics Ltd, Newcastle upon Tyne, UK) was used to analyse data files from LC-MS/MS runs via peak integration. The data files were used to generate a 2-D intensity map of the eluted peptides, using base peak ion chromatograms and mass to charge ratios of each peptide. All maps were aligned to a designated reference map (the run that best represented all the samples in the group). Features (candidate peptides) that had 2-6 charges and 1 isotope were selected for further analysis. The maps were then grouped according to the different comparative groups. Features were edited by inspecting their mass spectrum, retention time and expression profile. Features with low ANOVA scores ($p < 0.01$) and at least a 2 fold change in their expression profiles were selected for further statistical analysis. Fragmentation data from each run was exported as an *.mgf file into mascot for searching as described in section 2.12.4. The mascot results were imported as a *.xml file back into progenesis to gather sequence information and potential protein identifications. A peptide filter was then applied so as to remove scores less than 20 whilst resolving conflicting peptide assignments at the protein level.

2.11.3 Spectrum counting using Scaffold v2.0

Scaffold (version Scaffold_2_02_03, Proteome Software Inc., Portland, OR) was used to tally the frequency each particular MS/MS based spectra and peptide identification which occurred in a LC-MS data file. Data files after Mascot analysis (section 2.12.4) was imported and processed into Scaffold for processing. Peptide identifications were accepted if they had a greater than 80.0% probability as specified by the Peptide Prophet algorithm [121]. Protein identifications were accepted if they had a greater than 20.0%

probability and contained at least 1 identified peptide. Protein probabilities were assigned by the Protein Prophet algorithm [122].

2.12 LC-MS/MS for Peptide/Protein Identification

2.12.1 Quadrupole Time of Flight (Q TOF) analysis

Digests were analysed using an API Qstar Pulsar I hybrid tandem mass spectrometer (Applied Biosystems, Foster City, CA, USA). Peptides were separated by nano-LC using an Ultimate HPLC and Famos autosampler system (LC-Packings, Amsterdam, Netherlands). Samples were concentrated and desalted onto a micro C18 pre-column (500 µm x 2 mm, Michrom Bioresources, Inc. Auburn, CA, USA) with 2% ACN/0.05% HFBA/98% ultrapure water at 15-20 µL/min. After a 4 minute wash, the pre-column was switched (Switchos, LC Packings) into line with an in-house built fritless nano C18 column (75 µm x 10cm) packed with C18 Magic stationary phase (5 um, 200 Å pore size; Michrom Bioresources, Inc). LC mobile phase buffers comprised of A: 2% ACN/0.1% FA/98% ultrapure water and B: 80% ACN/0.1% FA/20% ultrapure water. Peptides were eluted using a linear gradient of 2% B to 50% B over 30 minutes followed by a 100% B wash over 1 minute at a flow rate of ~300nL/min.

High voltage was applied to low volume tee (Upchurch Scientific, Oak Harbor, WA, USA) and a column tip position at ~1cm from the orifice. Positive ions were generated by electrospray and the Qstar was operated in information dependant acquisition mode (IDA). A TOF-MS survey scan was acquired (m/z 350-1700, 1s) and the 2 most abundant multiply charged ions (counts > 15) were sequentially selected by Q1 for MS/MS analysis. Nitrogen was used as the collision gas and an optimum collision energy chosen (based on charge state and mass). Tandem mass spectra were acquired for 2.5 s (m/z 65-2000). Peak lists were generated using Mascot Distiller software (Matrix Science, London, England) using default parameters and submitted to the database search program Mascot (version 2.2, Matrix Science).

2.12.2 LTQ-FT analysis

Digests were analysed using a Linear Ion Trap/Fourier Transform ion cyclotron resonance (LTQ-FT) Ultra mass spectrometer (Thermo Electron, Bremen, Germany). Peptides were separated by nano-LC using an Ultimate 3000 HPLC and autosampler system (Dionex,

Amsterdam, Netherlands). Samples were concentrated and desalted onto a micro C18 pre-column (500 µm x 2 mm) with 0.05% (v/v) HFBA 20 µL/min. After a 4 minute wash, the pre-column was switched (Valco 10 port valve, Dionex) into line with an in-house built fritless nano C18 column (75 µm x 10cm) packed with C18 Magic stationary phase (5 µm, 200 Å pore size; Michrom Bioresources, Inc). Mobile phase buffers and peptide elution was performed using the same gradient and flow as previously described (Section 2.12.1).

High voltage was applied to low volume tee and a column tip position at ~0.5 cm from the heated capillary (T=200^{o}C) of the LTQ-FT. Positive ions were generated by electrospray and the LTQ-FT operated in DDA mode. A TOF-MS survey scan was acquired (m/z 350-1700) in the FT ICR cell (Resolution = 100 000 at m/z 400). Approximately 7 of the most abundant ions (>2000 counts) with charge states of +2 or +3 were sequentially isolated and fragmented within the linear ion trap using collision induced dissociation (CID). Mass to charge ratios selected for MS/MS were dynamically excluded for 60 seconds. Peak lists were generated using Mascot Daemon software (Matrix Science, London, England) using default parameters and submitted to the database search program Mascot (version 2.2).

2.12.3 2D LC-MS/MS

Peptides were separated by online cation exchange microtrap (1 x 8 mm, Michrom Bioresources, Auburn, CA) using an Ultimate HPLC, Switchos and Famos autosampler system. Peptides were eluted sequentially using 0, 5, 10, 15, 20, 30, 40, 50, 75, 150, 300, 1000mM ammonium acetate washes. The unbound load fraction (0 mM) and each salt step was concentrated and desalted on a micro C18 precolumn (500 µm x 2mm) with H_2O:ACN (98:2, 0.1% formic acid) at 20 µL/min. After a 10 minute wash the precolumn was switched into line with an in-house built fritless analytical column containing and C18 column (75 µm x 12 cm) [7]. Peptides were eluted using a linear gradient of H_2O:ACN (95:5, 0.1% formic acid to 95:5 0.1% formic acid) at 200 nl/min over 60 minutes. The column inlet was connected to a low volume tee (Upchurch Scientific) where high voltage was applied, and the column outlet was positioned ~1cm from the orifice of an API Qstar. Positive ions were generated by electrospray and the Qstar operated in IDA. A TOF MS survey scan was acquired (m/z 350-1700, 0.75s) and then the most abundant multiply charged ions sequentially selected by Q1 for MS/MS analysis. Nitrogen was used as the collision gas and optimum collision energy was automatically chosen based on charge state and mass. Tandem mass spectra were accumulated for 2 seconds.

2.12.4 Database Searching for In-Gel Digested and MF10 Samples

All MS/MS spectra were searched using Mascot. In-gel digested samples analysed on the Qstar and LTQ-FT Ultra were searched with the following criteria: precursor and product ion tolerances ±0.25 ppm and ± 0.2 Da respectively for the QStar and ± 6 ppm and ± 0.6 Da respectively for the LTQ-FT Ultra; variable modification of methionine oxidation, carbamidomethyl (C) and acrylamide (C); and two allowed missed cleavage specified. All data was searched against a human non-redundant NCBI (January 2009).

3

DEVELOPMENT OF A TEAR FRACTIONATION PROTOCOL TO DISCOVER PEPTIDE BIOMARKERS IN HUMAN TEARS

3.1 Introduction

The peptides found in tears can be released into the extracellular space in response to cellular signaling, various regulatory functions, the inflammatory response or cleavage of proteins. Their presence is ultimately controlled by the equilibrium between proteases and protease inhibitors within the tear film [46]. Disruption of this equilibrium, brought upon by changes to the ocular environment, may be reflected in changes in the abundance of lower abundance proteins and peptides [46].

The challenge in sampling and analysis of the tear fluid is reflected by the limited literature describing the tear peptidome and changes in expression related to the onset of an ocular pathology. Tears are typically collected in limited volumes (~5-10 µL) and analyses are further complicated by the large dynamic range of protein abundance in the tear sample, where over 80% of the total protein is represented by lipocalin, lysozyme and lactoferrin [123]. These higher abundance proteins will tend to mask lower abundance proteins and peptides, impeding investigation of the sample. From a study identifying over 491 proteins in the tear fluid proteome, de Souza et al. (2006) reported that in-gel digestion recovers more tear peptides and proteins than in-solution digestion. Such proteins and peptides were subsequently identifiable using a high-powered mass spectrometer [46].

Recent advances in proteomic technology have improved the capacity to investigate lower abundance proteins and peptides. Pre-fractionation strategies are available to not only isolate, but also enrich the lower-molecular weight protein and peptide species from complex samples, such as tears, prior to analysis. One such instrument is known as the Microflow MF10. The MF10 exploits the principles of liquid electrophoresis to separate and enrich peptides and proteins into defined mass ranges. Recent reports have illustrated some of the capabilities of this machine in the separation of $CD34^+$ haematopoietic stem/progenitor cells and $CD4^+$/$CD8^+$ T-cell proteins [124]. In addition to advances in separation technologies, the burgeoning field of peptidomics has been driven by the development of high-powered mass spectrometers that increase the ability to analyze complex peptidomes and proteomes in-depth. In particular, the recent development of the Linear Ion Trap Fourier Transform mass spectrometer (LTQ-FT MS) has introduced higher sequencing speeds, resolution and mass accuracy that have promoted a MS-based approach to biomarker discovery workflows.

After assessing a number of different technologies, this chapter describes the development of a tear fractionation protocol from which biomarkers can be successfully derived. Tear proteins were analysed by2-D electrophoresis and 2-D LC-MS/MS. Using these techniques, issues such as sample volume and instrument variation shifted the focus from total tear protein analysis to investigation of lower abundance peptides and proteins from which to isolate disease associated biomarker candidates. To investigate these lower abundance protein and peptide species several approaches were explored. These included;

- a pattern-based MALDI-MS discovery approach
- employment of spin filters to fractionate tears prior to LC MS/MS
- sample fractionation with a Microflow MF10 prior to MS analysis.

Peptides were quantitatively analysed with labelling (iTRAQ) and non-labelling (peak integration and spectral counting) strategies. The merits of each methodology and their utility in candidate biomarker discovery were considered while taking into account the limited volume of tears and the extent of sample preparation required.

3.2 Methods

3.2.1 Tear Collection

Tears were collected from healthy controls (Con), patients diagnosed with diabetes mellitus type 2 without retinopathy (DM) and patients diagnosed with diabetes mellitus type 2 with retinopathy (DR). Tears were collected from patients at the Wenzhou Hospital, Wenzhou, People's Republic of China as previously described (refer to Section 2.1). Patient data was also collected for reference.

Tears were collected from patients that were sex and age matched to controls. Control patients tears (*n=20*) were pooled together as were DM (*n=20*) and DR (*n=20*). Each pool was separated into 100 µg aliquots as determined by a Fluoroprofile™ quantitation assay (refer to section 2.3).

3.2.2 1 Dimensional Gel Electrophoresis (1-DE) Analysis of Tear Proteins

Individual tears from healthy subjects were analysed using 1D-E to investigate the extent of biological variation amongst subjects belonging to a cohort.

3.2.2.1 **Determining Protein Load by Volume**

A 1-DE gel was used to separate total tear protein from a standardized volume of tears collected from subjects. Aliquots of 2.5 µL and 5 µL of tears collected from a total of 10 subjects were separated on a 1-DE gel. To each tear sample, tears were diluted with water so that the final volume was 10 µL and separated by 1-DE gel as described in Section 1.6.2

3.2.2.2 **Determining Protein Load by Protein Concentration**

Ten aliquots from 10 individuals, each containing 10 µg of total tear protein as determined by Fluoroprofile™ quantitation, were separated on a 1-DE gel. Each tear sample was diluted with water so that the final volume was 10 µL. Samples were separated by 1-DE gel as described in Section 2.6.2

3.2.3 2 Dimensional Gel Electrophoresis (2-DE) Analysis of Tear Proteins

Tears collected from a healthy non-contact lens wearing male subject aged 23 years with no history of ocular pathology were separated by 2-DE as described in sections 2.4.1 – 2.4.4. Briefly, from pooled tears, aliquots containing 25 µg, 50 µg, 75 µg, 100 µg and 300 µg of total protein (section 2.3) were focused onto pH 4-7 IEF strips. Tears were then separated via SDS-PAGE (2.4.2) and visualized usingSypro Ruby staining before overstaining with Coomassie Brilliant Blue for visualization without fluorescence (section 2.4.3).

Manual comparison of the resulting 2-D protein profiles was performed. All tear proteins visualized on the 2-D gel loaded with 300 µg of protein and stained with Coomassie Brilliant Blue stain were excised, and identified using FT LC-MS/MS analysis as described in Section 2.12.4.

3.2.4 2D-LC Analysis of Tears

A 100 µg aliquot of pooled tears was diluted with 25 µL of 50 mM AMBIC. One microgram of trypsin in 50mM AMBIC (1µg/µL) was added to the tears and incubated overnight at 37^{o}C. Samples were dried down using a SpeedyVac® and reconstituted in 6 µL of 2% ACN/0.05% HFBA/98% ultrapure water. The digested protein was separated and analysed by online 2-D LC MS/MS as described in section 2.12.3.

3.2.5 MALDI Pattern Profiling of Tear Peptides

Five microlitres of unfractionated tear samples (*n* = 185) from pooled tears were diluted with 15 µL of one of the following mass spectrometry-compatible solutions: 0.1% (v/v) TFA, 0.1% (v/v) FA, 50 mM AMBIC or ultra-pure water. These samples were then incubated in the respective solutions overnight at 4^{o}C before they were treated using one of the following described methods (3.2.4.1-3.2.4.8). All techniques were performed in triplicate.

3.2.5.1 **C18 Reverse Phase Purification:** a C18 reverse phase microcolumn (PerfectPure, Eppendorf, Germany) was activated, equilibrated and the sample aspirated as per manufacturer's instructions. Bound peptides were eluted onto a MALDI target plate with α-cyano-4-hydroxycinnamic acid (CHCA) (8 mg/mL dissolved in 70% (v/v) ACN and 0.1% TFA).

3.2.5.2 **Centrifugation of Sample Followed by C18 Reverse Phase Purification:** diluted samples were centrifuged at 11 000 *g*, 30 min, 4°C before being subjected to C18 reverse phase filtration and spotting on to target plates (as described in procedure 3.2.5.1).

3.2.5.3 **Direct Thin Layer Preparation:** a thin layer of CHCA was placed on the target plate, washed in 0.1% TFA and allowed to dry. Subsequently, a 5 µL aliquot of diluted tear sample was placed onto the CHCA and left to dry.

3.2.5.4 **Reverse Thin Layer Preparation:** a 5 µL aliquot of the tear sample was placed on the target plate and left to dry. Subsequently, a thin layer of CHCA was spotted over the sample and left to dry. The sample was then washed with 5-10 µL of 0.1% TFA.

3.2.5.5 **Dried Droplet Application:** a 0.5-2 µL aliquot of diluted tears was mixed with 0.5 -1 µL of CHCA and allowed to air-dry on the plate. The sample was washed with 5-10 µL of 0.1% TFA for approximately 10 seconds.

3.2.5.6 **Acetone Precipitation:** tear samples (5 µL aliquots) were first diluted with 15 µL of cold acetone and left to precipitate at -20°C for a minimum of 1.5 hours. Proteins were pelleted at 24,000 g for 15 minutes, supernatant removed and the pellet air-dried for 10 minutes. Pellets were resuspended in 15 µL of one of the MS compatible solutions (TFA, FA, AMBIC or ultrapure water) and incubated overnight. Samples were then subjected to C18 reverse phase purification and spotted onto target plates (as described in procedure 1.2.4.1).

3.2.5.7 **Sample Concentration by Centrifugation:** a 5 µL aliquot of tears was diluted in 95 µL 50mM AMBIC and transferred into a YM-30 Microcon (Millipore) sample reservoir, then centrifuged at 14,000 *g* at 10°C for 30 minutes. The flow through was collected and then subjected to C18 reverse phase purification and spotted onto the target plate (as described in procedure 1.2.4.1).

3.2.5.8 **Reduction and Alkylation:** a 5 µL aliquot of tears was diluted in 95 µL 50mM AMBIC and then reduced and alkylated with dithiothreitol (DTT) (final concentration 10 mM) and iodoacetimide (IAA) (final concentration 50 mM) respectively for 10 minutes each. Samples were then subjected to C18 reverse phase purification and spotted onto the target plate (as described in procedure 1.2.4.1).

Peptide mass maps (PMM) of treated samples were generated by MALDI-TOF MS (Waters M@LDI^{TM}; Waters, Milford MA, USA). Samples were analysed in positive reflectron mode between the range 700-4000 m/z with an accelerating voltage of 15 kV. Three-point external calibration was performed using angiotensin (1064.543 Da), $P_{14}R$ (1533.858 Da) and adrenocorticotrophic hormone (2465.199 Da).

Statistical testing was performed on the number of peaks resolved on the PMM of tears. A multivariate analysis of variance was performed on log transformation of the number peaks derived from the tear PMM. Treatments were compared to each other based on each tear diluent. Significance levels were set at p = 0.05.

3.2.6 Spin Filter Fractionation and LC MS/MS

A 5 µL (*n*=3) aliquot of reflex tears was collected from a healthy control. Each 5 µL aliquot of tears was diluted in 95 µL of 50 mM AMBIC and transferred into a YM-30 Microcon (Millipore) sample reservoir. The reservoir was centrifuged at 14,000 *g* at 10^{o}C for 30 minutes. The flow through was collected and then subjected to C18 reverse phase purification and LC-MS/MS analysis (as described in section 2.12.2). Spectra produced from LC-MS/MS was searched against the MASCOT database as detailed in section 2.12.4

3.2.7 MicroFlow MF10

For peptide fractionation, a 3-chamber cartridge was assembled as illustrated in Figure 3.1 using 5, 25 and 65 kDa polyacrylamide membranes (NuSep, Sydney, Australia) and a 1 kDa regenerated cellulose membrane (Millipore, MA, USA). A 100 µg aliquot (*n*=2) of tears collected from a subject was fractionated as described in section 2.7. After fractionation, the 1-25 kDa fraction, 25-65 kDa fraction and >65 kDa fractions were collected from the chambers using gel-loading tips for subsequent sample preparation including removal of

interfering substances with StageTips™ (section 2.8), in solution tryptic digestion (section 2.9), analysis using LC-MS/MS (section 2.12.2). Data derived from the analysis was used to interrogate the Mascot database for identification (section 2.12.4). The 25-65 kDa and >65 kDa fractions were separated on a 1-DE gel (section 2.6.2).

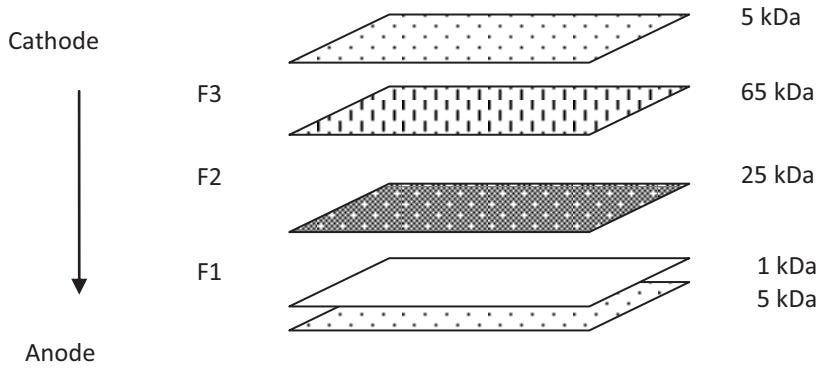

Figure 3.1 MF10 Chamber assemblies Protein and peptide standard fractionations (from the cathode): Fraction 1 (1-25 kDa), Fraction 2 (25-65 kDa) and Fraction 3 (65-5 kDa).

3.2.8 iTRAQ Labelling and Quantitation of Tear Peptides

Reflex tears were collected from each subject (*n*=20) in each disease group (Con, DM and DR) and then pooled and separated into 100 µg aliquots as determined by Fluoroprofile™ quantitation. One hundred micrograms of each pool was fractionated using the MF10 as described in section 2.4.

The 1-5 kDa and 5- 25kDa fractions collected were desalted and concentrated as described in section 2.6. Each fraction was labeled with iTRAQ reagents as previously described (section 2.8.1). For each fraction, Con, DM and DR were pooled after iTRAQ labelling and the samples were cleaned using cation exchange and reverse phase chromatography (section 2.10.1). The fractions were then separated and analysed by online 2-DLC MS/MS as described in section 2.12.3.

3.2.9 Non-labelling Quantitation Comparison

3.2.9.1 Peak Integration using Decyder MS

After MF10 fractionation of Con, DM and DR pools the 5-25 kDa fractions that were collected were then cleaned using C18 StageTips (refer to section 2.6) and analysed with the LTQ-FT (as described in Section 2.11.1). Each fractionated pool was injected into the LTQ-FT a total of 3 times so as to achieve statistical significance. Full scan LC-MS and MS/MS spectra from LTQ-FT MS/MS analysis were quantified and matched using Decyder MS as described in 2.10.1. Peptides were selected with the following peptide quantification values: ANOVA $p<0.001$ and two-sided students t-test $p<0.05$. Ten peptides were chosen on the basis they showed statistically different abundances between the following comparisons:

- Con and DM
- Con and DR
- DM and DR
- Con/DM and DR
- Con and DM/DR.

The 10 peptides showing the lowest p-values in each ANOVA were selected and identified. These peptides were chosen on the basis that they were significantly different in abundance (t-test results) when compared between the groups, ie. 10 peptides were chosen on the basis they showed statistical differential abundance between: Con and DM; Con and DR; DM and DR; Con/DM and DR; or Con and DM/DR. The 10 peptides showing the lowest p-values in each t-test were selected and identified. Each selected peptide was identified by exporting the peptide data as a *.mgf file into the MASCOT software. After MASCOT analysis, *.dat files containing sequence and peptide identification details were re-imported back into Decyder MS to generate the final report.

3.2.9.2 **Spectrum Counting using Scaffold**

Raw data files (*.raw) from the samples analysed using the LTQ-FT were processed via Scaffold as described in section 2.8.3. Briefly, the same raw files used in section 3.2.9.1 were analysed with Scaffold. Raw files were searched against a human non-redundant NCBI database using Mascot as described in section 2.12.4. The *.dat files from the resultant searches were loaded into Scaffold v2.0. Protein identifications were accepted if they had greater than 20.0% probability and contained at least 1 identified peptide. Protein changes between the three groups were deemed significant with an ANOVA score of $p < 0.05$.

3.3 Results

3.3.1 Protein Analysis

3.3.1.1 Biological variation and tear standardization

Individual tears from healthy subjects were analysed using 1-DE to investigate the extent of biological variation amongst subjects belonging to a cohort. Additionally, the study aimed to determine whether or not tears should be analysed based on standardized tear volume (as has been reported in numerous literature reports) or tear protein concentration. Figure 3.3 illustrates separation of tears using a standardized volume. Large variation can be observed in the 1-DE profiles of tears when loaded with either 2.5 or 5 µL aliquots of tears. The variation is indicated by the presence and absence of a variety of bands. Refer, for example, to that seen in the 70 kDa band and ~18 kDa band region. The variation in the lower molecular weight region (10 kDa) is most pronounced when loading with the larger volume.

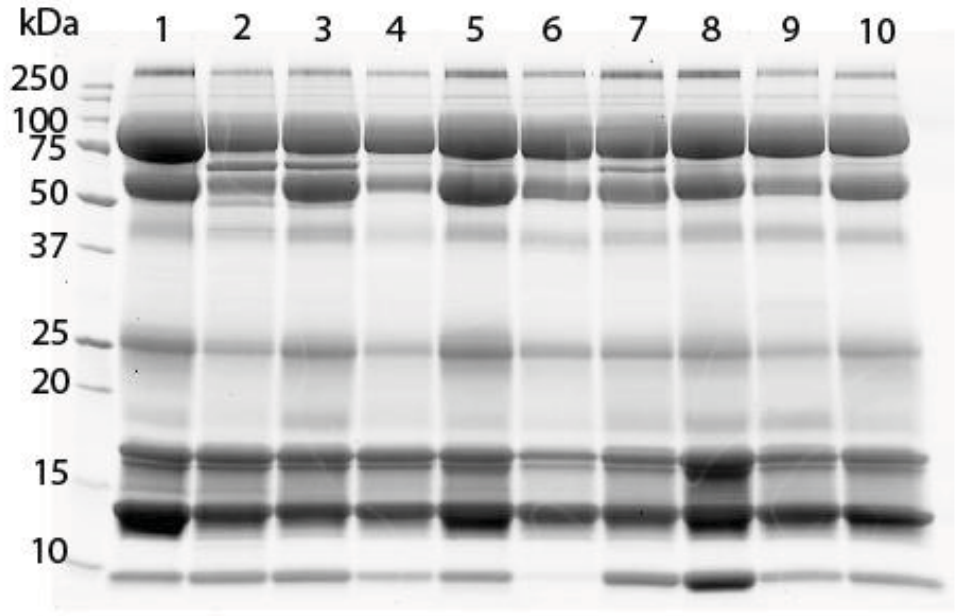

Figure 3.2 1-DE gel of tears standardised using volume. Lanes 1.-5 loaded with 2.5 µL aliquots of tears collected from 5 different subjects. Lanes 6-10 loaded with 5 µL aliquots of tears were collected from 5 different subjects. Proteins were separated on a 8-16% Tris-HCl gel and stained with Sypro Ruby (Bio-Rad).

Figure 3.4 illustrates separation of tears using a standardized protein concentration. A 10 µg aliquot as determined by Fluoroprofile™ quantitation was loaded from the same 10

subjects analysed in Figure 3.3. Whilst minimal variation is observed across the 1-DE separation profile of the tear proteins in comparison to the previous gel loaded with standardized volumes of tears, intensities of certain bands are observed to vary.

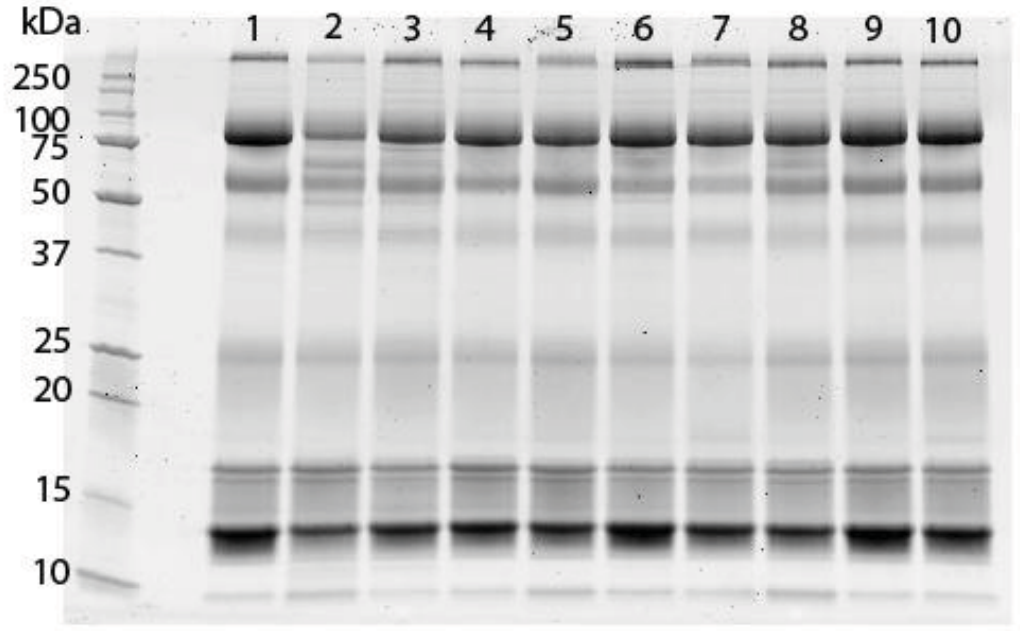

Figure 3.3 1-DE gel of tears standardised using amount. Gel was loaded with 10 µg aliquots of total tear protein as determined by Fluoroprofile™ (*n*=10) were separated on a 1-DE gel. Proteins were separated on a 8-16% Tris-HCl gel and stained with Sypro Ruby (Bio-Rad).

3.3.1.2 **2-DE of Tear Proteins**

Varying amounts of total tear protein as determined by the Fluoroprofile™ protein quantitation kit, were separated using 11cm 2D gels to determine the minimal protein amount for visualisation of the maximum number of protein species in human tears. Different protein loads (300, 100, 75, 50 and 25 µg) observed after Sypro staining are reported in Figure 3.5. The gel images indicate that gradual increases in protein load increase visualisation of a majority of the tear proteins. Lower abundance proteins cannot be clearly resolved on Sypro stained 2D gels until the gel is loaded with 300 µg of total tear protein, at which point many of the higher abundance proteins are saturated using this fluorescent dye.

The gels were over-stained with Coomassie Blue in order to visualise the protein spots without the use of fluorescence. Protein spots selected for excision and identification were

obtained from the 2D gel loaded with 300 μg of total protein. There was difficulty locating a majority of the lower intensity gel spots detectable on Sypro stained images, so although 75 spots were excised for analysis many of these spots were too faint to produce MS sequence data. Figure 3.6 indicates the proteins which were excised and successfully identified by MS analysis and their identifications are reported in Table 3.1.

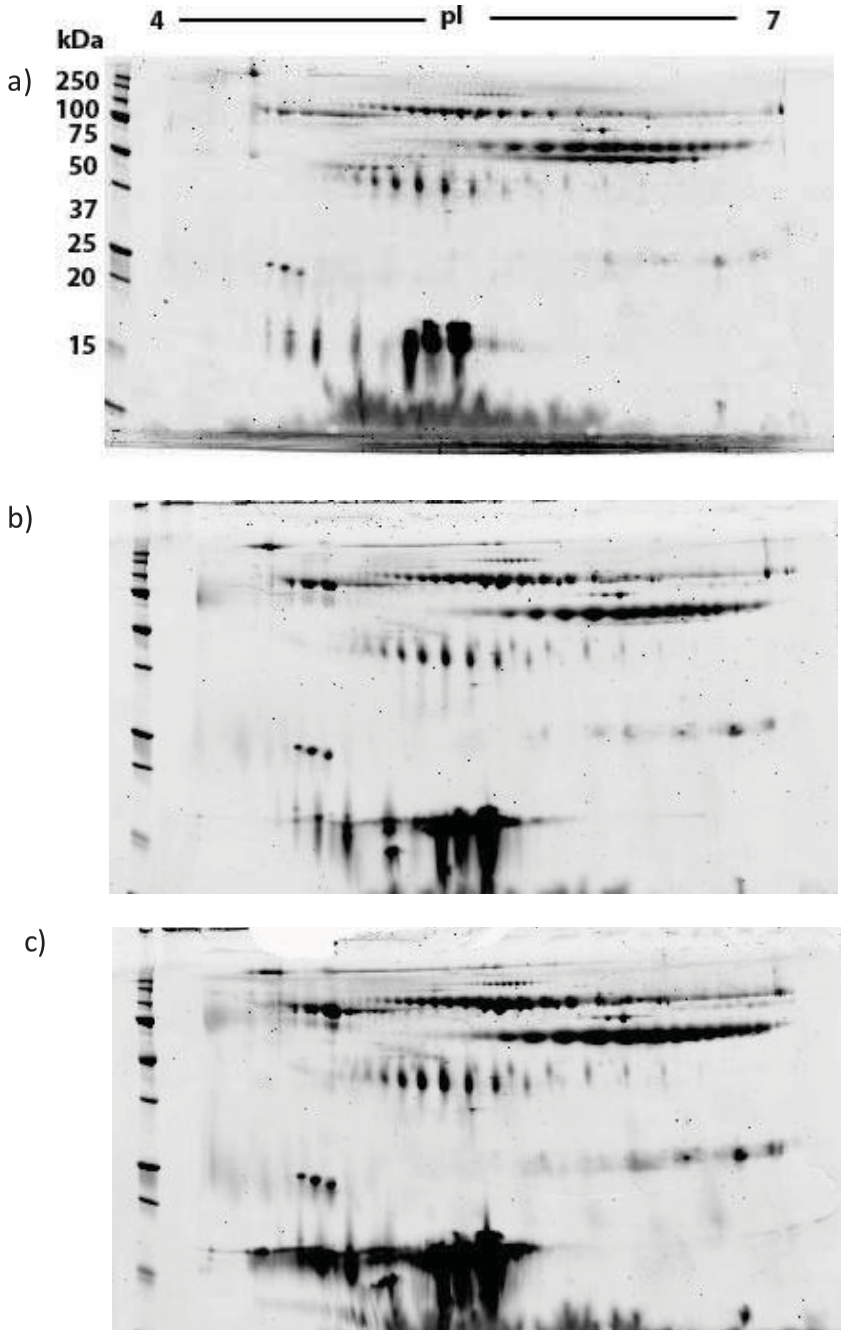

Figure 3.4 2-DE gels p*I* 4-7 separating different tear protein loads. Gels were loaded with a) 25 µg, b) 50 µg, c) 75 µg, d) 100 µg and e) 300 µg total tear protein as determined by Fluoroprofile™ protein assay. Proteins are separated on 11 cm IPG strips and 8-16% Tris-HCl gels and stained with Sypro Ruby.

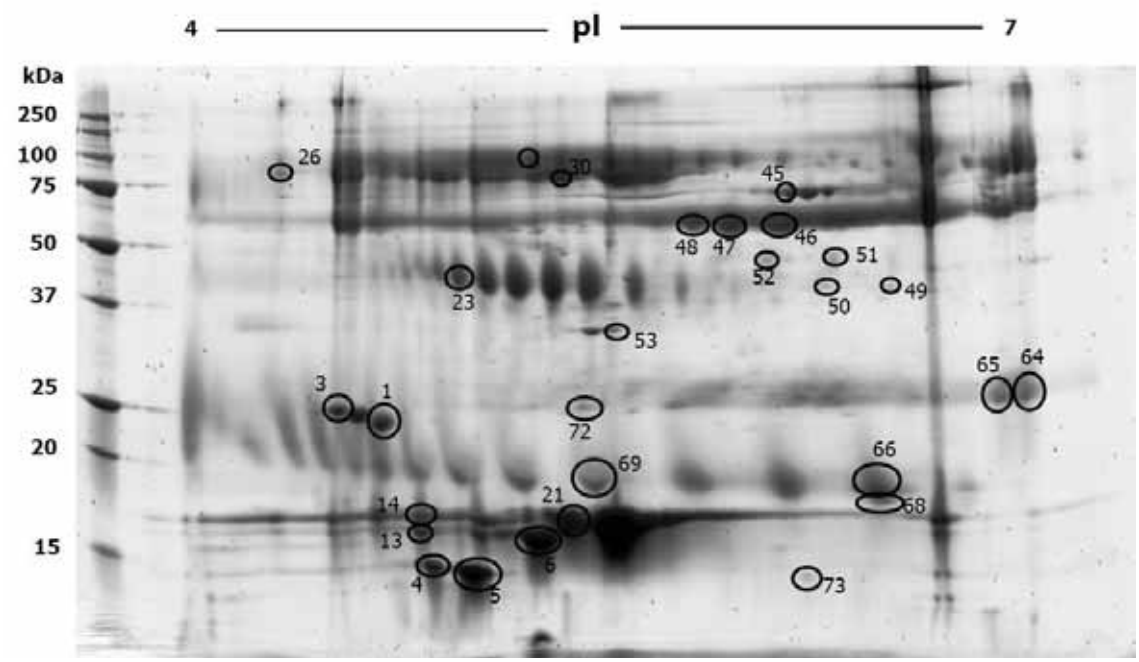

Figure 3.5 Proteins identified by mass spectrometry analysis from a 2D gel separating 300 µg of total tear protein. Identifications are tabulated in Table 3.1. Proteins were separated on 11 cm IPG strips and then an 8-16% Tris-HCl gels and stained with Sypro Ruby.

Table 3.1 Identification of tear proteins excised from a 2D-gel separating 300 µg of total tear protein. # unique peptides are the number of peptides that were matched via the database search to the proteins identified

Spot #	Protein/peptide identified	MOWSE score	# unique peptides	Sequence coverage (%)	Theoretical MW (Da)	NCBI accession no.
1	Immunoglobulin J chain	362	56	42	15585	gi|400044
3	Immunoglobulin J chain	328	48	35	15585	gi|400044
4	cystatin s	164	50	52	16204	gi|4503109
5	cystatin s	289	133	58	16204	gi|4503109
6	Lipocalin 1 precursor	1426	194	61	19238	gi|4504963
13	Prolactin induced protein	428	50	55	9061	gi|116642259
14	Prolactin induced protein	1463	118		16562	gi|4505821
21	lipocalin 1 precursor	1165		62		gi|4504963
23	Zn-alpha2-glycoprotein	347	66	53	34714	gi|38026
26	Lactoferrin	756	17	23	76147	gi|48425709
45	Chain A, Crystal structure of human serum albulmin	771	80	43	66410	gi|3212456
46	immunoglobulin alpha heavy chain variable region [Homo sapiens]	194	8	38	13725	gi|62871242
47	IGHA1 protein [Homo sapiens]	840	29	31	52831	gi|49257464
48	IGHA1 protein [Homo sapiens]	288	40	29	52831	gi|49257464
49	Keratin 2	773	17	29	65393	gi|47132620
50	Keratin type 2	402	11	18	65825	gi|547754
51	Chain A, Structure Of Human Diferric Lactoferrin At 2.5a Resolution Using Crystals Grown At Ph 6.5	110	3	4	76147	gi|48425709
52	Chain A, Structure Of Human Diferric Lactoferrin At 2.5a Resolution Using Crystals Grown At Ph 6.6	71	2	3	76147	gi|48425709
53	keratin 13	229	16	32	49613	gi|34033
64	keratin 9	261	8	14	62027	gi|55956899
65	Chain L, Neuropilin-1 B1 Domain In Complex With A Vegf-Blocking Fab	225	5	28	23269	gi|160877748
66	keratin 10 [Homo sapiens]	122	6	8	59492	gi|28317
68	keratin 1	318	10	16	66027	gi|11935049
69	keratin 9	124	4	7	62027	gi|5595689
72	keratin 9	366	9	17	62027	gi|55956899
73	Complex Between A Staphylococcus Aureus Domain And A Fab Fragment Of A Human Igm Antibody	249	4	24	23394	gi|442919

3.3.1.3 **Protein Identification using Online 2D LC-MS/MS**

To determine whether 2D LC-MS/MS was an optimal technique to study total tear protein samples, 100 µg of tear protein was analysed. Analysis generated an average of 765 CID spectra per fraction (8407 total). Data files derived from the MS/MS of each fraction were searched using Mascot. Redundant sequences were removed whilst unnamed and hypothetical proteins were searched using BLAST (http://blast.ncbi.nlm.nih.gov/Blast.cgi) against a non redundant database (nr) to determine the identity of the proteins leaving 48 proteins confidently identified (Table 3.2). Over 46% of proteins were matched to proteins on the NCBI database with 1 peptide (Figure 3.7).

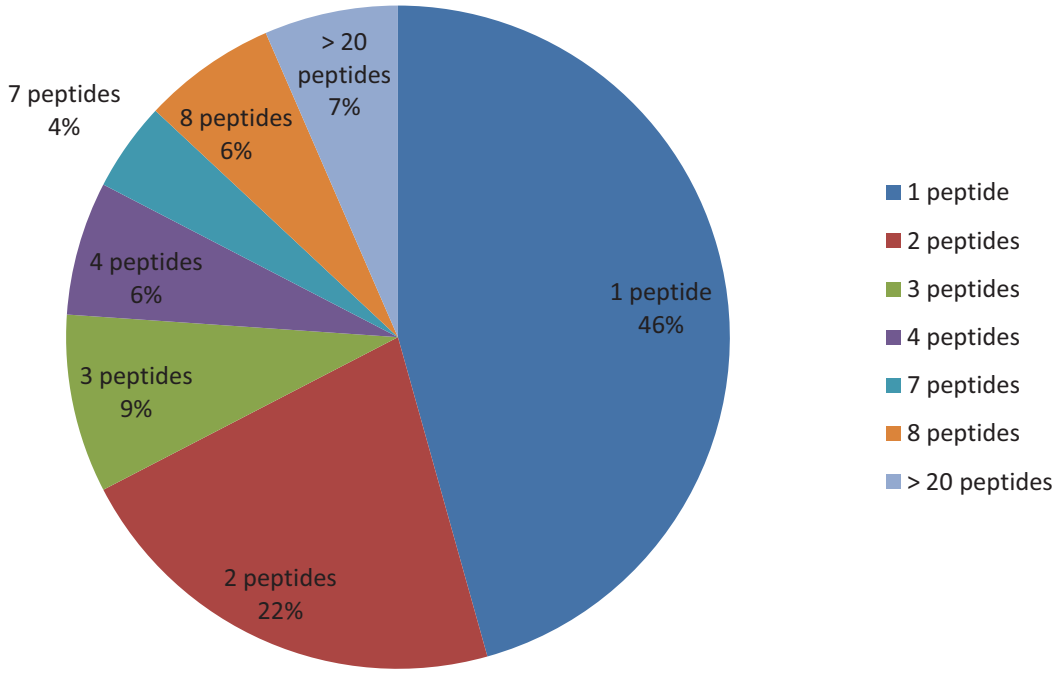

Figure 3.6 Number of peptides used to identify each protein after 2-D LC-MS/MS

Table 3.2 List of non-redundant proteins identified from 100 µg of total tear protein using 2-D LC-MS/MS

Accession #	Description	MOWSE Score	Mass	Non Redundant sequences	Sequence coverage (%)
gi|54607120	lactotransferrin precursor [Homo sapiens]	3186	78132	22	50.8
gi|75766355	Chain X, Structure Of Recombinant Human Lactoferrin Produced In The Milk Of Transgenic Cows	3154	76287	23	50.4
gi|45643462	growth-inhibiting protein 12 [Homo sapiens]	2992	78334	20	47.3
gi|1050983	pHL E1F1 [Homo sapiens]	1497	15088	8	55.2
gi|55667085	PREDICTED: similar to pHL E1F1 isoform 2 [Pan troglodytes]	1396	15116	8	54.5
gi|154448886	proline rich 4 (lacrimal) isoform 2 [Homo sapiens]	1330	15088	8	54.5
gi|58176763	Chain A, Zn-Alpha-2-Glycoprotein; Baculo-Zag Peg 200	1192	32126	7	62.6
gi|31377806	polymeric immunoglobulin receptor precursor [Homo sapiens]	1047	83232	6	25.1
gi|34527259	immunoglobulin heavy constant alpha 1 [Homo sapiens]	1046	53783	7	30.1
gi|229585	Ig A1 Bur	971	73331	6	24.3
gi|14424505	Mesothelin [Homo sapiens]	657	67968	3	21.4
gi|180620	complement cytolysis inhibitor precursor	530	52330	4	27.2
gi|221044882	deleted in malignant brain tumors 1 [Homo sapiens]	511	124419	2	8.6
gi|27728687	anti-rabies SOJB immunoglobulin lambda light chain [Homo sapiens]	500	24733	2	39.7
gi|157834215	Chain A, Contribution Of Hydrogen Bonds To The Conformational Stability Of Human Lysozyme	493	14675	2	46.9
gi|2914164	Chain L, Three-Dimensional Structure Of A Human Fab With High Affinity For Tetanus Toxoid	461	22665	1	41.2
gi|99031801	Chain L, Crystal Structure Of A Glycosylated Fab From An Igm Cryoglobulin With Properties Of A Natural Proteolytic Antibody	439	23331	4	35.8
gi|145579641	Chain B, Crystal Structure Of The Complex Formed Between Mhc-Like Zinc Alpha2-Glycoprotein And Prolactin Inducible Protein At 3 A Resolution	436	13514	3	55.9
gi|21669527	immunoglobulin lambda light chain VLJ region [Homo sapiens]	431	28247	1	26.2
gi|208435642	Chain A, Crystal Structure Of K63-Specific Fab Apu.3a8 Bound To K63- Linked Di-Ubiquitin	423	23694	4	32.3
gi|106586	Ig kappa chain V-III (KAU cold agglutinin) - human	409	23037	3	34.4
gi|4505171	secretoglobin, family 2A, member 1 [Homo sapiens]	392	10876	2	58.9
gi|4826762	haptoglobin isoform 1 preproprotein [Homo sapiens]	350	45177	2	19.2
gi|4503109	cystatin S precursor [Homo sapiens]	342	16204	1	41.8
gi|21284378	RecName: Full=Proline-rich protein 1; Short=PRL1; AltName: Full=Basic proline-rich lacrimal protein; Flags: Precursor	337	22856	2	20.9
gi|5729907	lipophilin A precursor [Homo sapiens]	332	9891	1	54.4
gi|350218	peptide PB,saliva	331	5807	1	93
gi|14278690	Chain A, Human Cystatin C; Dimeric Form With 3d Domain Swapping	280	13339	3	36.7
gi|41388180	monoclonal IgM antibody heavy chain [Homo sapiens]	265	64271	2	11
gi|21666732	NUCB2 protein [Homo sapiens]	261	50063	2	17.9
gi|48425723	Chain E, Structure Of Human Transferrin Receptor-Transferrin Complex	253	38222	1	10.4
gi|118188	RecName: Full=Cystatin-SN; AltName: Full=Cystatin-1; AltName: Full=Salivary cystatin-SA-1; AltName: Full=Cystain-SA-I; Flags: Precursor	229	16351	1	29.8
gi|3152360	anti-(ED-B) scFV [Homo sapiens]	228	25189	2	21.4
gi|34616	beta-2 microglobulin [Homo sapiens]	208	12791	1	35.5
gi|21263906	RecName: Full=Submaxillary gland androgen-regulated protein 3A; AltName: Full=Proline-rich protein 5; AltName: Full=Proline-rich protein PBI; Flags: Precursor	205	14108	2	20.9
gi|189053201	S100 calcium binding protein A9 [Homo sapiens]	201	13202	1	42.1
gi|239753333	PREDICTED: actin, beta-like 3 [Homo sapiens]	178	103670	1	4.8
gi|46253899	immunoglobulin heavy chain [Homo sapiens]	173	16609	1	18
gi|20149993	Chain A, Structure Of Human Trypsin Iv (Brain Trypsin)	172	24262	1	14.3
gi|21951802	SCC-112 [Homo sapiens]	164	146517	1	1.2
gi|112696627	immunoglobulin heavy chain variable region [Homo sapiens]	154	10755	1	46.5
gi|119571038	hCG1992932, isoform CRA_a [Homo sapiens]	130	28224	1	13.3
gi|21961605	Keratin 10 [Homo sapiens]	130	58792	1	6.7
gi|21961605	Keratin 10 [Homo sapiens]	130	58792	1	6.7
gi|21961605	Keratin 10 [Homo sapiens]	130	58792	1	6.7
gi|112697602	immunoglobulin heavy chain variable region [Homo sapiens]	128	10841	1	30.1
gi|400044	RecName: Full=Immunoglobulin J chain	126	15585	1	14.6
gi|198443201	Chain A, Crystal Structure Of Siderocalin (Ngal, Lipocalin 2) W79a- R81a Complexed With Ferric Enterobactin	121	22358	1	12.1

3.3.1.4 **Spectral Counting**

After MF10 separation of tear samples the 5-25kDa fractions from Con, DM and DR patients were analysed using LC-MS/MS and the data was interrogated by spectral counting in an effort to quantitate differences between tear peptides from each group. Results from the spectral count analysis are shown in Figure 3.8. Values plotted are the average counts for peptides found in the three technical replicates of the 5-25 kDa fraction of each group. Identifications of the proteins are detailed in Table 3.3. These values were normalized using Scaffold algorithms. All sequences used to identify the peptides were peptides that would be generated by digestion with trypsin.

When comparing the different groups (Con, DM and DR) using this method changes in abundance was identified in the case of ten different proteins. Two isoforms of proline rich protein 4 were observed to decrease in abundance with the onset of diabetes. The remaining proteins that were identified were seen to increase in abundance with the onset of the diabetic state (DM and/or DR).

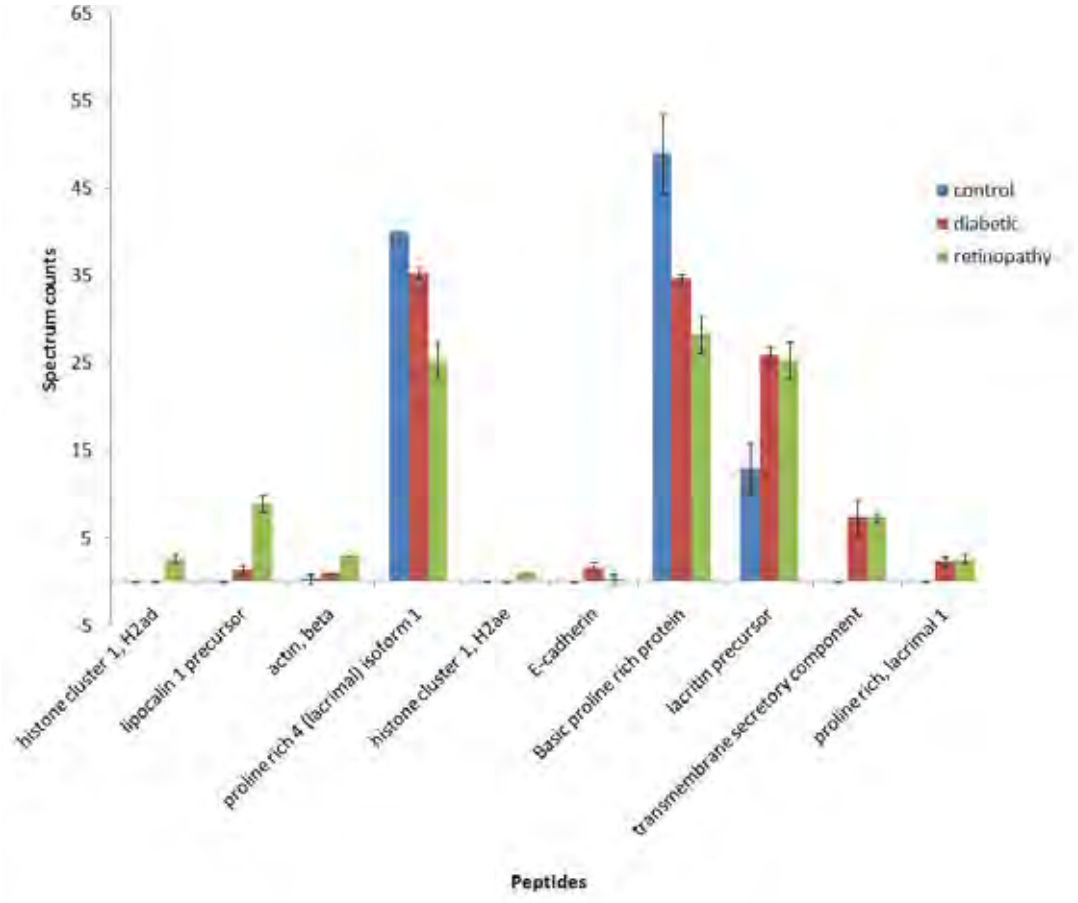

Figure 3.7 Tear proteins of interest identified using Scaffold analysis of 2-D. Values are average spectral counts for three technical replicates of a 5-25 kDa fraction. Identifications are detailed in table 3.2

Table 3.3 Identifications of proteins of interest using Scaffold

Values designate the number of spectra (±S.D) counted from technical analysis (n=3) of the samples.

					Spectral Count		
	Protein ID	Acession #	Molecular Weight	ANOVA Test (P-Value)	Control	Diabetes	Diabetic Retinopathy
1	histone cluster 1, H2ad [Homo sapiens]	gi|10800130	14 kDa	0.00000003	0 (0)	0 (0)	3 (0.6)
2	lipocalin 1 precursor [Homo sapiens]	gi|4504963	19 kDa	0.0000056	0 (0)	1 (0.6)	9 (1)
3	actin, beta [Homo sapiens]	gi|14250401	41 kDa	0.000011	0 (0.6	1 (0)	3 (0)
4	proline rich 4 (lacrimal) isoform 1 [Homo sapiens]	gi|154448882	17 kDa	0.000015	40 (0)	35 (0.6)	25 (2.1)
5	histone cluster 1, H2ae [Homo sapiens]	gi|10645195	14 kDa	0.000018	0 (0)	0 (0)	1 (0)
6	E-cadherin [Homo sapiens]	gi|1617084	91 kDa	0.000034	0 (0)	2 (0.6)	0 (0.6)
7	pHL E1F1 [Homo sapiens]	gi|1050983	15 kDa	0.00026	49 (4.6)	35 (0.6)	28 (2.1)
8	lacritin precursor [Homo sapiens]	gi|15187164	14 kDa	0.00048	13 (3)	26 (1)	25 (2.1)
9	transmembrane secretory component; poly-Ig receptor; SC [Homo sapiens]	gi|238236	83 kDa	0.00093	0 (0)	7 (2.1)	7 (0.6)
10	proline rich, lacrimal 1 [Homo sapiens]	gi|116805344	27 kDa	0.0012	0 (0)	2 (0.6)	3 (0.6)

3.3.2 Peptide Analysis

3.3.2.1 Pattern Based Method Development using MALDI-MS

Preliminary studies investigating seven different sample pre-treatment protocols were examined to determine the optimum technique for MALDI-TOF MS analysis of tears. Spectra obtained from the sample preparations (Figure 3.9) were compared to determine the method that would yield the greatest number of peptides on a tear PMM (Table 3.4). The best protocols were selected and used on 2 further samples each pooled from 3 separate individuals (Table 3.5).

Numbers of peptides produced from the various techniques were statistically compared after log-transformation of data using ANOVA and the Robust F test (computer package, SPSS). The direct thin layer preparation, reverse thin layer preparation or dried droplet sample preparation techniques did not show any discernible peptide peaks in their PMM. Samples subjected to a C18 reverse phase microcolumn purification only showed 34 to 63 peptide peaks on PMM depending on the initial diluent used, with FA or AMBIC giving higher numbers of peptide peaks than H_2O or TFA ($p < 0.025$). Reverse phase microcolumn purification of both the acetone precipitates and reduced and alkylated samples proved difficult, as there was a larger amount of physical effort required to aspirate the sample through the microcolumn. After subsequent C18 reverse phase microcolumn cleanup, only a modest number of peptide peaks were resolved. Centrifugation of tear samples followed by C18 reverse phase microcolumn purification also resolved a modest number of peptides. However this method was not superior to C18 reverse phase filtration alone for any tear diluent apart from using TFA where more peaks were resolved with prior sample centrifugation (Table 3.5; $p = 0.049$). The numbers of peaks resolved on a PMM were significantly improved once tear samples had been filtered through centrifugal filtration devices. Sample preparation using these filters produced an average of 126 peaks that were highly resolved on a PMM. Using this method, tears samples were collected from five individual subjects and the variations between each spectrum evaluated (Figure 3.9).

To investigate variability between the tear profiles of individuals using the method of choice tears from five individuals were collected were analysed (Figure 3.8). Tears were analysed by MALDI-TOF MS after dilution in AMBIC buffer followed by filtration with a 30

kDa cut-off filter and C18 reverse phase microcolumn purification.The variation between individuals was examined. A total of 235 peaks were resolve between all 5 PMM. Additionally, there was an average of 107.6 peaks with a standard deviation of 30. Eighteen percent of the 235 total peaks were resolved between all of the 5 PMM.

a) Incubation of tears in 50 mM AMBIC buffer followed by C18 microcolumn purification

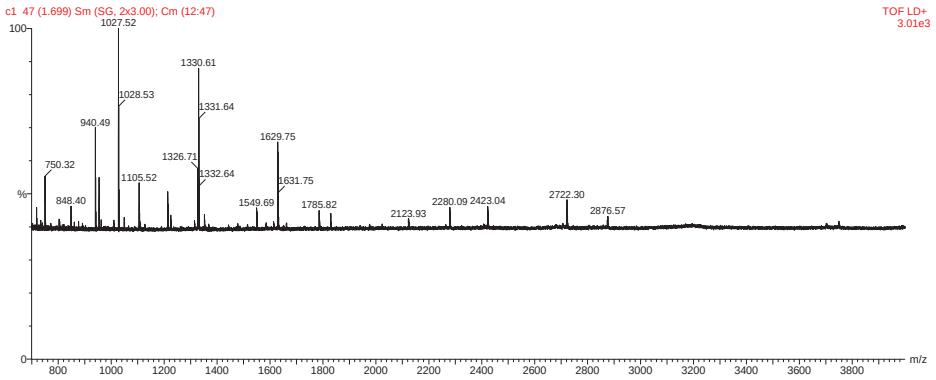

b) Centrifugation of tears followed by C18 purification after incubation in 50 mM AMBIC buffer

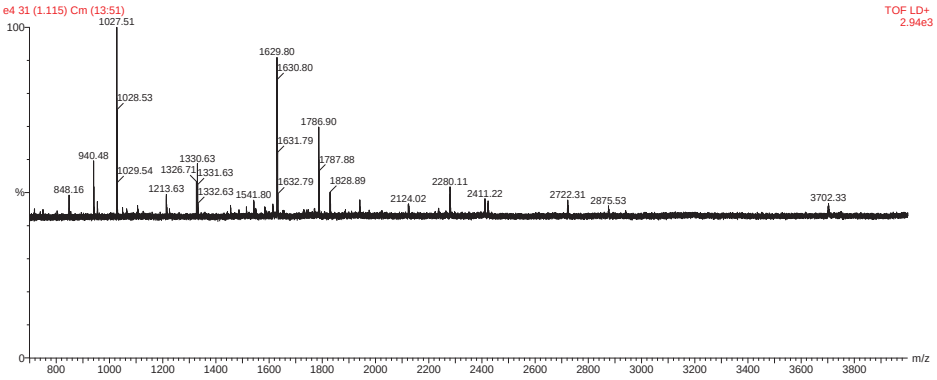

c) Dried Droplet of tears after dilution with 50mM AMBIC

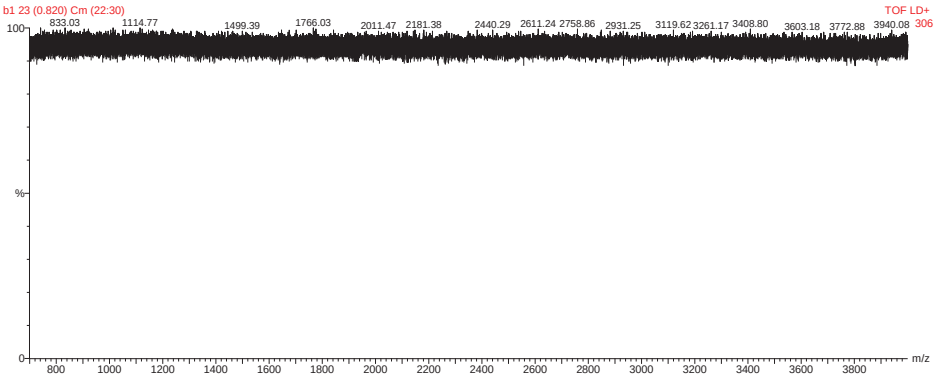

d) Thin layer preparation of tears after dilution with 50 mM AMBIC buffer

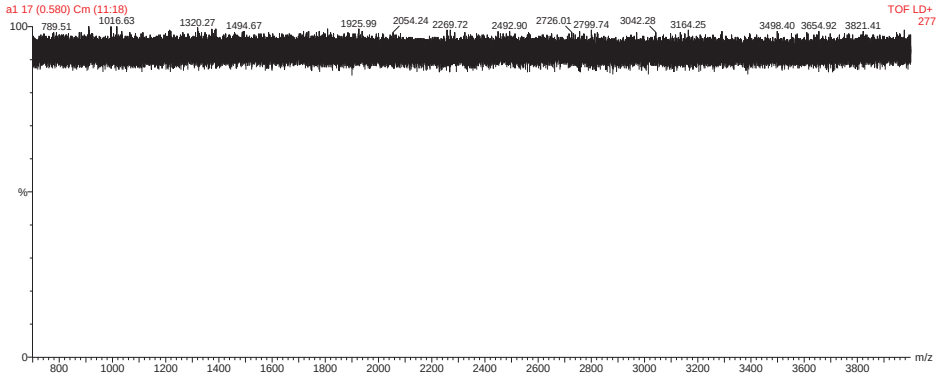

e) Reverse thin layer preparation of tears after dilution with 50 mM AMBIC buffer

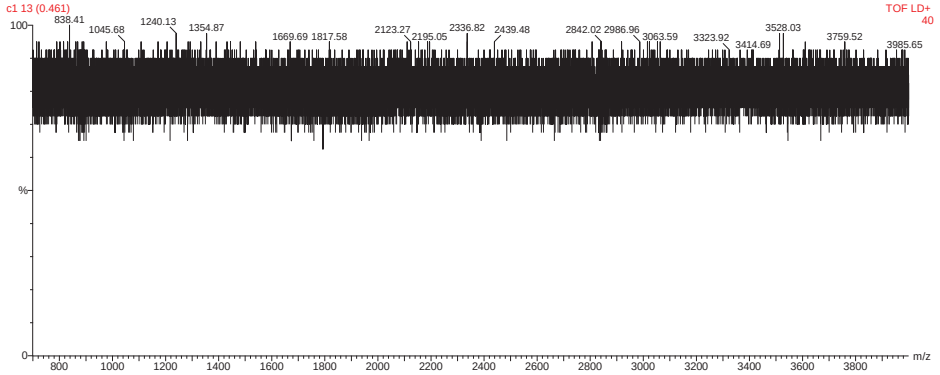

f) Acetone precipitation of tears followed by dilution in 50 mM AMBIC buffer prior to C18 purification

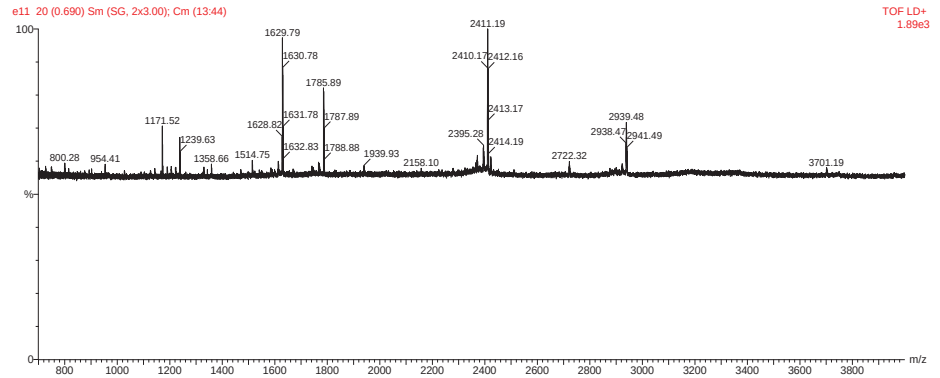

g) Dilution of tears with 50 mM AMBIC followed by 30 kDa cutoff spin filter fractionation

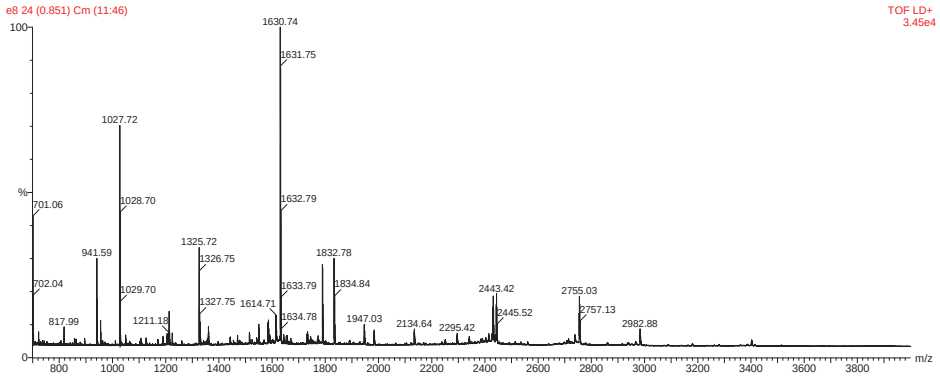

h) Dilution of tears with 0.1% TFA followed by 30 kDa cutoff spin filter fractionation

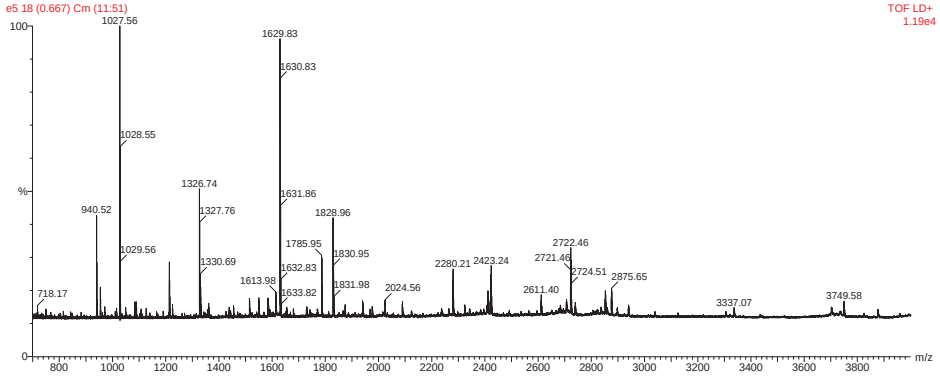

i) Dilution of tears with 0.1% FA followed by 30 kDa cutoff spin filter fractionation

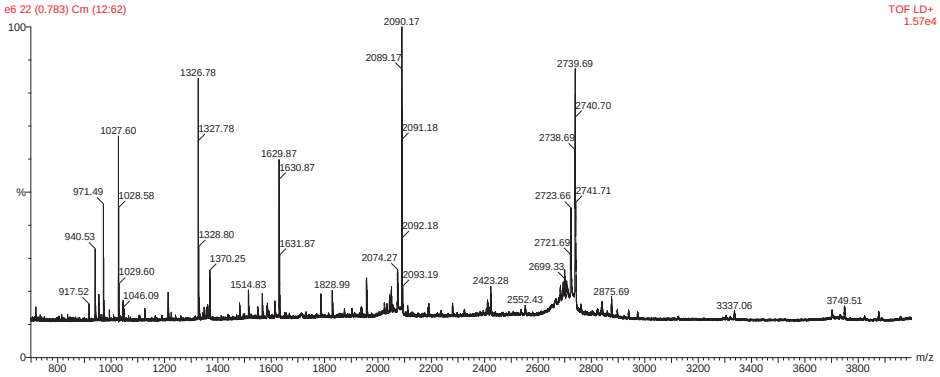

j) Dilution of tears with ultra-pure water followed by 30 kDa cutoff spin filter fractionation

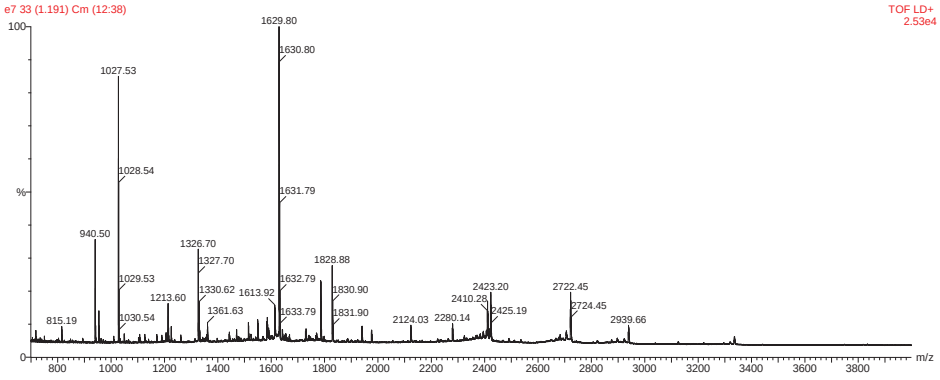

k) Reduction and alkylation of tears in 50 mM AMBIC followed by C18 purification

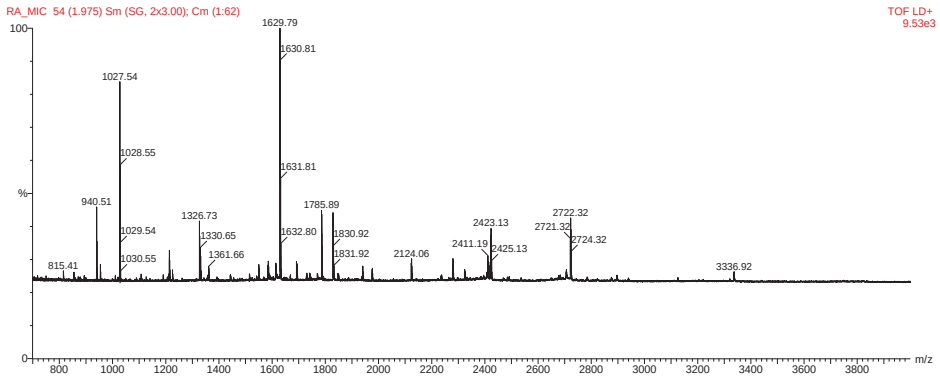

Figure 3.8 Reflectron mode MALDI mass spectra of tears, prepared with (a) Incubation of tears in 50 mM AMBIC buffer followed by C18 purification (b) centrifugation of tears followed by incubation in 50 mM AMBIC buffer and C18 purification (c) Dried Droplet of tears after dilution with 50mM AMBIC (d) Thin layer preparation of tears after dilution with 50 mM AMBIC buffer (e) Reverse thin layer preparation of tears after dilution with 50 mM AMBIC buffer (f) Acetone precipitation of tears followed by dilution in 50 mM AMBIC buffer and C18 purification (g) dilution in 50 mM AMBIC followed by 30 kDa cutoff spin filter purification (h) diluting in 0.1% TFA followed by 30 kDa cutoff spin filter purification (i) dilution in 0.1% FA followed by 30 kDa cutoff spin filter purification (j) dilution in ultra-pure water followed by 30 kDa cutoff spin filter purification (k) reduction and alkylation of tears in 50 mM ABC followed by C18 purification. The number of peptides resolved on each PMM is shown in Table 3.4.

a)

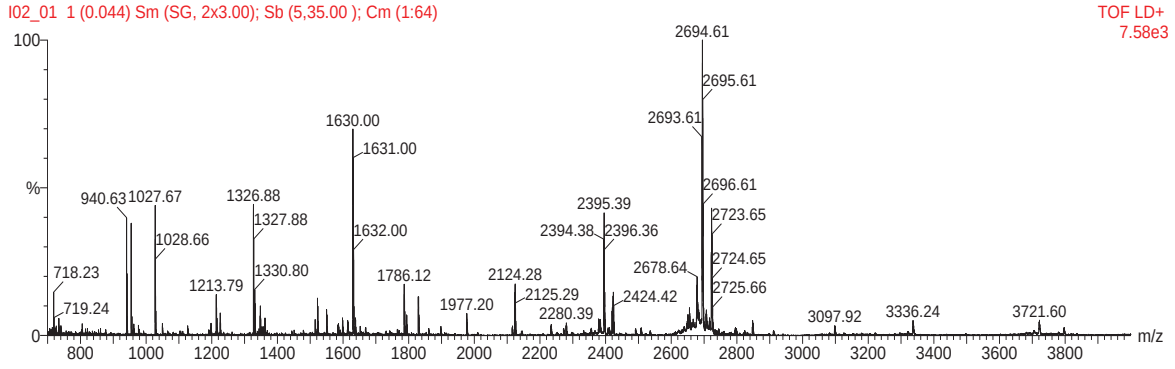
I02_01 1 (0.044) Sm (SG, 2x3.00); Sb (5,35.00); Cm (1:64)
TOF LD+
7.58e3
100
%
0
m/z
800 1000 1200 1400 1600 1800 2000 2200 2400 2600 2800 3000 3200 3400 3600 3800
2694.61
2695.61
2693.61
1630.00
1631.00
940.63
1027.67
1326.88
1327.88
2395.39
2696.61
2723.65
2394.38
2396.36
1028.66
1632.00
2724.65
718.23
1330.80
2678.64
2725.66
1213.79
1786.12
2124.28
2125.29
2424.42
719.24
1977.20
2280.39
3097.92
3336.24
3721.60

b)

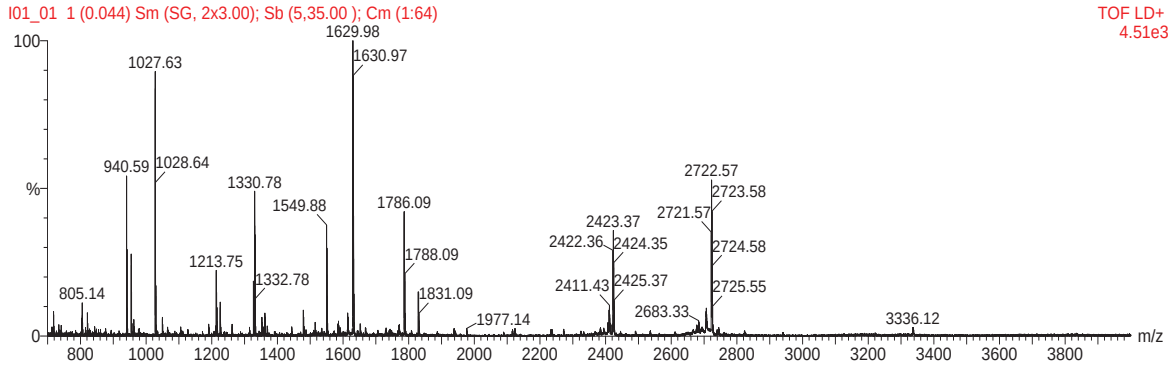
I01_01 1 (0.044) Sm (SG, 2x3.00); Sb (5,35.00); Cm (1:64)
TOF LD+
4.51e3
100
%
0
m/z
800 1000 1200 1400 1600 1800 2000 2200 2400 2600 2800 3000 3200 3400 3600 3800
1629.98
1630.97
1027.63
940.59
1028.64
1330.78
2722.57
2723.58
1549.88
1786.09
2721.57
2423.37
2422.36
2424.35
2724.58
1213.75
1788.09
1332.78
2425.37
805.14
1831.09
2411.43
2725.55
2683.33
1977.14
3336.12

c)

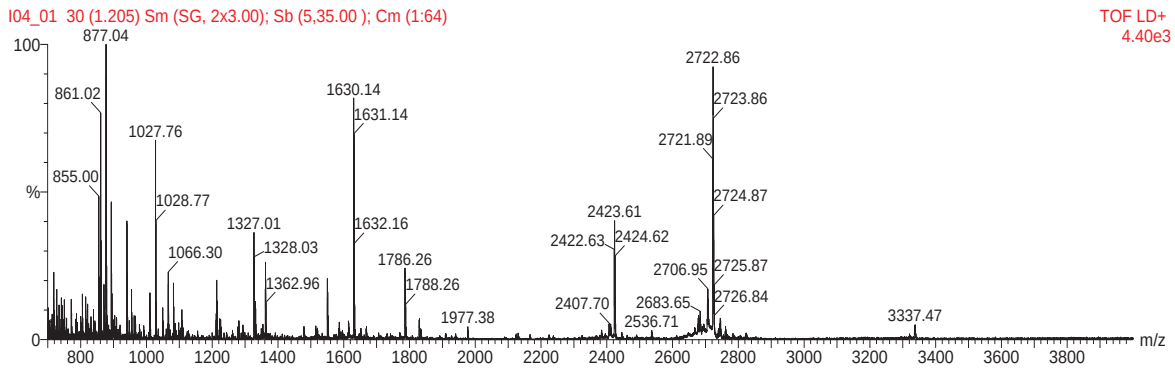
I04_01 30 (1.205) Sm (SG, 2x3.00); Sb (5,35.00); Cm (1:64)
TOF LD+
4.40e3
100
%
0
m/z
800 1000 1200 1400 1600 1800 2000 2200 2400 2600 2800 3000 3200 3400 3600 3800
877.04
2722.86
861.02
1630.14
2723.86
1631.14
1027.76
2721.89
855.00
2724.87
1028.77
2423.61
1327.01
1632.16
2422.63
2424.62
1066.30
1328.03
1786.26
2706.95
2725.87
1362.96
1788.26
2726.84
2407.70
2683.65
1977.38
2536.71
3337.47

d)

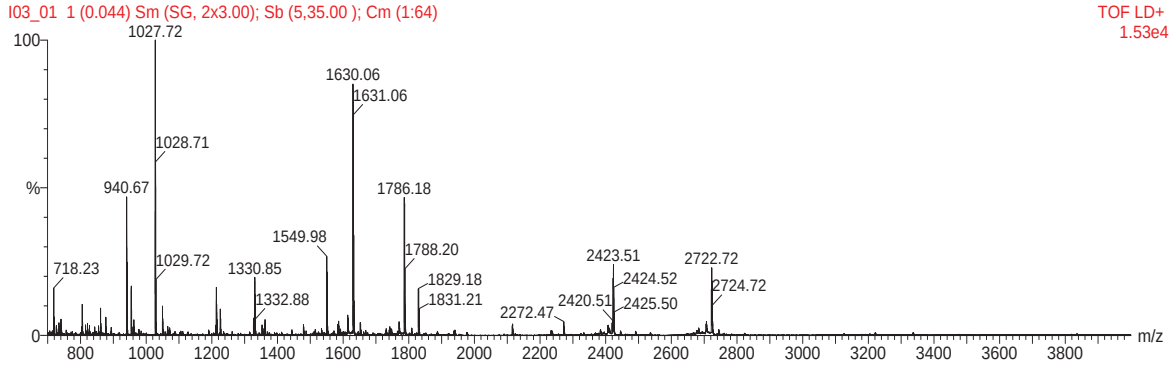

e)

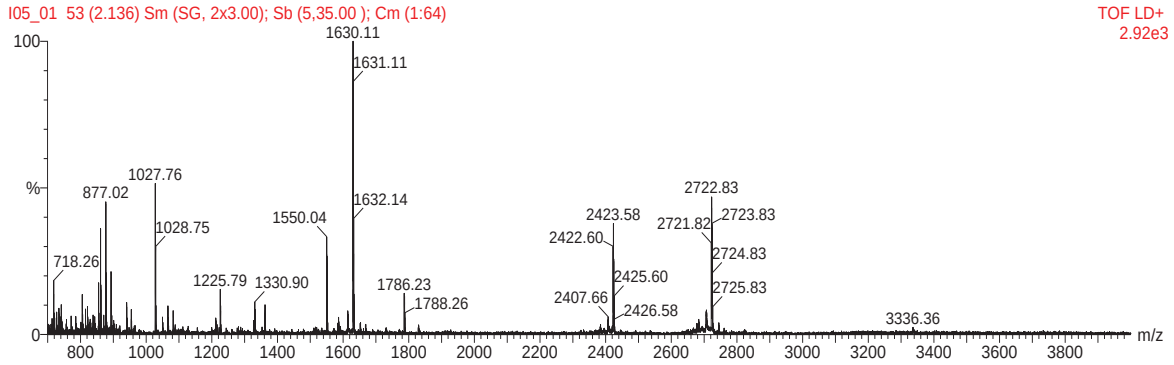

Figure 3.9 Comparison of variation between PMM of 5 individuals using the optimised protocol. Tears extracted from 5 individual healthy controls and a 5 µL aliquot from each individual was diluted in 50 mM AMBIC before being washed through a YM-30 spin filter. The flow through was collected and then subjected to C18 reverse phase filtration and analysis by MALDI-TOF. Spectra have been background subtracted and smoothed.

Table 3.4 Peptide count averages for various treatments on human tears. Tears were either treated in 0.1% trifluoroacetic acid (TFA), 0.1% formic acid (FA) ultrapure water (dH_2O) or 50 mM ammonium bicarbonate (AMBIC). Numbers in parentheses are standard deviations of triplicate analyses of the respective treatment. The best protocols were repeated on 2 further samples each pooled from 3 separate individuals (see Table 3.5).

Treatment	C18 reverse phase microcolumn purification	Spin and C18 reverse phase microcolumn purification	Thin Layer	Reverse Thin Layer	Dried Droplet	Acetone and C18 reverse phase microcolumn purification	Centrifugal filters and C18 reverse phase microcolumn purification	Reduction and Alkylation
TFA	33.7 (+3.8)	82.3(+31.4)	0.0 (+0.0)	0.0 (+0.0)	0.0 (+0.0)	13.3 (+5.7)	122.7 (+20.6)	N/A
FA	52.0 (+40.6)	78.0 (+22.6)	0.0 (+0.0)	0.0 (+0.0)	0.0 (+0.0)	2.0 (+0.0)	123.3 (+21.0)	N/A
dH_2O	39.0 (+4.0)	43.3 (+10.8)	0.0 (+0.0)	0.0 (+0.0)	0.0 (+0.0)	6.7 (+5.8)	115.7 (+7.8)	N/A
AMBIC	63.0 (+18.1)	56.3 (+13.6)	0.0 (+0.0)	0.0 (+0.0)	0.0 (+0.0)	13.7 (+17.6)	145.3 (+11.5)	73.3 (+19.7)

Table 3.5 Peptide count averages for various treatments on human tears. Experiments that produced a high number of peptides in the preliminary study were performed on 3 samples each pooled from separate individuals.

		C18 reverse phase microcolumn purification			Spin and C18 reverse phase microcolumn purification			Acetone and C18 reverse phase microcolumn purification			Centrifugal filters and C18 reverse phase microcolumn purification		
	Number	Average	S.D	CV (%)	Average	S.D	CV (%)	Average	S.D	CV (%)	Average	S.D	CV (%)
TFA	1	37	9.54	25.78	22.67	10.07	44.41	30.33	8.74	28.8	112	23.26	20.77
	2	80.67	8.33	10.32	46.67	38.4	82.28	34.67	10.6	30.57	111.67	13.05	11.69
	3	33.7	3.8	11.25	107	14	13.08	16	1.7	10.83	122.7	20.6	16.75
FA	1	29.67	14.29	48.18	46.33	15.37	33.18	35.5	9.19	25.89	98	19.29	19.68
	2	79	13.9	17.59	81.33	21.13	25.98	37	2.83	7.64	139.67	4.16	2.98
	3	69.67	32.52	46.67	100	10.1	10.15	2	0	0	123.3	21	17.05
AMBIC	1	13.33	5.69	42.65	14	3.61	25.75	29.2	9.52	32.62	96.67	10.21	10.57
	2	12.67	2.08	16.43	12.33	3.06	24.77	26	16.16	62.14	145.67	1.15	0.79
	3	39	4	10.26	43.3	10.8	24.89	19.3	16.2	83.62	115.7	7.8	6.72
H2O	1	8.67	7.37	85.05	9.67	3.21	33.25	37	41.58	112.38	98	19.29	19.68
	2	19.33	5.69	29.41	22	15.13	68.79	27.33	18.5	67.69	139.67	4.16	2.98
	3	63	18.1	28.7	56.3	13.6	24.1	19	14.5	76.45	145.3	11.5	7.92

3.3.3 Biomarker Discovery using MALDI

Peptide mass maps from tears of patients of Con, DM and DR backgrounds were compared to discern peptides differentially expressed between the three different groups. A total of 43 peptide masses were found to have altered with the onset of diabetes and diabetic retinopathy. Peptide masses found to be differentially expressed were categorised into two "priority" groups. "Priority one masses" were peptide masses observed to either appear or disappear with the onset of diabetes or diabetic retinopathy. "Priority two masses" were peptide masses observed to alter in intensity with the development of diabetes and/or diabetic retinopathy.

Figure 3.11 displays examples of spectra demonstrating alterations in intensity between healthy controls, diabetic and diabetic retinopathy patients. Table 3.6 displays a summary of the peptides of interest detected and organised into the two priority lists.

Spectra for the m/z range 100-1300

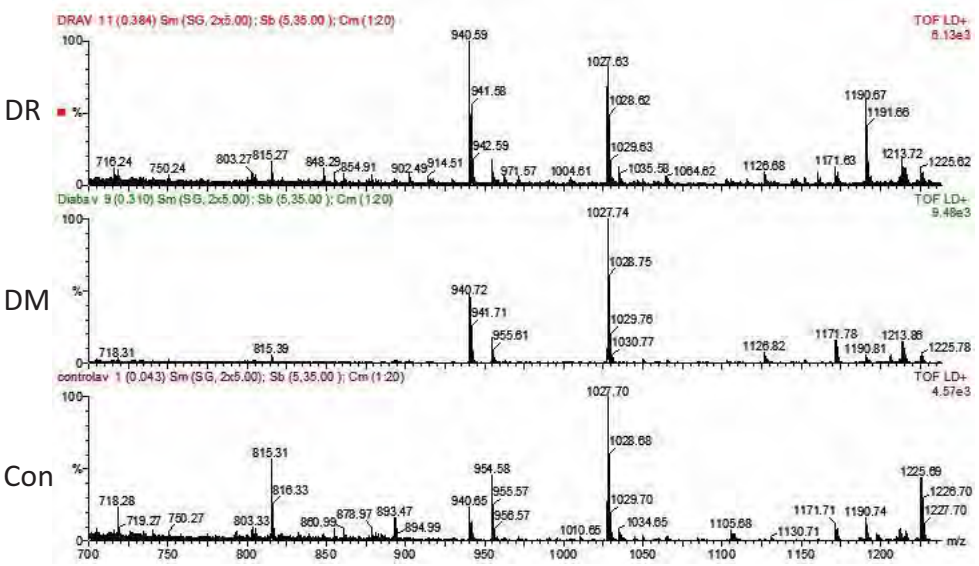

Spectra for the m/z range 1280-1390

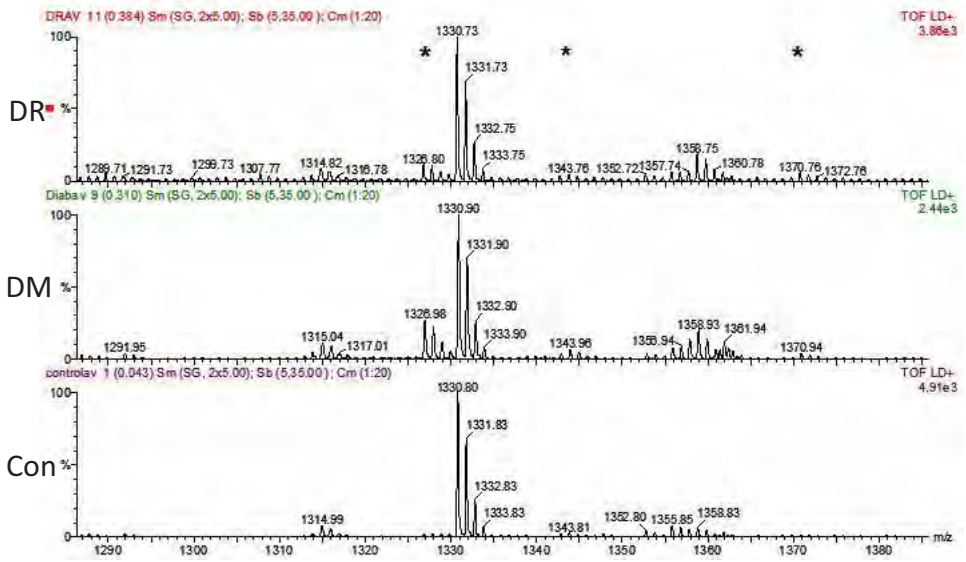

Spectra for the m/z range 1690-2000

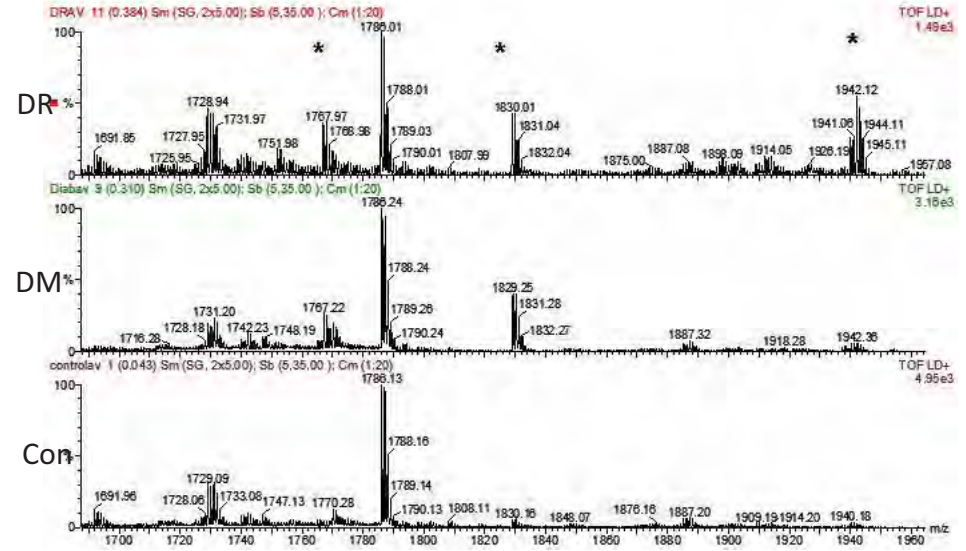

Figure 3.10 MALDI-MS spectra displaying relative abundance differences of peptide masses between pooled tears (*n=5*) of subjects with diabetes and retinopathy, diabetic and healthy controls. Peptide shown to be different in abundance are listed in Table 3.6

Table 3.6 Peptides that were shown to change in abundance as determined by MALDI-MS. Masses were organised into two "priority" groups. "Priority one masses" was observed to either appear or disappear with the onset of diabetes or diabetic retinopathy. "Priority two masses" were peptide masses observed to alter in intensities with the development of diabetes and/or diabetic retinopathy.

Priority 1 (m/z)		Priority 2 (m/z)			
716.24	1752	750.24	1126.68	1358.75	1786.01
848.29	1767.97	893.41	1151.66	1360	1848.07
929.57	1829.01	902.49	1197.83	1370.76	1887.32
971.57	1940.06	940.59	1213.72	1398.79	
1143.81	1492.12	954.61	1225.69	1430.8	
1160.7	2234.48	962.57	1238.7	1514.88	
1326.8	3336.09	990.84	1261.7	1541.09	
1326.95	3836.49	1102.68	1307.75	1585.9	

3.3.4 Spin Filter Fractionation and Analysis by LC-MS/MS

Tear samples were analysed by LC-MS/MS in an effort to identify the peptides of interest (masses listed in Table 3.6). Fractions under 30 kDa were collected after spin filter fractionation (section 3.2.6) and analysed via LC-MS/MS. The analysis did not produce any viable data as no peptides were matched to the data that was collected.

3.3.5 MF10 Microflow Fractionation

As a result of the inability to identify the peptides from the masses of interest using LC-MS/MS, an alternative technique was required to identify and quantitate peptides of interest in the tear samples. Fractionation would need to be compatible with LC-MS/MS whilst maintaining the ability to quantitate using additional labeling chemistries such as iTRAQ labeling.

In the initial runs using a control sample to test the method's suitability for analysis of patient samples, 1-25kDa fractions collected after MF10separation were analysed by LC-MS/MS. Use of this method resulted in an increased number of peptides being identified compared to fractionation using spin filters coupled with LC-MS/MS. An average of 2673 (±

667.5) peptides resulting from this method was observed for queries using MASCOT, whilst only 62 (± 22.6) peptides on average were observed with spin filters.

A large amount of high abundance tear peptides were detected such as lactoferrin. Large amounts of keratin were also found in the fractions, which could be present due to the highly abundant nature of this protein species in tears or possibly as a result of contamination as this method requires a reasonable amount of user handling. MF10 fractions containing higher molecular weight proteins: 25 kDa–65 kDa and >65 kDa, were collected and separated on a 1D-E gel. SDS-PAGE analysis of the tear fractions collected after separation on an MF10 demonstrated that there was efficient separation of tear proteins into their constituent sized fractions (Figure 3.11).

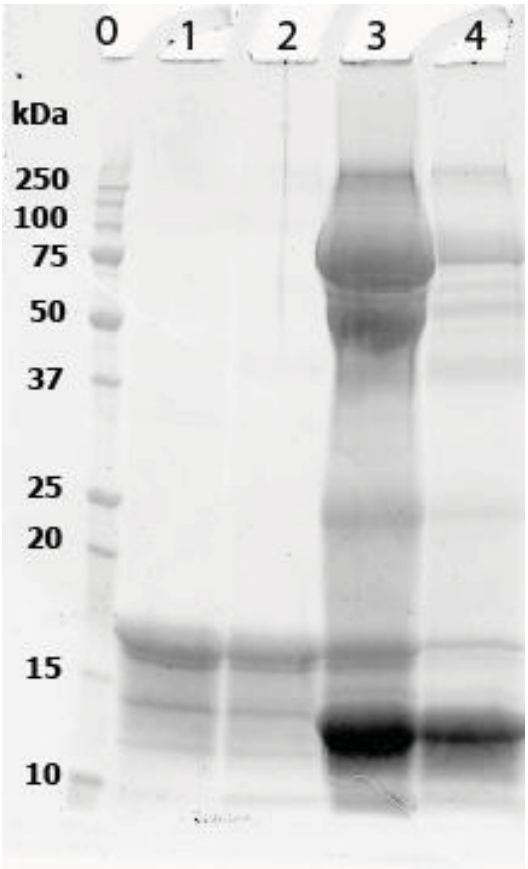

Figure 3.11 Comparison of MF10 fractionation of tears. Fractions 3 and Fraction 4 from MF10 fractionation of tears (*n*=2) were separated on a 1D-gel. Lanes 0 - MW marker; Lanes 1 and 2 – fraction 3 (25-65 kDa); Lanes 3 and 4 – fraction 4 (>65 kDa).Proteins were separated on a 8-16% Tris-HCl gel and stained with Sypro Ruby (Bio-Rad).

3.3.6 iTraq Labelling, Quantitation and Idenfitication

Following the MF10 fractionation, the iTRAQ protocol was trialed using fractions 1 (1-5kda) and 2 (5-25 kDa) fractionated tears collected from Con (*n=20*), DM (*n=20*) and DR patients (*n=20*). Each group was pooled and 100 µg from each pool was used in the analysis. All patients' tears were sex and age matched. The aim of this experiment was to provide the foundation of a preliminary study of differences in tear protein and peptide abundance between the three groups, as well as an evaluation on the efficiency of the iTRAQ technology coupled with MF10 fractionation to monitor such abundance differences. However, no human proteins were identified via 2D LC MS/MS.

3.3.7 Label-free Quantitation of Peptides

3.3.7.1 Peak Integration using Decyder MS

Tear Peptides 5-25 kDa

Decyder was used to interrogate the results of the 5-25 kDa MF10 fraction of tears analysed by LC MS/MS to determine significant quantitative changes to tear peptides. After the pooled tears of healthy controls (*n*=20), diabetic (*n*=20) and diabetic retinopathy patients (*n*=20) were separated by MF10 and processed (Section 2.8), the 5-25 kDa fractions from each pool were injected 3 times into the LC-FT MS and the data processed using Decyder MS.

This analysis identified 2440 peptides representing 1842 proteins and protein isoforms which were present in either Con, DM or DR. This analysis identified 2057 peptides of interest to have altered in abundance on progression from Con to DM to DR. These peptides displayed extremely low ANOVA p-statistics ($1e^{-1}$ – $1e^{-11}$). The potential biomarkers were categorized into different categories based on the degree of change across Con, DM and DR. Figure 3.13 illustrates the top ten peptides which demonstrated the highest degree of change between tear peptides of:

- Con/DM and DR
- Con and DM
- Con and DR
- Con and DM/DR
- DM and DR.

The peptides from these categories that were successfully sequenced and identified are tabulated in Table 3.7. Analysis of the total data shown in table 3.7 suggests overall, there are a relatively small number of peptides that are increased in abundance within DR tears compared to Con and DM tears.

a) Peptides changing in abundance between both Control and Diabetic as compared with Retinopathy

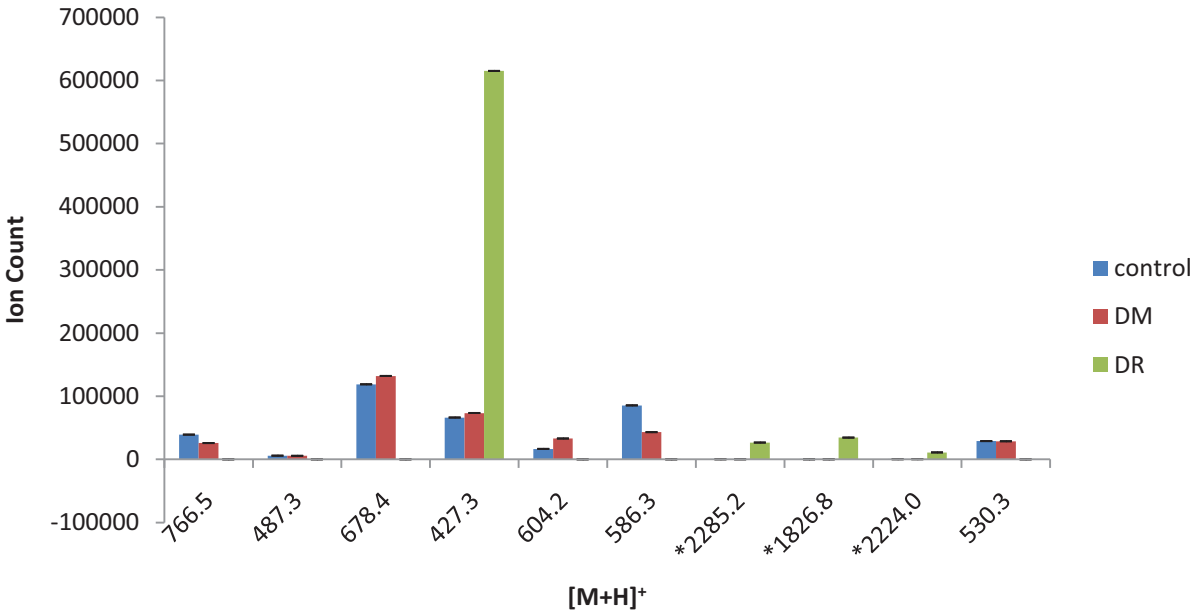

b) Peptides changing in abundance between Control and Diabetic

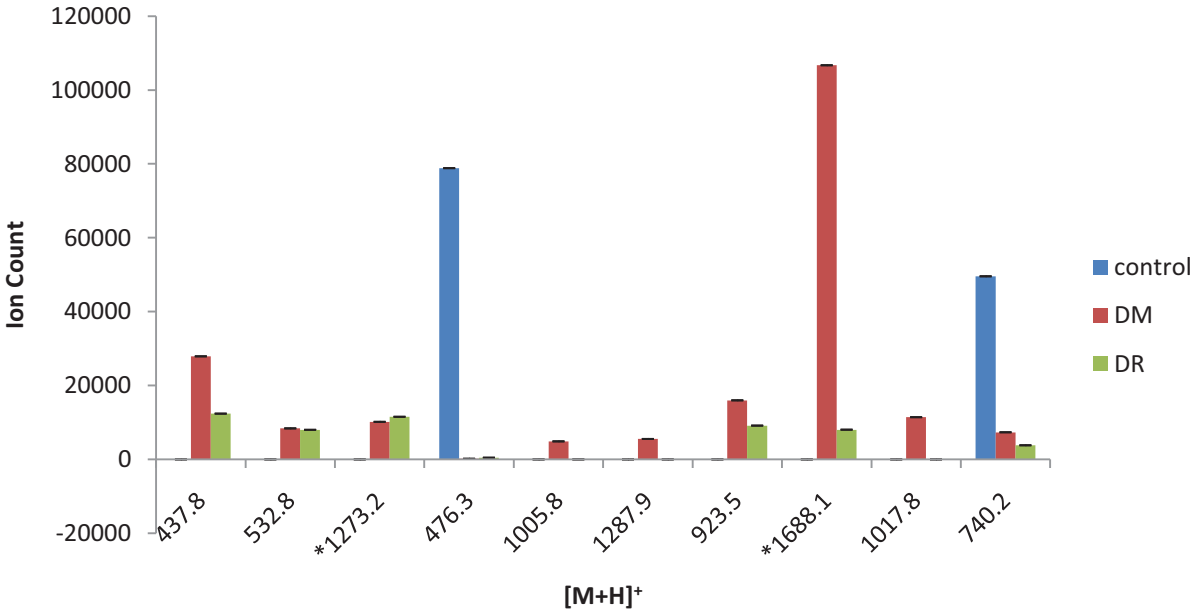

c) Peptides changing in abundance between Control and Retinopathy

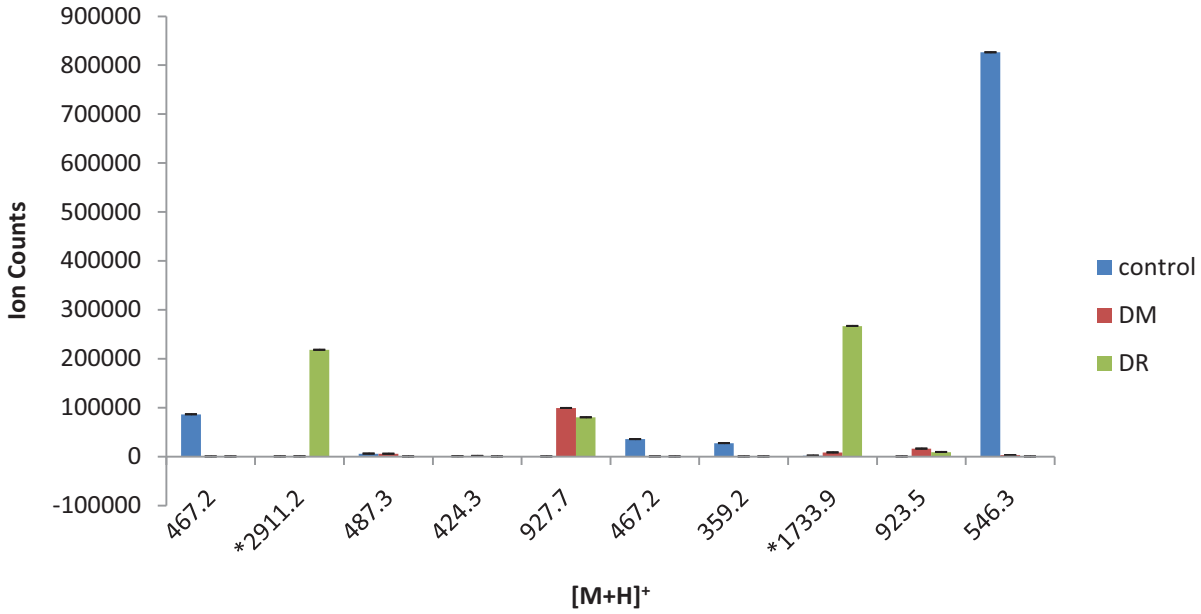

d) Peptides changing in abundance between both Diabetic and Retinopathy as compared with Control

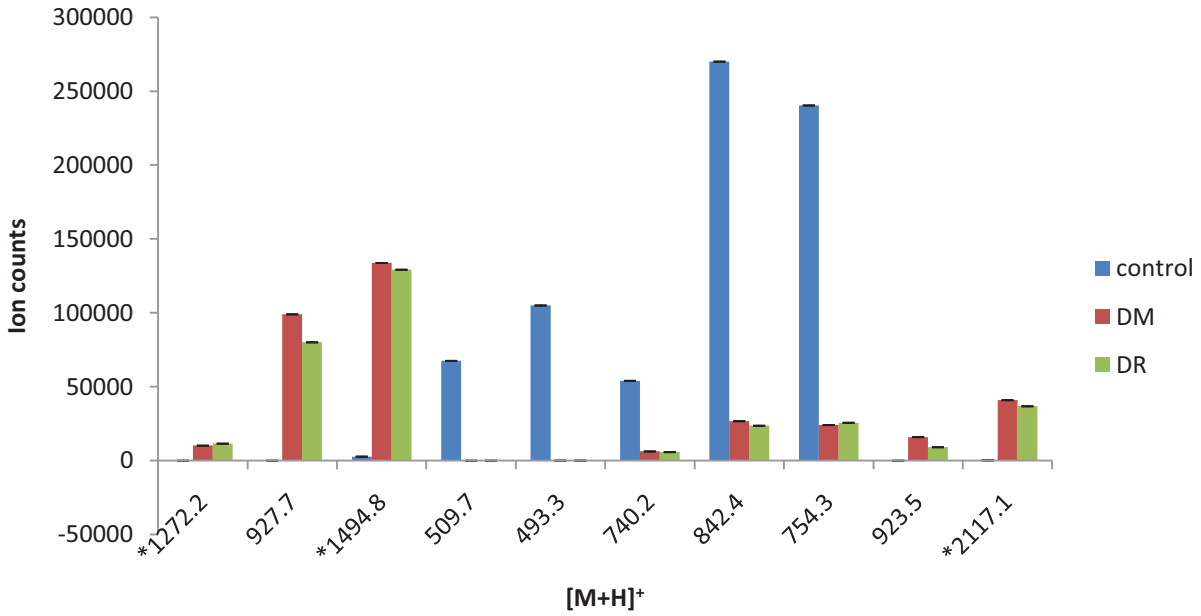

e) Peptides changing in abundance between Diabetic and Retinopathy

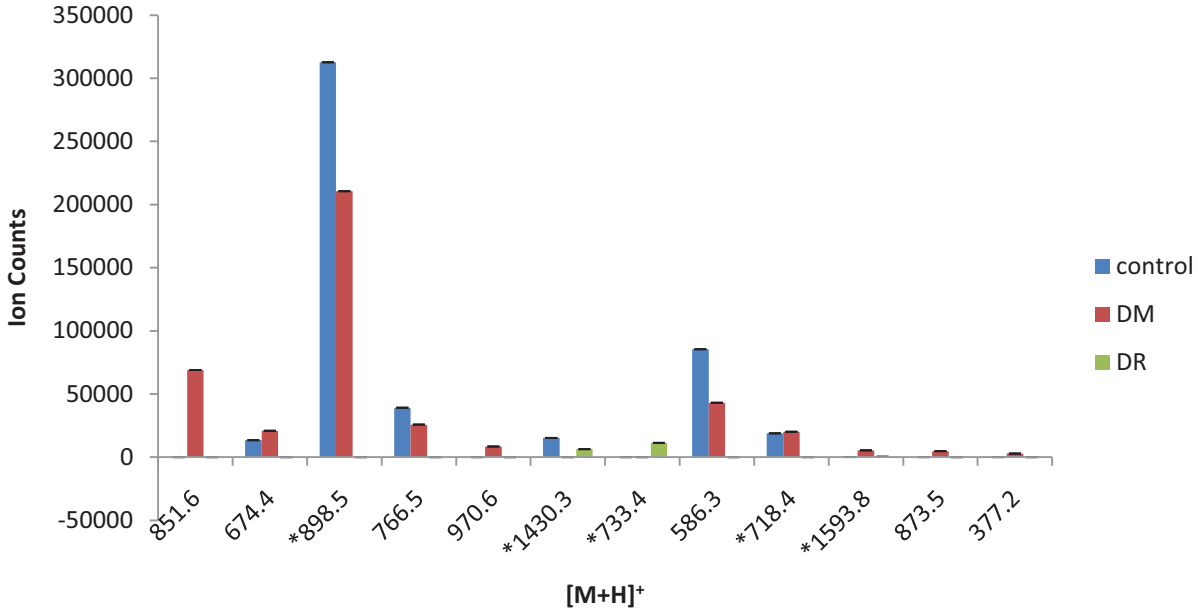

Figure 3.12 Comparisons between Con, DM and DR tear peptides identified in 5-25 kDa. Peptides of interest are organised into a) Con/DM vs DR; b) Con vs DM; c) Con vs DR; d) Con vs DM/DR and e) DM vs DR. Illustrated are average ion counts (cps) (± 1 S.D.) after 3 injections of the respective pooled samples. Peptide masses marked with a * were successfully identified and are tabulated in table 3.7.

Table 3.7 Peptides successfully identified in a comparison between control diabetic and retinopathy tear samples in a 5-25 kDa fraction after MF10 fractionation. All peptides were found in varying abundances in control, diabetic without retinopathy and diabetic with retinopathy.

$[M+H]^+$	ID Score	Peptide	ID Details	Protein	ANOVA p
2286.2	28.3	KLVGRDPKNNLEALEDFEKA	lipocalin 1 precursor [Homo sapiens]	gi|4504963	4.01E-07
1827.8	15.8	CLCASLHVCVCVYVC	hypothetical protein [Homo sapiens]	gi|169178571	8.32E-07
2225	14.8	NTTXSAGRCCCPCWPLRSSVS	PIK4CA variant protein [Homo sapiens]	gi|169215728	9.24E-07
1273.2	35.6	LPRFPSVSLQE	pHL E1F1 [Homo sapiens]	gi|1050983	1.40E-10
1689.1	15.2	ECSECGKIFSMKKSL	zinc finger protein 157 [Homo sapiens]	gi|113204607	1.04E-10
2912.2	20.3	MAYPCGDMNSFSQGLCLSCKKGRCN	hepatic lipase precursor [Homo sapiens]	gi|307129	4.18E-09
1734.9	65.4	TINSDISIPEYKELL	secretoglobin, family 2A, member 1 [Homo sapiens]	gi|4505171	3.79E-08
1273.2	35.6	LPRFPSVSLQE	pHL E1F1 [Homo sapiens]	gi|1050983	1.40E-10
1495.8	61.8	FIENGSEFAQKLL	lacritin precursor [Homo sapiens]	gi|15187164	7.05E-09
2118.1	52	SGSSEEQGGSSRALVSTLVPLG	transmembrane secretory component; poly-Ig receptor; SC [Homo sapiens]	gi|238236	5.71E-08
899.5	8.2	GQGKGRLAL	hypothetical protein [Homo sapiens]	gi|5912020	9.83E-09
1431.3	29.9	SLPRFPSVSLQEA	pHL E1F1 [Homo sapiens]	gi|1050983	8.21E-09
734.4	26.1	ITKYPL	pleckstrin homology domain containing, family G (with RhoGef domain) member 6 [Homo sapiens]	gi|8922581	1.24E-07
719.4	9.7	KKSAXSA	YRRM	gi|1205999	2.22E-06

3.4 Discussion

The general aim of this work was to determine an optimal approach to investigate the tear proteome of multiple samples rather than perform a thorough investigation of a single tear proteome. As such it was not necessary for the strategies used to analyse the entire proteome or peptidome; more importance was placed on the quality of the resulting data and ease of implementation for multiple samples. The p*I* 4-7 region of the proteome was investigated using 2D gel electrophoresis as previous studies have demonstrated the majority of tear proteins are found in this region [38, 125-126]. In these experiments, a single gel were of each pooled sample (*n=20*) was run. Any variation would be attributed to technical variation from the instruments used in this study. It is anticipated that variation observed in future experiments assaying larger sample numbers will reflect biological variation between subjects and of the disease-associated tears.

The sampling method is critical in proteomic and peptidomic investigations as different sampling methods will induce both environmental changes and reflex changes to the tear film. Several tear sampling methods are available; however, the most efficient one would avoid irritation and stimulation of the surrounding epithelial cells of the ocular region [127-128]. Glass capillaries would sample tears via capillary action. This resulted in minimal contact to the ocular environment whilst maximizing tear collection thus so this method was chosen for use in the current study.

3.4.1 Biological Variation

Due to the limited volume of tears that can be collected from a subject at any one time, most studies have reported using tear volume rather than protein concentration in their investigations into tear biomarkers [37-38, 125-126, 129] [130] [57]. This study illustrated the extensive variation that can be observed when comparing a standard volume of tears. This variation can be reduced by standardizing sample loading with tear protein concentration.

Multiple studies have assessed the biological variation between reflex and open-eye tears, as well as day-to-day variation between healthy subjects. Several studies report that proteins such as lysozyme, sIgA and serum albumin do increase when comparing reflex to open to closed eye tears [131]. On the contrary, there is a body of studies that suggest proteins such as tear specific prealbumin and lactoferrin do not alter in abundance

between the different types of tears [65, 67]. There is no consensus as to the changes to the total protein content between the types of tears collected. Evidence suggests regulated tear proteins are relatively stable as they change with the pace of the tear flow rate. On the other hand, secreted proteins are increased on the occasion where the ocular region is under stress such as hypoxia incurred within the closed eye environment. As a result of these differences, collection of the tears from subjects for future experiments was restricted to 10 am to 12 pm every day.

3.4.2 Analysis of Proteins

Unless one can maximize the resolution of the complex tear protein mixture, one cannot easily identify proteins of interest. Different concentrations of tear protein were used to determine the optimal load separated on a 2-DE gel to interrogate the tear proteome. The results suggest that a large amount of protein, coupled with detection using a fluorescent dye is required to resolve the lower abundance proteins within a tear sample. Difficulty in discerning these proteins in a Coomassie Brilliant Blue stained gel emphasizes the limitations associated with the resolution, visualization and isolation of lower abundance proteins that impedes efficient analysis using current proteomic paradigms. Taking into account the limited volume of tears that can be collected comfortably with minimal irritation of the ocular environment, current proteomic platforms using 2-DE technology cannot be used to efficiently interrogate the differences between samples. A platform is required that can concentrate and enrich tear proteins from its wide dynamic range, which must be analysed using highly sensitive technology.

3.4.3 Shotgun Proteome Analysis of Tears

A shotgun approach using 2-D LC-MS/MS analysis of tears demonstrated that this sample type could be successfully separated and analysed using shotgun strategies. A comparison with 2-DE demonstrated that through 2-D LC-MS/MS analysis of tears a significantly higher number of tear proteins can be identified per µg of tear protein analysed. Specifically, using 2-DE technology, 0.09 proteins were identified per µg of protein analysed compared to 0.45 proteins identified per µg of protein analysed by 2-D LC-MS/MS. The technology however, is not without its issues. In this study quantitative labelling analysis (iTRAQ) coupled to 2-D LC-MS/MS after MF10 fractionation was unsuccessful due to incompatibility between the reagents for each technique (refer to section 3.4.5). Whilst

this study did not explore non-labelling quantitative analysis strategies with 2-D LC-MS/MS, it is foreseen that the volume of data generated from such an analysis would increase exponentially and potentially unmanageable for a multiple sample study. Furthermore, studies have indicated through a 2-D LC-MS/MS approach, repeatability is reduced with every replicate analysis – an important feature to confirm statistical significance. Such a decrease in repeatability is due to slight variations in elution patterns and loss of peptides during analyte transfer between the two modes of separation [100]. Whilst the technique identified a significant number of proteins over one run, several issues inherent with the technology concluded continuation of the quantitative analysis of the tear proteins in this study were impractical.

3.4.4 Peptidomic Strategies using MALDI-MS

From the 2-DE analysis of tears performed in this study, it is clear that a spectrum of proteins and peptides remains undetected using this technology. This region is of high interest for investigation of changes to the protein content of tears associated with the onset of diabetes and diabetic retinopathy. In a recent comprehensive analysis of tears using high powered mass spectrometers, de Souza et al., determined an equal number of protease and protease inhibitors [46]. These enzymes complement each other, maintaining equilibrium of the dynamic protein turnover in a secreted fluid [46, 132-133]. Studies have also established that an imbalance of these enzymes will indicate or lead to disease states in the ocular environment, placing importance on peptide investigation.

MALDI-MS technology can be used to investigate the peptidomic profile of tears. We initially examined various sampling treatments using MALDI-MS with the focus on maximising the resolution of peptides from the low molecular weight proteome of tears. This study demonstrated that centrifugal filtration coupled with C18 reverse phase microcolumn purification maximizes the amount of peptides visualised on a tear peptide mass map (PMM). The optimised method reduced lengthy analysis time and minimised effort required for sample preparation and resulted in efficient recovery and resolution of peptides.

Sample dilution with mass spectrometry-compatible solvents is necessary due to the small volumes of tears that can be collected per patient and the larger volumes required for sample preparation technology i.e. centrifugal filters. The use of sample diluents such as

ammonium bicarbonate (AMBIC), trifluoroacetic acid (TFA), formic acid (FA) and ultra-pure water did not affect the number of peptides to be concentrated by C18 reverse phase microcolumn purification. From this study, AMBIC is the preferred solvent for the treatment of tear samples for a number of reasons;

(i) the use of ultra-pure water has the potential to activate proteases [134],

(ii) FA in particular is used in the chemical digestion of proteins and peptides. Thus, their use could inadvertently cause non-specific digestion, perhaps hampering peptidomic analysis of tears [135].

(iii) Peptides are treated with TFA and/or FA in later mass spectrometry sample preparation stages, thus, treatments with TFA and FA would be redundant in the early stages of tear sample preparation. The use of AMBIC permits the possibility for future enzymatic reactions to occur should this be required by the experimental design [136].

Whilst collecting tears using glass capillaries is advantageous over other tear sampling methods, this method also collects non-volatile compounds such as non-polar sterol esters and wax within the lipid layer of the tear film. The complexity of tears might render redundant any “on-target” sample preparations such as dried-droplet, thin-layer and reverse thin-layer techniques. These sample preparations would concentrate all non-volatile contaminants that can cause ion-suppression with any MALDI analysis [137]. Whilst protein concentration techniques, such as acetone precipitation, remove the aforementioned contaminants they do not remove larger molecular weight proteins present in tears. High MW range proteins in tears will physically congest the C18 reverse phase microcolumn purification, thus preventing the maximal number of peptides in tears to be cleaned, concentrated to be resolved using MALDI-TOF MS. Additionally, the failure to enrich small peptides in this experiment can be explained limited success acetone precipitation methods generally have with precipitating small peptides.

In an attempt to maximize the number of low molecular weight species of tears seen in MS analysis, reduction and alkylation of large complexes native to tears is necessary. This process coupled with C18 microcolumn purification suffers from limitations associated with the presence of high MW residual proteins in solution. These proteins will physically congest the C18 reverse phase microcolumn purification, albeit not to the extent of that following acetone precipitation.

Centrifugal filters are an efficient method, physically removing the larger proteins, salts, detergents and contaminants from the population of small proteins and peptides in the filtrate which are later concentrated and cleaned with C18 reverse phase microcolumn purification. The attraction of the centrifugal filtration protocol for tears lies with the ease, speed and efficiency of sample cleanup and concentration of highly complex biological samples. Additionally micro centrifuge filtration devices have the capacity to concentrate peptides whilst also eliminating contaminants that could otherwise suppress ions resolved on a MS.

The advantage of using a pattern-based test for a diagnostic to detect diabetic retinopathy and diabetes resides in the fact that such a diagnostic is potentially fast, requires minimal processing and the appearance of a suite of peptide masses rather than identification of a gold standard biomarker for the disease. This ensures easier, higher specificity detection for the disease. Prefractionation of tears coupled with MALDI will increase the resolution of lower molecular weight species of protein and peptides. What has been developed is equivalent to a SELDI approach to finding biomarkers, instead using a standard MALDI mass spectrometer.

Unfortunately, the technology does carry substantial caveats. From a research standpoint, this analysis is quite similar to a SELDI technology and as such, several considerations must be made before using this technology for biomarker discovery. The technology lacks the potential for absolute quantitation, thus abundance changes between and within runs cannot be adequately monitored. Discoveries would not characterize potential post-translational modification details. Furthermore, the capital costs to maintain the technology behind the assay would render it out of reach of most health professionals and more amenable in a preclinical setting. Ideally, this strategy would be best used as a basic preliminary approach to discovery phases of experiments to assess current research strategies [138].

Nonetheless, from this study, it is clear that there are definite changes that can be found between the tears of healthy controls, diabetic and diabetic retinopathy patients. The nature of the preliminary MALDI study means these changes could not be identified or the exact abundance profiles described accurately. There is a need to identify the suite of

markers from within the pattern-based signatures to provide an appropriate test for low-cost use. Thus, effort needs to be directed towards sequencing and identification of these markers using MS technologies such as LC-MS/MS. Nonetheless it is envisioned that once biomarkers are identified, such technology could be used to develop a fast and easy assay or diagnostic to detect the onset of DM or DR.

3.4.5 Sample Recovery and MF10 Fractionation

A major issue shared amongst the technologies used in this study is sample recovery. Ideally, with all strategies, sample recovery must be at a high level for every process in the experiment to allow the maximum concentration of proteins for analysis. This is critical for discovery experiments that are looking at low abundance proteins in a bio-fluid which itself is in limited supply. Unfortunately protocols used in this method development suffered from minimal protein recovery associated with rigorous clean-up steps to remove contaminating buffers, denaturants and surfactants introduced during fractionation that were incompatible with downstream MS analysis.

Separated on the gel in figure 3.11 are proteins that were fractioned in the MF10 under denatured and reduced conditions. The size of the membranes the machine is fitted with are nominal for native conditions. Denatured proteins do not have the same clean separation seen for native samples resulting in overlapping size fractionation as was seen here. Nonetheless, the gels demonstrated successful fractionation of lower molecular weight species in tear samples.

An indirect comparison between methods using spin filters and MF10 fractionation demonstrates that relatively large sample loss is experienced through peptide partitioning with spin filters. One hundred and forty five peaks were observed alone in spin filter coupled with MALDI analysis (table 3.5) compared to >6000 peptides identified in 5-25kDa MF10 fractionation after DeCyder analysis (Section 3.3.7.1). In part, this is explained by the difference in membrane structure between spin filters and those used MF10 separation. MF10 membranes are lined with polyacrylamide and as such, create turbulence during separation which limits accumulation of protein and thus membrane fouling, which is experienced with spin filters. Membrane fouling events during spin filter fractionation may also in part explain the difficulty sequencing peptides isolated from the 1-30 kDa fractions of tears with LC-MS/MS in addition to the presence of any residual contaminating salts etc.

Additionally, separation occurs over differing time periods. Spin filters are limited by a 30 minute run time, whilst separation on the MF10 occurs across 2.5 hrs, allowing greater time for separation and thus enrichment of the tear peptidomic fraction. Peptide recovery was not efficient and compatible between analysis with MALDI-MS and LC-MS/MS technology, using spin filter technology. Based on the aforementioned circumstances, MF10 fractionation was a far superior technology to use in the detection of changes in low abundance proteins and peptides in a complex and limited bio-fluid such as tears.

Unfortunately, buffers used to fractionate using the MF10 are amine based, which interfere with amine-tagging technology such as iTRAQ [139]. Furthermore, the additional chromatography steps introduced to remove buffer and concentrate peptides before iTRAQ tagging such as SCX and C18 chromatography are rigorous steps, that, while necessary, do remove a significant proportion of the tear peptidome prior to MS sequencing. For these reasons label free quantitation was attempted.

3.4.6 Label-free Quantitation

Label-free quantitation by-passes the sample loss challenges associated with label quantitation strategies. There are minimal clean-up preparative steps required prior to MS sequencing. Whilst a chromatographic cleanup of the sample is required it is less rigourous than the multiple cleanups required using iTRAQ protocols. As demonstrated by the data, there is minimal peptide loss between MF10 fractionation and peak integration using the Decyder MS analysis software. Peak integration performs a comprehensive and exhaustive interrogation of all the peptides amongst the data generated by the LC-MS/MS. An indirect comparison between the number of peptides queried after MF10 analysis using MASCOT (2673 ± 667.5 in the 1-25 kDa fraction) and the number of peptides queried using Decyder MS (2057 peptides in a 5-25 kDa fraction) tends to suggest that there is minimal loss of peptides between the stages in the workflow. Thus, differences between lower molecular weight peptidomes and proteomes of diseased and healthy control patients can be compared and scrutinized effectively. Taking into account the variable nature of proteotypic peptides, it must be stressed that it is fundamental to repeat runs so as to generate consistent results during biomarker discovery and validation. As the method that was developed was potentially a high throughput quantitative approach such repeats were possible (see chapter 4).

Two distinct mass-spectrometry based quantitative approaches were studied in this experiment. Spectral counting and peak integration were used to compare changes to tear peptides and proteins in a 5-25 kDa fraction of tears between control, DM and DR. Limitations of current mass spectrometry technology means that peak integration is preferable over spectral counting in biomarker discovery strategies. Due to the duty cycle of a mass spectrometer the top 4 peptides are fragmented in an MS scan. With peak integration, every precursor ion within the MS sensitivity range can be extracted and included in the quantification process, since peak integration correlates the total ion chromatogram (TIC) of a peptide. For those peptides that are too low in intensity to undergo fragmentation, an inclusion list can be made and sample re-injected to gather qualitative data for that peptide. Unfortunately, with spectral counting this is not a viable option, since the method relies on counting MS/MS spectra rather than comparing MS scans. Thus, differences in the MS scans cannot be discerned and as such, the dynamic range of peptides/proteins can't be compared between samples.

Nonetheless, when looking at these preliminary results derived from both the Scaffold and Peak integration analysis, it is clear that there is a substantial difference between the peptide and protein abundance profiles of healthy controls, diabetic and diabetic retinopathy patients. It is evident from these preliminary investigative experiments that there is a characteristic decrease in the abundance of the majority of peptides with the onset of DR. Interestingly, there tends to be an increase in abundance of the tear peptides in DM. However, this observation is not a definitive description of tear biomarker candidates. Biomarkers will need to undergo rigorous statistical and replicative testing to confirm or invalidate the trends seen in this study.

3.4.7 Concluding Remarks

In this chapter, several methodologies were assessed as to its efficiency to detect protein and peptide species from tears, a bio-fluid limited by its quantity. The strategy which can resolve a large number of protein and peptide species is the ideal method to mine tears for potential biomarker candidates. In assessing the benefits of each method, it should be acknowledged that each fractionation and MS detection method is dependent upon the different chemistries and biophysical characteristics of the protein and peptide species within tear samples. Thus while it is inevitable that several lists of proteins and peptides vary between different detection and fractionation methods, it is essential that the search

parameters are stringent so as to ensure the problems with false positive identification is negated.

Data derived from both the Decyder MS analysis and MALDI-MS pattern profiling suggests there are significant changes that occur amongst tear peptide populations with the onset and maturation of diabetes and diabetic retinopathy. At this point, caution must be exercised as to the over-interpretation of such proteins as diagnostic markers for both the diabetes and diabetic retinopathy. Further validation of the data is required on a larger scale of patients.

In a complex biological sample, fractionation and enrichment of peptide fractions coupled with non-labelling quantitation strategies will maximize the magnitude and resolution of the peptides. This method offers a comprehensive interrogation of the tear peptidome, which itself is a difficult sample to analyse as a result of the small volume and large dynamic range of protein abundance. At this stage, the data presented here can attest to the constant flux of abundance that would influence the peptidomic nature of the tears with the onset and development of diabetic retinopathy. Whilst the technique described in this chapter will be used to identify and validate peptide abundance fluctuations with the onset of diabetic retinopathy using a large number of patients for statistical significance, it is also applicable to monitor tear peptides across other pathologies.

4

IDENTIFICATION OF TEAR PEPTIDE BIOMARKERS FOR DIABETES AND DIABETIC RETINOPATHY

4.1 Introduction

Diabetic retinopathy (DR) is a common complication of diabetes. In 2004-05, 700,000 Australians, representing 3.6% of the population, were reported to have some form of diabetes [140]. Of the population with this condition 83% were reported to have diabetes type 2, a number that is ever increasing with an ageing population. Fifteen percent of diabetic patients within Australia are diagnosed with some form of DR [1-3]. Amongst patients with type 2 diabetes, 22% had developed DR, whilst 6% of newly diagnosed patients with type 2 diabetes had developed DR. Recently, studies have also shown that retinopathy has a propensity to develop 7 years prior to the detection of diabetes [4-5].

Several studies have reported an association between changes to the tear film and its constituent protein population with the onset of diabetes type 2 and diabetic retinopathy. Herber *et al*., (2001) demonstrated a significant increase in tear film global protein content in diabetic patients [38]. HPLC analysis has demonstrated increased abundance of secretory immunoglobulin A (sIgA) and lysozyme in diabetic and diabetic retinopathy patients respectively, and a decreased abundance of tear specific pre-albumin in diabetic retinopathy patients, when compared with healthy controls [141]. Additionally, Yu *et al.* demonstrated that onset of diabetic proliferative retinopathy decreased tear film function and decreased concentration of lactoferrin and lipocalin [141]. On the other hand, apolipoprotein A-1 concentrations have been reported to increase with onset of both diabetes and diabetic retinopathy [78].

In summary, there is a global change to the tear film environment with the onset of diabetes and diabetic retinopathy. In effect, this will alter the abundance of the tear film protein population. To complement recent studies on the proteomic changes to the tear film, this study investigates the changes to the low abundance proteins and peptide species in the tear film. This is done through a non-labeling quantitative strategy involving fractionation and enrichment of lower abundance proteins and peptides employing the MF10, LC-MS/MS analysis using a highly sensitive MS LTQ-FT followed by peak integration with Progenesis LC-MS.

4.2 Methods

4.2.1 Tear Collection

Tears were collected from healthy controls (Con), patients diagnosed with diabetes mellitus without retinopathy (DM) and patients diagnosed with diabetes with retinopathy (DR). Tears were collected from patients at the Wenzhou Hospital, Wenzhou, People's Republic of China as previously described (Refer to Section 2.1). Patient data was also collected for reference.

Patients tears were sex and aged matched. Con patients tears (*n=30*) were pooled together as were tear samples from 30 DM and 30 DR subjects. Each pool was separated into 100 µg aliquots as determined by Fluoroprofile^{TM} quantitation assay (Refer to section 2.3).

4.2.2 MF10 Fractionation of Tear Proteins

MF10 fractionation was performed on 3 x 100 µg tear aliquots each of Con, DM and DR pooled tears. All MF10 fractionations were performed as described in section 3.2.4.1.

4.2.3 Protein Cleanup and Digestion

All 1-5 kDa and 5-25 kDa fractions from each MF10 fractionation run were desalted and concentrated as described in section 2.8. The larger fractions, 25-65 kDa and >65 kDa, were precipitated as described in section 2.4 and stored for future use.

The peptide fractions of interest, namely all 1-5 kDa and 5-25 kDa fractions, were digested with trypsin. Fractions were reconstituted with 25 µL of 50 mM AMBIC and 2 µg of trypsin was added to each fraction and incubated overnight at 37^{o}C. The digested fractions were then dried down in a SpeedVac (Savant, Thermo Scientific, Waltham, MA, USA).

4.2.4 LC-MS/MS using a LTQ-FT

LC-MS/MS using the LTQ ultra was performed according to section 2.12.2.

4.2.5 Biomarker Discovery using Peak Integration with Progenesis LC-MS

Data files (*.raw) generated from the LC-MS/MS were analysed according to section 2.12.2. Briefly, all data files were imported into Progenesis LC-MS. Each data file containing peptides (features), with their characteristic isotope, charge and m/z information was used to generate a signal intensity map separated by the m/z and elution time of each feature. The data files were then aligned to a designated reference map and filtered so only features exhibiting a 2-6 charge state were analysed further. Fragment data was exported for searching through Mascot as described in section 2.12.4. Peptide sequences were imported back into Progenesis LC-MS. Some peptides not able to be identified from MSMS spectra were chosen for further analysis.

Samples were injected into the mass spectrometer and specific m/z were chosen within an inclusion list. The inclusion list was generated from features which generated: no MS/MS data; faint MS/MS data; or MS/MS data which contained high background noise. Inclusion lists were then used to selectively fragment the peptides from the samples again so as to determine the peptide sequence and identification. This information was imported into Progenesis LC-MS.

4.2.6 Statistics

Intensity of the peptides were statistically compared using two-sided ANOVA. Precursor ions with significantly different (ANOVA $p < 0.01$) and at least a 2 fold change across their expression profiles were selected as the candidate biomarkers.

4.2.7 Gene Ontology Analysis

Gene ontology was performed on the peptides that were identified in the study. Uniprot accession numbers for proteins from which the peptides were identified were imported as a list into an online Database for Annotation, Visualisation and Integrated Discovery (DAVID, http://david.abcc.ncifcrf.gov/tools.jsp) [142-143]. Peptides were annotated and clustered according to their cellular component, biological process and molecular function.

4.3 Results

A non-labelling peptidomic approach was used to determine the abundance of peptides present in tears of patients that were healthy, diabetic or diabetic with retinopathy.

A reference intensity map was generated based on the peptides eluted, as identified by their retention times and the m/z values on the base ion chromatogram. Initially, there were a total of 27,114 and 25,723 precursor ions with a charge between 2-6+ in the 1-5 kDa and 5-25 kDa fractions respectively (Figure 4.1).

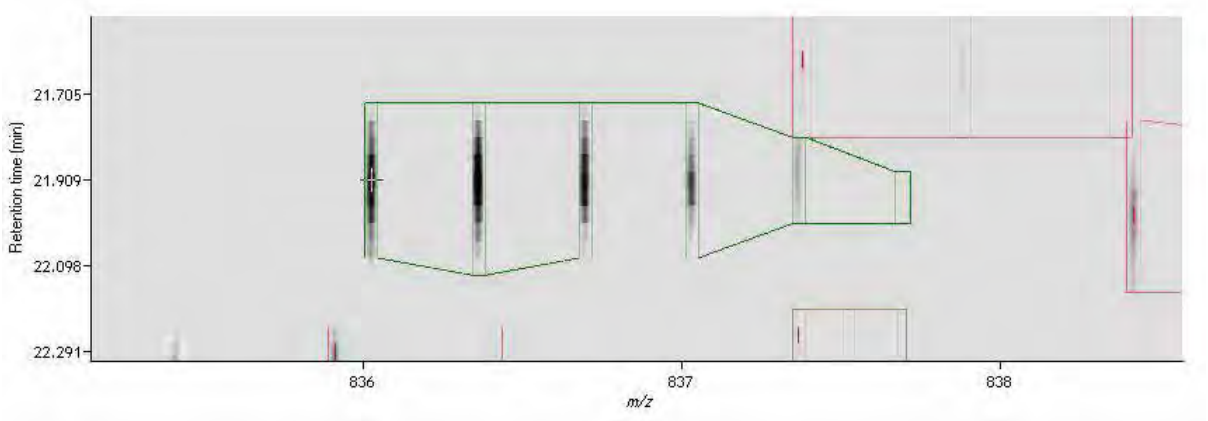

Figure 4.1 Example of a typical isotopic pattern on an intensity plot map, defined by the retention time and m/z on a base-ion chromatogram. Precursor ions demonstrating this pattern with minimal background noise and strong intensity were selected for further analysis.

4.3.1 Peptides 1-5 kDa

Seventy-nine peptides were identified as significant peptides of interest based on the statistical analysis of their abundance when their ion counts (cps) were compared between the patient groups (Table 4.1a).

Of these peptides, 12 peptides were successfully sequenced and identified (Table 4.2). The remaining peptides did not match to any sequences in the NCBI using the Mascot algorithm and may be modulated in some form. The 12 identified peptides represented 7 different proteins. As described in table 4.1 showing their abundance profiles between each disease group, peptides derived from proline rich protein 4 (pHL E1F1; $SLQEASSFFR^{2+}$ / $HPQEQPL^{2+}$) were observed to drop in abundance in diabetic retinopathy patients. This trend was also observed for peptides of lacritin ($QFIENGSEFA^{2+}$ /

EDASSDSTGADPAQEAGTSKPNEEI^{3+} / LTEQALAK^{2+}), mesothelin (VLPLTVAEVQK^{2+}) and secretoglobin 2A (TINSDISIPEYK^{2+}). Peptides from the proteins lipocalin (TLEGGNLEAK^{2+}) and Apolipoprotin J (Clusterin; ASSIIDELFQDR^{2+} / SIIDELFQDR^{2+}) were observed to increase in abundance in diabetic tears only. Peptides of actin (DSYVGDEAQSK^{2+} / VLSGGTTMYPGIADR^{2+}) were shown to gradually decrease with the progression of diabetes and diabetic retinopathy.

4.3.2 Peptides 5-25 kDa

Thirty peptides were identified from the 5-25kDa fraction as significant peptides of interest based on the statistical analysis of their abundance when their signal intensity maps were compared (Table 4.1b).

Two of these 30 peptides were able to be sequenced and identified (Table 4.1b Table 4.2). Of the two peptides that were observed to have altered, a peptide from actin (DSYVGDEAQSK^{2+}) was observed to gradually decrease with the progression of diabetes and diabetic retinopathy. This peptide was also identified in the 1-5 kDa fraction exhibiting the same profile changes. The peptide identified from caspase 14 (FQQAIDSR^{2+}), was observed to increase in abundance only in diabetic tears relative to tears of controls and people with diabetic retinopathy.

4.3.3 One Hit Wonders

A major issue with peptidomic biomarker discoveries is whether or not “one hit wonders” are in fact true biomarkers. “One hit wonders” are false positive peptides which would only occur once in one sample despite being of high interest or statistical significance [144]. Table 4.3 tallies the frequency at which the spectra for each peptide sequence occurs in each sample. Though many of the peptides may occur once in a sample, they are present and sequenced amongst subsequent replicates.

4.3.4 Gene Ontology Analysis

Gene Ontology analysis was performed on the peptides which were identified and sequenced. Not all peptides and their corresponding proteins are annotated as many proteins do not yet have their biological details and function assigned. Figure 4.4 tabulates the different known gene ontology attributes of the peptides including biological activity, cell compartmentalisation and features. From the Gene Ontology analysis of the peptides

identified in this study several of the proteins were ambiguous and multidimensional in terms of their molecular function and cellular compartmentalisation.

Table 4.1 Heatmap of the precursor ions found to significantly alter in abundance. Intensity of colours (red = high, orange = moderate, yellow = low abundance) is based on an arbitrary normalised volume unit (± 1 S.D) and is relative to the respective precursor mass. A total of 79 and 30 precursor ions were found in the A) 1-5 kDa and B) 5-25 kDa fractions respectively. These precursor ions were significantly altered in abundance across healthy control, DM and DR. Data represents technical triplicate analysis of a pool of *n=30* from each group.

a)

			control		diabetes without retinopathy		diabetes with retinopathy			
#	m/z	charge	Average	S.D	Average	S.D	Average	S.D	Max fold change	Anova
1	586.29	2	45804.27	857.69	77242.57	32220.63	21279.03	1503.42	4	0.005
2	562.82	2	331.24	218.52	20453.85	13893.95	8768.04	3966.29	62	0.002
3	903.72	3	55096.50	35595.30	18597.17	13645.95	1519.57	872.39	36	0.003
4	568.84	2	262.72	133.32	15393.05	8514.16	6951.56	3963.64	59	0.001
5	424.72	2	7502.36	979.92	2919.79	1266.79	924.31	560.25	8	0.003
6	571.26	2	7842.98	4722.86	10726.18	8204.94	707.84	234.28	15	0.005
7	517.26	2	5130.53	2796.43	3207.09	1456.45	12200.13	18236.64	4	0.908
8	540.31	2	461.76	214.92	17624.58	9554.09	9844.67	1427.05	38	0.000
9	825.96	2	2115.37	148.64	49055.71	26385.81	15774.57	7688.47	23	0.001
10	1054.77	3	70565.91	32247.78	18338.45	12673.25	1035.10	542.57	68	0.001
11	576.30	2	273.22	82.90	12159.35	9977.36	3819.96	973.71	45	0.001
12	650.85	2	810.20	267.62	13166.04	6048.95	6825.74	468.64	16	0.000
13	382.69	2	116.32	65.05	4752.21	5220.06	2531.13	1153.29	41	0.005
14	504.79	2	72.62	32.16	3625.41	1485.75	2192.02	482.94	50	0.000
15	595.34	2	2594.09	308.38	1848.01	1007.89	379.52	113.65	7	0.003
16	711.41	2	253.14	169.05	12413.16	8374.07	6869.79	2370.98	49	0.001
17	571.75	2	5349.93	3552.91	3972.60	1569.06	347.91	203.76	15	0.004
18	516.27	2	98.36	33.42	2717.34	2447.07	26.62	12.55	102	0.000
19	1031.42	2	527.35	261.10	11138.79	9454.60	11104.95	2810.69	21	0.002
20	364.23	2	2310.06	604.51	1531.81	392.79	1112.47	633.00	2	0.115
21	550.79	2	91.46	54.17	8010.33	3624.52	3165.51	207.61	88	0.000
22	836.03	3	8905.37	8002.71	6722.07	5128.48	193.86	39.92	46	0.006
23	697.35	2	648.62	205.57	5423.51	2010.59	840.30	546.51	8	0.002
24	599.76	2	3492.85	2190.79	1219.53	472.21	116.45	65.48	30	0.002
25	777.39	2	12195.75	8334.25	1768.86	649.40	423.07	249.63	29	0.005
26	690.36	2	3758.00	917.67	4157.36	1449.16	1685.96	1377.49	2	0.082
27	914.40	2	9962.31	6453.30	5082.68	1539.43	702.91	359.37	14	0.002
28	501.26	2	22.91	23.34	1976.38	1155.88	2076.01	956.47	91	0.007
29	483.29	2	370.52	141.93	5493.43	4237.07	5683.08	1856.49	15	0.004
30	766.92	2	1024.03	283.50	16528.57	8621.86	7698.79	1182.89	16	0.000
31	540.31	2	289.82	162.06	4495.52	2668.87	2660.24	785.09	16	0.002
32	776.42	2	593.91	130.61	6895.29	3611.35	4050.47	1406.85	12	0.002
33	660.88	2	179.62	171.12	5097.21	4195.85	2174.01	664.62	28	0.009
34	437.26	2	651.69	363.60	248.54	73.85	84.37	47.36	8	0.010
35	586.78	2	2673.61	2780.90	200.36	80.57	73.69	28.10	36	0.004
36	1253.54	2	9355.21	6991.08	7104.55	5135.47	378.00	334.59	25	0.013
37	1151.80	3	18279.43	10042.89	5386.44	3386.46	555.25	188.72	33	0.003
38	499.26	2	81.70	53.27	1941.70	1436.61	912.85	266.55	24	0.005
39	864.95	2	2480.28	140.52	11500.67	3139.19	5831.21	1091.61	5	0.000

40	1355.08	2	12536.71	6222.17	3315.27	2302.88	426.69	235.31	29	0.004
41	696.06	3	1017.81	579.95	8386.29	2146.74	3974.04	1244.18	8	0.001
42	1060.45	3	14237.42	11246.55	2533.66	1526.31	555.13	613.84	26	0.013
43	607.33	2	59.43	6.97	999.57	495.82	906.99	410.46	17	0.000
44	909.40	3	6101.52	1906.40	1886.41	1165.94	243.32	65.11	25	0.001
45	691.07	3	732.60	65.07	11957.32	2081.52	4829.47	2875.49	16	0.001
46	598.87	2	1021.84	1115.05	1012.10	212.03	99.12	72.47	10	0.020
47	729.41	3	650.29	301.18	7324.35	662.67	3278.21	1436.51	11	0.001
48	571.33	2	45.00	24.08	1353.84	957.57	658.72	313.74	30	0.007
49	763.90	2	251.41	143.46	3479.04	1618.45	1428.93	229.09	14	0.002
50	669.35	2	59.61	11.60	2400.81	2112.21	638.98	433.05	40	0.003
51	751.38	2	989.48	227.97	3744.94	669.80	2566.83	717.97	4	0.001
52	664.83	2	543.19	304.40	1171.03	183.24	345.05	176.08	3	0.025
53	560.78	2	1156.02	692.45	128.38	69.48	142.03	158.38	9	0.025
54	538.80	2	347.18	111.76	293.81	126.48	60.27	39.40	6	0.005
55	971.41	3	3718.76	1870.50	4643.77	3023.00	334.77	164.94	14	0.009
56	1053.48	2	716.83	338.48	5820.43	2671.70	3975.25	1068.44	8	0.003
57	678.33	2	86.71	14.42	2245.42	1831.16	854.45	132.53	26	0.001
58	971.41	3	4876.39	2541.46	1116.14	892.51	154.51	115.99	32	0.014
59	577.33	2	61.06	23.47	844.66	597.92	594.67	134.85	14	0.005
60	674.85	2	126.73	72.12	1632.88	1006.31	728.51	301.55	13	0.005
61	591.34	2	153.41	41.09	806.42	437.73	816.23	283.84	5	0.004
62	586.78	2	4.45	4.14	696.72	457.01	37.36	45.19	157	0.005
63	706.37	2	208.44	104.94	2270.84	832.03	1340.11	139.48	11	0.001
64	699.35	2	206.15	65.49	1456.64	810.76	311.30	212.44	7	0.019
65	684.34	2	285.96	72.12	598.04	169.52	168.01	125.58	4	0.052
66	545.30	2	217.88	97.47	1365.00	792.46	943.56	490.16	6	0.017
67	729.41	3	891.84	358.83	4625.81	902.41	3476.21	2434.49	5	0.016
68	485.27	2	17.64	13.12	446.96	405.24	160.17	101.37	25	0.009
69	1039.11	3	2634.75	1362.96	811.36	555.82	234.01	177.77	11	0.016
70	717.91	2	55.66	40.76	903.36	577.47	401.96	59.56	16	0.003
71	618.32	2	101.97	9.42	734.28	214.18	123.87	36.87	7	0.000
72	659.36	2	51.86	12.04	547.22	234.74	468.46	233.35	11	0.001
73	765.37	2	172.52	77.99	723.24	238.67	41.15	51.74	18	0.006
74	449.73	2	132.23	85.06	162.21	28.79	10.20	8.83	16	0.014
75	703.84	2	313.80	60.12	184.93	90.30	42.32	9.97	7	0.002
76	830.87	2	89.73	40.14	925.77	484.71	423.88	248.02	10	0.011
77	681.82	2	33.00	6.32	433.54	250.12	50.82	22.60	13	0.003
78	507.77	2	3.44	3.02	143.06	120.49	37.42	19.33	42	0.008
79	1157.48	3	2818.80	2539.44	677.35	360.21	238.73	108.09	12	0.028

b)

#	m/z	Charge	Control		Diabetes without Retinopathy		Diabetes with Retinopathy		Statistics	
			Average	S.D	Average	S.D	Average	S.D	Max fold change	Anova
80	770.37	2	6057.29	1311.99	2196.17	566.76	4527.39	849.37	3	0.008
81	657.82	4	8629.03	1747.69	3671.14	140.11	7738.58	1413.23	2	0.002
82	842.90	2	6780.37	442.45	3065.02	1116.05	2014.46	319.03	3	0.008
83	635.04	4	3908.07	982.52	1744.36	266.59	3903.34	968.95	2	0.010
84	692.40	2	577.41	33.09	1168.45	125.07	1762.62	359.03	3	0.002
85	645.31	3	1609.80	256.39	507.34	143.81	1292.43	309.93	3	0.007
86	883.73	3	629.83	146.96	3004.36	471.88	2553.27	863.00	5	0.004
87	914.41	2	2779.94	1562.90	2012.15	1088.69	308.74	68.32	9	0.008
88	806.39	3	4768.52	1522.50	1557.91	319.64	1034.66	231.18	5	0.003
89	659.90	2	742.00	48.25	1542.53	878.84	104.43	66.93	15	0.007
90	931.11	3	2568.19	11.18	586.26	99.93	1239.51	339.50	4	0.001
91	652.65	3	715.81	145.44	304.24	46.28	481.06	72.46	2	0.006
92	529.26	3	232.13	54.49	102.99	9.12	208.79	34.86	2	0.004
93	800.90	4	882.54	88.11	361.64	35.58	831.05	118.85	2	0.000
94	482.75	2	26.53	7.36	177.59	87.79	42.38	9.26	7	0.006
95	482.24	2	42.73	10.92	168.64	53.90	67.60	15.44	4	0.010
96	411.69	2	212.80	59.35	61.07	16.08	59.22	14.34	4	0.005
97	697.31	2	804.16	117.55	180.02	11.62	158.89	33.56	5	0.000
98	598.87	2	21.06	12.04	345.66	236.38	21.90	6.91	16	0.006
99	500.77	2	93.08	9.94	50.69	9.21	109.33	22.83	2	0.009
100	1044.84	3	757.44	119.90	402.52	102.10	1131.01	271.76	3	0.006
101	599.76	2	142.08	2.77	130.14	50.67	26.91	5.59	5	0.001
102	757.62	4	78.17	11.94	568.03	148.89	107.69	50.00	7	0.005
103	396.22	3	7.37	2.37	56.34	6.73	15.31	10.28	8	0.006
104	560.29	2	253.25	127.32	57.56	9.58	60.61	10.03	4	0.005
105	894.41	2	286.39	73.60	713.58	207.03	175.86	13.94	4	0.002
106	811.86	2	255.46	48.61	62.44	24.46	101.25	14.80	4	0.005
107	910.44	4	52.74	22.53	242.69	14.84	92.16	17.43	5	0.002
108	939.98	2	5.94	1.07	252.23	86.14	30.63	26.76	42	0.004
109	618.26	2	43.56	0.06	18.99	2.32	47.63	12.22	3	0.003

Table 4.2 Peptides identified from the 1-5 kDa and 5-25 kDa fractions using LC-MS/MS, MASCOT using NCBI database (2009).

#	m/z	Charge	Max fold change	Anova	Score	Protein	Sequence	Variable modifications	Description
1-5 kDa									
1	586.29	2	3.6	0.0045	62.87	gi|1050983	SLQEASSFFR		pHL E1F1 [Homo sapiens]
5	424.72	2	8.1	0.0033	28.87	gi|1050983	HPQEQPL		pHL E1F1 [Homo sapiens]
6	571.26	2	15.2	0.0051	61.39	gi|15187164	QFIENGSEFA		lacritin[Homo sapiens]
18	516.27	2	102.1	0.0002	59.67	gi|4504963	TLEGGNLEAK		lipocalin 1 precursor [Homo sapiens]
22	836.03	3	45.9	0.0064	51.82	gi|15187164	EDASSDSTGADPAQEAGTSKPNEEI		lacritin precursor [Homo sapiens]
23	697.35	2	8.4	0.0017	63.3	gi|178855	ASSIIDELFQDR		apolipoprotein J precursor [Homo sapiens]
24	599.76	2	30.0	0.0015	67.3	gi|49168516	DSYVGDEAQSK		ACTG2 [Homo sapiens]
25	777.39	2	28.8	0.0052	81.28	gi|49168516	VLSGGTTMYPGIADR	[8] Oxidation (M)	ACTG2 [Homo sapiens]
26	690.36	2	2.5	0.0820	60.3	gi|4505171	TINSDISIPEYK		secretoglobin, family 2A, member 1 [Homo sapiens]
34	437.26	2	7.7	0.0095	44.42	gi|15187164	LTEQALAK		lacritin precursor [Homo sapiens]
46	598.87	2	10.3	0.0198	47.66	gi|1145724	VLPLTVAEVQK		mesothelin or CAK1 antigen precursor
71	618.32	2	7.2	0.0002	45.43	gi|178855	SIIDELFQDR		apolipoprotein J precursor [Homo sapiens]
5-25 kDa									
95	482.746	2	6.7	0.0056	54.31	gi|6912286	FQQAIDSR		caspase 14 precursor [Homo sapiens]
101	599.7648	2	5.3	0.0014	28.37	gi|169213772	DSYVGEDAQSK		actin alpha 1 skeletal muscle protein [Homo sapiens]

Table 4.3 Peptides and number of MS/MS spectra of the corresponding samples. Data was tallied through manual inspection of the annotated spectra during analysis with Progenesis LC-MS. Blue designates that more than one spectrum for the corresponding sequence was found. Scores are MOWSE scores derived from searching ncbi database through Mascot.

#	Protein	Description	Sequence	Control			Diabetic without retinopathy			Diabetes with Retinopathy		
1-5 kDa				Con01	Con02	Con03	DM01	DM02	DM03	DR01	DR02	DR03
1	gi|1050983	pHL E1F1 [Homo sapiens]	SLQEASSFFR			1				2		
5	gi|1050983	pHL E1F1 [Homo sapiens]	HPQEQPL	1	1	1		1	1			
6	gi|15187164	lacritin[Homo sapiens]	QFIENGSEFA	2	2	2	2	2	2			
18	gi|4504963	lipocalin 1 precursor [Homo sapiens]	TLEGGNLEAK				2	2	2			
22	gi|15187164	lacritin precursor [Homo sapiens]	EDASSDSTGADPAQEAGTSKPNEEI	1	2		2		2			
23	gi|178855	apolipoprotein J precursor [Homo sapiens]	ASSIIDELFQDR				2	2	2			
24	gi|49168516	ACTG2 [Homo sapiens]	DSYVGDEAQSK	2	3	2	2	2	2			
25	gi|49168516	ACTG2 [Homo sapiens]	VLSGGTTMYPGIADR	2	1	2	1		1			
26	gi|4505171	secretoglobin, family 2A, member 1 [Homo sapiens]	TINSDISIPEYK	1	2	2	1		1			
34	gi|15187164	lacritin precursor [Homo sapiens]	LTEQALAK			2						
46	gi|1145724	mesothelin or CAK1 antigen precursor	VLPLTVAEVQK			2	2	2				
71	gi|178855	apolipoprotein J precursor [Homo sapiens]	SIIDELFQDR				2	1				
5-25 kDa												
94	gi|6912286	caspase 14 precursor [Homo sapiens]	FQQAIDSR				1	2	2			
101	gi|169213772	actin alpha 1 skeletal muscle protein [Homo sapiens]	DSYVGEDAQSK	2	3	2	2	2	2			

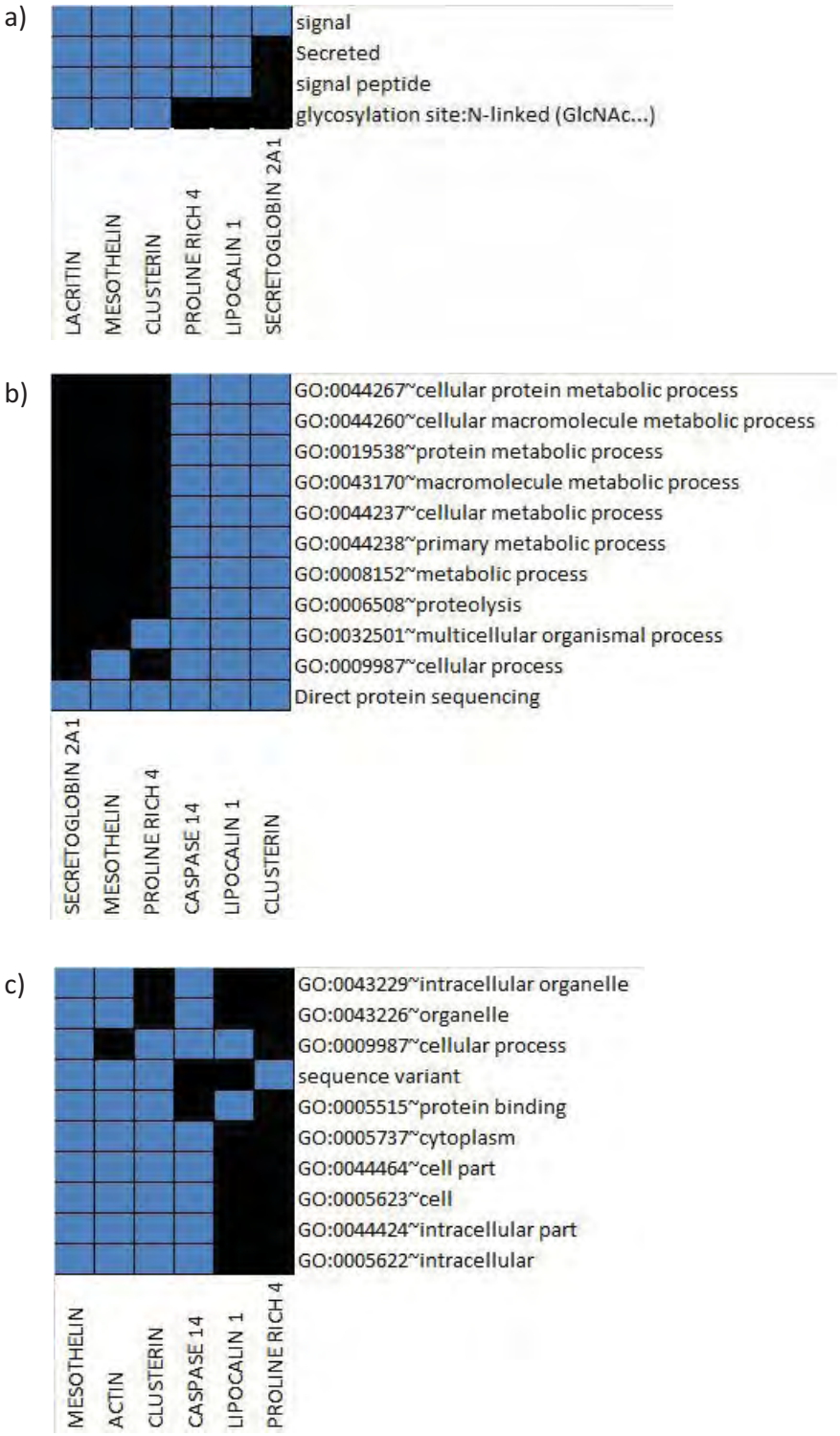

Figure 4.4 Functional annotation clustering of the precursor proteins identified successfully based on their a) features, b) Biological Processes and c) Cellular component. Uniprot accession references of proteins from which the peptides were identified were imported into DAVID for gene ontology analysis. Blue designates positive protein association, black designates negative protein association.

4.4 Discussion

Together, enrichment strategies, sensitive mass spectrometry instruments and a label free-quantitation analysis were used in this study to characterise changes to the peptidomic abundance profiles of the tear film with the onset of diabetes and diabetes with retinopathy. Over 109 peptides were profiled which could potentially be used as peptide biomarkers for diabetes and diabetes with retinopathy. Despite the many clinical classifications of diabetes and diabetes with retinopathy, the goal of this study was to identify changes to both diseases. Further work is needed to correlate these peptides to the changes to the different stages of diabetic and diabetic retinopathy development. Of these peptides, a total of only 13 were sequenced and identified. Gene Ontology analysis revealed the isolated peptides encompassed a variety of biological functions and cellular locations indicating the broad effects that come with the onset of the diabetes and diabetic retinopathy.

Ion-count/peak integration analysis was performed using Progenesis LC-MS. Though similar in principle to DeCyder MS, Progenesis LC-MS analysis program is another label-free quantitative analysis which is more rigorous and allows significantly more selective fine tuning of molecular ion over noise data as well as exploring data in specific terms. Biomarkers identified were of high significance. Additionally, there was a change in chromatography columns between the preliminary and the current study. This changed the elution profiles such that alignments from previous experiments (Section 3.3.7.1) was no longer possible and thus comparison between the samples from both studies.

4.4.1 Peptidomic Analysis

Although 13 peptides were successfully identified from this analysis the majority of potential peptide biomarkers profiled were not. Most importantly, the complexity of biological samples still presents a challenge. Conventional MS methods take into account the success of identification and favour the selection of the most abundant precursor ions at any given time for MS/MS. Current methods select (once for 40 sec exclusion window) up to 6 of the most abundant ions within a 1 Da ion window at any one time measured on the nsec scale. Lower abundance, smaller peptides with poorly charged termini are therefore disadvantaged. The success of the enrichment process prior to MS is thus essential to increase chances of good MSMS for these peptides.

A challenge of this study is the peptidomic study of tears using proteomic databases. Currently, a majority of all protein identification search programs are protein-centric. The algorithm must determine whether the MS/MS ion spectra is a good match to the peptide and the peptide is a good match to the protein (Wasinger pers. Comm.), via statistic-based and cross correlative algorithms (Sequest)[97] and probability based algorithms (Mascot) [145] [146-147]. In a peptide–centric study, as there are fewer peptides per protein, the chance that this peptide can be matched to multiple proteins is increased. The false positive assignment will be much greater for these studies. Peptides assigned using protein biased algorithms may therefore influence identifications, particularly for 'one-hit wonders'. Characterisation of these peptides at the protein level is therefore unreliable. In this study we have realized this challenge and have:

a) Confirmed the repeated occurrence of these single peptide assignments in multiple samples at the correct retention time and m/z.
b) Selected a number of these molecular peptide ions for further MS/MS using inclusion lists to help improve identification prospects.
c) Used the m/z of the peptide to follow up quantitation between samples rather than focusing on whole protein identifications.
d) Used statistical tests to show the value of pursuing these molecular ions irrespective of identification.

Of the peptides that were sequenced, a majority of the peptides are found in the peptide partition after fractionation, it is highly likely that they are a product of protease activity. This is not defined well within MASCOT algorithm or protein-biased databases thus they remain unidentified at this stage. De novo sequencing is needed to adequately sequence these peptides. However, this would require further extensive effort, which is beyond the scope of this thesis. Furthermore, coupled with the state of protein flux in a biological fluid, protein concentration is ever-changing. As such, peptides identified in this study cannot be a direct reflection of the concentration of the associated protein. Rather, these peptides are only potential biomarker candidates associated with DM and DR.

4.4.2 Gene Ontology Analysis and Functional Roles of Identified Proteins

The onset of an ocular disease will alter the metabolic pathways and environment of the tear film. This hypothesis is supported by the diverse biological roles of the proteins from which the peptides are identified in this study. Gene Ontology (GO) analysis of the proteins

from which the peptides are derived, demonstrated that the onset of diabetes and diabetic retinopathy did affect tear proteins that are multi-functional and integral to a wide range of cellular and metabolic processes.

A significant portion of the peptides that were identified are derived from proteins indigenous to the tear film. Proline rich protein (PRP) 4 is known to have high expression levels in the tear lacrimal gland [148-149]. Also found in saliva and mucosal lining, PRP is involved in oral defense and aggregation of microorganisms, thus retarding their capacity to colonise tissue surfaces [149]. Another component of the lacrimal gland found in this study is actin, which is integral to the role of exocytosis in the lacrimal environment [150]. Additionally, common tear proteins such as lacritin, lipocalin and secretoglobin were also identified in this study to change with the disease status. Lacritin is a prosecretory mitogen, elicited in meibomian gland secretion and is primarily responsible for increasing the volume of basal tear secretion [151]. Lacritin is downregulated in Sjorgrens syndrome and blepharitis [79]. Lipocalin is a protein integral to tear film stability. It is involved in lipid transport and removal, thus contributing to the stability and integrity of the lipid/aqueous/mucousal layers of the tear film [152]. Furthermore, lipocalin is the principle endonuclease in human tears [153]. This is particularly important in the prevention of viral propagation by transformation. In this study, these species have been reduced in abundance with the onset of DR. On consideration, the possible down regulation of these peptides as seen in this experiment may be an indication to tear instability and reduced tear film function.

Whilst a majority of the proteins are involved intimately with the function of the tear film, some proteins could potentially be involved in tear deficiencies such as dry eye which is a common symptom in the tear film function of diabetic and diabetic retinopathy patients. Clusterin (Apolipoprotein J) is a major component of secreted fluids [154]. Clusterin is primarily associated with apoptosis, however, reports have also associated this protein with a diverse range of physiological processes such as lipid transport, complement inhibition, sperm maturation, tissue re-modelling, facilitating cell-cell/substrate interactions, membrane recycling and chaperone function [155]. This highly glycosylated protein is strongly expressed in normal conjunctival epithelium. However, reduced clusterin expression is associated with keratinized conjunctival epithelia and tear deficiencies such as dry eye [156]. Additionally, a decrease in clusterin abundance in the

vitreous is associated with the onset of proliferative diabetic retinopathy [157]. Current literature has not described a link between the vitreous and tear film. Further work would need to establish the presence or absence of a relationship between the two. Capase 14 is only expressed in the epidermis and involved in keratinocyte differentiation. Its primary role is to assist in the formation of epidermal layers that protects against dehydration and UVB radiation [158]. In relation to disease, expression of this protein is also moderated in several cancer cell lines [159]. For example, it is reduced in UVB cell carcinomas and there is a reduced caspase 14 differentiation in advanced tumours [158]. Capase 14 can be observed in cervix and lung squamous cell carcinomas [160]. Furthermore, caspase 14 is downregulated in psoriatic lesions leading to uncontrolled proliferation of keratinocytes and thus impaired cornification [161-163]. In this study, both caspase 14 and clusterin demonstrated similar abundance profile changes. Both were at least 5 fold higher in the tears of diabetics than in healthy controls and diabetic retinopathy patients. It is thus postulated that caspase 14 and clusterin abundance may reflect the degree of keratinization and in turn, the severity of dry eye in the tear film with the onset of diabetes and diabetic retinopathy. In this study, abundances of caspase 14 and clusterin are not concurrent with expression (mRNA) studies which suggest that their decreased expression is intrinsic to keratinization and dry eye [156]. However, the existence of their peptides may suggest that the structural and thus functional attributes of such proteins are compromised. Further work is required to support this hypothesis.

Other proteins found in this study which are associated with ocular diseases such as dry eye include secretoglobin 2A1 and mesothelin. Secretoglobin 2A1 (SCGB 2A1) is a protein of unknown function, yet, it has been reported as both a tear and serum marker for breast, lung, colon, ovary and prostate cancers [72]. Of note, androgen-dependant expression of SCGB 2A1 is observed in prostate tissue [164]. Androgen-dependant expression of SCGB 2A1 can be observed in keratinized stratified squamous epithelium of the eyelid, in stratified epithelium of conjunctiva and in orbicularis oculi muscle [165]. It is known that patients with complete androgen insensitivity demonstrate dry eye symptoms [166]. Its decreasing abundance with the onset of diabetes and retinopathy in this study may well correlate with its likely contribution to dry eye with the onset of the aforementioned diseases. Mesothelin is a protein which has been identified in tears in many studies [167-168]. Mesothelin is a cell-surface membrane protein that has been detected in the sera of patients with ovarian cancer and malignant pleural mesotheliomas

– cancer of lining of organ cavities [169-170]. Not much is known about its functional role in tears, however, studies have illustrated its down-regulation in the conjunctival epithelium of patients with Sjorgrens syndrome which itself is characterized by dry eye [167]. It is thus postulated that the observed decrease in abundance of the aforementioned peptides would be an indication of the compromised stability of the conjunctival epithelium associated with the onset of DM and DR. This remains speculative, and further work is needed to validate this association.

It is important to note at this point that biological pathways in the tear film have not been mapped in detail. Thus, the nature of interaction between these peptides and proteins cannot be correlated to changes to the systems biology. Nonetheless, their presence or absence at certain stages of disease may indicate their catabolism and turnover, particularly as they are found in low molecular range fractions. Proteins may be effectors of biological process such as dry eye or by-products of that biological process. They may also be effectors of biological processes to counteract events which can upset homeostasis in the tear environment. The changes to the abundance of peptides reported here represent a cross-sectional snapshot of the population of peptides. Further work is required to sequence and identify the unidentified peptides in this study. This would assist with correlating the changes in systems biology to biological pathways of the tear film.

4.4.3 Concluding Remarks

The study represented here is a proof of concept study that identifies low abundant peptide biomarkers specific to diabetes and diabetes with retinopathy. Indeed, there are many changes that occur to the tear film with the onset and development of diabetes. Though there are various stages to diabetes and retinopathy, it is more efficacious to distinguish overall biomarkers, validate them before monitoring the changes across different stages of diabetes and retinopathy. Being a biomarker study, it is not necessary to determine the biological role these changes have brought upon the tear film. Nevertheless, it has been determined that these peptides are of diverse function, compartmentation and biological process.

Validation studies are required to authenticate the trends and biomarker candidates identified in this study. This could possibly be taken down two avenues; mass spectrometry based validation or antibody validation. Both require that the peptides to be

validated are identified. Validation of identified biomarker candidates was performed using a mass spectrometry based strategy. This is described in chapter 5.

5

MRM VALIDATION OF PEPTIDOMIC BIOMARKERS

5.1 Introduction

Biomarkers are objectively measured characteristics that can correlate with a biological or pathological process or pharmacological response to some therapeutic intervention [171]. Specifically, protein or peptide biomarkers are endogenous species whose presence and/or metabolism indicate a physiological or pathological state. As of 2006, there were over 150,000 disease-associated biomarkers in the current literature [172]. Unfortunately, very few biomarkers are of robust clinical utility due to the absence of established validation of these biomarkers via extensive (> 1000 patients) clinical trials [172]. Most biomarker candidates identified during the discovery phase are debated through reputable journals as to the utility of the biomarker in the clinic and are rarely developed any further [172].

Validation of biomarkers firstly involves assessment and verification using methods clinically relevant to the biomarker of interest [119]. This stage of the validation process involves testing the biomarker using a sample size representing a population close to that which a clinical trial would employ [119]. The pre-validation process works to reduce the list of candidates to only those that merit the extensive effort and expense of a clinical validation. In many instances the lack of validated and/or pre-validated biomarkers are ascribed to the limitations associated with antibody based assays which are the current gold-standard method of biomarker validation [173-176].These assays include techniques such as ELISA, FACS, western blotting and tissue microarrays which are time consuming and labour intensive to develop [119].

Mass spectrometry based techniques of validation have recently become a popular alternative validation method to antibody based approaches. Multiple reaction monitoring (MRM)analysis compares ion chromatograms of a peptide between samples and there is little requirement for further identification as the fragmentation ions which generate the chromatograms are used to identify the presence of the selected peptide [120]. In an MRM assay, samples are assayed using 3 quadrupoles. Specifically, the ion of interest (precursor ion) is preselected using the first quadrupole (Q1), fragmentation is induced using a collision gas in the second quadrupole (Q2). The resulting fragment ion (product ion) counts are then measured for analysis using the third and final quadrupole (Q3) [120, 177]. The instrument used in this study is a hybrid instrument using an ion trap as Q3 and having the advantage of reducing duty cycle while maintaining/improving sensitivity. In

doing so, the parent and associated daughter ions pairs could be simultaneously scanned and measured with high accuracy. Assaying peptides using MRM overcomes potential problems with immunoassays associated with protein-folding and protein-complexes [119]. Furthermore, multiplexing with MRMs does not rely on potentially irreproducible and non-specific antibody labeling chemistries. Being a mass spectrometry-based approach, MRMs are an efficient high-throughput method of validation, particularly when evaluating a panel of potential biomarkers in one sample. However, the rate-limiting step of MRM validation is method development which includes optimizing the instrument settings required for each quadrupole to resolve the transitions (Q1/Q3 filtered masses). In developing the assay, one should be mindful that whilst they should select a small panel of ions that is unique for their target proteins, in a majority of cases, there is a propensity for the instrument to sequence peptides with the most intense signals or "proteotypic peptides" [178].

MRM technology has largely been used to monitor the presence of metabolites and drug targets [179]. As such, related protocols and instruments are available for this process, which only require minimal optimisation to use for protein biomarker validation. Additionally, programs and repositories are available to assist the researcher in this process to produce a high-throughput validation method. Skyline is an example of a Windows based client application for building MRM methods and analysing the resulting MS data [180]. Through this application, methods can be created and iteratively refined for large-scale qualification.

There are numerous approaches which can be used to quantitate using MRM including label-free, stable isotope or labeling methods. Whilst all methods require considerable time to develop and optimize, label-free strategies provide an expeditious approach to validating biomarkers using MRM [120]. Variation in the samples and sensitivity of the instruments to be used must be determined before the specificity of the assay to the disease can be adequately assessed.

The aim of the study reported in this chapter was to develop an MRM assay to test the utility of the biomarkers identified in the previous chapter. The current chapter describes MRM assay development and monitoring performed using Skyline.

5.2 Method

5.2.1 Sample collection

Tears were collected as previously described (Section 2.1) from healthy controls (Con), patients diagnosed with diabetes mellitus without retinopathy (DM) and patients diagnosed with diabetes mellitus with retinopathy (DR). Tears were collected from patients at the Wenzhou Hospital, Wenzhou, and People's Republic of China as previously described (Refer to section 2.1). Patient information was also collected to aid in data analysis.

5.2.2 Sample Preparation

5.2.2.1 **Reduction and alkylation**

A 21 µg aliquot of total tear protein, as determined by amino acid analysis (AAA), was diluted with 45 µL of 50 mM AMBIC/4M urea. The sample was reduced by incubating with 2.5 µL of 200 mM TBP (Bio-Rad) at room temperature for 2 hours and then alkylated by incubation with 2 µL of 25% acrylamide at room temperature for 30 minutes.

5.2.2.2 **StageTip cleanup**

Tear proteins were desalted and concentrated for MRM using StageTips as described in section 2.6.

5.2.2.3 **Digestion**

Samples were digested as described in section 2.7. Briefly, samples were dried in a SpeedVac^{TM} (Savant), reconstituted in 25 µL of 50 mM AMBIC and incubated with 0.2 µg of trypsin at 37^{o}C overnight. Digested samples were then dried using a SpeedVac^{TM} and resuspended in 5 µL of 2% acetic acid /0.1% HFBA /2% ACN.

5.2.3 Amino Acid Analysis

Amino acid analysis (AAA) of the collected individual tears was carried out at the Australian Proteome Analysis Facility (APAF, Macquarie University, Sydney, Australia) to quantify the amount of protein present in each sample. One microlitre of each crude unfractionated tear sample was analysed. Samples were dissolved in 40 µL 20% ACN/0.1% TFA and subjected to gas phase hydrolysis for 24 hrs with 6 M HCl at 110^{o}C. Amino acids were then analysed using AccQ.Tag chemistry (Waters, Milford, MA, USA). Analyses were performed in duplicate.

5.2.4 MRM assay development

5.2.4.1 **Assay development using Skyline**

A healthy control sample was injected into the QTrap (*n=3*) to assess the technical variation of the assay for the peptides identified in chapter 4.

Thirteen peptide candidates with suitable physicochemical properties, including length of 7–24 amino acids, +2 peptide charge state and, where possible, the omission of peptides containing methionine (M), tryptophan (W) or cysteine (C), were selected for further MRM development. Amino acid sequences of these peptides were entered into Skyline v0.5 (MacCoss Lab, University of Washington, Seattle, USA) [180]. A transition list of the peptides of interest was automatically generated which included an appropriate collision energy and declustering potential, as determined by Skyline. The dwell time for these transitions was set to 50 ms. These settings were optimized for an 'ABI instrument' then exported from Skyline and imported into a 4000 QTRAP hybrid triple quadrupole linear ion-trap mass spectrometer (Applied Biosystem/MDS Sciex) as a *.csv format.

5.2.4.2 **MRM assay**

MRM analyses were performed on a 4000 QTRAP hybrid triple quadrupole linear ion-trap mass spectrometer (Applied Biosystems, Foster City, CA, USA) interfaced with a nanospray ion source operated in positive ion mode. One microgram of tear peptides (2 µg for intra-variation assay) prepared as described in section 5.2.2 were concentrated and desalted onto a micro C18 precolumn (500 µm x 2 mm, Michrom Bioresources, Auburn, CA) with H_2O:ACN (98:2, 0.05 % TFA) at 15 µL/minute. After 4 min washing, the pre-column was automatically switched (Valco 10 port valve, Houston, TX) into line with a fritless nano column manufactured according to the protocol of Gatlin *et al*.[181]. Peptides were eluted using a linear gradient of H_2O:ACN(98:2, 0.1 % FA) to H_2O:ACN (36:64, 0.1 % FA) at ~300 nL/min over 50 min. The pre-column was connected via a fused silica capillary (10 cm column, 25 µm) to a low volume tee (Upchurch Scientific, Oak Harbor, WA) via a fused silica capillary (25 cm, 25 µm) and introduced into the 4000 QTRAP mass spectrometer. Samples were analyzed with an ion spray voltage 2.4 kV, curtain gas flow of 12 and nebulizing gas flow of 5. For MRM studies, quadrupoles were operated in the low resolution, and the dwell time was 50 ms. For validation runs, the MRM experiment

triggered MS/MS spectrum acquisition. MS/MS spectra were acquired in the trap mode (enhanced product ion) with dynamic fill time; Q1 was operated in low resolution.

5.2.4.3 **MRM data analysis**

Data files generated from the MRM assay were re-imported into Skyline v0.5. The extracted ion chromatograms (XIC) generated by the QTrap were automatically matched to theoretical transitions generated. Methods were refined by editing transitions for each peptide. Briefly, this involved comparing the results of each MRM method to theoretical transition values as calculated by Skyline, as well as to the validated MS/MS spectra and sequenced peptides. Transitions of each peptide were ranked based on the observed intensities from each run. The fragment *y*-ions above the precursor ion (Q1) were selected as the Q3 transitions. A transition was removed if it did not correlate with the theoretically ranked transitions calculated by Skyline and no confirmation from MS/MS was present.

5.2.5 MRM assay

Samples from Con, DM and DR (*n=10*) were processed as described in Section 5.2.2. One microgram from each tear sample was injected into the QTrap and assayed using the optimized MRM assay settings (Table 5.2). Ion counts, and area under the curve (AUC) of the targeted transitions were analysed using Skyline v0.5 (Section 5.2.4.3)

5.2.6 Intra sample variation method

An assay of the peptides from one sample was assessed for intra-variation. A control sample used to assay the peptides (Section 5.3.2) was re-injected into the QTrap (*n=2*) using the developed and optimized MRM assay settings (Table 5.2).Ion counts, and area under the curve (AUC) targeted transitions were analysed using Skyline v0.5 (Section 5.2.4.3)

5.3 Results

5.3.1 Method Development

5.3.1.1 Amino Acid Analysis

An AAA of individual tear samples (*n=4*) from each disease group revealed that there was significant variation in total protein between samples (Table 5.1).The coefficient of variance (CV) of total tear protein concentration ranged from 39% amongst control groups, 20% amongst diabetic mellitus and 31% amongst diabetic retinopathy. It was expected that variation was higher using individual samples rather than the triplicate analysis of the pool of biological replicates (*n=30*) used in Chapter 4 to identify the peptide biomarker candidates. The average concentration for each sample group was used to normalize the initial total tear protein amount to be processed prior to MRM assay.

Table 5.1 Protein concentrations of four samples of tears from control (Con), diabetic (DM) and diabetic retinopathy (DR) candidates as determined by amino acid analysis. The average was used to standardise samples to be tested with the developed MRM assay.

	Protein concentration µg/µL				Average	Std Dev	CV (%)
Group	1	2	3	4			
Con	10.4	4.9	3.9	6.2	6.4	2.5	39.0
DM	8.1	12.5	7.9	8.8	9.3	1.9	20.0
DR	11.9	11	5.9	6.2	8.8	2.7	31.1

5.3.1.2 Assay settings

MRM transitions were developed for successfully sequenced peptides that were shown to change in abundance with the onset of diabetes and diabetes with retinopathy. Thirteen peptides were selected for MRM development. Transitions were predicted using Skyline and the appropriate Q3 values were selected after experimental Q3 values were correlated with predicted Q3 values.

Table 1.2 displays the optimal settings for MRM transitions selected. Lacritin peptide EDASSDSTGADPAQEAGTSKPNEEI^{3+} and proline rich protein 4 peptide HPQEQPL^{2+}were removed from the final analysis as transitions were not successfully developed due to poor correlation between the triplicate analysis.

Table 5.2 Optimised transition settings for MRM of tear peptides. Skyline was used to determine settings includingprecursor ion (Q1) and fragment ions (Q3) values, collision energy (CE) and declustering potential (DP).

Protein	Amino Acid Sequence	Q1	Q3	Dwell time (ms)	CE	DP
LACRITIN	LTEQALAK	437.26	760.42	50	63	23.6
			659.37	50	63	23.6
			530.33	50	63	23.6
LACRITIN	QFIENGSEFA	571.26	866.39	50	72.8	29.4
			753.30	50	72.8	29.4
			624.26	50	72.8	29.4
ACTG2	DSYVGDEAQSK	599.76	833.40	50	74.8	30.6
			734.33	50	74.8	30.6
			677.31	50	74.8	30.6
ACTG2	VLSGGTTMYPGIADR	769.39	1238.58	50	87.2	37.9
			1181.56	50	87.2	37.9
			1124.54	50	87.2	37.9
			1023.49	50	87.2	37.9
			922.45	50	87.2	37.9
			791.40	50	87.2	37.9
			628.34	50	87.2	37.9
APOLIPOPROTEIN J	SIIDELFQDR	618.32	1035.51	50	76.2	31.4
			922.43	50	76.2	31.4
			807.40	50	76.2	31.4
			678.36	50	76.2	31.4
APOLIPOPROTEIN J	ASSIIDELFQDR	697.35	1035.51	50	82	34.8
			922.43	50	82	34.8
			807.40	50	82	34.8
pHL E1F1	SLQEASSFFR	586.29	971.46	50	73.9	30
			843.40	50	73.9	30
			714.36	50	73.9	30
			643.32	50	73.9	30
SECRETOGLOBIN FAMILY 2A	TINSDISIPEYK	690.36	1165.57	50	81.4	34.5
			849.47	50	81.4	34.5
			736.39	50	81.4	34.5
			536.27	50	81.4	34.5
LIPOCALIN 1 PRECURSOR	TLEGGNLEAK	516.27	930.49	50	68.8	27
			817.41	50	68.8	27
			688.36	50	68.8	27
			631.34	50	68.8	27
			574.32	50	68.8	27
MESOTHELIN PRECURSOR	VLPLTVAEVQK	598.87	1097.66	50	74.8	30.6
			984.57	50	74.8	30.6
			887.52	50	74.8	30.6
			774.44	50	74.8	30.6
			673.39	50	74.8	30.6
CASPASE 14 PRECURSOR	FQQAIDSR	482.75	689.36	50	66.3	25.6
			561.30	50	66.3	25.6

5.3.1.3 **Analysis of CV of individual peptides**

The reproducibility of the MRM assay developed for each peptide was assessed (Figure 5.1) and the CV of each assay calculated. Briefly this involved comparing the area under the curve (AUC) for the combined transitions that were refined for each peptide assayed.

Peptides in the assay displayed a small range of variation between the transitions. The largest variation was measured for caspase 14 peptide FQQAIDSR^{+}with CVof 41.7%. The lowest variation was measured for proline rich protein 4 peptide SLQEASSFFR^{2+}with CV of 5%. The AUC of the peptides ranged from 557.3 (± 41.7%) for caspase 14 peptide FQQAIDSR^{2+} to 20 x 10^{06} cps (± 23.3%)for secretoglobin peptide TINSDISIPEYK^{2+}. Overall, the average CV of each peptide measured was deemed an appropriate level of variation for the assay to be used to validatethe biomarkers on a larger cohort of samples.

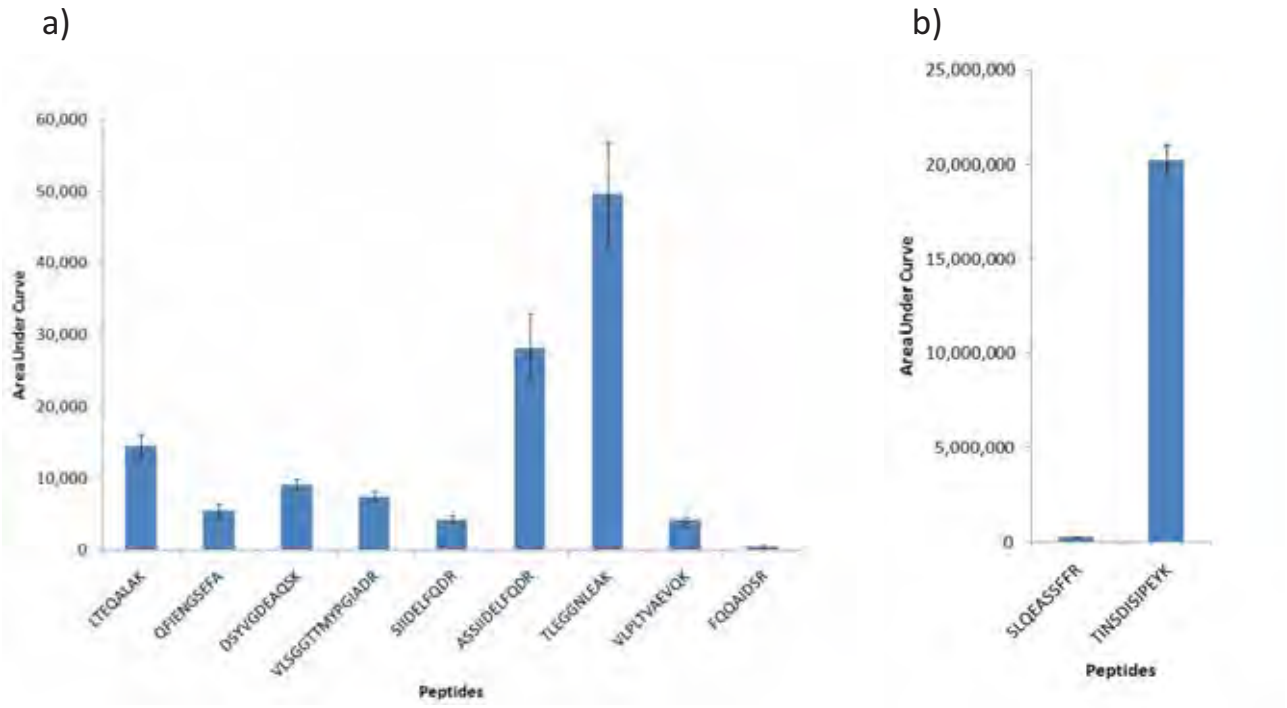

Figure 5.1 Abundance of tear peptide biomarker candidates in control sample. Area under curve (AUC) measured by 4000 QTrap analysis from triplicate analysis of one biological replicate. Data represents area under curve (AUC) for biomarker candidates listed in table 5.2.

5.3.2 MRM analysis of Tear Peptides

The 11 MRM assays developed for tear peptides (Section 5.3.1.3) were evaluated using tear samples from 10 patients from each group of DM, DR and healthy controls. Data from this work was used to further evaluate the variation in relative abundance on an individual patient basis.

All peptides displayed high variation in all sample groups and demonstrated a decrease in abundance in diabetic and diabetic retinopathy samples (Figure 5.2).Area under the curve

quantitation ranged from1,872,859 ± 1,688,277 (TINSDISIPEYK^{2+}) to 553.7 ± 473.8 (QFIENGSEFA^{2+}) amongst controls; 1,504,155 ± 1,046,920 (TINSDISIPEYK^{2+}) to 416 ± 572.3 (SIIDELFQDR^{2+}) for DM and from1,109,852 ± 667,980 (TINSDISIPEYK^{2+}) to 238.7± 183.55 (FQQAIDSR^{2+}) for DR.The largest variation was seen amongst control groups with the average CV being 113%. The peptide showing the largest variation amongst all samples was SLQEASSFFR^{2+} with an average of 129% variation in intensity between control, diabetes and diabetes with retinopathy (Table 5.3).

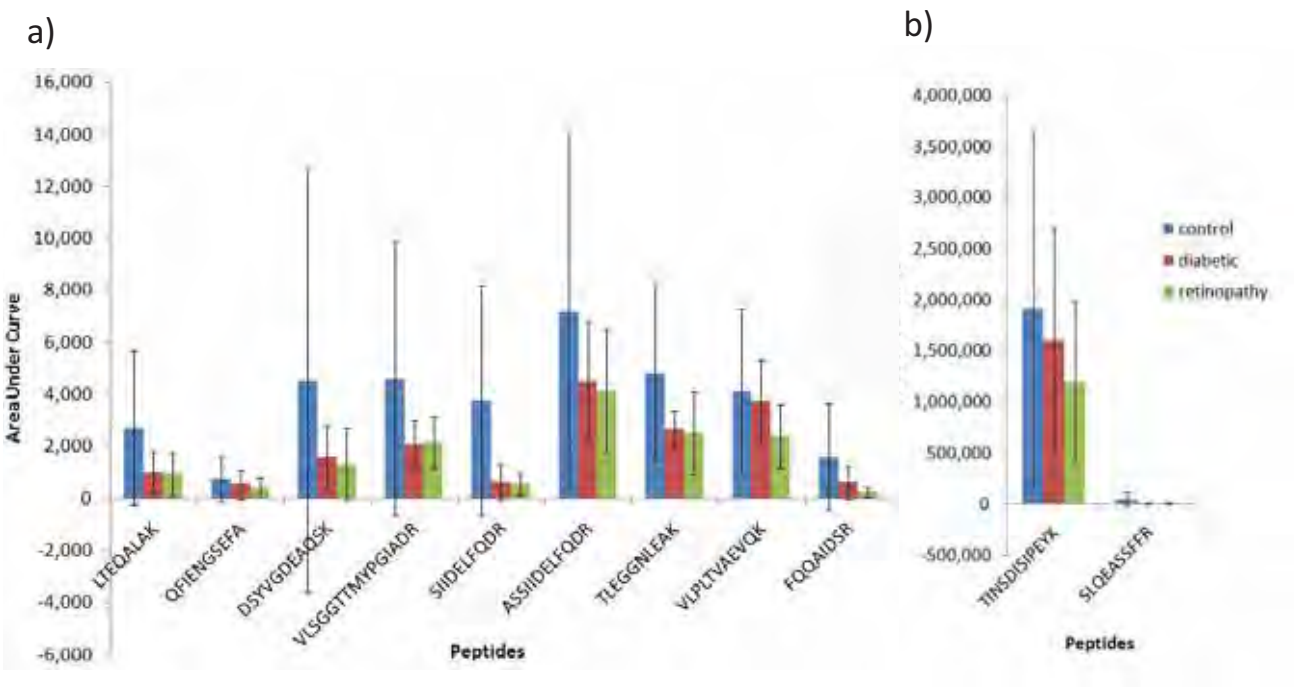

Figure 5.2 Abundance of the tear peptide biomarker candidates in control, diabetic and diabetic retinopathy candidates. Area under curve (AUC) measured by analysis from 1 µg aliquot of tears (*n*=10 for each sample group). Data represents AUC counts for biomarker candidates listed in table 5.2.

Table 5.3 Coefficient of Variance (CV) for peak area of each peptide as measured by MRM assays in control (Con), diabetic (DM) and diabetic with retinopathy (DR). Values are calculated based on *n=10*.

	Con	DM	DR
LTEQALAK	108.9	80.3	89.0
QFIENGSEFA	120.0	103.2	93.2
DSYVGDEAQSK	179.9	77.5	106.6
VLSGGTTMYPGIADR	114.4	44.5	46.4
SIIDELFQDR	117.4	113.0	74.3
ASSIIDELFQDR	94.9	50.3	56.8
SLQEASSFFR	149.3	125.9	113.3
TLEGGNLEAK	69.4	26.0	63.1
VLPLTVAEVQK	76.9	42.2	50.7
FQQAIDSR	129.0	104.7	75.4
TINSDISIPEYK	91.2	68.4	67.2

5.3.3 Comparison between Peak integration and MRM

5.3.3.1 Abundance profiles

A comparison was made between the abundance profiles between the MRM data and the peak integration data in chapter 4to determine whether there was a direct correlation between the abundance profiles of the two sets of data. As both sets of data were quantitatively measured using different instruments, the area under the curve (AUC) data from both instruments was measured using different scales. As a result, each dataset was transformed using an arcsinh transformation allowing the data sets to be compared using a scale within one magnitude, whilst still preserving the mean/variance relationship between each of the peptides;
(http://www.biology.ed.ac.uk/research/groups/jdeacon/statistics/tress4.html).

Figure 5.3describes abundance profiles of the tear peptides between peak integration data (Progenesis PI) and measured AUC using MRM (MRM AUC) values for Con (Figure 5.3a), DM (Figure 5.3b) and DR (Figure 5.3c). The three graphs illustrate the abundance profiles between each MRM and peak integration dataset do not correlate well in any of the three groups. Variation is relatively high amongst control samples compared to DM and DR. Figure 5.4 describes abundance profiles for Con, DM and DR between peak integration data (Figure 5.4a) and MRM data (Figure 5.4b). It is evident that even though Progenesis

data shows significant differences between all three groups in terms of abundance, MRM data illustrate similar trends between the analysed groups, which suggest the peptide abundance levels are dependent on the sample load into the instrument.

a)

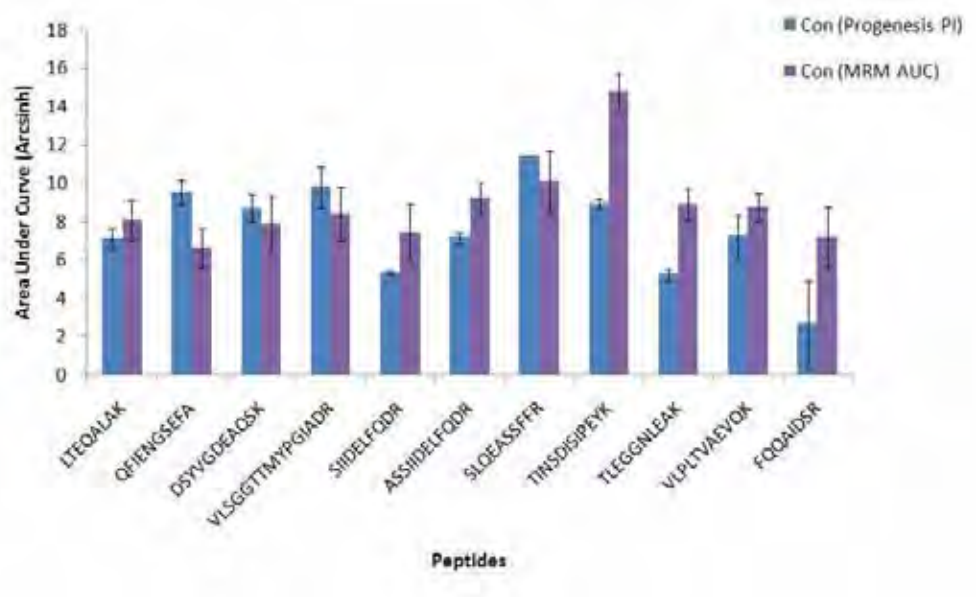

b)

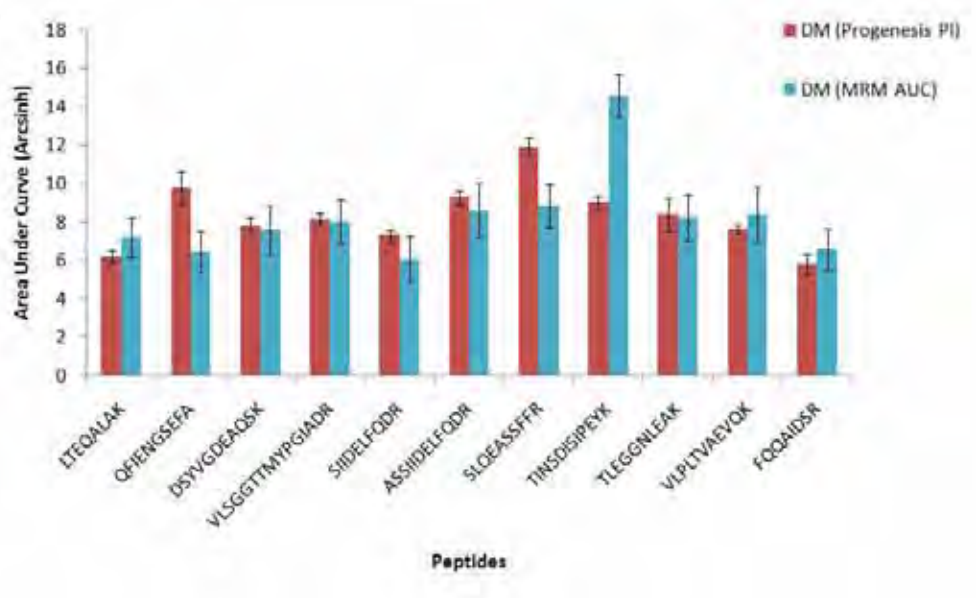

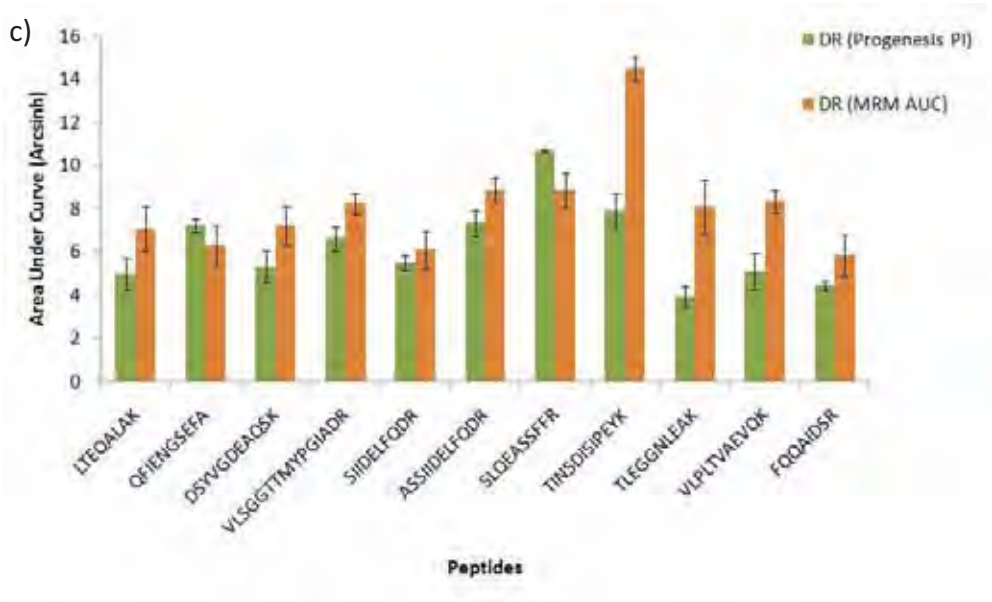

Figure 5.3 Comparison between area under curve (AUC) of the tear peptides between peak integration data (Progenesis PI) and measured MRM (MRM AUC) values for a) Con, b) DM and c) DR. All data has undergone arcsinh transformation of the AUC for the respective groups to allow direct comparison. Data represents averages (± 1 S.D.).

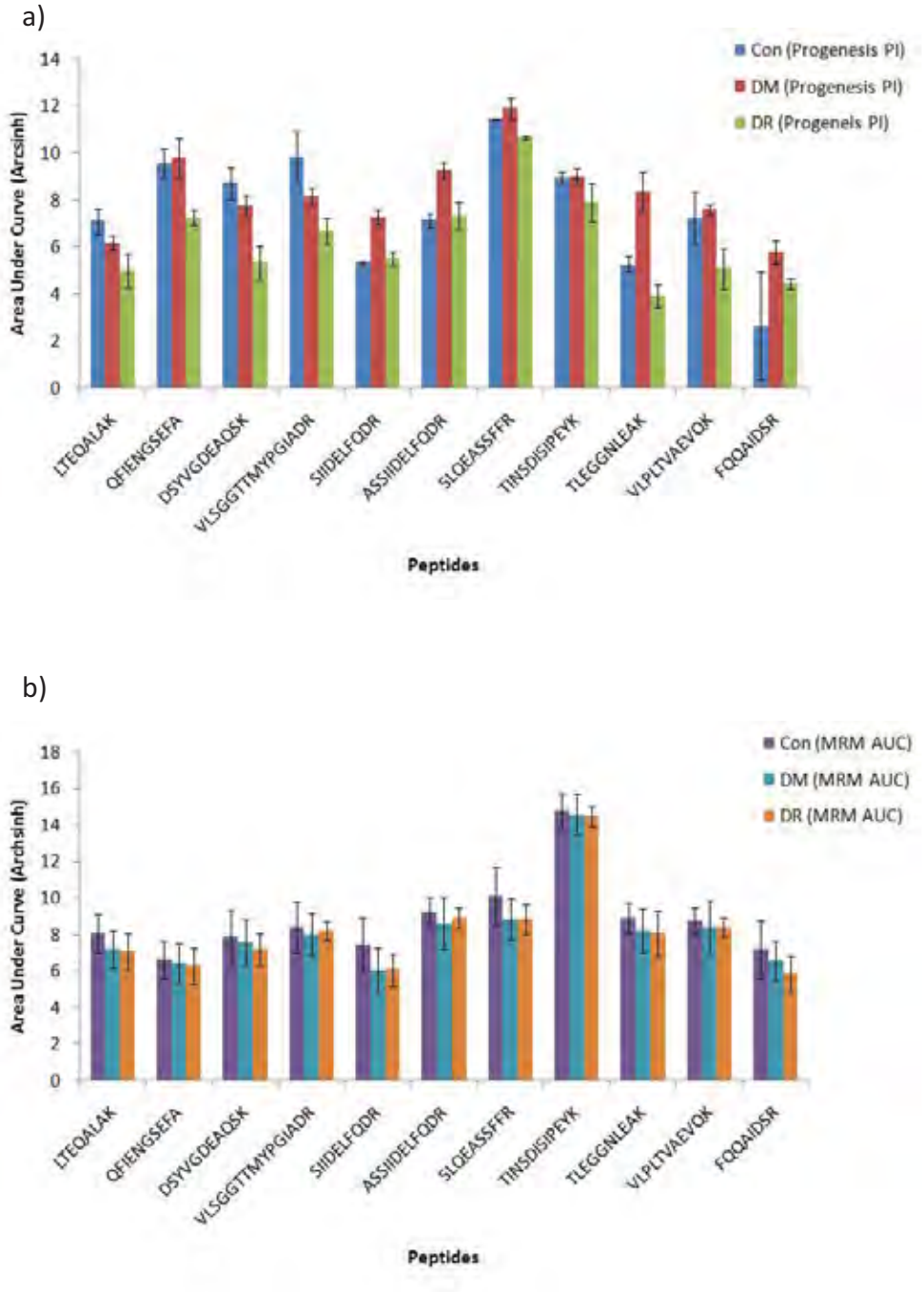

Figure 5.4 Comparison of the area under the curve (AUC) and abundance profiles for Con, DM and DR between a) peak integration data and b) MRM data. All data has undergonearcsinh transformation of the AUC for the respective groups to allow direct comparison. Data represents averages (± 1 S.D.).Whilst there are differences between the groups with peak integration data, peptides from all groups measured with MRM showed similar abundance profiles.

5.3.4 Variation

A comparison of the variation between the two quantitative methods (peak integration and MRM) was performed (Figure 5.5). Variation is high amongst peptides measured with MRM compared to those measured with peak integration.

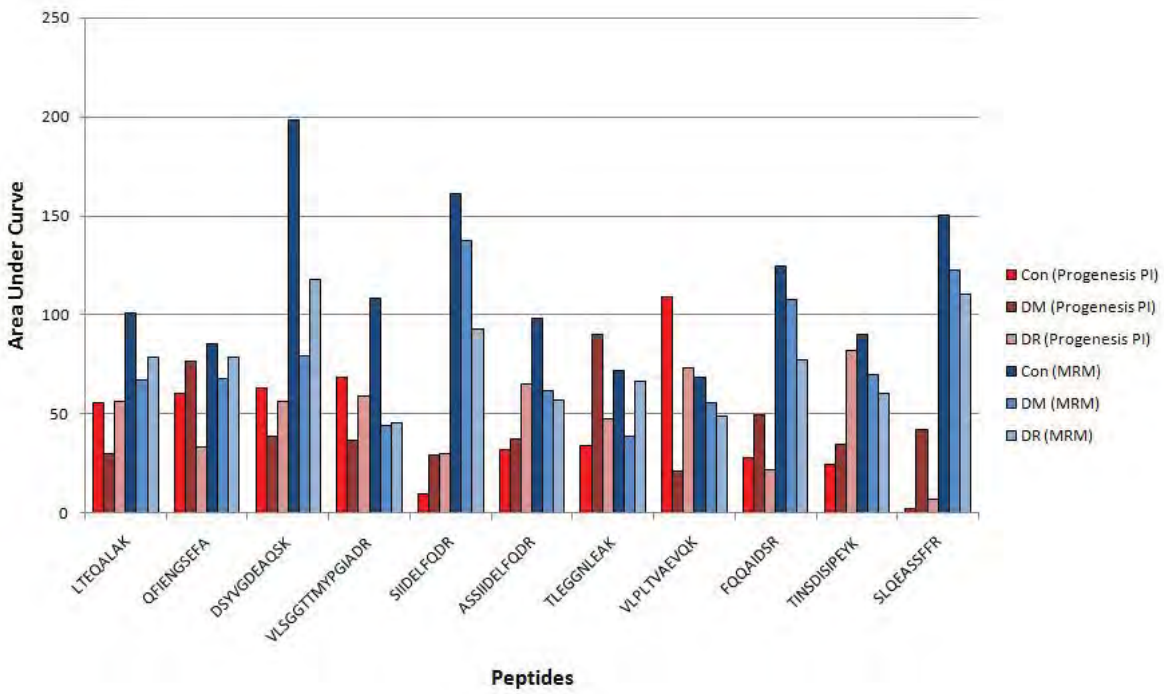

Figure 5.5 A comparison of the variation in Con, DM and DR samples observed using the MF10 fractionation and peak integration method (Progenesis PI) (triplicate of biological replicate of *n=30*) and the MRM method (*n=10*).

5.4 Discussion

5.4.1 Assay Development.

MRM assays have been used to validate several disease associated biomarker candidates [173, 182-184]. In these studies, protein biomarkers are quantitated by analysing proteotypic peptides using MRM. To our knowledge, this chapter describes the first study to optimise an MRM assay which allowed the successful measurement and quantitative validation of tear peptide biomarkers. In this study, there are large differences in results between methodologies which were used to detect and quantitate the tear biomarkers. Firstly, the discovery stage where these peptides were detected as potentially having differential expression between disease states involved LTQ-FT MS, which itself is far more sensitive and different in configuration, ionisation, collision energies and sensitivity when compared to the 4000 QTrap. Secondly, there is a large degree of fractionation in the discovery experiments so as to enrich the peptides for discovery. Ideally, in validation, an assay should be conducive to the high-throughput validation of large numbers of samples [119, 185]. Thus, sample preparation is reduced, removing the need for any fractionation.

Following from these prerequisites ,this chapter reports the successful development of MRM assays for 11 peptides which have been shown to differ in abundance between Con, DM and DR (Chapter 4).This involved several fundamental stages;

1. Preparation of peptides for MRM assay using tears collected from one individual subject rather than a pool of people from one group. No fractionation was required. Sample preparation required inclusion of tryptic digestion and reduction and alkylation to prevent unnecessary complexes forming via disulphide bridges.
2. Development of MRM transition settings and protocols.
3. Testing the variability of sample runs to assess the technical variation in the MRM assay. It was expected that variation would be significantly high owing to interference from the matrix of the low abundance peptides.
4. Refining the methodology for better performing peptides.

In developing these assays, several candidate peptides were omitted. In particular, lacritin peptide EDASSDSTGADPAQEAGTSKPNEEI^{3+} and proline rich protein 4 peptide HPQEQPL^{2+} were removed from analysis. Whilst, the lacritin peptide EDASSDSTGADPAQEAGTSKPNEEI^{3+} could not be detected at all, Skyline had difficulty generating any instrument settings for proline rich protein 4 peptide HPQEQPL^{2+}.Mallick

(2007) noted that proteotypic peptides vary across different configurations of mass spectrometers [178]. This is not surprising considering the differences in source configuration, ionization, collision energies and sensitivity. The LTQ-FT used in the initial biomarker discovery phase of this project is a far more sensitive instrument than the QTrap, used in MRM assay development. Thus, although the LTQ-FT may identify the most promising targets for MRM, detection and signal intensity may not display complete correlation between the two instruments.

Development of the assay involved assessing its sensitivity to detect the peptides of interest. Several factors such as the ion source parameters, ion types chosen for detection and collision energy for the selected peptides were optimized using Skyline. Most of the peptides were subsequently detected with a satisfactory series of transitions that could qualitatively and quantitatively characterize the peptides, with low variation between the ion counts of the peptides in a single sample. Ideally, the specificity of the assay in detecting the targeted peptides would be complemented by additional MS/MS data so as to reduce monitoring of false positive peaks from non-canonical fragments or natural isotope distribution [120, 186]. In developing this assay, peptides were selected for subsequent fragmentation on the proviso that ion counts would surpass 5000 counts per second (cps). This did not occur in this experiment and it is hypothesized that this is a result of assaying low abundant peptides. Whilst peptide detection could be improved by increasing the initial loading of the sample onto the QTrap, caution was exercised to avoid overloading the chromatography column which could elute into succeeding runs, leading to erroneous quantitation.

5.4.2 MRM validation of tear biomarkers

The MRM validation of the tear biomarker candidates for diabetes and diabetic retinopathy did not demonstrate any statistically significant changes amongst the peptides assayed. Data suggested that all peptides were reduced in abundance with the onset of diabetes and diabetic retinopathy. Unfortunately, with such high variation amongst all samples, it is difficult to determine that this is the biological trend. The high variations observed in the experiments are attributed to several oversights regarding sample variation and injection into the QTrap. It is a more accurate conclusion that inconsistent sample loading between the samples contributed to the trends that were observed.

In comparison to the variation observed in Chapter 4, it was expected in this study, that there would be a relatively larger degree of variation. Data measured via peak integration was based on a triplicate analysis of a pool of biological replicate of 30. On the other hand, the data described in this chapter is based on individual biological replicates of 10. Pooling would dilute any major abundance differences and thus, little variation is observed. The variation observed in this experiment could be derived from a number of sources. In this chapter, the sample load introduced into the QTrap was normalized based on the average protein concentration from each disease group, despite the within-group variation. Samples collected varied from 1 µL to 5 µL and so in some cases, the volume collected was not available for both AAA and the developed MRM. On a larger number of samples, variation could easily be exaggerated. Normalization using protein concentration on four individuals assayed for AAA did not show any potential differences. An important source of variation would have been derived from biological variation between individuals. As mentioned earlier, open, closed and reflex tears vary in terms of their constitutive and regulated protein populations [66, 187-189]. Despite efforts to minimize such variation when collecting tears, the variation observed is amplified by the different degrees of open, closed or reflex tears produced by each subject prior to and during collection.

A comparison of data from MRM quantitation with the data from peak integration (Chapter 4) shows that abundance profiles between both experiments did not correlate well. Additionally, peptides between the different groups measured with MRM showed similar AUC values. In this experiment, MF10 fractionation on individual samples prior to MRM assay was not feasible due to small sample volumes available for analysis. A contributing factor to the differences in the trend between the two is the absence of sample fractionation for experiments performed in this chapter. Enriched in the 1-25 kDa fractions are specific proteins and peptide isoforms which have been targeted for protease activity (as an effect of the change in biological environment with the onset of DM/DR). Without fractionation, selectivity and potential to discriminate between the protein and peptides isoforms is absent; quantitation of the specific peptides observed in chapter 4 is overwhelmed by an abundance of tear proteins and peptides isoforms. For this reason it is suggested that methodologies shared in both biomarker discovery and validation should be consistent with minimal or limited adjustments. This is particularly the case in the context of biomarker discovery and validation using a complex biofluid, such as tears, where the large dynamic range of abundance of proteins is a major characteristic.

5.4.3 Conclusions

This chapter describes the successful refinement of a list of potential biomarker peptides which were identified as altering in abundance between Con, DM and DR in chapter 4. Furthermore, an MRM assay has been optimized to test the range of relative abundances of the peptides from an individual subject. When tested against a small population, it is evident that several strategies need to be implemented during sample preparation to ensure the targeted quantitation is specific for the peptides identified in chapter 4. An analysis of the power calculation for the experiments illustrates that the number of samples used in this validation was insufficient to verify the peptides with high confidence. To achieve a power of at least 80%, $p<0.05$ and a small effect size, there would need to be at least 115 samples per group. This experiment used 10 samples, which was not sufficient to produce high confidence. A greater number of samples are required to ensure statistical confidence is high for quantitative validation.

Sample preparation, including fractionation processes, is an important facet of detection and targeted quantitation of the peptides. As discussed, enrichment and fractionation are important steps to ensure the specific targeting of the peptides identified in the biomarker discovery experiments. To ensure adequate normalization of ion intensities, tear peptide concentration of each sample would need to be accurately determined before sample loading onto a QTrap. In doing so, a standard amount of each sample would be loaded, thus increasing the confidence of the quantitation and validation process. Unfortunately due to the limited volume of each tear sample, methods such as AAA and total protein content may inevitably consume a large portion of the sample before any analysis is performed.

Alternatively, there are several other MRM strategies available. One such strategy is that of isotope-based quantification. Here, a standard, such as a mixture of the samples or the peptides to be analysed, is labeled with heavy stable isotopes and spiked into individual samples. An MRM assay would have to be developed for the heavy isotope prior to validation. Quantitation is thus based on relative intensity of the unknown analyte signals and the known internal standard. Using this method, transitions of the heavy (labeled) and light (unlabelled) peptides must be selectively optimized. Currently stable isotope labeling approaches are used in many quantitative shotgun proteomics techniques such as Isotope

Coded Affinity Tags (ICAT) [190], Stable Isotope Labeling with amino acids (AQUA)[191] and Isotope Coded Protein Labeling (ICPL)[192] amongst others[119, 193].

Another strategy involves labeling the sample with isobaric tags such as in mTRAQ or TMT experiments. Samples are labeled with unique isobaric reporter tags and then pooled. The precursor mass of the targeted peptide is selected at the Q1 stage to qualitatively identify the peptide, whilst the reporter ions detected at the Q3 stage will determine relative intensity of each peptide in the MRM assay. The major limitation behind this approach is that peptides sharing similar precursor masses can also be selected and quantitated, thus reducing the specificity of the two-stage filtering process of MRMs. Nevertheless, iTRAQ labeling coupled with MRM analysis has been successfully applied to the analysis of highly enriched samples of low complexity [194].

Labeling strategies are an expensive and complex addition to an MRM experiment. However, they do allow precise quantitation. Matrix effects at higher concentrations are negated and thus larger sample loading is also permitted which, in turn, can increase the sensitivity of the assay provided sample amount is not limiting. Future experiments would need to address the issues outlined in this study so as to evaluate and efficiently determine the peptides which warrant clinical validation, and ultimately develop a test which can increase disease management for diabetes and diabetic retinopathy.

6

GENERAL DISCUSSION

Diabetic retinopathy (DR) is a disease primarily centering on abnormal blood vessel growth within the retinal regions of the eye. Initially, the structural integrity of local blood vessels weakens increasing microaneurysm events. Such vascular rupturing, which increases with the progression of the disease, deprives the retina of sufficient blood supply. The advanced stage of retinopathy is characterised by the growth of abnormal and fragile blood vessels, which have a high propensity to rupture, leading to severe vision loss and blindness.

Currently available diagnostics do not offer a great deal of benefit to DR disease management. Most diagnostics rely on the clinical presentation of DR and by this point maturation of the disease and possible damage to the retinal tissue is significant. This emphasizes the need to develop a diagnostic technology that can detect the disease in its infancy. At this stage, disease management and preventative strategies such as glycemic control would be less intensive and invasive.

It was the aim of this project to identify biomarkers in human tears that would constitute a non-invasive diagnostic for DR and/or diabetes spell out what the disease is (DM). To our knowledge, this thesis describes the first study to identify a suite of peptidomic biomarker candidates that correlate with the onset of DM and DR. Due to the complexity and low volumes of tear samples collected from subjects, a conservative approach to biomarker discovery was taken. This process involved extensive method development to determine the most reproducible methodology to efficiently identify quantitative changes to the tear peptidome and proteome. The optimised developed method was used to measure quantitative changes to the tear peptidome in subjects across three groups; healthy controls, DM and DR. Candidate biomarkers were then verified and validated using a mass spectrometry based assay, multiple reaction monitoring (MRM), which was developed and optimized for the candidate biomarkers.

6.1 Novel findings

During this study, several techniques have been developed, optimised and assessed for their utility in tear biomarker discovery and validation. In this thesis, several of the techniques used could be applied to analyse other complex bio-fluids in addition to further tear biomarker studies for other ocular-related diseases. Furthermore, these studies have produced several outcomes;

- This is the first study to use MF10 technology and peak integration analysis to interrogate the peptidome fraction of tears between different subject groups. This technology overcomes the limitation of conventional proteomics in resolving lower abundance proteins from a tear source limited in volume.

- Improvements to visualize the lower molecular weight proteins and peptides of human tears using MALDI, through the application of spin filters to partition higher molecular weight tear proteins from analysis.

- It is also the first study to mine the peptidomic population in tears for disease associated biomarkers. Comparison of peptide mass maps of tear samples from DM and DR subjects revealed that peptides in tear film do change in abundance with the onset of DM and DR.

- One hundred and nine peptides in the 1-25 kDa MF10 fractions of the tear samples were found to alter between DM and DR subjects in comparison to healthy controls. Thirteen peptides were sequenced and identified. Most of the peptides were derived from proteins indigenous to the tear film, suggesting an alteration to the environment of the tear film with the progression of DM and DR. Changes to these proteins could be attributed to secondary tear film deficiencies characteristic of DM or DR, such as dry eye [91, 195]. Moreover, several proteins have been reported to exist as biomarkers for other diseases such as several cancers [53, 72, 126].

- Development of a MRM assay to quantify, verify and validate candidate tear peptide biomarkers. This has value both in the present study and for future work investigating the tear peptidome. Briefly this involved; 1) development of a sample preparation method for tear samples which promotes the proteotypic nature of peptide detection and includes reduction and alkylation to prevent unnecessary formation of complexes between peptides. 2) Development of MRM transitions and protocol, facilitated using the MRM method development application Skyline. 3) Testing the variability of sample runs by assessing the range of relative abundances from an individual subject rather than the pooled subject samples

used in biomarker discovery. 4) Assessing the variability of multiple sample runs between each group.

- Finally, it has been demonstrated that fractionation is an important part of both biomarker discovery and validation, especially in the context of identifying biomarkers in a complex biofluid such as tears.

6.2 Comparison with/advantages over previous work

The current study is a first to describe the development of a novel methodology to investigate a peptidomic fraction of the tear film. The methodology used has brought together the two technologies MF10 fractionation and peak integration MS analysis. Current literature describes MF10 microflow technology as a relatively young technology, but one which has allowed successful enrichment fractionation and identification of less than 50 μgtotal protein from differentially expressed $CD4^+$/$CD8^+$ T-cells and $CD34^+$ cells [124] . Similar to tears, both samples are inherently limited in volume, relatively complex and over-represented by a small population of higher abundance protein species. The advantages of the MF10 lie in its ability to concentrate whilst fractionating and desalting proteins. On the other hand, peak integration analysis is designed to overcome limitations of labelling quantitative analysis in which inefficient labelling is a major problem[110-111]. Both technologies have been developed to address the common problems with biomarker mining, namely, limited sample volume and the extensive sample complexity inherent in bio-fluids.

A significant progression from this method development is the identification of peptide biomarkers within the tear film which are characteristic of both DM and DR. Many studies have correlated relative changes in abundance in tear proteins with these conditions. Apolipoprotein A-I has been shown to increase in relative abundance in DR [78], whilst a relative increase in abundance of the global protein profile of tears with DR has also been demonstrated [37-38]. de Souza et al., reported the presence of an equilibrium of proteases and protease inhibitors within normal tears and proposed that with the onset of an ocular-related disease this equilibrium is disrupted [46]. It is thus anticipated that the development of DR will coincide with altered peptide abundances as a result of the disruption of this equilibrium. It should be noted that many of the peptides identified have

also been elicited in other ocular and non-ocular diseases. Thus, potentially, these tear peptide biomarkers may fall into the category of acute-phase response peptides and proteins whose concentrations will alter with the onset of secondary complications to the ocular region as a result of the onset of DM and DR. It is important that validation studies be introduced to assess the specificity of these peptides for both diseases.

In terms of development of a validation method for peptidomic biomarkers, data in this work provides an argument for sharing the same methodologies between biomarker discovery and validation. The dominant opinion is that sample preparation should be kept to a minimum during validation assays. As such, relative sample complexity will re-introduce the variation minimized in biomarker discovery, allowing the assessment of biomarker specificity [119]. Additionally, validation should ideally be high-throughput to increase the number of samples processed and in effect increase the power of statistical analysis [185]. MRM is an MS based strategy that has been developed to facilitate biomarker research following these assertions. Unfortunately, as observed in this study, a reduced degree of sample preparation can ultimately expose the quantitation steps to false-positive peptides derived from various isoforms of the protein and peptide in a complex sample such as tears. Without measures to fractionate during sample preparation prior to validation, specificity related to the isoforms observed in biomarker discovery is removed.

6.3 Potential outcomes - Future work/directions

It is envisioned that the biomarkers identified in this thesis will form the intrinsic components of a non-invasive diagnostic developed specifically for DM and DR. Such a diagnostic could help to identify the onset of the disease prior to its maturation or development when less invasive treatments such as glycemic or dietary control would suffice. In doing so, the biomarkers identified hold promising potential to improve the disease management of DR, in turn improving lifestyle of those afflicted with diabetes and its vision complications. The findings from this study provide principles for future work in tear peptide biomarker discovery, validation and possible development of clinical diagnostics specific for DM and DR.

Despite successfully identifying a collection of biomarkers, a significant number of potential candidates remain unidentified. Future work following from the data presented

in this study should focus on identification of the remaining potential biomarker candidates. *De novo* sequencing is currently the best option to identify these potential biomarker candidates and can eliminate any false positive quantitative changes in the process. Furthermore, through *de novo* sequencing, potential PTMs would be identified, thus adding further dimension to understanding the overall changes to the peptidomic character of the ocular tear film with the onset of DM and DR.

The current study has established an MRM protocol to verify the candidate biomarkers for DM and DR. It is suggested that future work introduce internal standards or label candidate peptides using stable isotopes whilst improving current sample preparation strategies. Fractionation of tear samples could constitute an elemental facet of sample preparation prior to MRM quantitation so as to avoid the identification of false-positive peptide candidates. Furthermore, absolute normalization should also be an elemental aspect during MRM analysis. A non-labelling standard experiment could involve the introduction of another MRM assay developed for a constitutive protein such as sIgA, whose secretion is dependent on the rate of tear protein synthesis, rather than tear protein flow. Known labeled standards such as a stable isotope of the targeted peptide would need to be introduced into the sample prior to sample preparation to ensure that the quantitative information is conserved through fractionation, capture and elution. For biomarker candidates that are too low for a reliable assay, sensitivity can be improved using anti-peptide antibodies to enrich for the targeted peptides prior to MRM analysis.

A simple power analysis demonstrates on the back of Progenesis^{TM} data that a significant amount of individual samples are needed to increase the power of the biomarker candidates that have been identified. Through this study, samples were verified using *n=10*. Ideally, pre-validation and certainly validation experiments would extend this targeted analysis to a larger number of subjects, whilst incorporating a broader range of cases and controls, therefore testing environmental, biological and genetic variation in the population.

From a broad view, this thesis has established principles for future peptidomic or low abundance protein studies with complex bio-fluids. Both MF10 and peak integration quantitation have been developed to improve the concentration of peptide content whilst minimising sample loss which could result from labelling strategies. Furthermore, the work

describes the isolation, and identification of several proteins which may possibly be a characteristic to other ocular or non-ocular related diseases. For example, we have described the characterization of mesothelin peptide VLPLTVAEVQK. Using the aforementioned method, one could potentially isolate these peptides in other bio-fluids as well as tears as potential biomarkers or effectors in other biological processes. Coupled with validation through targeted quantitative mass spectrometry, the workflow described is a powerful tool in biomarker discovery and validation of clinical utility.

References

[1] Tapp, R. J., Shaw, J. E., Harper, C. A., de Courten, M. P.*, et al.*, The prevalence of and factors associated with diabetic retinopathy in the Australian population. *Diabetes Care* 2003, *26*, 1731-1737.

[2] Klein, R., Klein, B. E., Moss, S. E., The Wisconsin epidemiological study of diabetic retinopathy: a review. *Diabetes Metab Rev* 1989, *5*, 559-570.

[3] Klein, R., Moss, S. E., Klein, B. E., New management concepts for timely diagnosis of diabetic retinopathy treatable by photocoagulation. *Diabetes Care* 1987, *10*, 633-638.

[4] Fong, D. S., Aiello, L. P., Ferris, F. L., 3rd, Klein, R., Diabetic retinopathy. *Diabetes Care* 2004, *27*, 2540-2553.

[5] Harris, M. I., Undiagnosed NIDDM: clinical and public health issues. *Diabetes Care* 1993, *16*, 642-652.

[6] Lim, A., Stewart, J., Chui, T. Y., Lin, M.*, et al.*, Prevalence and risk factors of diabetic retinopathy in a multi-racial underserved population. *Ophthalmic Epidemiol* 2008, *15*, 402-409.

[7] Kolb, H., Nelson, R., Ahnelt, P., Cuenca, N., Cellular organization of the vertebrate retina. *Prog Brain Res* 2001, *131*, 3-26.

[8] Steuer, H., Jaworski, A., Elger, B., Kaussmann, M.*, et al.*, Functional characterization and comparison of the outer blood-retina barrier and the blood-brain barrier. *Invest Ophthalmol Vis Sci* 2005, *46*, 1047-1053.

[9] Larsen, J., Lund-Andersen, H., Krogsaa, B., Transient transport across the blood-retina barrier. *Bull Math Biol* 1983, *45*, 749-758.

[10] Tso, M. O., Cunha-Vaz, J. G., Shih, C. Y., Jones, C. W., Clinicopathologic study of blood-retinal barrier in experimental diabetes mellitus. *Arch Ophthalmol* 1980, *98*, 2032-2040.

[11] Wu, S. W., [A preliminary report on the measurement of retinal function by electro-oculography]. *Zhonghua Yan Ke Za Zhi* 1983, *19*, 23-27.

[12] Frank, R. N., Diabetic retinopathy. *N Engl J Med* 2004, *350*, 48-58.

[13] Mathews, M. K., Merges, C., McLeod, D. S., Lutty, G. A., Vascular endothelial growth factor and vascular permeability changes in human diabetic retinopathy. *Invest Ophthalmol Vis Sci* 1997, *38*, 2729-2741.

[14] Antonetti, D. A., Barber, A. J., Bronson, S. K., Freeman, W. M.*, et al.*, Diabetic retinopathy: seeing beyond glucose-induced microvascular disease. *Diabetes* 2006, *55*, 2401-2411.

[15] van Dijk, H. W., Kok, P. H., Garvin, M., Sonka, M.*, et al.*, Selective loss of inner retinal layer thickness in type 1 diabetic patients with minimal diabetic retinopathy. *Invest Ophthalmol Vis Sci* 2009, *50*, 3404-3409.

[16] Chu, J., Ali, Y., Diabetic retinopathy: A review. *Drug Develop Res* 2008, *69*, 1-14.

[17] Ciulla, T. A., Amador, A. G., Zinman, B., Diabetic retinopathy and diabetic macular edema - Pathophysiology, screening, and novel therapies. *Diabetes Care* 2003, *26*, 2653-2664.

[18] Yam, J. C., Kwok, A. K., Update on the treatment of diabetic retinopathy. *Hong Kong Med J* 2007, *13*, 46-60.

[19] Sheth, B. P., Does pregnancy accelerate the rate of progression of diabetic retinopathy? *Curr Diab Rep* 2002, *2*, 327-330.

[20] Dorchy, H., Screening for subclinical complications in young type 1 diabetic patients: experience acquired in Brussels. *Pediatr Endocrinol Rev* 2004, *1*, 380-403.

[21] Wong, T. Y., Mitchell, P., The eye in hypertension. *Lancet* 2007, *369*, 425-435.

[22] Mohamed, Q., Gillies, M. C., Wong, T. Y., Management of diabetic retinopathy: a systematic review. *JAMA* 2007, *298*, 902-916.

[23] Photocoagulation treatment of proliferative diabetic retinopathy: the second report of diabetic retinopathy study findings. *Ophthalmology* 1978, *85*, 82-106.

[24] Retinopathy and nephropathy in patients with type 1 diabetes four years after a trial of intensive therapy. The Diabetes Control and Complications Trial/Epidemiology of Diabetes Interventions and Complications Research Group. *N Engl J Med* 2000, *342*, 381-389.

[25] Stratton, I. M., Kohner, E. M., Aldington, S. J., Turner, R. C*., et al.*, UKPDS 50: risk factors for incidence and progression of retinopathy in Type II diabetes over 6 years from diagnosis. *Diabetologia* 2001, *44*, 156-163.

[26] Intensive blood-glucose control with sulphonylureas or insulin compared with conventional treatment and risk of complications in patients with type 2 diabetes (UKPDS 33). UK Prospective Diabetes Study (UKPDS) Group. *Lancet* 1998, *352*, 837-853.

[27] Smiddy, W. E., Flynn, H. W., Jr., Vitrectomy in the management of diabetic retinopathy. *Surv Ophthalmol* 1999, *43*, 491-507.

[28] Moss, S. E., Meuer, S. M., Klein, R., Hubbard, L. D*., et al.*, Are seven standard photographic fields necessary for classification of diabetic retinopathy? *Invest Ophthalmol Vis Sci* 1989, *30*, 823-828.

[29] Fransen, S. R., Leonard-Martin, T. C., Feuer, W. J., Hildebrand, P. L., Clinical evaluation of patients with diabetic retinopathy: accuracy of the Inoveon diabetic retinopathy-3DT system. *Ophthalmology* 2002, *109*, 595-601.

[30] Huang, D., Swanson, E. A., Lin, C. P., Schuman, J. S*., et al.*, Optical coherence tomography. *Science* 1991, *254*, 1178-1181.

[31] Grunwald, J. E., Riva, C. E., Sinclair, S. H., Brucker, A. J., Petrig, B. L., Laser Doppler velocimetry study of retinal circulation in diabetes mellitus. *Arch Ophthalmol* 1986, *104*, 991-996.

[32] Berkowitz, B. A., Adult and newborn rat inner retinal oxygenation during carbogen and 100% oxygen breathing. Comparison using magnetic resonance imaging delta Po2 mapping. *Invest Ophthalmol Vis Sci* 1996, *37*, 2089-2098.

[33] Aebersold, R., Anderson, L., Caprioli, R., Druker, B., *et al.*, Perspective: a program to improve protein biomarker discovery for cancer. *J Proteome Res* 2005, *4*, 1104-1109.

[34] Vitzthum, F., Behrens, F., Anderson, N. L., Shaw, J. H., Proteomics: from basic research to diagnostic application. A review of requirements & needs. *J Proteome Res* 2005, *4*, 1086-1097.

[35] Aebersold, R., Mann, M., Mass spectrometry-based proteomics. *Nature* 2003, *422*, 198-207.

[36] Grus, F. H., Podust, V. N., Bruns, K., Lackner, K., *et al.*, SELDI-TOF-MS ProteinChip array profiling of tears from patients with dry eye. *Invest Ophthalmol Vis Sci* 2005, *46*, 863-876.

[37] Grus, F. H., Sabuncuo, P., Dick, H. B., Augustin, A. J., Pfeiffer, N., Changes in the tear proteins of diabetic patients. *BMC Ophthalmol* 2002, *2*, 4.

[38] Herber, S., Grus, F. H., Sabuncuo, P., Augustin, A. J., Two-dimensional analysis of tear protein patterns of diabetic patients. *Electrophoresis* 2001, *22*, 1838-1844.

[39] Lemp, M. A., Report of the National Eye Institute/Industry workshop on Clinical Trials in Dry Eyes. *CLAO J* 1995, *21*, 221-232.

[40] de Godoy, L. M., Olsen, J. V., de Souza, G. A., Li, G., *et al.*, Status of complete proteome analysis by mass spectrometry: SILAC labeled yeast as a model system. *Genome Biol* 2006, *7*, R50.

[41] Goebbels, M., Tear secretion and tear film function in insulin dependent diabetics. *Br J Ophthalmol* 2000, *84*, 19-21.

[42] Foulks, G. N., Bron, A. J., Meibomian gland dysfunction: a clinical scheme for description, diagnosis, classification, and grading. *Ocul Surf* 2003, *1*, 107-126.

[43] Guzman-Aranguez, A., Mantelli, F., Argueso, P., Mucin-type O-glycans in tears of normal subjects and patients with non-Sjogren's dry eye. *Invest Ophthalmol Vis Sci* 2009, *50*, 4581-4587.

[44] Davidson, H. J., Kuonen, V. J., The tear film and ocular mucins. *Vet Ophthalmol* 2004, *7*, 71-77.

[45] Baum, J. L., The Castroviejo Lecture. Prolonged eyelid closure is a risk to the cornea. *Cornea* 1997, *16*, 602-611.

[46] de Souza, G. A., Godoy, L. M., Mann, M., Identification of 491 proteins in the tear fluid proteome reveals a large number of proteases and protease inhibitors. *Genome Biol* 2006, *7*, R72.

[47] Holly, F. J., Lemp, M. A., Tear physiology and dry eyes. *Surv Ophthalmol* 1977, *22*, 69-87.

[48] Bron, A. J., Tiffany, J. M., The meibomian glands and tear film lipids. Structure, function, and control. *Adv Exp Med Biol* 1998, *438*, 281-295.

[49] Dartt, D. A., in: Albert, D. M., Jakobiec, F. A. (Eds.), *Principles and practice of ophthalmology*, WB Saunders Company, Philadelphia 2000, pp. 960-981.

[50] Bron, A. J., Tiffany, J. M., The contribution of meibomian disease to dry eye. *Ocul Surf* 2004, *2*, 149-165.

[51] McCulley, J. P., Shine, W. E., Meibomian gland function and the tear lipid layer. *Ocul Surf* 2003, *1*, 97-106.

[52] Brown, S. I., Dervichian, D. G., The oils of the meibomian glands. Physical and surface characteristics. *Arch Ophthalmol* 1969, *82*, 537-540.

[53] de Freitas Campos, C., Cole, N., Van Dyk, D., Walsh, B. J.*, et al.*, Proteomic analysis of dog tears for potential cancer markers. *Res Vet Sci* 2008, *85*, 349-352.

[54] Milder, B., in: Moses, R. A. a. H., W.M. (Ed.), *Adler's Physiology of the Eye*, Mosby, St Louis 1987, pp. 15-35.

[55] Dartt, D. A., Regulation of tear secretion. *Adv Exp Med Biol* 1994, *350*, 1-9.

[56] Bothelo, S. Y., Tears and the lacrimal gland. *Science American* 1964, *211*, 78.

[57] Green-Church, K. B., Nichols, K. K., Kleinholz, N. M., Zhang, L., Nichols, J. J., Investigation of the human tear film proteome using multiple proteomic approaches. *Mol Vis* 2008, *14*, 456-470.

[58] Redl, B., Holzfeind, P., Lottspeich, F., cDNA cloning and sequencing reveals human tear prealbumin to be a member of the lipophilic-ligand carrier protein superfamily. *J Biol Chem* 1992, *267*, 20282-20287.

[59] Flower, D. R., North, A. C., Attwood, T. K., Structure and sequence relationships in the lipocalins and related proteins. *Protein Sci* 1993, *2*, 753-761.

[60] Chmurzynska, A., The multigene family of fatty acid-binding proteins (FABPs): function, structure and polymorphism. *J Appl Genet* 2006, *47*, 39-48.

[61] Sariri, R., Ghafoori, H., Tear proteins in health, disease, and contact lens wear. *Biochemistry (Mosc)* 2008, *73*, 381-392.

[62] Seal, D. V., McGill, J. I., Mackie, I. A., Liakos, G. M.*, et al.*, Bacteriology and tear protein profiles of the dry eye. *Br J Ophthalmol* 1986, *70*, 122-125.

[63] Farris, R. L., Tear analysis in contact lens wearers. *Trans Am Ophthalmol Soc* 1985, *83*, 501-545.

[64] Craig, J., *The tear film. Structure, function and clinical examination*, Butterworth Heinmann, Edinburgh 2002, pp. 19-50.

[65] Ng, V., Cho, P., Wong, F., Chan, Y., Variability of tear protein levels in normal young adults: diurnal (daytime) variation. *Graefes Arch Clin Exp Ophthalmol* 2001, *239*, 257-263.

[66] Fullard, R. J., Tucker, D. L., Changes in human tear protein levels with progressively increasing stimulus. *Invest Ophthalmol Vis Sci* 1991, *32*, 2290-2301.

[67] Sack, R. A., Conradi, L., Krumholz, D., Beaton, A.*, et al.*, Membrane array characterization of 80 chemokines, cytokines, and growth factors in open- and closed-eye tears: angiogenin and other defense system constituents. *Invest Ophthalmol Vis Sci* 2005, *46*, 1228-1238.

[68] Willcox, M. D., Morris, C. A., Thakur, A., Sack, R. A.*, et al.*, Complement and complement regulatory proteins in human tears. *Invest Ophthalmol Vis Sci* 1997, *38*, 1-8.

[69] Rohen, J. W. a. L.-D., E., *The Dry Eye. A comprehensive Guide*, Springer-Verlag, Berlin 1992, pp. 35-63.

[70] Kaura, R. a. T., J.M., in: Holly, F. J. (Ed.), *The Preocular Tear Film in Health, Disease and Contact Lens Wear*, Dry Eye Institute, Lubbock 1986, pp. 728-732.

[71] Hu, S., Loo, J. A., Wong, D. T., Human body fluid proteome analysis. *Proteomics* 2006, *6*, 6326-6353.

[72] Evans, V., Vockler, C., Friedlander, M., Walsh, B., Willcox, M. D., Lacryglobin in human tears, a potential marker for cancer. *Clin Experiment Ophthalmol* 2001, *29*, 161-163.

[73] Assouti, M., Vynios, D. H., Anagnostides, S. T., Papadopoulos, G.*, et al.*, Collagen type IX and HNK-1 epitope in tears of patients with pseudoexfoliation syndrome. *Biochim Biophys Acta* 2006, *1762*, 54-58.

[74] Jacob, J. T., Ham, B., Compositional Profiling and Biomarker Identification of the Tear Film. *Ocul Surf* 2008, *6*, 175-185.

[75] Zhou, L., Beuerman, R. W., Barathi, A., Tan, D., Analysis of rabbit tear proteins by high-pressure liquid chromatography/electrospray ionization mass spectrometry. *Rapid Commun Mass Spectrom* 2003, *17*, 401-412.

[76] Ham, B. M., Jacob, J. T., Cole, R. B., Single eye analysis and contralateral eye comparison of tear proteins in normal and dry eye model rabbits by MALDI-ToF mass spectrometry using wax-coated target plates. *Anal Bioanal Chem* 2007, *387*, 889-900.

[77] Zhou, L., Beuerman, R. W., Huang, L., Barathi, A.*, et al.*, Proteomic analysis of rabbit tear fluid: Defensin levels after an experimental corneal wound are correlated to wound closure. *Proteomics* 2007, *7*, 3194-3206.

[78] Kawai, S., Nakajima, T., Hokari, S., Komoda, T., Kawai, K., Apolipoprotein A-I concentration in tears in diabetic retinopathy. *Ann Clin Biochem* 2002, *39*, 56-61.

[79] Koo, B. S., Lee, D. Y., Ha, H. S., Kim, J. C., Kim, C. W., Comparative analysis of the tear protein expression in blepharitis patients using two-dimensional electrophoresis. *J Proteome Res* 2005, *4*, 719-724.

[80] Ohashi, Y., Ishida, R., Kojima, T., Goto, E.*, et al.*, Abnormal protein profiles in tears with dry eye syndrome. *Am J Ophthalmol* 2003, *136*, 291-299.

[81] Tomosugi, N., Kitagawa, K., Takahashi, N., Sugai, S., Ishikawa, I., Diagnostic potential of tear proteomic patterns in Sjogren's syndrome. *J Proteome Res* 2005, *4*, 820-825.

[82] ter Rahe, B. S., van Haeringen, N. J., Cystatins in tears of patients with different corneal conditions. *Ophthalmologica* 1998, *212*, 34-36.

[83] Fodor, M., Facsko, A., Rajnavolgyi, E., Harsfalvi, J.*, et al.*, Enhanced release of IL-6 and IL-8 into tears in various anterior segment eye diseases. *Ophthalmic Res* 2006, *38*, 182-188.

[84] Zhou, L., Huang, L. Q., Beuerman, R. W., Grigg, M. E.*, et al.*, Proteomic analysis of human tears: defensin expression after ocular surface surgery. *J Proteome Res* 2004, *3*, 410-416.

[85] Yokota, H., Mori, F., Kai, K., Nagaoka, T.*, et al.*, Serum prorenin levels and diabetic retinopathy in type 2 diabetes: new method to measure serum level of prorenin using antibody activating direct kinetic assay. *Br J Ophthalmol* 2005, *89*, 871-873.

[86] Izuora, K. E., Chase, H. P., Jackson, W. E., Coll, J. R.*, et al.*, Inflammatory markers and diabetic retinopathy in type 1 diabetes. *Diabetes Care* 2005, *28*, 714-715.

[87] Masmiquel, L., Segura, R. M., Mateo, C., Calatayud, M.*, et al.*, Serum laminin as a marker of diabetic retinopathy development: a 4-year follow-up study. *Am J Ophthalmol* 2000, *129*, 347-352.

[88] Watanabe, D., Suzuma, K., Suzuma, I., Ohashi, H.*, et al.*, Vitreous levels of angiopoietin 2 and vascular endothelial growth factor in patients with proliferative diabetic retinopathy. *Am J Ophthalmol* 2005, *139*, 476-481.

[89] Hernandez, C., Segura, R. M., Fonollosa, A., Carrasco, E.*, et al.*, Interleukin-8, monocyte chemoattractant protein-1 and IL-10 in the vitreous fluid of patients with proliferative diabetic retinopathy. *Diabet Med* 2005, *22*, 719-722.

[90] Funatsu, H., Yamashita, H., Noma, H., Mimura, T.*, et al.*, Aqueous humor levels of cytokines are related to vitreous levels and progression of diabetic retinopathy in diabetic patients. *Graefes Arch Clin Exp Ophthalmol* 2005, *243*, 3-8.

[91] Manaviat, M. R., Rashidi, M., Afkhami-Ardekani, M., Shoja, M. R., Prevalence of dry eye syndrome and diabetic retinopathy in type 2 diabetic patients. *BMC Ophthalmol* 2008, *8*, 10.

[92] Cordwell, S. J., Technologies for bacterial surface proteomics. *Curr Opin Microbiol* 2006, *9*, 320-329.

[93] Haynes, P. A., Roberts, T. H., Subcellular shotgun proteomics in plants: looking beyond the usual suspects. *Proteomics* 2007, *7*, 2963-2975.

[94] Penque, D., Two-dimensional gel electrophoresis and mass spectrometry for biomarker discovery. *Proteom Clin Appl* 2009, *3*, 155-172.

[95] Righetti, P. G., Castagna, A., Antonioli, P., Boschetti, E., Prefractionation techniques in proteome analysis: the mining tools of the third millennium. *Electrophoresis* 2005, *26*, 297-319.

[96] Wu, C. C., Yates, J. R., 3rd, The application of mass spectrometry to membrane proteomics. *Nat Biotechnol* 2003, *21*, 262-267.

[97] Washburn, M. P., Wolters, D., Yates, J. R., 3rd, Large-scale analysis of the yeast proteome by multidimensional protein identification technology. *Nat Biotechnol* 2001, *19*, 242-247.

[98] Chen, E. I., Hewel, J., Felding-Habermann, B., Yates, J. R., 3rd, Large scale protein profiling by combination of protein fractionation and multidimensional protein identification technology (MudPIT). *Mol Cell Proteomics* 2006, *5*, 53-56.

[99] Haynes, P. A., Roberts, T. H., Subcellular shotgun proteomics in plants: Looking beyond the usual suspects. *Proteomics* 2007, *7*, 2963-2975.

[100] Delmotte, N., Lasaosa, M., Tholey, A., Heinzle, E., *et al.*, Repeatability of peptide identifications in shotgun proteome analysis employing off-line two-dimensional chromatographic separations and ion-trap MS. *J Sep Sci* 2009, *32*, 1156-1164.

[101] Liu, H., Sadygov, R. G., Yates, J. R., 3rd, A model for random sampling and estimation of relative protein abundance in shotgun proteomics. *Anal Chem* 2004, *76*, 4193-4201.

[102] Zybailov, B., Coleman, M. K., Florens, L., Washburn, M. P., Correlation of relative abundance ratios derived from peptide ion chromatograms and spectrum counting for quantitative proteomic analysis using stable isotope labeling. *Anal Chem* 2005, *77*, 6218-6224.

[103] Gygi, S. P., Rist, B., Griffin, T. J., Eng, J., Aebersold, R., Proteome analysis of low-abundance proteins using multidimensional chromatography and isotope-coded affinity tags. *J Proteome Res* 2002, *1*, 47-54.

[104] Zhang, Y., Wolf-Yadlin, A., Ross, P. L., Pappin, D. J., *et al.*, Time-resolved mass spectrometry of tyrosine phosphorylation sites in the epidermal growth factor receptor signaling network reveals dynamic modules. *Mol Cell Proteomics* 2005, *4*, 1240-1250.

[105] Hu, J., Qian, J., Borisov, O., Pan, S., *et al.*, Optimized proteomic analysis of a mouse model of cerebellar dysfunction using amine-specific isobaric tags. *Proteomics* 2006, *6*, 4321-4334.

[106] Wu, W. W., Wang, G., Baek, S. J., Shen, R. F., Comparative study of three proteomic quantitative methods, DIGE, cICAT, and iTRAQ, using 2D gel- or LC-MALDI TOF/TOF. *J Proteome Res* 2006, *5*, 651-658.

[107] Liao, L., Pilotte, J., Xu, T., Wong, C. C., *et al.*, BDNF induces widespread changes in synaptic protein content and up-regulates components of the translation machinery: an analysis using high-throughput proteomics. *J Proteome Res* 2007, *6*, 1059-1071.

[108] Nagalla, S. R., Canick, J. A., Jacob, T., Schneider, K. A., *et al.*, Proteomic analysis of maternal serum in down syndrome: identification of novel protein biomarkers. *J Proteome Res* 2007, *6*, 1245-1257.

[109] Pereira, L., Reddy, A. P., Jacob, T., Thomas, A., *et al.*, Identification of novel protein biomarkers of preterm birth in human cervical-vaginal fluid. *J Proteome Res* 2007, *6*, 1269-1276.

[110] Stevenson, S. E., Chu, Y., Ozias-Akins, P., Thelen, J. J., Validation of gel-free, label-free quantitative proteomics approaches: applications for seed allergen profiling. *J Proteomics* 2009, *72*, 555-566.

[111] Guillaume, E., Berger, B., Affolter, M., Kussmann, M., Label-free quantitative proteomics of two Bifidobacterium longum strains. *J Proteomics* 2009, *72*, 771-784.

[112] Fricker, L. D., Lim, J., Pan, H., Che, F. Y., Peptidomics: identification and quantification of endogenous peptides in neuroendocrine tissues. *Mass Spectrom Rev* 2006, *25*, 327-344.

[113] Schulz-Knappe, P., Zucht, H. D., Heine, G., Jurgens, M., *et al.*, Peptidomics: the comprehensive analysis of peptides in complex biological mixtures. *Comb Chem High Throughput Screen* 2001, *4*, 207-217.

[114] Strand, F. L., Neuropeptides: general characteristics and neuropharmaceutical potential in treating CNS disorders. *Prog Drug Res* 2003, *61*, 1-37.

[115] Farrokhi, N., Whitelegge, J. P., Brusslan, J. A., Plant peptides and peptidomics. *Plant Biotechnol J* 2008, *6*, 105-134.

[116] Baggerman, G., Boonen, K., Verleyen, P., De Loof, A., Schoofs, L., Peptidomic analysis of the larval Drosophila melanogaster central nervous system by two-dimensional capillary liquid chromatography quadrupole time-of-flight mass spectrometry. *J Mass Spectrom* 2005, *40*, 250-260.

[117] Horvath, Z. S., Corthals, G. L., Wrigley, C. W., Margolis, J., Multifunctional apparatus for electrokinetic processing of proteins. *Electrophoresis* 1994, *15*, 968-971.

[118] Wasinger, V., Ly, L., Fitzgerald, A., Walsh, B., Prefractionation, enrichment, desalting and depleting of low volume and low abundance proteins and peptides using the MF10. *Methods Mol Biol* 2008, *424*, 257-275.

[119] Rifai, N., Gillette, M. A., Carr, S. A., Protein biomarker discovery and validation: the long and uncertain path to clinical utility. *Nat Biotechnol* 2006, *24*, 971-983.

[120] Lange, V., Picotti, P., Domon, B., Aebersold, R., Selected reaction monitoring for quantitative proteomics: a tutorial. *Mol Syst Biol* 2008, *4*, 222.

[121] Keller, A., Nesvizhskii, A. I., Kolker, E., Aebersold, R., Empirical statistical model to estimate the accuracy of peptide identifications made by MS/MS and database search. *Anal Chem* 2002, *74*, 5383-5392.

[122] Nesvizhskii, A. I., Keller, A., Kolker, E., Aebersold, R., A statistical model for identifying proteins by tandem mass spectrometry. *Anal Chem* 2003, *75*, 4646-4658.

[123] Azzarolo, A. M., Brew, K., Kota, S., Ponomareva, O.*, et al.*, Presence of tear lipocalin and other major proteins in lacrimal fluid of rabbits. *Comp Biochem Physiol B Biochem Mol Biol* 2004, *138*, 111-117.

[124] Ly, L., Wasinger, V. C., Mass and charge selective protein fractionation for the differential analysis of T-cell and CD34+ stem cell proteins from cord blood. *J Proteomics* 2010, *73*, 571-578.

[125] Grus, F. H., Augustin, A. J., Evangelou, N. G., Toth-Sagi, K., Analysis of tear-protein patterns as a diagnostic tool for the detection of dry eyes. *Eur J Ophthalmol* 1998, *8*, 90-97.

[126] Molloy, M. P., Bolis, S., Herbert, B. R., Ou, K.*, et al.*, Establishment of the human reflex tear two-dimensional polyacrylamide gel electrophoresis reference map: new proteins of potential diagnostic value. *Electrophoresis* 1997, *18*, 2811-2815.

[127] Stuchell, R. N., Feldman, J. J., Farris, R. L., Mandel, I. D., The effect of collection technique on tear composition. *Invest Ophthalmol Vis Sci* 1984, *25*, 374-377.

[128] Choy, C. K., Cho, P., Chung, W. Y., Benzie, I. F., Water-soluble antioxidants in human tears: effect of the collection method. *Invest Ophthalmol Vis Sci* 2001, *42*, 3130-3134.

[129] Grus, F. H., Kramann, C., Bozkurt, N., Wiegel, N.*, et al.*, Effects of multipurpose contact lens solutions on the protein composition of the tear film. *Cont Lens Anterior Eye* 2005, *28*, 103-112.

[130] Reitz, C., Breipohl, W., Augustin, A., Bours, J., Analysis of tear proteins by one- and two-dimensional thin-layer iosoelectric focusing, sodium dodecyl sulfate electrophoresis and lectin blotting. Detection of a new component: cystatin C. *Graefes Arch Clin Exp Ophthalmol* 1998, *236*, 894-899.

[131] Haggerty, C. M., Larke, J. R., Human tear protein fractions during waking hours. *Ophthalmic Physiol Opt* 1982, *2*, 187-191.

[132] Sathe, S., Sakata, M., Beaton, A. R., Sack, R. A., Identification, origins and the diurnal role of the principal serine protease inhibitors in human tear fluid. *Curr Eye Res* 1998, *17*, 348-362.

[133] Barka, T., Asbell, P. A., van der Noen, H., Prasad, A., Cystatins in human tear fluid. *Curr Eye Res* 1991, *10*, 25-34.

[134] Sreenivasan, U., Axelsen, P. H., Buried water in homologous serine proteases. *Biochemistry* 1992, *31*, 12785-12791.

[135] Li, A., Sowder, R. C., Henderson, L. E., Moore, S. P.*, et al.*, Chemical cleavage at aspartyl residues for protein identification. *Anal Chem* 2001, *73*, 5395-5402.

[136] Manza, L. L., Stamer, S. L., Ham, A. J., Codreanu, S. G., Liebler, D. C., Sample preparation and digestion for proteomic analyses using spin filters. *Proteomics* 2005, *5*, 1742-1745.

[137] Annesley, T. M., Ion suppression in mass spectrometry. *Clin Chem* 2003, *49*, 1041-1044.

[138] White, M. Y., Gundry, R. L., Cordwell, S. J., When does a fingerprint constitute a diagnostic? *Lancet* 2006, *368*, 971-973.

[139] Griffiths, S. D., Burthem, J., Unwin, R. D., Holyoake, T. L.*, et al.*, The use of isobaric tag peptide labeling (iTRAQ) and mass spectrometry to examine rare, primitive hematopoietic cells from patients with chronic myeloid leukemia. *Mol Biotechnol* 2007, *36*, 81-89.

[140] Australia, C. o., Australian Bureau of Statistics 2006.

[141] Yu, L., Chen, X., Qin, G., Xie, H., Lv, P., Tear film function in type 2 diabetic patients with retinopathy. *Ophthalmologica* 2008, *222*, 284-291.

[142] Dennis, G., Jr., Sherman, B. T., Hosack, D. A., Yang, J.*, et al.*, DAVID: Database for Annotation, Visualization, and Integrated Discovery. *Genome Biol* 2003, *4*, P3.

[143] Huang da, W., Sherman, B. T., Lempicki, R. A., Systematic and integrative analysis of large gene lists using DAVID bioinformatics resources. *Nat Protoc* 2009, *4*, 44-57.

[144] Veenstra, T. D., Conrads, T. P., Issaq, H. J., What to do with "one-hit wonders"? *Electrophoresis* 2004, *25*, 1278-1279.

[145] Perkins, D. N., Pappin, D. J., Creasy, D. M., Cottrell, J. S., Probability-based protein identification by searching sequence databases using mass spectrometry data. *Electrophoresis* 1999, *20*, 3551-3567.

[146] Kristensen, D. B., Brond, J. C., Nielsen, P. A., Andersen, J. R.*, et al.*, Experimental Peptide Identification Repository (EPIR): an integrated peptide-centric platform for validation and mining of tandem mass spectrometry data. *Mol Cell Proteomics* 2004, *3*, 1023-1038.

[147] Yen, C. Y., Russell, S., Mendoza, A. M., Meyer-Arendt, K., *et al.*, Improving sensitivity in shotgun proteomics using a peptide-centric database with reduced complexity: protease cleavage and SCX elution rules from data mining of MS/MS spectra. *Anal Chem* 2006, *78*, 1071-1084.

[148] Zhou, L., Beuerman, R. W., Foo, Y., Liu, S., *et al.*, Characterisation of human tear proteins using high-resolution mass spectrometry. *Ann Acad Med Singapore* 2006, *35*, 400-407.

[149] Fung, K. Y., Morris, C., Sathe, S., Sack, R., Duncan, M. W., Characterization of the in vivo forms of lacrimal-specific proline-rich proteins in human tear fluid. *Proteomics* 2004, *4*, 3953-3959.

[150] Jerdeva, G. V., Wu, K., Yarber, F. A., Rhodes, C. J., *et al.*, Actin and non-muscle myosin II facilitate apical exocytosis of tear proteins in rabbit lacrimal acinar epithelial cells. *J Cell Sci* 2005, *118*, 4797-4812.

[151] Ma, P., Wang, N., McKown, R. L., Raab, R. W., Laurie, G. W., Focus on molecules: lacritin. *Exp Eye Res* 2008, *86*, 457-458.

[152] Tsai, P. S., Evans, J. E., Green, K. M., Sullivan, R. M., *et al.*, Proteomic analysis of human meibomian gland secretions. *Br J Ophthalmol* 2006, *90*, 372-377.

[153] Laurie, G. W., Olsakovsky, L. A., Conway, B. P., McKown, R. L., *et al.*, Dry eye and designer ophthalmics. *Optom Vis Sci* 2008, *85*, 643-652.

[154] Zhang, L. Y., Ying, W. T., Mao, Y. S., He, H. Z., *et al.*, Loss of clusterin both in serum and tissue correlates with the tumorigenesis of esophageal squamous cell carcinoma via proteomics approaches. *World J Gastroenterol* 2003, *9*, 650-654.

[155] Jordan-Starck, T., Witte, D. P., Aronow, B. J., Harmony, J. A., Apolipoprotein J: a membrane policeman? *Current opinion in Lipidology* 1992, *3*.

[156] Nakamura, T., Nishida, K., Dota, A., Kinoshita, S., Changes in conjunctival clusterin expression in severe ocular surface disease. *Invest Ophthalmol Vis Sci* 2002, *43*, 1702-1707.

[157] Gao, B. B., Chen, X., Timothy, N., Aiello, L. P., Feener, E. P., Characterization of the vitreous proteome in diabetes without diabetic retinopathy and diabetes with proliferative diabetic retinopathy. *J Proteome Res* 2008, *7*, 2516-2525.

[158] Denecker, G., Hoste, E., Gilbert, B., Hochepied, T., *et al.*, Caspase-14 protects against epidermal UVB photodamage and water loss. *Nat Cell Biol* 2007, *9*, 666-674.

[159] Denecker, G., Ovaere, P., Vandenabeele, P., Declercq, W., Caspase-14 reveals its secrets. *J Cell Biol* 2008, *180*, 451-458.

[160] Koenig, U., Sommergruber, W., Lippens, S., Aberrant expression of caspase-14 in epithelial tumors. *Biochem Biophys Res Commun* 2005, *335*, 309-313.

[161] Lippens, S., Kockx, M., Knaapen, M., Mortier, L., *et al.*, Epidermal differentiation does not involve the pro-apoptotic executioner caspases, but is associated with caspase-14 induction and processing. *Cell Death Differ* 2000, *7*, 1218-1224.

[162] Lippens, S., Kockx, M., Denecker, G., Knaapen, M.*, et al.*, Vitamin D3 induces caspase-14 expression in psoriatic lesions and enhances caspase-14 processing in organotypic skin cultures. *Am J Pathol* 2004, *165*, 833-841.

[163] Walsh, D. S., Borke, J. L., Singh, B. B., Do, N. N.*, et al.*, Psoriasis is characterized by altered epidermal expression of caspase 14, a novel regulator of keratinocyte terminal differentiation and barrier formation. *J Dermatol Sci* 2005, *37*, 61-63.

[164] Xiao, F., Mirwald, A., Papaioannou, M., Baniahmad, A., Klug, J., Secretoglobin 2A1 is under selective androgen control mediated by a peculiar binding site for Sp family transcription factors. *Mol Endocrinol* 2005, *19*, 2964-2978.

[165] Stoeckelhuber, M., Messmer, E. M., Schmidt, C., Xiao, F.*, et al.*, Immunohistochemical analysis of secretoglobin SCGB 2A1 expression in human ocular glands and tissues. *Histochem Cell Biol* 2006, *126*, 103-109.

[166] Cermak, J. M., Krenzer, K. L., Sullivan, R. M., Dana, M. R., Sullivan, D. A., Is complete androgen insensitivity syndrome associated with alterations in the meibomian gland and ocular surface? *Cornea* 2003, *22*, 516-521.

[167] Kawasaki, S., Kawamoto, S., Yokoi, N., Connon, C.*, et al.*, Up-regulated gene expression in the conjunctival epithelium of patients with Sjogren's syndrome. *Exp Eye Res* 2003, *77*, 17-26.

[168] Li, N., Wang, N., Zheng, J., Liu, X. M.*, et al.*, Characterization of human tear proteome using multiple proteomic analysis techniques. *J Proteome Res* 2005, *4*, 2052-2061.

[169] Hassan, R., Alexander, R., Antman, K., Boffetta, P.*, et al.*, Current treatment options and biology of peritoneal mesothelioma: meeting summary of the first NIH peritoneal mesothelioma conference. *Ann Oncol* 2006, *17*, 1615-1619.

[170] Hassan, R., Remaley, A. T., Sampson, M. L., Zhang, J.*, et al.*, Detection and quantitation of serum mesothelin, a tumor marker for patients with mesothelioma and ovarian cancer. *Clin Cancer Res* 2006, *12*, 447-453.

[171] Etzioni, R., Urban, N., Ramsey, S., McIntosh, M.*, et al.*, The case for early detection. *Nat Rev Cancer* 2003, *3*, 243-252.

[172] Lost in validation. *Nat Biotechnol* 2006, *24*, 869.

[173] Kuzyk, M. A., Smith, D., Yang, J., Cross, T. J.*, et al.*, Multiple reaction monitoring-based, multiplexed, absolute quantitation of 45 proteins in human plasma. *Mol Cell Proteomics* 2009, *8*, 1860-1877.

[174] Matt, P., Fu, Z., Fu, Q., Van Eyk, J. E., Biomarker discovery: proteome fractionation and separation in biological samples. *Physiol Genomics* 2008, *33*, 12-17.

[175] Pang, S., Smith, J., Onley, D., Reeve, J.*, et al.*, A comparability study of the emerging protein array platforms with established ELISA procedures. *J Immunol Methods* 2005, *302*, 1-12.

[176] Fu, Q., Van Eyk, J. E., Proteomics and heart disease: identifying biomarkers of clinical utility. *Expert Rev Proteomics* 2006, *3*, 237-249.

[177] Anderson, L., Hunter, C. L., Quantitative mass spectrometric multiple reaction monitoring assays for major plasma proteins. *Mol Cell Proteomics* 2006, *5*, 573-588.

[178] Mallick, P., Schirle, M., Chen, S. S., Flory, M. R.*, et al.*, Computational prediction of proteotypic peptides for quantitative proteomics. *Nat Biotechnol* 2007, *25*, 125-131.

[179] Roschinger, W., Olgemoller, B., Fingerhut, R., Liebl, B., Roscher, A. A., Advances in analytical mass spectrometry to improve screening for inherited metabolic diseases. *Eur J Pediatr* 2003, *162 Suppl 1*, S67-76.

[180] MacLean, B., Tomazela, D. M., Shulman, N., Chambers, M.*, et al.*, Skyline: an open source document editor for creating and analyzing targeted proteomics experiments. *Bioinformatics* 2010, *26*, 966-968.

[181] Gatlin, C. L., Kleemann, G. R., Hays, L. G., Link, A. J., Yates, J. R., 3rd, Protein identification at the low femtomole level from silver-stained gels using a new fritless electrospray interface for liquid chromatography-microspray and nanospray mass spectrometry. *Anal Biochem* 1998, *263*, 93-101.

[182] Stahl-Zeng, J., Lange, V., Ossola, R., Eckhardt, K.*, et al.*, High sensitivity detection of plasma proteins by multiple reaction monitoring of N-glycosites. *Mol Cell Proteomics* 2007, *6*, 1809-1817.

[183] Nicol, G. R., Han, M., Kim, J., Birse, C. E.*, et al.*, Use of an immunoaffinity-mass spectrometry-based approach for the quantification of protein biomarkers from serum samples of lung cancer patients. *Mol Cell Proteomics* 2008, *7*, 1974-1982.

[184] Berna, M. J., Zhen, Y., Watson, D. E., Hale, J. E., Ackermann, B. L., Strategic use of immunoprecipitation and LC/MS/MS for trace-level protein quantification: myosin light chain 1, a biomarker of cardiac necrosis. *Anal Chem* 2007, *79*, 4199-4205.

[185] Ye, X., Blonder, J., Veenstra, T. D., Targeted proteomics for validation of biomarkers in clinical samples. *Brief Funct Genomic Proteomic* 2009, *8*, 126-135.

[186] Unwin, R. D., Griffiths, J. R., Leverentz, M. K., Grallert, A.*, et al.*, Multiple reaction monitoring to identify sites of protein phosphorylation with high sensitivity. *Mol Cell Proteomics* 2005, *4*, 1134-1144.

[187] Sen, D. K., Sarin, G. S., Biological variations of lysozyme concentration in the tear fluids of healthy persons. *Br J Ophthalmol* 1986, *70*, 246-248.

[188] Sack, R. A., Tan, K. O., Tan, A., Diurnal tear cycle: evidence for a nocturnal inflammatory constitutive tear fluid. *Invest Ophthalmol Vis Sci* 1992, *33*, 626-640.

[189] Huth, S. W., Miller, M. J., Leopold, I. H., Calcium and protein in tears: diurnal variation. *Arch Ophthalmol* 1981, *99*, 1628-1633.

[190] Gygi, S. P., Rist, B., Gerber, S. A., Turecek, F.*, et al.*, Quantitative analysis of complex protein mixtures using isotope-coded affinity tags. *Nat Biotechnol* 1999, *17*, 994-999.

[191] Ong, S. E., Blagoev, B., Kratchmarova, I., Kristensen, D. B.*, et al.*, Stable isotope labeling by amino acids in cell culture, SILAC, as a simple and accurate approach to expression proteomics. *Mol Cell Proteomics* 2002, *1*, 376-386.

[192] Schmidt, A., Kellermann, J., Lottspeich, F., A novel strategy for quantitative proteomics using isotope-coded protein labels. *Proteomics* 2005, *5*, 4-15.

[193] Ong, S. E., Mann, M., Mass spectrometry-based proteomics turns quantitative. *Nat Chem Biol* 2005, *1*, 252-262.

[194] Wolf-Yadlin, A., Hautaniemi, S., Lauffenburger, D. A., White, F. M., Multiple reaction monitoring for robust quantitative proteomic analysis of cellular signaling networks. *Proc Natl Acad Sci U S A* 2007, *104*, 5860-5865.

[195] Kaiserman, I., Kaiserman, N., Nakar, S., Vinker, S., Dry eye in diabetic patients. *Am J Ophthalmol* 2005, *139*, 498-503.

Appendix I

DOI 10.1002/pmic.200701161

TECHNICAL BRIEF

Improvements for the visualization of low-molecular weight protein and peptides of human tears using MALDI

Terry Nguyen-Khuong[1, 2], Anna Fitzgerald[1], Zhejun Zhao[2], Mark Willcox[2] and Bradley J. Walsh[1]

[1] Minomic Pty Ltd, Frenchs Forest, NSW Australia
[2] Institute for Eye Research and School of Optometry and Vision Science, University of New South Wales, Sydney, NSW Australia

Many low-molecular weight proteins and peptides in human tears are potentially bioactive proteins but the range and number of these is yet to be fully characterized. A number of different sample preparation techniques were used to maximize the visualization of peptides from reflex tears. Samples were pretreated using precipitation and filtration techniques prior to analyses using MALDI-TOF MS. Peptides were searched for between 700 to 4000 *m/z*. Sample dilution in several different buffer systems followed by filtration with a 30-kDa cutoff filter and C18 reverse phase microcolumn purification produced significantly ($p = 0.049$) more peaks in tears than other methods used to prepare tears prior to MALDI-TOF MS. This study has established a technique for optimizing the visualization of naturally occurring peptides in tears.

Received: December 16, 2007
Revised: April 2, 2008
Accepted: May 1, 2008

Keywords:
Matrix-assisted laser desorption/ionization time of flight mass spectrometry / Peptide / Tears

The tear film is a multi-functional fluid involved in the lubrication and protection of the eye. Recent studies have demonstrated that changes in tear film composition can occur during eye diseases such as dry eye, Sjögren's syndrome, conjunctivitis, blepharitis and other general inflammatory conditions [1–4]. The tear film has the potential to be used as a relatively easy to obtain fluid for monitoring diseases, of the eye or perhaps elsewhere in the body. To date, the complex mixture of the tear proteome has not been completely characterized as problems are frequently encountered in finding, sensitive, rapid and simple techniques for the analysis of tears [5]. In particular, proteomic and peptidomic analysis of tears can prove to be challenging due to the small volumes (<5 μL) of tears that are collected in a clinical setting [6]. Recent studies have applied MALDI-TOF MS to the successful analysis of peptides present in human tears albeit with a low number of peptides [7, 8]. For these reasons, we established an inexpensive microscale purification technique that allows for the rapid and efficient concentration and cleanup of small quantities of tears prior to MALDI-TOF MS analysis.

In a preliminary study, reflex tears were recovered from healthy candidates aged between 24–31 years with no history of ocular pathology. Tears (2 to 5 μL) were collected once a day over 3 days between 11 am and 2 pm from the inferior cul-de-sac using a 10-μL microcapillary tube (Blaubrand Intramark, Wertheim, Germany). After collection, tears were pooled and stored in capped, 1.5-mL polyethylene centrifuge tubes at –80°C until use.

Five microliters of unfractionated tear samples ($n = 185$) from pooled tears were diluted with 15 μL of one of the following MS-compatible solutions: 0.1% v/v TFA (Sigma-Aldrich, USA), 0.1% v/v formic acid (FA; BDH, Germany), 50 mM ammonium bicarbonate (ABC; Sigma-

Correspondence: Dr. Bradley J. Walsh, Minomic Pty Ltd, PO Box 664, Harbord 2096, New South Wales, Australia
E-mail: brad.walsh@minomic.com
Fax: +612-9975-3888

Abbreviations: **ABC**, ammonium bicarbonate; **FA**, formic acid; **PMM**, peptide mass maps

Aldrich) and ultra-pure water (H_2O). These samples were then incubated in the respective solutions overnight at 4°C before they were treated using one of the following described methods (i-viii). All techniques were repeated in triplicate.

(i) C18 RP purification: a C18 RP microcolumn purification (PerfectPure, Eppendorf, Germany) was activated, equilibrated and the sample aspirated as per manufacturer's instructions. Bound peptides were eluted onto a MALDI target plate (the plate) with CHCA (8 mg/mL dissolved in 70% v/v ACN and 0.1% TFA).

(ii) Centrifugation of sample followed by C18 RP purification: diluted samples were centrifuged at $11\,000 \times g$, 30 min, 4°C before being subjected to C18 reverse phase filtration (as described in procedure (i).

(iii) Direct thin layer preparation: a thin layer of CHCA was placed on the target plate, washed in 0.1% TFA and allowed to dry. Subsequently, a 5-μL aliquot of diluted tear sample was placed onto the CHCA and left to dry.

(iv) Reverse thin-layer preparation: a 5-μL aliquot of the tear sample was placed on the target plate and left to dry. Subsequently, a thin layer of CHCA was spotted over the sample and left to dry. The sample was then washed with 5–10 μL of 0.1% TFA for approximately 10 s.

(v) Dried droplet application: a 0.5–2-μL aliquot of diluted tears was mixed with 0.5–1 μL of CHCA and allowed to air-dry on the plate. The sample was washed with 5–10 μL of 0.1% TFA for approximately 10 s.

(vi) Acetone precipitation: tear samples (5-μL aliquots) were first diluted with 15 μL of cold acetone and left to precipitate at −20°C for a minimum of 1.5 h. Proteins were pelleted at $24\,000 \times g$ for 15 min, supernatant removed and the pellet air-dried for 10 min. Pellets were resuspended in 15 μL of one of the MS-compatible solutions (TFA, FA, ABC or H_2O) and incubated overnight. Samples were then subjected to C18 RP filtration and MALDI-TOF.

(vii) Sample concentration by centrifugation: a 100-μL aliquot of diluted tears was transferred into an YM-30 Microcon (Millipore) sample reservoir, and then spun at $14\,000 \times g$ at 10°C for 30 min. The flow through was collected and then subjected to C18 RP filtration and MALDI-TOF.

(viii) Reduction and alkylation: a 100-μL aliquot of diluted tears diluted in 50 mM ABC was reduced and alkylated with 10 mM DTT and 50 mM iodoacetimide (IAA), respectively, for 10 min each. Samples were then subjected to C18 RP filtration and MALDI-TOF.

Peptide mass maps (PMM) of treated samples were generated by MALDI-TOF MS (Waters M@LDI™; Waters, Milford, MA). Samples were analyzed in positive reflectron mode in the range 700–4000 *m/z* with an accelerating voltage of 15 kV. A three-point external calibration was performed using angiotensin (1064.543 Da), $P_{14}R$ (1533.858 Da) and adrenocorticotrophic Hormone (2465.199 Da) (Sigma Aldrich).

Preliminary studies on the aforementioned protocols were examined (Table 1). The best protocols were selected and used on two further samples each pooled from three separate individuals (Table 2). Sample dilution in several different buffer systems followed by filtration with a 30-kDa cutoff filter and C18 RP microcolumn purification produced significantly ($p = 0.049$) more peaks in tears than other methods used to prepare tears prior to MALDI-TOF MS. Using this method, five candidate's tears were obtained and the variations between each spectra were evaluated (Fig. 2).

Spectra obtained from the sample preparations (Fig. 1) were compared to determine the method that would yield the greatest number of peptides on a tear PMM (Table 1). Numbers of peptides produced from the various techniques were statistically compared after log-transformation of data using ANOVA and the Robust F test (computer package, SPSS). The direct thin-layer preparation, reverse thin-layer prepara-

Table 1. Peptide count averages for various treatments on human tears.

Treatment	(i) C18 RP microcolumn purification	(ii) Spin and C18 RP purification	(iii) Thin layer	(iv) Reverse thin layer	(v) Dried droplet	(vi) Acetone and C18 RP microcolumn purification	(vii) Centrifugal filters and C18 RP microcolumn purification	(viii) Reduction and Alkylation
	Average (Std Dev)	*Average (Std Dev)*	*Average (Std Dev)*	*Average (Std Dev)*	*Average (Std Dev)*	*Average (Std Dev)*	*Average (Std Dev)*	*Average (Std Dev)*
TFA	33.7 (+3.8)	82.3 (+31.4)	0.0 (+0.0)	0.0 (+0.0)	0.0 (+0.0)	13.3 (+5.7)	122.7 (+20.6)	N/A
FA	52.0 (+40.6)	78.0 (+22.6)	0.0 (+0.0)	0.0 (+0.0)	0.0 (+0.0)	2.0 (+0.0)	123.3 (+21.0)	N/A
dH_2O	39.0 (+4.0)	43.3 (+10.8)	0.0 (+0.0)	0.0 (+0.0)	0.0 (+0.0)	6.7 (+5.8)	115.7 (+7.8)	N/A
ABC	63.0 (+18.1)	56.3 (+13.6)	0.0 (+0.0)	0.0 (+0.0)	0.0 (+0.0)	13.7 (+17.6)	145.3 (+11.5)	73.3 (+19.7)

Tears were either treated in 0.1% TFA, 0.1% FA, ultra-pure water (dH_2O) or 50 mM ammonium bicarbonate (ABC). Numbers in parentheses are SD of triplicate gels of the respective treatment. Sample dilution in several different buffer systems followed by filtration with a 30-kDa cut off filter and C18 RP microcolumn purification produced significantly ($p = 0.049$) more peaks in tears than other methods used to prepare tears prior to MALDI-TOF MS. The best protocols were repeated on two further samples each pooled from three separate individuals.

Table 2. Peptide count averages for various treatments on human tears.

		C18 reverse phase microcolumn purification			Spin and C18 reverse phase microcolumn purification			Acetone and C18 reverse phase microcolumn purification			Centrifugal filters and C18 reverse phase microcolumn purification		
	Number	Average	S.D	CV (%)	Average	S.D	CV (%)	Average	S.D	CV (%)	Average	S.D	CV (%)
TFA	1	37.00	9.54	25.78	22.67	10.07	44.41	30.33	8.74	28.80	112.00	23.26	20.77
	2	80.67	8.33	10.32	46.67	38.40	82.28	34.67	10.60	30.57	111.67	13.05	11.69
	3	33.7	3.8	11.25	107.0	14.0	13.08	16.0	1.7	10.83	122.7	20.6	16.75
FA	1	29.67	14.29	48.18	46.33	15.37	33.18	35.50	9.19	25.89	98.00	19.29	19.68
	2	79.0	13.9	17.59	81.33	21.13	25.98	37.00	2.83	7.64	139.67	4.16	2.98
	3	69.67	32.52	46.67	100.0	10.1	10.15	2.0	0.0	0.00	123.3	21.0	17.05
ABC	1	13.33	5.69	42.65	14.00	3.61	25.75	29.20	9.52	32.62	96.67	10.21	10.57
	2	12.67	2.08	16.43	12.33	3.06	24.77	26.00	16.16	62.14	145.67	1.15	0.79
	3	39.0	4.0	10.26	43.3	10.8	24.89	19.3	16.2	83.62	115.7	7.8	6.72
H_2O	1	8.67	7.37	85.05	9.67	3.21	33.25	37.00	41.58	112.38	98.00	19.29	19.68
	2	19.33	5.69	29.41	22.00	15.13	68.79	27.33	18.50	67.69	139.67	4.16	2.98
	3	63.0	18.1	28.70	56.3	13.6	24.10	19.0	14.5	76.45	145.3	11.5	7.92

Experiments, which produced a high number of peptides in the preliminary study (Table 1) were performed on three samples each pooled from separate individuals (Table 2).

tion or dried-droplet sample preparation techniques did not show any discernible peptide peaks in their PMM. These on-target sample preparations are free of pre-sample treatment and thus would concentrate all non-volatile contaminants such as non-polar sterol esters and wax. Furthermore, large cellular debris within the tear film would also be present. These non-peptide contaminants might cause ion-suppression during the MALDI analysis. In contrast, sample preparations that involve a degree of sample cleaning such as acetone precipitation, centrifugation, centrifugal filtration or C18 microcolumns filtration resolved many peptides. The tear film is a heterogeneous mixture of proteins, peptides, salts, lipids and other compounds and it appears that these non-peptide contaminants must be removed and the sample concentrated in order for the peptides to be better resolved by MS.

Samples subjected to a C18 RP microcolumn purification only showed 34 to 63 peptide peaks on PMM, depending on the initial diluent used, with FA or ABC giving higher numbers of peptide peaks than H_2O or TFA ($p < 0.025$). However, RP microcolumn purification of both the acetone precipitates and reduced and alkylated samples proved difficult, as there was a larger amount of physical effort required to aspirate the sample through the RP microcolumn. After subsequent C18 RP microcolumn cleanup, only a modest number of peptide peaks were resolved. Centrifugation of tear samples followed by C18 RP microcolumn purification also only resolved a modest number of peptides. This method was not superior to C18 RP filtration alone for any tear diluent apart from using TFA where more peaks were resolved with prior sample centrifugation (Table 1; $p = 0.000$). The numbers of peptides resolved on a PMM were significantly improved once tear samples had been filtered through centrifugal filtration devices. Sample preparation using these filters produced an average of 126 peptides that were highly resolved on a PMM.

Whilst protein concentration techniques, such as acetone precipitation, remove the aforementioned contaminants, they do not remove larger molecular weight proteins present in tears. High-MW range proteins in tears might physically congest access of peptides to the C18 RP microcolumn purification, thus reducing the ability to detect peptides in tears. Reduction and alkylation of crude tears would denature large protein complexes, and perhaps release small proteins and peptides. However, larger residual proteins from such complexes would be concentrated by subsequent C18 RP microcolumn purification and again congest the C18 RP microcolumn purification. Centrifugal filters are an efficient method of physically removing the larger proteins, from the population of small proteins and peptides in the filtrate. Salts, detergents and contaminants are cleared from this population later after it is cleaned and concentrated using a C18 RP microcolumn purification.

Sample dilution with MS-compatible solvents is necessary due to the small volumes of tears that can be collected per patient as compared with larger volumes required for sample preparation apparati, *i.e.* centrifugal filters. In general, the use of sample diluents such as TFA, FA and ultrapure water did not affect the number of peptides resolved after C18 RP microcolumn filtration. Whilst there are a few additional peptides resolved above 3000 m/z using TFA or FA, this did not constitute a major difference between solvents. ABC is the preferred solvent for the treatment of tear samples as it consistently allowed resolution of a large num-

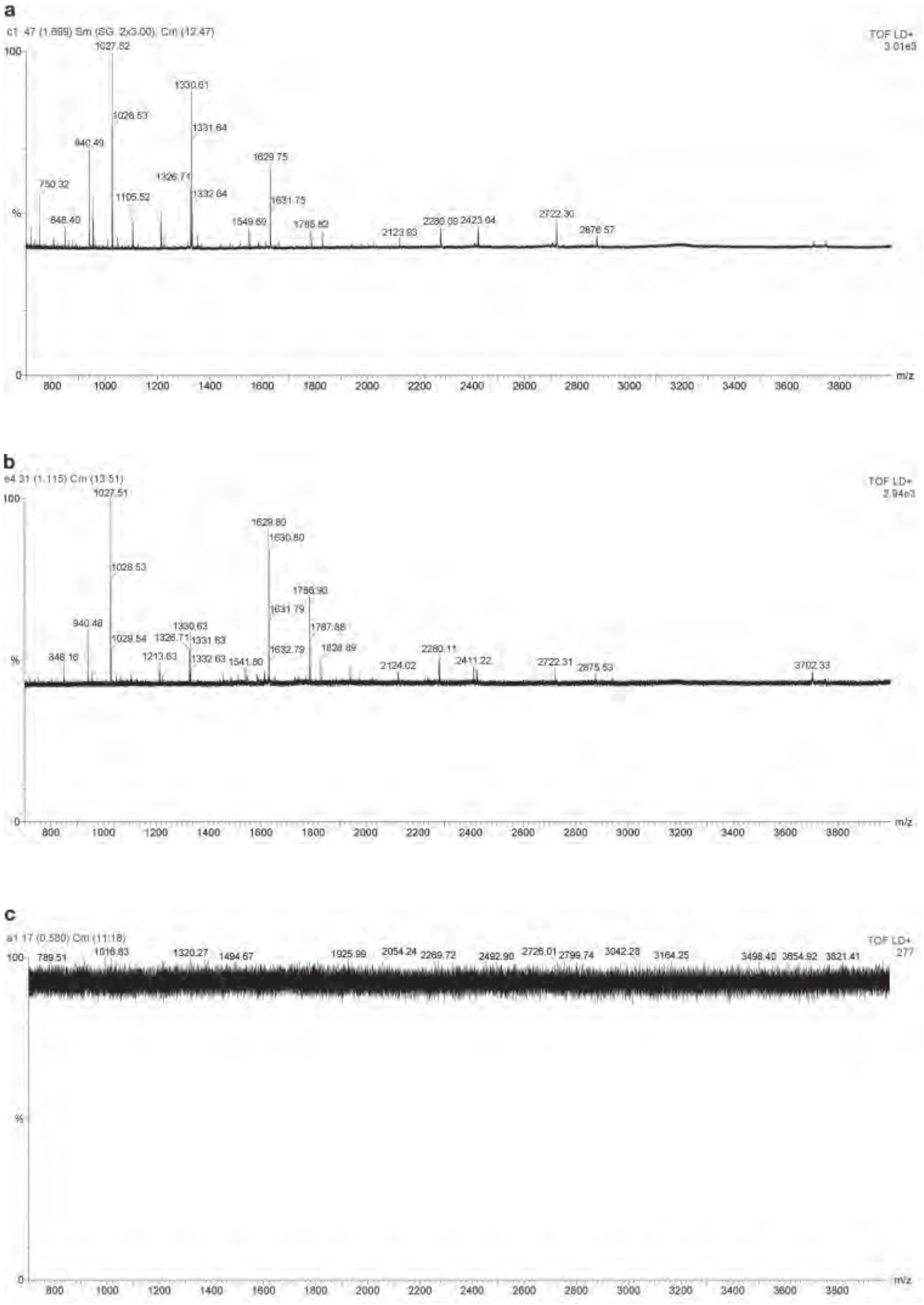

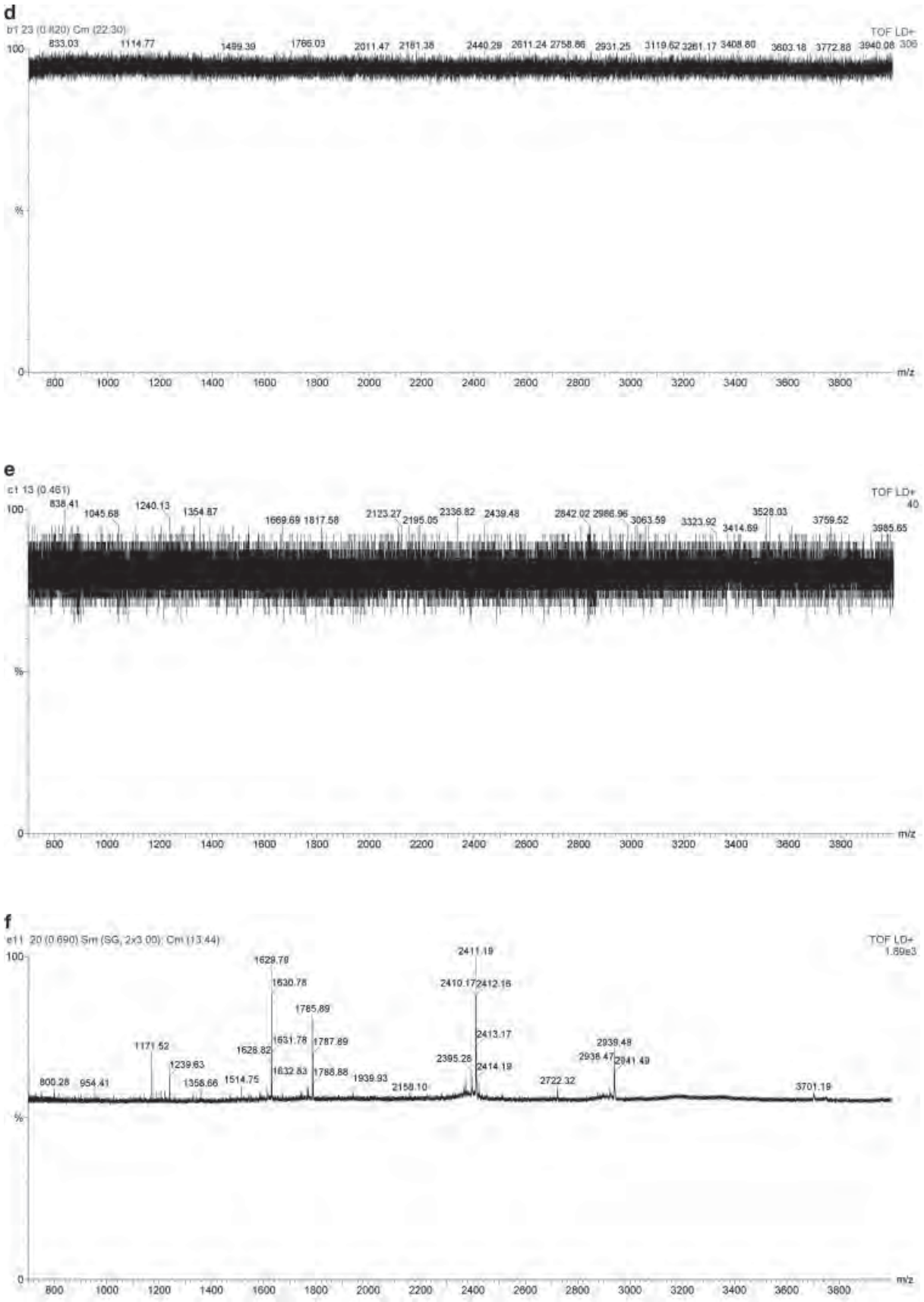

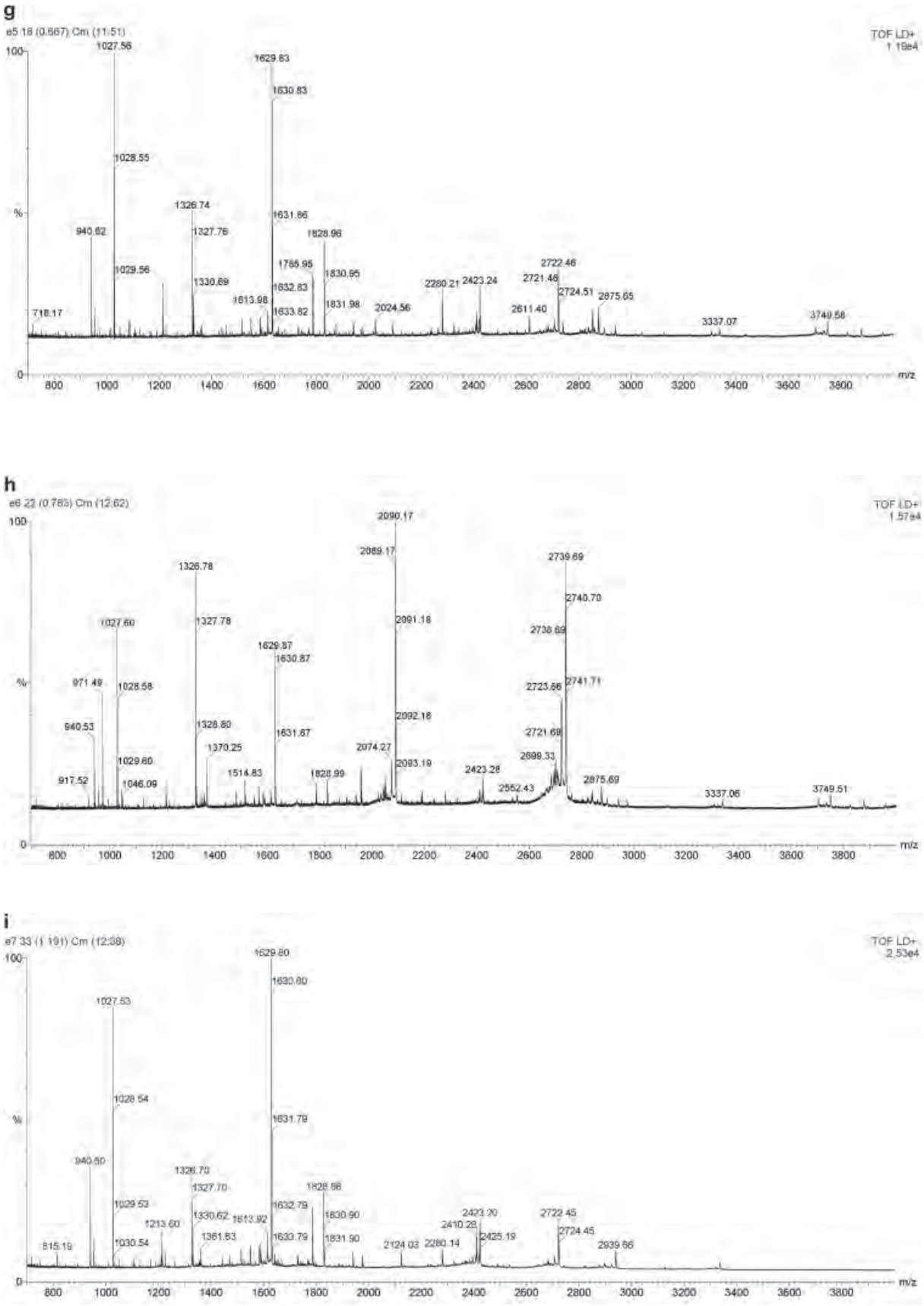

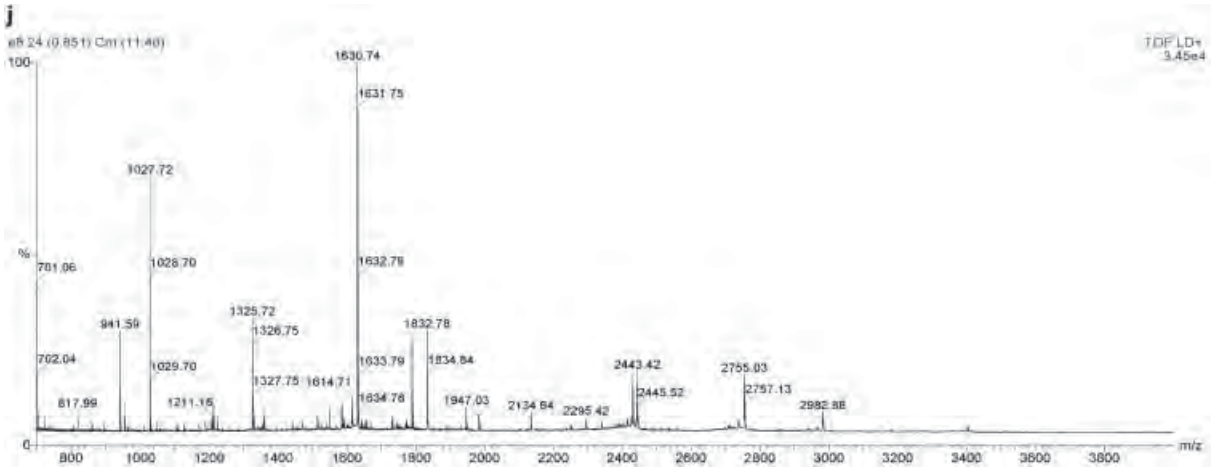

Figure 1. Reflectron mode MALDI mass spectra of tears. (a) Incubation of tears in 50 mM ABC buffer before C18 RP microcolumn purification. (b) Spinning tears down before simple cleanup with C18 RP microcolumn purification after incubation in 50 mM ABC buffer. (c) Dried droplet of tears after dilution with 50 mM ABC. (d) Thin layer preparation of tears after dilution with 50 mM ABC buffer. (e) Reverse thin-layer preparation of tears after dilution with 50 mM ABC buffer. (f) Acetone precipitation of tears followed by dilution in 50 mM ABC buffer prior to C18 RP microcolumn purification. (g) Diluting tears with 50 mM ABC before centrifuging them down through a 30-kDa cutoff spin filter (Microcon – Millipore, USA). (h) Diluting tears with 0.1% TFA before centrifuging them down through a 30-kDa cutoff spin filter. (i) Diluting tears with 0.1% FA before centrifuging them down through a 30-kDa cutoff spin filter. (j) Diluting tears with ultra-pure water before centrifuging them down through a 30-kDa cutoff spin filter. (k) Reduction and alkylation of tears in 50 mM ABC before concentration with C18 RP microcolumn purification. Note; all techniques involved with spin filters were purified with a C18 RP microcolumn prior to MALDI analysis. The numbers of peptides resolved on each PMM are shown in Table 1. Dilution with an MS-compatible solvent followed by centrifugal filtering resolved the most number of peaks. The dilution with various solvents did not affect the resolution of the peaks as seen when panels (g), (i), (h) and (j) are compared.

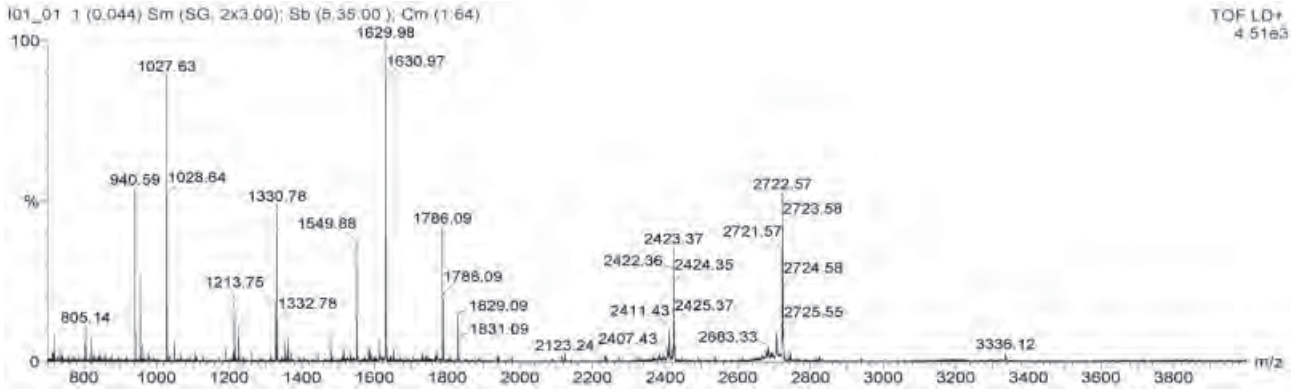

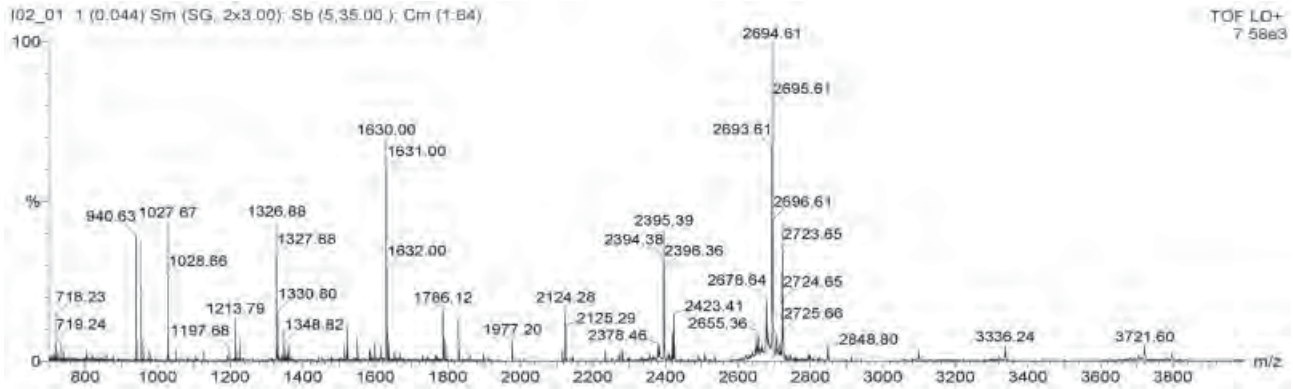

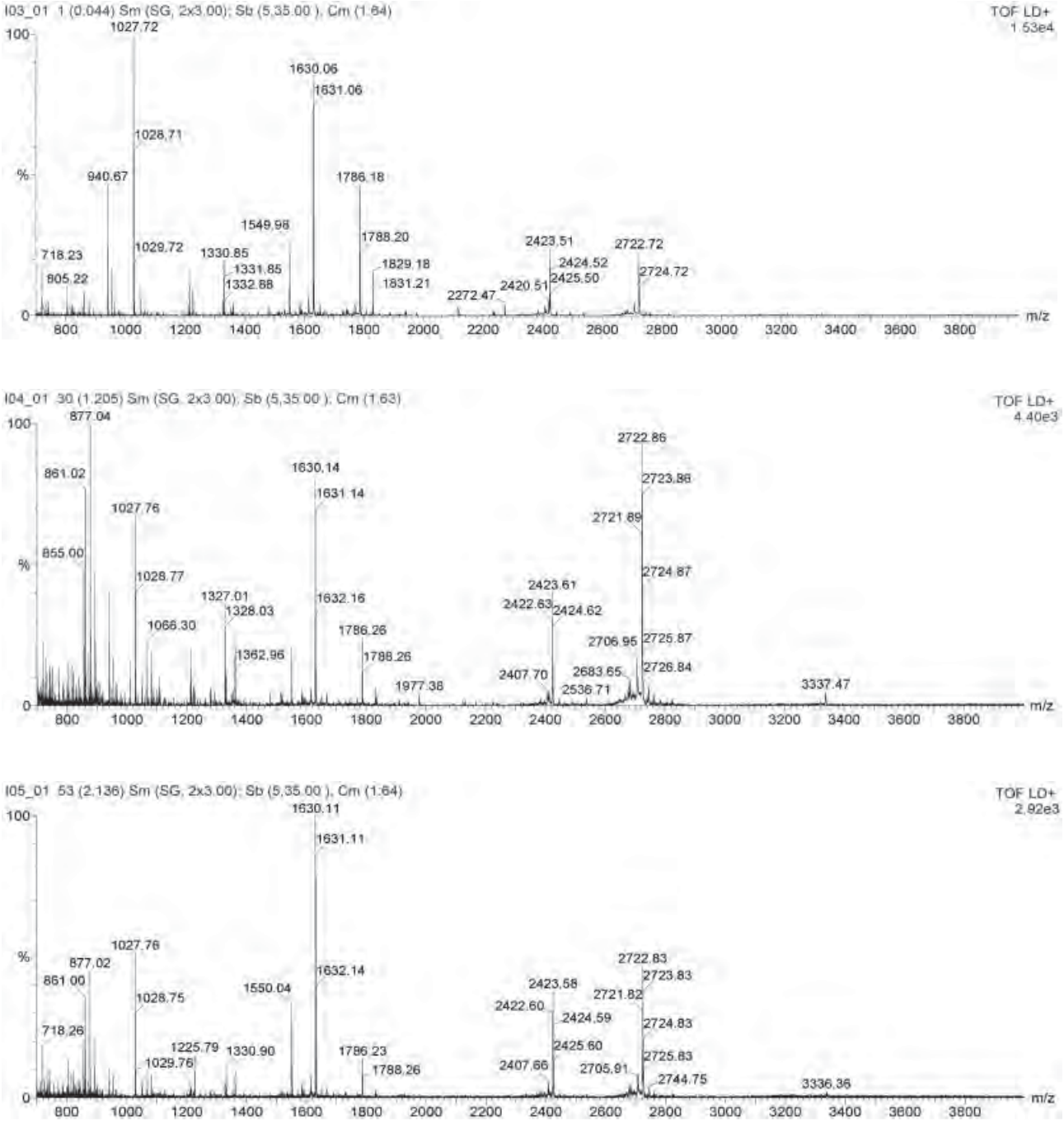

Figure 2. Comparison of variation between PMM of five individuals was made using tears extracted from five individual healthy controls. Five microliters tears taken from each individual was diluted in 50 mM ABC then washed through a YM-30 spin filter. The flow-through was collected and then subjected to C18 RP filtration and MALDI-TOF. Spectra are background subtracted and smoothed.

ber of peptides regardless of subsequent sample preparation. There are potential problems associated with the use of other solvents such as (i) ultra-pure water, which has the potential to activate proteases [9]; (ii) FA, which could inadvertently cause nonspecific digestion, perhaps hampering a peptidomic analysis of tears [10]; (iii) TFA and/or FA, which are used in later MS sample preparation stages, thus, treatment in either of these solutions would be redundant in the early stages of tear sample preparation. In addition to potential limitations of other solvents, the use of ABC would ensure that tear peptides and proteins are in their physiological pH range whilst permitting immediate sample manipulation

such as trypsin digestion without buffer exchange should this be required by the experimental design [11].

Five individual tears were collected and analyzed using the protocol of choice (Fig. 2). Tears were analyzed using protocol (vii) after diluting the tears with 50 mM ABC. The variation between individuals was examined. A total of 235 peaks were resolved between all five PMM. Additionally, there was an average of 107.6 peaks with an SD of 30. Eighteen percent of the 235 total peaks were resolved between all of five PMM. Furthermore, 50% of the total peaks were observed in two or more of the five individuals analyzed. The use of centrifugal filters followed by C18 RP microcolumn purification allows for reproducibility whilst permits variations amongst lower-range proteins and peptides in the tear film that can reflect pathological conditions of, but not limited, to the eye

Comprehensive identification of peptides and proteins is necessary to identify biological markers for diseases of the eye. In this study, we examined various sampling treatments using MALDI-MS with the focus on maximizing the number of highly resolved peptides in a low-molecular proteome profile of tears. This study has demonstrated that centrifugal filtration coupled with a C18 RP microcolumn purification maximizes the amount of peptides visualized on a tear PMM. In the current study, an easy, fast, and efficient technique for maximizing the amount and resolution of peptides in tears was established. Methods described in this study may be advantageous not only to the study of tears, but also various other complex biological samples.

This project is supported by the Australian Research Council, and the University of New South Wales. We thank Kieran Scott for his assistance and advice and Thomas John for his assistance with statistical analysis of the data.

The authors have declared no conflict of interest.

References

[1] Grus, F. H., Podust, V. N., Bruns, K., Lackner, K. *et al.*, SELDI-TOF-MS ProteinChip array profiling of tears from patients with dry eye. *Invest. Ophthalmol. Vis. Sci.* 2005, *46*, 863–876.

[2] Grus, F. H., Sabuncuo, P., Dick, H. B., Augustin, A. J., Pfeiffer, N., Changes in the tear proteins of diabetic patients. *BMC Ophthalmol.* 2002, *2*, 4.

[3] Herber, S., Grus, F. H., Sabuncuo, P., Augustin, A. J., Two-dimensional analysis of tear protein patterns of diabetic patients. *Electrophoresis* 2001, *22*, 1838–1844.

[4] Lemp, M. A., Report of the National Eye Institute/Industry workshop on Clinical Trials in Dry Eyes. *Clao J.* 1995, *21*, 221–232.

[5] Sack, R. A., Conradi, L., Krumholz, D., Beaton, A. *et al.*, Membrane array characterization of 80 chemokines, cytokines, and growth factors in open- and closed-eye tears: angiogenin and other defense system constituents. *Invest. Ophthalmol. Vis. Sci.* 2005, *46*, 1228–1238.

[6] Hu, S., Loo, J. A., Wong, D. T., Human body fluid proteome analysis. *Proteomics* 2006, *6*, 6326–6353.

[7] Mulvenna, I., Stapleton, F., Hains, P. G., Cengiz, A. *et al.*, Low molecular weight analysis of tears using matrix assisted laser desorption ionization-time of flight mass spectrometry. *Clin. Experiment. Ophthalmol.* 2000, *28*, 205–207.

[8] Fung, K., Morris, C., Duncan, M., Mass spectrometric techniques applied to the analysis of human tears: a focus on the peptide and protein constituents. *Adv. Exp. Med. Biol.* 2002, *506*, 601–605.

[9] Sreenivasan, U., Axelsen, P. H., Buried water in homologous serine proteases. *Biochemistry* 1992, *31*, 12785–12791.

[10] Li, A., Sowder, R. C., Henderson, L. E., Moore, S. P. *et al.*, Chemical cleavage at aspartyl residues for protein identification. *Anal. Chem.* 2001, *73*, 5395–5402.

[11] Manza, L. L., Stamer, S. L., Ham, A. J., Codreanu, S. G., Liebler, D. C., Sample preparation and digestion for proteomic analyses using spin filters. *Proteomics* 2005, *5*, 1742–1745.

Experimental Eye Research 90 (2010) 344–349

Contents lists available at ScienceDirect

Experimental Eye Research

journal homepage: www.elsevier.com/locate/yexer

Tear lipocalin is the predominant phosphoprotein in human tear fluid

Zhenjun Zhao [a,b,*], Jingfang Liu [a], Valerie C. Wasinger [c], Tammy Malouf [a], Terry Nguyen-Khuong [d], Brad Walsh [d], Mark D.P. Willcox [a,b]

[a] Institute for Eye Research, Sydney, Australia
[b] The School of Optometry and Vision Science, University of New South Wales, Kensington, Australia
[c] Bioanalytical Mass Spectrometry Facility, University of New South Wales, Kensington, Australia
[d] Minomic Pty Ltd, French Forest, Australia

ARTICLE INFO

Article history:
Received 29 September 2009
Accepted in revised form
23 November 2009
Available online 29 November 2009

Keywords:
tear proteins
phosphoproteins
tear lipocalin

ABSTRACT

Proteins are very important components in tears. Their phosphorylation is an important post-translational modification affecting biological activity. Using proteomic techniques, this study was designed to analyze phosphoproteins found in open eye basal tears from normal human subjects. Proteins in tear samples were separated in 1-dimensional (1D) and 2-dimensional (2D) gels and phosphoproteins were selectively stained with Pro-Q diamond dye before visualization of all proteins using Sypro Ruby. Potential phosphoproteins in 2D gels were identified by liquid chromatography-mass spectrometry (LC-MS/MS) after trypsin digestion and phosphopeptide enrichment using titanium dioxide (TiO_2) columns. The tryptic digests of the tear samples were also analyzed to identify phosphoproteins directly by LC-MS/MS after phosphopeptide enrichment. The major phosphoprotein stained by Pro-Q diamond in the gels and identified by LC-MS/MS from the spots was tear lipocalin. Tear lipocalin was separated into 3 different isoforms and one phosphorylation site (serine at position 24) was identified in one of the isoforms. Prolactin-induced protein, nucleobindin-2 and lipophilin C were also stained with Pro-Q diamond although no phosphorylated peptides from these proteins could be found using LC-MS/MS. Direct analysis of the tear tryptic digests by LC-MS/MS identified a further 12 potential phosphoproteins with tear lipocalin predominant. Four phosphorylation sites (position 24 (serine), 32 (serine), 34 (threonine) and 36 (tyrosine)) were identified for tear lipocalin using this method. These results indicate that tear lipocalin is the predominant phosphoprotein in normal human basal tears. Nucleobindin-2, prolactin-induced protein and lipophilin C also appear to be phosphorylated in basal tear samples.

1. Introduction

Human tear film has a complex multilayered fluid structure (Tiffany, 2008). Although up to six layers have been proposed, most researchers agree that some form of three-layered structure is probably operational in the normal eye, comprising an extensive aqueous layer situated between a mucin layer and a lipid layer (Holly, 1987; Tiffany, 1994). Maintenance of this structure is important in performing tear film function and minimizing tear fluid evaporation (Bron et al., 2004; Craig and Tomlinson, 1997). The aqueous layer, which is mainly secreted from the lacrimal gland, contains locally synthesized and serum-derived proteins (Janssen and van Bijsterveld, 1983; Liotet et al., 1982). Quantitatively, the major tear proteins are lysozyme, tear lipocalin, secretory immunoglobulin A (sIgA) and lactroferrin (Molloy et al., 1997). Nearly 500 other low abundant proteins have also been reported in human tear fluid (de Souza et al., 2006; Li et al., 2008; Zhou et al., 2006). Knowledge of the functions and modifications of individual components comprising tear film and their specific interactions with each other will lead to an improved understanding of tear film.

One of the fundamental functions of human tear film is protection and health maintenance of the cornea and conjunctiva. Protein components perform vital tasks in achieving this goal (Sariri and Ghafoori, 2008). To help prevent corneal or conjunctiva infection, tear proteins such as lactoferrin, lysozyme and complement proteins comprise the non-adaptive antimicrobial factors, while sIgA comprises the predominant adaptive protein, along with

* Corresponding author. Institute for Eye Research, Gate 14 Barker Street, Rupert Myers Building, UNSW Sydney 2052, Australia. Tel.: +61 2 93857593; fax: +61 2 93857401.
E-mail address: z.zhao@ier.org.au (Z. Zhao).

0014-4835/$ – see front matter © 2009 Elsevier Ltd. All rights reserved.
doi:10.1016/j.exer.2009.11.013

anatomical barriers and mucous secretions (Chandler and Gillette, 1983). Other tear proteins such as tear lipocalin, a lipid-binding protein, may help stabilize the tear film (Gasymov et al., 2005; Glasgow et al., 2002). Tear proteins have other functions such as promoting wound healing (Flanagan and Willcox, 2009) by affecting the migration of ocular surface epithelial cells. Bioactive proteins and peptides such as cytokines have also been detected in tears and may participate in regulating the biochemical processes inside corneal and conjunctival epithelial cells (Klenkler et al., 2007; Li et al., 2008).

Posttranslational modification regulates the bioactivity of proteins (Takahashi, 2005). Protein phosphorylation has been recognized as an important posttranslational modification affecting the activity of many proteins (Greengard, 1978; Kurosawa, 1994). Protein kinases catalyze protein phosphorylation, while protein phosphatases work in the opposite fashion to remove phosphate moieties from proteins at specific sites. Coordination of these enzyme systems fine-tune many biological processes (Kurosawa, 1994). Several kinases (mitogen-activated protein kinase 3, serine/threonine protein kinase MST4, phosphoglycerate kinase 1 and UMP-CMP kinase) and phosphatases (serine/threonine protein phosphatase, inositol polyphosphate 1 phosphatase, protein tyrosine phosphate and Q15257 protein phosphatase 2A) have been identified in human tear fluid (de Souza et al., 2006). Phosphopeptides from tear lipocalin have been detected in tears (Li et al., 2005), suggesting these enzymes regulate the phosphorylation state of proteins within the tear fluid and affect tear film functions. Abnormalities in phosphorylation have been implicated in many diseases (Cohen, 2001). The aim of the present study was to identify phosphoproteins in basal tear fluid from healthy subjects using systematic proteomic techniques.

2. Materials and methods

2.1. Chemicals and reagents

LavaPep™ peptide quantification kit was purchased from Fluorotechnics Pty Limited (Sydney, NSW, Australia). Titanium dioxide (TiO_2, Titansphere, 5 μm) was a product of GL Sciences (Torrance, CA). Sequencing grade modified trypsin was from Promega (Madison, WI), Immobilized pH gradient (IPG) strips, 4–12% Bis-Tris 1.0 mm minigel and Criterion Tris–HCl 8–16% 11 cm gels were products of Bio-Rad Laboratories (Hercules, CA). Pro-Q diamond stain kit, Peppermint stick phosphoprotein molecular weight standard, Sypro Ruby protein gel stain were from Invitrogen (Carlsbad, CA). MiPrep F buffer was from Minomic Pty Ltd (Frenchs Forest, NSW, Australia).

2.2. Tear collection

Open eye basal tears from three non-contact lens-wear volunteers (2 males and 1 female, age 26–45 yr old) without any ocular pathology or dry-eye symptoms were collected using a blunt glass capillary tube from the outer canthus of the eye. Informed consent was obtained from the subjects after explanation of the nature and possible consequences of the study. All experimental protocols complied with the Declaration of Helsinki for Experimentation on Humans, 1975 and revised in 1983.

Routinely around 5 μL tears could be collected from each subject each time. Repeated collections from each subject, each time at a different day, were needed to produce sufficient samples for analysis. Tears were pooled and then stored at 80 °C. Total protein concentration of each pooled sample was assayed using a LavaPep protein quantitation kit according to the manufacturer's instructions.

2.3. SDS gel electrophoresis analyses

For 1-dimensional (1D) gel separation of tear proteins, 3 μL (21 μg) tears was first mixed with 15 μL PBS and 6 μL 4 × sample buffer (0.125 M Tris–HCl, 2% SDS, 40% v/v glycerol, 0.8% bromophenol blue, pH 6.8) and incubated at ambient temperature (AT) for 20 min. Twenty μL was loaded onto a Bio-Rad 4–12% Bis-Tris 1.0 mm minigel. The stacking gel contained 4% acrylamide/bis. Electrophoresis was carried out at 100 V in Laemmli buffer (25 mM Tris base, 0.1% SDS, 250 mM glycine, pH 8.3). Protein bands were visualized by Pro-Q diamond stain kit and then Sypro Ruby according to the manufacturer's instructions.

For 2-dimensional (2D) gel separation of tear proteins, tear samples (280 μg, ~40 μL) were first cleaned by mixing with 600 μL methanol and 150 μL chloroform. Next 450 μL ultrapure water was added and the samples were mixed by vortexing, followed by centrifugation at 12000 rpm for 5 min. The supernatant was discarded and the precipitate was washed in 450 μL methanol, recollected by centrifugation at 12000 rpm for 5 min and dried in a vacuum centrifuge for 10 min. The pellet was dissolved in 100 μL MiPrep F.

An IPG strip (11 cm, pH 4–7) was first rehydrated using 200 μL MiPrep F for 4–5 h. Then cup loading of the sample (100 μL of the prepared sample) was performed using 2 cups, which were placed at the cathode and anode ends of the strip, each containing 50 μL sample. A Bio-Rad Protean IEF cell was used to carry out isoelectric focusing at AT. The total Vh was approximately 50,000. The strip was frozen at −80 °C for 1 h, then treated with reduction solution (6 M urea, 2% SDS, 20% glycerol, 65 mM DTT in Tris–HCl gel buffer pH 8.8) and alkylation solution (6 M urea, 2% SDS, 20% glycerol, 2.5% acrylamide in Tris–HCl gel buffer pH 8.8) consecutively, for 15 min each. Tris–HCl 8–16% 11 cm gels were used for the 2nd dimension and Peppermint stick Phosphoprotein Molecular Weight Standard (1 μL) as the marker. The electrophoresis was carried out at 200 V at AT.

After electrophoresis, the gels were stained with Pro-Q diamond and then Sypro Ruby according to the protocol provided by their manufacturers. A Pharos Imager was used to visualize the spots using dye specific settings.

2.4. LC-MS/MS identification of protein gel spots

Protein spots from the 2D gels were excised into 1 mm cubes and transferred into 1.5 mL Eppendorf tubes. Samples were washed with 200 μL 50% acetonitrile/50 mM ammonium bicarbonate for 30 min at 37 °C, dehydrated with 100% acetonitrile, then dried at 37 °C for 30 min. Utilizing a method described by Herbert and colleagues (Herbert et al., 1998), proteins were reduced and alkylated with 50 μL freshly prepared solution containing 5 mM tributyl phosphine and 10 mM acrylamide in 50 mM ammonium bicarbonate by incubation at AT for 1 h. Samples were washed, dehydrated and dried again as described above. Samples were digested for 17 h at 37 °C with 50 μL of 6 μg/mL sequencing grade trypsin in 50 mM ammonium bicarbonate. Resulting peptides were extracted twice, each with 100 μL 10% acetonitrile/0.1% trifluoroacetic acid and sonicated in a water bath for 10 min.

Extracts were combined and dried using a SpeedVac (Thermo Scientific, Waltham, MA). Peptides were dissolved in 20 μL loading/washing solution containing 80% acetonitrile and 5% trifluoacetic acid. Phosphopeptides were enriched using an in-house built TiO_2 micro-column (Jensen and Larsen, 2007) as follows. A syringe needle was used to cut a frit from C8 Empore disk (St Paul, MN) and inserted into a crystal loader tip. A TiO_2 slurry was prepared and packed into the column to a 2 mm length and washed with wash solution. The sample was loaded in wash solution, washed with

20 μL of wash solution and eluted in 10 μL of 6% ammonia and 20% acetonitrile and then dried in the SpeedVac.

Peptides were resuspended in 0.1% HFBA/1% formic acid and separated by nano-LC using an Ultimate 3000 HPLC and autosampler system (Dionex, Amsterdam, Netherlands). Samples were concentrated and desalted onto a micro C18 pre-column (500 μm × 2 mm, Michrom Bioresources, Inc. Auburn, CA) with 0.05% HFBA at 20 μL/min. After a 4 min wash the pre-column was switched (Valco 10 port valve, Dionex, Amsterdam, Netherlands) into line with an in-house built fritless nano C18 column. LC mobile phase buffers comprised of A: 2% CH_3CN/0.1% formic acid/98% deionised water and B: 80% CH_3CN/0.1% formic acid/20% deionised water. Peptides were eluted using a linear gradient of 2–50% B over 30 min and then 100% B wash over 1 min at a flow rate of ~300 nL/min. The LTQ-FT ultra hybrid ion trap Fourier transform high resolution mass spectrometer (Thermo Scientific, Waltham, MA) was operated as described previously (Ly and Wasinger, 2008). Peak lists were generated using 'Mascot Daemon/extract_msn' (Matrix Science, Boston, MA) and submitted to the database search program Mascot using parameters of: Precursor and product ion tolerances ± 0.6 and 0.6 ppm respectively; Met(O), Acrylamide (C), Carbamidomethyl (C), Phospho (STY) specified as variable modifications, enzyme specificity was trypsin, 1 missed cleavage was possible and a non-redundant database (NCBI, Feb 2007) searched. For protein identification, p value (probability that the observed match is a random event) was set at $p \leq 0.05$.

2.5. Direct LC-MS/MS analysis of the tear samples

Tear samples (56 μg, 8 μL) were mixed with 50 mM ammonium bicarbonate (pH 8.0) to a final volume of 50 μL. Trypsin (1 μL, 1 μg/μL in 50 mM acetic acid) was added and the mixture was incubated at 37 °C overnight (17 h). After evaporating the solvent using the SpeedVac, resulting peptides were dissolved in 20 μL loading/washing solution containing 80% acetonitrile and 5% trifluoacetic acid. Phosphopeptides were enriched using the in-house built TiO_2 micro-column and then the samples were run using LC-MS/MS on an LTQ-FT instrument as previously described. A 'Decoy' database search gave a calculated false positive rate of 1.96% for the peptides matching above the identity threshold.

3. Results

3.1. Analysis of phosphoproteins in normal basal tears using Pro-Q diamond staining of SDS gels

Tear proteins were separated by 1D and 2D gels and stained with Pro-Q diamond, a dye specifically staining phosphoproteins, and subsequently Sypro Ruby, a dye staining all proteins. In 1D gels, a protein with a molecular weight of 18 kDa was strongly stained by Pro-Q diamond (Fig. 1, top right). The next most strongly stained band corresponded to a molecular weight of approximately 14 kDa. A few other faint bands were also visible. All these bands were strongly stained by Sypro Ruby (Fig. 1, bottom right).

To explore the details of Pro-Q diamond staining pattern of tear proteins, 2D gel analysis was preformed and a group of spots with molecular weight of 16–19 kDa and isoelectric point (PI) of 4.8–5.3 were visible after staining using Pro-Q diamond dye (Fig. 1, top left). In comparison with the image of Sypro Ruby staining of the same gel, spots 1 and 3 were stained mainly by Pro-Q diamond, only weakly by Sypro Ruby, indicating that these proteins are potentially phosphorylated but their abundances in the sample are low. In contrast, spots 2 and 4 were weakly stained in the Pro-Q diamond gel but strongly stained by Sypro Ruby, indicating these high abundant proteins in the sample are weakly or not phosphorylated (non-specific staining). Another train of spots (within circle A, Fig. 1 left), normally corresponding to different isoforms of the same protein (Kim et al., 2007; Pietrogrande et al., 2006), could be seen clearly in the Pro-Q diamond gel but were very faint in the Sypro Ruby gel, indicating this protein may be phosphorylated but of very low abundance in the sample. Some other faint spots could also be seen in the Pro-Q diamond stained gel. Since these proteins are highly abundant in the sample (heavily stained in Sypro Ruby gel, Fig. 1, bottom left), these spots were regarded as background (non-specific) staining.

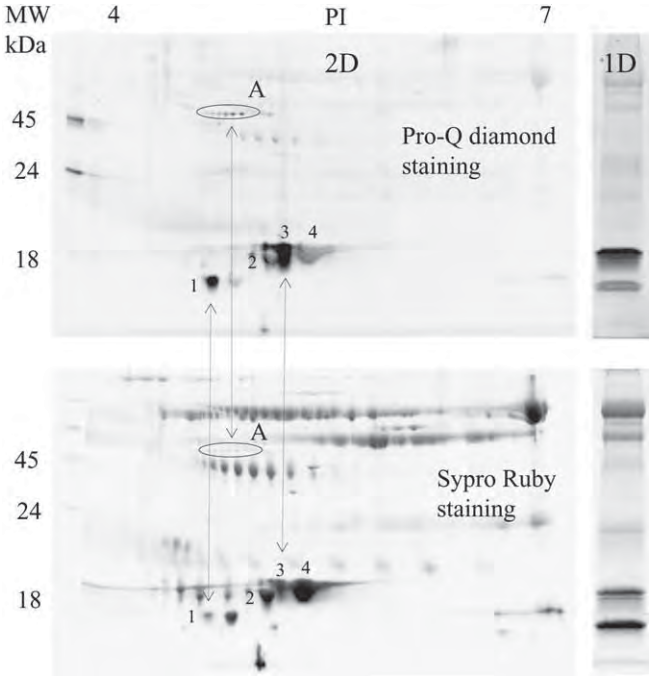

Fig. 1. 1D (right) and 2D (left) gel images of tear samples stained with Pro-Q diamond (top) first and then Sypro Ruby (bottom). The arrows linked by dot lines indicate the same spots after the different dye staining. Spots 1, 3 and within circle A in the 2D gel were selectively stained by Pro-Q diamond, a phosphoprotein specific dye.

3.2. LC-MS/MS identification of the spots

The major spots in the 2D gels stained with Pro-Q diamond were cut and the phosphoproteins analyzed by LC-MS/MS (Table 1). Spot 1 was identified as prolactin-induced protein. Spots 2 and 3 were tear lipocalin. Spot 4 was a mixture of tear lipocalin and lipophilin C. The train of spots in circle A was identified as nucleobindin-2. The most intensive spot in Pro-Q diamond stained gel was spot 3 (lipocalin), which was found to have a phosphorylation site at position

Table 1
LC-MS/MS identification of the Pro-Q diamond stained spots in tear 2D gels.

Spot	Accession#	Protein name	Mascot score	emPAI[a]
1	gi|4505821	Prolactin-induced protein	640	0.39
2	gi|4504963	Tear lipocalin	498	28.33
3	gi|4504963	Tear lipocalin	898	326.69
4	gi|6831582	Lipophilin C	101	1.28
4	gi|4504963	Tear lipocalin	59	0.19
A	gi|4826870	Nucleobindin-2	192	0.29

[a] Exponentially modified protein abundance index.

24 (serine). No further phosphorylation site was detected by MS in other gel samples.

3.3. Direct LC-MS/MS analysis of the tear samples

The tear sample was digested with trypsin and the phosphopeptides enriched using the TiO_2 column and analyzed by LC-MS/MS. NCBI database search of the results identified a total of 13 proteins (Table 2). Tear lipocalin obtained the highest ranking Mascot score, the highest exponentially modified protein abundance index (emPAI) value indicating abundance, and was the only tear protein from which phosphorylated peptides could be detected. No further phosphoproteins could be confirmed by phosphorylation site analysis in the samples. This result was reproducible in another two repeated analyses. The detected phosphopeptides are shown in Fig. 2. The detected phosphorylation sites in tear lipocalin were located within a defined region, i.e. position 24 (serine), 32 (serine), 34 (threonine) and 36 (tyrosine) (Fig. 2). Non-phosphorylated tear lipocalin, i.e. the same peptide sequences but not phosphorylated, or tear lipocalin only partially phosphorylated at some of four sites were also found in the samples. Fully phosphorylated lipocalin, i.e. all the four sites were phosphorylated in a single peptide, was not detected.

4. Discussion

In the present study, tear lipocalin, previously referred to as 'tear-specific prealbumin', was found to be the predominant phosphoprotein in normal basal tears from healthy subjects, and the only protein for which phosphorylation sites were confirmed. Pro-Q diamond staining suggested prolactin-induced protein and nucleobindin-2 may also be phosphorylated, despite the lack of confirmation of a phosphorylation site by LC-MS/MS. The identification of the phosphoproteins other than tear lipocalin by LC-MS/MS method from the phosphopeptide enriched tear tryptic digests could not be confirmed as there were no phosphopeptides detected from these proteins in these samples. As with other phosphor-enrichment techniques, TiO_2 suffers from non-specific binding (Jensen and Larsen, 2007). Non-phosphorylated peptides are commonly found in the phosphopeptide fraction. Thus identification of phosphopeptides in the tryptic digests was limited to those that could be confirmed by the presence of phosphorylated amino acids within the sequence. Certainly, the presence of highly abundant tear proteins such as lysozyme and sIgA in the TiO_2 fraction, but their absence in the Pro-Q stained gels, indicates that these are likely not phosphorylated. The presence of these high abundant proteins increases the risk of depressing the detection of some low abundant phosphopeptides. This may be the reason why the two likely phosphorylated proteins found in 2D gels, prolactin-induced protein and nucleobindin-2, were not identified in the tryptic digests of tears.

Table 2
LC-MS/MS identification of potential phosphoproteins in tryptic digests of tear samples.

Accession #	Protein name	Mascot score	emPAI
gi|4504963	Tear lipocalin	1273	39.47
gi|6831582	Lipophilin C	434	14.57
gi|152031723	Protein UNQ773	200	0.51
gi|125145	Ig kappa chain C region	185	0.67
gi|150421625	Polymeric immunoglobulin receptor	172	0.17
gi|33301325	Extracellular glycoprotein lacritin	170	1.92
gi|399336	Cystatin-S	136	0.21
gi|85687556	Deleted in malignant brain tumors 1 protein	129	0.01
gi|116242732	Proline-rich protein 4	93	0.83
gi|113584	Ig alpha-1 chain C region	88	0.09
gi|48428995	Lysozyme C	85	0.74
gi|116533	Clusterin/apolipoprotein J	84	0.20
gi|400044	Immunoglobulin J chain	65	0.22

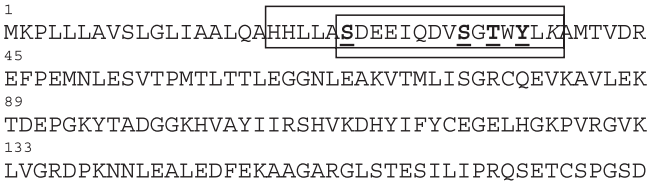

Fig. 2. Lipocalin amino acid sequence and the detected phosphorylation sites (underlined bold). The two boxes indicate the phosphopeptides detected by LC-MS/MS in tryptic digests of the tear sample. The numbers show the sequence positions of the first amino acid of each line.

Tear lipocalin, produced in the lacrimal gland as well as in von Ebner's gland, is a member of the lipocalin superfamily (Blaker et al., 1993; Delaire et al., 1992; Inada, 1984; Redl et al., 1992) and has lipid-binding properties (Flower, 1996). This group of proteins has been classified as extracellular transport proteins and possesses many different and potentially significant biological functions including roles in mediating pheromone activity, olfaction, cryptic coloration, enzymatic synthesis, immunomodulation and the regulation of cell homoeostasis (Flower, 1996). Tear lipocalin is one of major tear proteins. Normally, the open eye basal tears contain approximately 1.5 mg/mL of this protein (Yamada et al., 2005), which comprises 15–33% of the mass of total protein in tears (Fullard and Kissner, 1991). It is believed that tear lipocalin is the principal lipid-binding protein in tears (Glasgow et al., 1995) and has been proposed to help clear lipids from the ocular surface (Gasymov et al., 2005). Apart from this, tear lipocalin is the major endonuclease in tears (Yusifov et al., 2008) and has been demonstrated to have antibacterial activity (Fluckinger et al., 2004) and inhibit cysteine proteinases (van't Hof et al., 1997). Tear lipocalin has also been shown to interact with other tear proteins (Gasymov et al., 1999) and its concentration changes in some ocular surface diseases (Caffery et al., 2008; Glasson et al., 2002; Navone et al., 2005; Yamada et al., 2005).

It is clear that tear lipocalin possess multiple biological functions. As a group of proteins, the activity of lipocalins has been shown to be regulated by posttranslational modifications such as glycosylation (Loebel et al., 2000). The current study found 4 phosphorylation sites within a small region (position 24–36) of the protein sequence and non-phosphorylated lipocalin or lipocalin only partially phosphorylated at some of four sites was also detected in the samples. Positions 32 and 34 have been showed to be phosphorylated previously (Li et al., 2005). From the published 3D structure of this protein related to lipid binding (Breustedt et al., 2005; Gasymov et al., 2009, 2001), these amino acids located outside of the lipid-binding cavity and, therefore, seem not participate in external or intracavitary lipid binding. The phosphorylation status unlikely affects its lipid-binding property. Since lipocalin has many other functions, significance of the phosphorylation in these activities should be the focus of future investigation.

In 2D gels, tear lipocalin was separated into 3 distinct spots (Fig. 1 left, spots 2–4, PI 5.1, 5.2, 5.3 respectively). These may be the different isoforms of tear lipocalin, as detected by others previously (Fullard and Kissner, 1991; Lassagne and Gachon, 1993). It is unknown whether or not there is any difference in phosphorylation status among these isoforms. The detection of phosphopeptides in spot 3 only, but not in spots 2 and 4, and spot 3's much stronger phosphorylation staining suggests that this isoform only is

significantly phosphorylated. The single phosphorylation site (Serine 24) detected from this spot may mean tear lipocalin is more regularly phosphorylated at this site. Taking into consideration that this isoform is very low in abundance (see the Sypro Ruby stained 2D gel in Fig. 2), phosphorylation at other sites may exist but the amounts of the corresponding phosphopeptides may be too low for detection. Likewise, the phosphorylation may also exist in spots 2 and 4 but their amounts are also below the detection limit.

One concern about Pro-Q diamond staining of the gels is that the dye may stain any proteins that bind to phospholipids, not necessarily phosphorylated proteins. We know that native tear lipocalin can bind phospholipids but we do not believe that this is a major concern in the present study. Prior to 2D-gel electrophoresis the samples were subjected to cleaning with a chloroform/methanol mixture which would remove lipids from the sample. Under the condition of electrophoresis, all the tear proteins were denatured and reduced so that it is unlikely that tear lipocalin (or other proteins) would still binds phospholipids.

Two other proteins were identified by Pro-Q diamond staining, namely prolactin-induced protein and nucleobidin-2. However, no phosphopeptides were detected in these spots upon LC-MS/MS. Again, this may only mean that their amount may be too low for detection, and this same reason may also explain why these two proteins were not identified in direct LC-MS/MS analysis of tear tryptic digests. The location of nucleobindin-2 in the 2D gel approximately agrees with its molecular weight (50.2 kDa) and PI (5.0) (from Swiss-Prot protein database http://au.expasy.org/sprot/). For prolactin-induced protein, its location in the 2D gel roughly agrees with molecular weight (13.5 kDa) and PI (5.5) of the mature protein (without the signal peptide 1–28) but not with its full sequence of 16.6 kDa and PI 8.3 (Swiss-Prot protein database http://au.expasy.org/sprot/). The result is consistent with other investigators who have also identified this protein in 2D gels in tears (Green-Church et al., 2008) and sperm (Martinez-Heredia et al., 2008).

Spot 4 is the most intensive spot in the Sypro Ruby stained 2D gel but it is faint in Pro-Q diamond stained the same gel. LC-MS/MS identification showed this spot to be a mixture of lipophilin C and tear lipocalin. Lipophilin C, also known as mammaglobin-B, appeared also in the potential phosphoprotein list generated from the direct LC-MS/MS analysis results of tear tryptic digests. It is a part of tear lipophilin, a heterodimer consisting of lipophilin A (7.6 kDa, PI 9.5) and lipophilin C (8.9 kDa, PI 4.9). Lipophilin, also named lacryoglobin, is a low abundant tear protein (45 μg/mL in stimulated tears) (Lehrer et al., 1998) and can only be detected in a proportion of normal human subjects (Evans et al., 2001). This protein has been very well characterized in tears (Lehrer et al., 1998). The heterodimers are held together by 3 disulfides. Spot 4 on Fig. 1, showing a mass of about 15–18 kDa, seems to represent the unreduced heterodimer. Its low PI (5.3), which is close to that of monomer lipophilin C, may implicate modifications. The result may also indicate incomplete reduction under the condition used.

Lipophilin C should contribute a small portion for spot 4's intensity in Sypro Ruby stained gels. The function of this protein is unknown but a report showed that it was expressed in the prostate (Xiao et al., 2005). This protein has been found to be over expressed in some colon cancers and down-regulated in hepatoma cells (Aihara et al., 2000) and a potential biomarker for some cancers in tears (Evans et al., 2001).

In general protein phosphorylation plays a significant role in a wide range of cellular processes (Graves and Krebs, 1999). It is rational to propose that most phosphoproteins are located within cells. Indeed, 20–30% of proteins inside the cell are estimated to be phosphorylated (Cohen, 2000). However, phosphorylation and dephosphorylation regulate protein activities in all parts of animal body so it is not surprising that tear fluid, normally a cell-free body fluid, also contains phosphoproteins. The tear fluid covers the epithelium cells of the ocular surface and the phosphorylation status of tear proteins may also implicate in the health of ocular surface epithelium cells.

In conclusion tear lipocalin is the predominant phosphoprotein in normal basal tears. The phosphorylation status of various tear lipocalin isoforms may be different. Nucleobindin-2, prolactin-induced protein and lipophilin C are three proteins potentially phosphorylated in tears. The biological relevance of the phosphorylation remains to be explored.

Acknowledgments

We thank Dr Judith Flanagan for editing the manuscript and Val Valova (CMRI) for acquisition of TiO_2 column techniques. This work is supported in part by the Australian Federal Government through the Cooperative Research Centres Program.

References

Aihara, T., Fujiwara, Y., Miyake, Y., Okami, J., Okada, Y., Iwao, K., Sugita, Y., Tomita, N., Sakon, M., Shiozaki, H., et al., 2000. Mammaglobin B gene as a novel marker for lymph node micrometastasis in patients with abdominal cancers. Cancer Lett. 150, 79–84.

Blaker, M., Kock, K., Ahlers, C., Buck, F., Schmale, H., 1993. Molecular cloning of human von Ebner's gland protein, a member of the lipocalin superfamily highly expressed in lingual salivary glands. Biochim. Biophys. Acta 1172, 131–137.

Breustedt, D.A., Korndorfer, I.P., Redl, B., Skerra, A., 2005. The 1.8-A crystal structure of human tear lipocalin reveals an extended branched cavity with capacity for multiple ligands. J. Biol. Chem. 280, 484–493.

Bron, A.J., Tiffany, J.M., Gouveia, S.M., Yokoi, N., Voon, L.W., 2004. Functional aspects of the tear film lipid layer. Exp. Eye Res. 78, 347–360.

Caffery, B., Joyce, E., Boone, A., Slomovic, A., Simpson, T., Jones, L., Senchyna, M., 2008. Tear lipocalin and lysozyme in sjogren and non-sjogren dry eye. Optom. Vis. Sci. 85, 661–667.

Chandler, J.W., Gillette, T.E., 1983. Immunologic defense mechanisms of the ocular surface. Ophthalmology 90, 585–591.

Cohen, P., 2000. The regulation of protein function by multisite phosphorylation–a 25 year update. Trends Biochem. Sci. 25, 596–601.

Cohen, P., 2001. The role of protein phosphorylation in human health and disease. The Sir Hans Krebs Medal Lecture. Eur. J. Biochem. 268, 5001–5010.

Craig, J.P., Tomlinson, A., 1997. Importance of the lipid layer in human tear film stability and evaporation. Optom. Vis. Sci. 74, 8–13.

Delaire, A., Lassagne, H., Gachon, A.M., 1992. New members of the lipocalin family in human tear fluid. Exp. Eye Res. 55, 645–647.

Evans, V., Vockler, C., Friedlander, M., Walsh, B., Willcox, M.D., 2001. Lacryglobin in human tears, a potential marker for cancer. Clin. Experiment. Ophthalmol. 29, 161–163.

Flanagan, J.L., Willcox, M.D., 2009. Role of lactoferrin in the tear film. Biochimie 91, 35–43.

Flower, D.R., 1996. The lipocalin protein family: structure and function. Biochem. J. 318 (Pt 1), 1–14.

Fluckinger, M., Haas, H., Merschak, P., Glasgow, B.J., Redl, B., 2004. Human tear lipocalin exhibits antimicrobial activity by scavenging microbial siderophores. Antimicrob. Agents Chemother. 48, 3367–3372.

Fullard, R.J., Kissner, D.M., 1991. Purification of the isoforms of tear specific prealbumin. Curr. Eye Res. 10, 613–628.

Gasymov, O.K., Abduragimov, A.R., Glasgow, B.J., 2009. Intracavitary ligand distribution in tear lipocalin by site-directed tryptophan fluorescence. Biochemistry 48, 7219–7228.

Gasymov, O.K., Abduragimov, A.R., Prasher, P., Yusifov, T.N., Glasgow, B.J., 2005. Tear lipocalin: evidence for a scavenging function to remove lipids from the human corneal surface. Invest. Ophthalmol. Vis. Sci. 46, 3589–3596.

Gasymov, O.K., Abduragimov, A.R., Yusifov, T.N., Glasgow, B.J., 1999. Interaction of tear lipocalin with lysozyme and lactoferrin. Biochem. Biophys. Res. Commun. 265, 322–325.

Gasymov, O.K., Abduragimov, A.R., Yusifov, T.N., Glasgow, B.J., 2001. Site-directed tryptophan fluorescence reveals the solution structure of tear lipocalin: evidence for features that confer promiscuity in ligand binding. Biochemistry 40, 14754–14762.

Glasgow, B.J., Abduragimov, A.R., Farahbakhsh, Z.T., Faull, K.F., Hubbell, W.L., 1995. Tear lipocalins bind a broad array of lipid ligands. Curr. Eye Res. 14, 363–372.

Glasgow, B.J., Abduragimov, A.R., Gasymov, O.K., Yusifov, T.N., 2002. Tear lipocalin: structure, function and molecular mechanisms of action. Adv. Exp. Med. Biol. 506 (Pt A), 555–565.

Glasson, M., Stapleton, F., Willcox, M., 2002. Lipid, lipase and lipocalin differences between tolerant and intolerant contact lens wearers. Curr. Eye Res. 25, 227–235.
Graves, J.D., Krebs, E.G., 1999. Protein phosphorylation and signal transduction. Pharmacol. Ther. 82, 111–121.
Green-Church, K.B., Nichols, K.K., Kleinholz, N.M., Zhang, L., Nichols, J.J., 2008. Investigation of the human tear film proteome using multiple proteomic approaches. Mol. Vis. 14, 456–470.
Greengard, P., 1978. Phosphorylated proteins as physiological effectors. Science 199, 146–152.
Herbert, B.R., Molloy, M.P., Gooley, A.A., Walsh, B.J., Bryson, W.G., Williams, K.L., 1998. Improved protein solubility in two-dimensional electrophoresis using tributyl phosphine as reducing agent. Electrophoresis 19, 845–851.
Holly, F.J., 1987. Tear film physiology. Int. Ophthalmol. Clin. 27, 2–6.
van't Hof, W., Blankenvoorde, M.F., Veerman, E.C., Amerongen, A.V., 1997. The salivary lipocalin von Ebner's gland protein is a cysteine proteinase inhibitor. J. Biol. Chem. 272, 1837–1841.
Inada, K., 1984. Studies of human tear proteins. 3. Distribution of specific tear prealbumin in lacrimal glands and other ocular adnexa. Jpn. J. Ophthalmol. 28, 315–330.
Janssen, P.T., van Bijsterveld, O.P., 1983. Origin and biosynthesis of human tear fluid proteins. Invest. Ophthalmol. Vis. Sci. 24, 623–630.
Jensen, S.S., Larsen, M.R., 2007. Evaluation of the impact of some experimental procedures on different phosphopeptide enrichment techniques. Rapid Commun. Mass Spectrom. 21, 3635–3645.
Kim, H., Eliuk, S., Deshane, J., Meleth, S., Sanderson, T., Pinner, A., Robinson, G., Wilson, L., Kirk, M., Barnes, S., 2007. 2D gel proteomics: an approach to study age-related differences in protein abundance or isoform complexity in biological samples. Methods Mol. Biol. 371, 349–391.
Klenkler, B., Sheardown, H., Jones, L., 2007. Growth factors in the tear film: role in tissue maintenance, wound healing, and ocular pathology. Ocul. Surf. 5, 228–239.
Kurosawa, M., 1994. Phosphorylation and dephosphorylation of protein in regulating cellular function. J. Pharmacol. Toxicol. Methods 31, 135–139.
Lassagne, H., Gachon, A.M., 1993. Cloning of a human lacrimal lipocalin secreted in tears. Exp. Eye Res. 56, 605–609.
Lehrer, R.I., Xu, G., Abduragimov, A., Dinh, N.N., Qu, X.D., Martin, D., Glasgow, B.J., 1998. Lipophilin, a novel heterodimeric protein of human tears. FEBS Lett. 432, 163–167.
Li, N., Wang, N., Zheng, J., Liu, X.M., Lever, O.W., Erickson, P.M., Li, L., 2005. Characterization of human tear proteome using multiple proteomic analysis techniques. J. Proteome Res. 4, 2052–2061.
Li, S., Sack, R., Vijmasi, T., Sathe, S., Beaton, A., Quigley, D., Gallup, M., McNamara, N. A., 2008. Antibody protein array analysis of the tear film cytokines. Optom. Vis. Sci. 85, E653–E660.
Liotet, S., Warnet, V.N., Arrata, M., 1982. Functional exploration of the lacrimal gland by tear electrophoresis. Ophthalmologica 184, 87–91.
Loebel, D., Scaloni, A., Paolini, S., Fini, C., Ferrara, L., Breer, H., Pelosi, P., 2000. Cloning, post-translational modifications, heterologous expression and ligand-binding of boar salivary lipocalin. Biochem. J. 350 (Pt 2), 369–379.
Ly, L., Wasinger, V.C., 2008. Peptide enrichment and protein fractionation using selective electrophoresis. Proteomics 8, 4197–4208.
Martinez-Heredia, J., de Mateo, S., Vidal-Taboada, J.M., Ballesca, J.L., Oliva, R., 2008. Identification of proteomic differences in asthenozoospermic sperm samples. Hum. Reprod. 23, 783–791.
Molloy, M.P., Bolis, S., Herbert, B.R., Ou, K., Tyler, M.I., van Dyk, D.D., Willcox, M.D., Gooley, A.A., Williams, K.L., Morris, C.A., et al., 1997. Establishment of the human reflex tear two-dimensional polyacrylamide gel electrophoresis reference map: new proteins of potential diagnostic value. Electrophoresis 18, 2811–2815.
Navone, R., Lunardi, C., Gerli, R., Tinazzi, E., Peterlana, D., Bason, C., Corrocher, R., Puccetti, A., 2005. Identification of tear lipocalin as a novel autoantigen target in Sjogren's syndrome. J. Autoimmun. 25, 229–234.
Pietrogrande, M.C., Marchetti, N., Dondi, F., Righetti, P.G., 2006. Decoding 2D-PAGE complex maps: relevance to proteomics. J. Chromatogr. B Analyt. Technol. Biomed. Life Sci. 833, 51–62.
Redl, B., Holzfeind, P., Lottspeich, F., 1992. cDNA cloning and sequencing reveals human tear prealbumin to be a member of the lipophilic-ligand carrier protein superfamily. J. Biol. Chem. 267, 20282–20287.
Sariri, R., Ghafoori, H., 2008. Tear proteins in health, disease, and contact lens wear. Biochemistry (Mosc) 73, 381–392.
de Souza, G.A., Godoy, L.M., Mann, M., 2006. Identification of 491 proteins in the tear fluid proteome reveals a large number of proteases and protease inhibitors. Genome Biol. 7, R72.
Takahashi, N., 2005. Change in protein function due to post-translational modification. Seikagaku 77, 481–483.
Tiffany, J.M., 1994. Composition and biophysical properties of the tear film: knowledge and uncertainty. Adv. Exp. Med. Biol. 350, 231–238.
Tiffany, J.M., 2008. The normal tear film. Dev. Ophthalmol. 41, 1–20.
Xiao, F., Mirwald, A., Papaioannou, M., Baniahmad, A., Klug, J., 2005. Secretoglobin 2A1 is under selective androgen control mediated by a peculiar binding site for Sp family transcription factors. Mol. Endocrinol. 19, 2964–2978.
Yamada, M., Mochizuki, H., Kawai, M., Tsubota, K., Bryce, T.J., 2005. Decreased tear lipocalin concentration in patients with meibomian gland dysfunction. Br. J. Ophthalmol. 89, 803–805.
Yusifov, T.N., Abduragimov, A.R., Narsinh, K., Gasymov, O.K., Glasgow, B.J., 2008. Tear lipocalin is the major endonuclease in tears. Mol. Vis. 14, 180–188.
Zhou, L., Roger, W.B., Foo, Y., Liu, S., Leonard, P.A., Donald, T.T., 2006. Characterisation of human tear proteins using high-resolution mass spectrometry. Ann. Acad. Med. Singapore 35, 400–408.